



UNIVERSITAT DE
BARCELONA

Proliferative and positional instructions underlying planarian regeneration and tissue renewal

Instrucciones proliferativas y posicionales subyacentes a la regeneración y el recambio tisular en planaria

José Ignacio Rojo Laguna

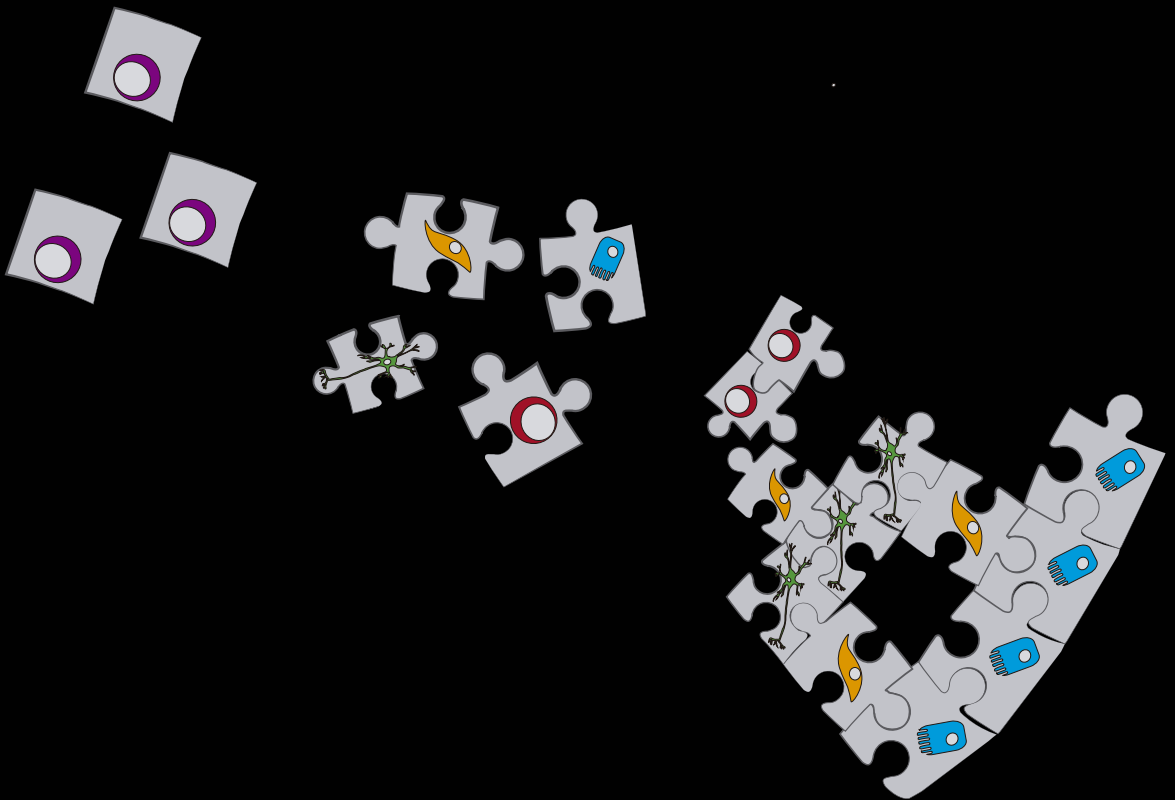
ADVERTIMENT. La consulta d'aquesta tesi queda condicionada a l'acceptació de les següents condicions d'ús: La difusió d'aquesta tesi per mitjà del servei TDX (www.tdx.cat) i a través del Dipòsit Digital de la UB (diposit.ub.edu) ha estat autoritzada pels titulars dels drets de propietat intel·lectual únicament per a usos privats emmarcats en activitats d'investigació i docència. No s'autoritza la seva reproducció amb finalitats de lucre ni la seva difusió i posada a disposició des d'un lloc aliè al servei TDX ni al Dipòsit Digital de la UB. No s'autoritza la presentació del seu contingut en una finestra o marc aliè a TDX o al Dipòsit Digital de la UB (framing). Aquesta reserva de drets afecta tant al resum de presentació de la tesi com als seus continguts. En la utilització o cita de parts de la tesi és obligat indicar el nom de la persona autora.

ADVERTENCIA. La consulta de esta tesis queda condicionada a la aceptación de las siguientes condiciones de uso: La difusión de esta tesis por medio del servicio TDR (www.tdx.cat) y a través del Repositorio Digital de la UB (diposit.ub.edu) ha sido autorizada por los titulares de los derechos de propiedad intelectual únicamente para usos privados enmarcados en actividades de investigación y docencia. No se autoriza su reproducción con finalidades de lucro ni su difusión y puesta a disposición desde un sitio ajeno al servicio TDR o al Repositorio Digital de la UB. No se autoriza la presentación de su contenido en una ventana o marco ajeno a TDR o al Repositorio Digital de la UB (framing). Esta reserva de derechos afecta tanto al resumen de presentación de la tesis como a sus contenidos. En la utilización o cita de partes de la tesis es obligado indicar el nombre de la persona autora.

WARNING. On having consulted this thesis you're accepting the following use conditions: Spreading this thesis by the TDX (www.tdx.cat) service and by the UB Digital Repository (diposit.ub.edu) has been authorized by the titular of the intellectual property rights only for private uses placed in investigation and teaching activities. Reproduction with lucrative aims is not authorized nor its spreading and availability from a site foreign to the TDX service or to the UB Digital Repository. Introducing its content in a window or frame foreign to the TDX service or to the UB Digital Repository is not authorized (framing). Those rights affect to the presentation summary of the thesis as well as to its contents. In the using or citation of parts of the thesis it's obliged to indicate the name of the author.

PROLIFERATIVE AND POSITIONAL INSTRUCTIONS UNDERLYING PLANARIAN REGENERATION AND TISSUE RENEWAL

José Ignacio Rojo Laguna
PhD Thesis 2017



Departamento de Genética, Microbiología y Estadística
Programa de Doctorado en Genética de la Facultad de Biología
Universidad de Barcelona

**PROLIFERATIVE AND POSITIONAL INSTRUCTIONS UNDERLYING PLANARIAN
REGENERATION AND TISSUE RENEWAL**

(Instrucciones proliferativas y posicionales subyacentes a la regeneración y el
recambio tisular en planaria)

Memoria presentada por

José Ignacio Rojo Laguna

Para optar al grado de

Doctor

por la Universidad de Barcelona



UNIVERSITAT DE
BARCELONA

Tesis doctoral realizada bajo la dirección del Dr. Emili Saló Boix y la Dra. María Teresa
Adell Creixell.

Barcelona, Abril 2017

Departamento de Genética, Microbiología y Estadística
Programa de Doctorado en Genética de la Facultad de Biología
Universidad de Barcelona

**PROLIFERATIVE AND POSITIONAL INSTRUCTIONS UNDERLYING PLANARIAN
REGENERATION AND TISSUE RENEWAL**

(Instrucciones proliferativas y posicionales subyacentes a la regeneración y el
recambio tisular en planaria)

Memoria presentada por

José Ignacio Rojo Laguna

Para optar al grado de

Doctor

por la Universidad de Barcelona



UNIVERSITAT DE
BARCELONA

Tesis doctoral realizada bajo la dirección del Dr. Emili Saló Boix y la Dra. María Teresa
Adell Creixell.

Firmado, los directores:

Firmado, el autor:

Dr. Emili Saló Boix

Dra. María Teresa Adell Creixell

José Ignacio Rojo Laguna

Barcelona, Abril 2017

“Si pudiera inventarse algo -dije impulsivamente- para embotellar los recuerdos, como los perfumes... Para que no se disipasen, para que nunca pudieran ponerse rancios... Cuando quisiéramos, podríamos destapar el frasco y sería como vivir de nuevo el momento guardado.”

- Daphne du Maurier

ACKNOWLEDGEMENTS

Una etapa de mi vida llega a su final, bueno no solo de mi vida, sino de toda la gente que está a mi alrededor, sin cuya inestimable ayuda no habría podido finalizar. Cómo he llegado hasta aquí implica muchos acontecimientos y situaciones que no voy a describir aquí y ahora ya que me darían para escribir una novela. Sin embargo, no puedo dejar pasar la oportunidad de recalcar algunos aspectos que han sido vitales para que este proyecto no se haya quedado en solo un intento. Mi familia (pobres de ellos) ha aguantado con mucha entereza todos mis altibajos sin los que una tesis no sería tal; no solo me han dado consuelo, sino que también me han dado fuerzas para continuar en los peores momentos y han celebrado junto a mí los buenos. Yo sé que no terminan de comprender por lo que pasa un doctorando, ya que somos una especie rara, y menos aun los proyectos en los que andamos metidos. Aun así, me han escuchado felizmente explicarles historias que les habrán sonado de lo más extraño, he incluso lo habrán intentado transmitir a conocidos; posiblemente con frases como “mi hijo/hermano/novio/sobrino corta y pincha lombrices y estudia como regeneran”.

Durante esta etapa he conocido a muchas personas a nivel tanto personal como laboral que, incluso sin saberlo, me han ayudado de diversas maneras. Dentro de este grupo, no puedo dejar de mencionar a la persona que más me ha ayudado y más ha sufrido mis altibajos debido a experimentos fallidos, animales que se ponen enfermos y no me dejan continuar, nervios por charlas o congresos, y un eterno etcétera. Esta persona me ha hecho madurar influenciando, aunque no lo sepa, en el desarrollo de la tesis, haciéndome valorar aspectos de la vida que ahora son esenciales para mí y como no, mi futuro. Por otra parte, no podría olvidar la ayuda incondicional que me han proporcionado mis “tutores” o directores de tesis. Nunca he sabido muy bien como denominarlos, tutores, directores de tesis, jefes... Todas ellas no responden realmente al trabajo que han volcado en mí, ya que su comportamiento es más cercano al de un familiar que cuida de ti y te intenta guiar por el camino correcto a pesar de mi elevada tozudez (característica de buen aragonés), mis frecuentes despistes y olvidos o mis inquietudes. Al final, creo que pueden estar orgullosos, ya que hacen una gran labor, pues han conseguido que YO esté donde estoy ahora mismo. Finalmente, me gustaría agradecer a todos los amigos y amigas que me han apoyado, me han hecho formar parte de sus vidas y me han hecho tal y como soy, pues yo soy yo y mis circunstancias.

ACKNOWLEDGEMENTS

A pesar de que se supone que estas palabras son de agradecimiento, no puedo evitar pedir perdón a todas aquellas personas que, debido a la alta dedicación que una tesis conlleva, han visto menguada mi atención hacia ellos, bien sea por comunicarme menos, verlos menos o prestarles menos ayuda de la que a lo mejor podría esperar de mí.

Finalmente, agradezco a todas estas personas el haber hecho quien soy, el haber imbuido en mí millones de recuerdos, los cuales nos determinan como las personas que somos. Por eso quiero animar a todos a que se aferren a los recuerdos, que los valoren por lo que son y por lo que significan, que recuerden a las personas que han sido importantes pues aunque se perdiesen nuestros recuerdos, siempre viviremos tal y como somos en los recuerdos de los demás.

A todos vosotros, GRACIAS.

GLOSSARY OF FIGURES	vi-xi
GLOSSARY OF ABBREVIATIONS	xiii-xiv
GLOSSARY OF GENES	xv-xix
INTRODUCTION	1-43
1. Regeneration and homeostasis	2-5
2. Planarian as a model system: <i>Schmidtea mediterranea</i>	5-18
2.1. Nervous system	7-8
2.2. Digestive system	9
2.3. Excretory system	10
2.4. Reproductive system	10-11
2.5. Parenchyma tissue	11
2.6. Epidermal tissue	11-12
2.7. Muscular tissue	12-14
2.8. Neoblast	14-18
3. Mechanisms required for proper regeneration and tissue turn over.	19-42
3.1. Control of cell number: balance between proliferation and apoptosis	19-28
3.1.1. Jun-N-terminal kinase: a mayor regulator of proliferation and apoptosis	23-25
3.1.2. Krüppel like factors (KLF): Their role regulating proliferation and apoptosis.	26-28
3.2. Stem cell specification	28-33
3.2.1. Nuclear Factor Y: a transcriptional complex	31-33

INDEX

required for proper cell specification.	
3.3. Positional instructions	33-43
3.3.1 Planarian AP axis establishment:	35-37
3.3.2. Planarian DV axis establishment:	37-39
3.3.3. Planarian ML establishment:	39-42
3.3.3.1. Midline and CNS establishment	40-42
OBJECTIVES	45-47
RESULTS	49-102
4. CHAPTER I: Nuclear Factor Y complex controls neoblast differentiation avoiding the proper regeneration and homeostasis.	53-63
4.1. The Nuclear Factor Y elements were found in a Digital Gene Expression Analysis	53-54
4.2. Protein structure of NF-Y elements	54-55
4.3. Expression of <i>nf-y</i> subunits in planarian	55-57
4.4. Functional analysis of <i>nf-y</i> subunits in planarian	58-63
5. CHAPTER II: Krüppel-like Factor 10/11 controls the onset of mitosis in planarian stem cells and triggers apoptotic cell death required for regeneration and remodelling.	65-78
5.1. Expression pattern of planarian klf members	67-69
5.2. Functional characterisation of the planarian Klfs	70-78
5.2.1. Functional analysis of <i>Smed-klf10/11</i>	70-76
5.2.1.1 Klf10/11 attenuates the progression of the cell cycle	71-74
5.2.1.2 Klf10/11 triggers the apoptosis required	75-76

for proper remodelling	
5.2.2. Klf10/11 has putative AP-1 binding sites	77-78
6. Chapter III: WNT5-ROR2 and SLIT-ROBO-c signals generate a mutually dependent system to position the CNS along the medio-lateral axis in planarians	79-102
6.1. Wnt5 acts as a repellent for neuronal growth	81-84
6.2. WNT5 and SLIT act through ROR and ROBO-c receptors, respectively, to guide neuron positioning	84-88
6.2.1. <i>Ror</i> and <i>Robo-c</i> are co-expressed in neuronal cells	87-88
6.3. <i>Ror</i> and <i>Robo-c</i> are expressed in muscular cells that express <i>slit</i> and <i>wnt5</i> , respectively.	89-92
6.4. Wnt5-Ror/Slit-Robo-c signalling systems could act as a self-regulatory system to define their respective expression domains	93-102
6.4.1. Modeling of the Wnt5-Ror/Slit-Robo-c signalling system	93-94
6.4.2. The boundary of expression between <i>Wnt5</i> and <i>Slit</i> is not defined at early regeneration stages	94-95
6.4.3. WNT5-ROR and SLIT-ROBO-c regulation occurs by transcriptional changes	96-97
6.4.4. Wnt5 is required to establish the <i>slit</i> expression domain	97-99
6.4.5. An ectopic source of WNT5 in the <i>slit</i> expression domain locally inhibits <i>slit</i> expression	100-102

INDEX

DISCUSSION	103-136
7. Nuclear Factor Y complex controls neoblast differentiation interfering regeneration and homeostasis	107-113
7.1. The NF-Y heterotrimeric complex is required to drive target gene expression in planarians	109-110
7.2. Duplication and functional specialisation of NF-Yb	108-109
7.3. Function of NF-Y in <i>Schmidtea mediterranea</i>	111-113
8. Krüppel-like Factor 10/11 controls the onset of mitosis in planarian stem cells and triggers apoptotic cell death required for regeneration and remodelling	115-121
8.1. klf10/11 controls the onset of mitosis and triggers the apoptosis required for regeneration and remodelling possibly as a JNK target	117-121
9. WNT5-ROR2 and SLIT-ROBO-c signals generate a mutually dependent system to position the CNS along the medio-lateral axis in planarians	125-136
9.1. Wnt5/Ror and Slit/Robo-c generate a mutually dependent system	127-130
9.2. Mechanism through which Wnt5 and Slit position the CNS	130-133
9.3. The Wnt5/Slit system controls the M-L position of all tissues	133-134
9.4. Was the Wnt5/Slit system controlling the number of longitudinal nerve cords along evolution?	135-136
10. General discussion	137-140

CONCLUSIONS	141-144
MATERIALS AND METHODS	145-152
ANNEXES	153-191
Annex I: Digital gene expression approach over multiple RNA-Seq data sets to detect neoblast transcriptional changes in <i>Schmidtea mediterranea</i> . Rodríguez-Esteban, Gustavo; González-Sastre, Alejandro; Rojo-Laguna, José Ignacio; Saló, Emili; Abril, Josep F. BMC Genomics. 2015.	155-179
Annex II: Alignment of planarian NF-Y with different species.	181-184
Annex III: Alignment of planarian NF-Y with different planarian species.	185-187
Annex IV: Expression levels of neural genes after <i>wnt5</i> and <i>slit</i> RNAi. <i>Ovo+</i> cells positioning is affected after <i>wnt5</i> and <i>slit</i> RNAi.	189-191
BIBLIOGRAFY	193-211

GLOSSARY OF FIGURES

Figure	Page
Figure 1: Phylogenetic tree showing the animal phyla that contain species with high regenerative potential, either as larvae or as adult.	1
Figure 2: Schematic view of cell turnover process.	3
Figure 3: Overview of differentiation, transdifferentiation and dedifferentiation.	4
Figure 4: In vivo images of <i>Schmidtea mediterranea</i> .	6
Figure 5: Planarian Central Nervous System.	8
Figure 6: Planarian digestive system.	9
Figure 7: Planarian excretory system.	10
Figure 8: Generalized reproductive system in the sexual planarian.	11
Figure 9: Photomicrograph of a longitudinal section through epidermis	12
Figure 10: Immunostaining showing different types of muscular fibers in planarian.	13
Figure 11: PCG expression in muscle specifies the identity of new cell types made in tissue turnover.	14
Figure 12: Planarian Neoblasts.	14
Figure 13: Fluorescence-activated cell sorting (FACS) profiles of	16

FIGURE GLOSSARY

cells derived from non-irradiated and X-ray-irradiated adult planarians.

Figure 14: Schematic view of the two main theories about the generation of differentiated cells from neoblasts. 17

Figure 15: Model of planarian stem cell hierarchies. 18

Figure 16: Mitotic and apoptotic dynamics during planarian regeneration. 21

Figure 17: Proliferative and apoptotic response during growth and degrowth. 22

Figure 18: JNK pathway described in drosophila. 24

Figure 19: Schematic showing role of JNK in planarian regeneration and homeostatic degrowth. 25

Figure 20: Structural properties of vertebrate Sp1-like/KLF proteins. 26-27

Figure 21: KLF family members in the cell cycle control. 28

Figure 22: Overview of cell specification in planarian. 30

Figure 23: NF-Y complex 32

Figure 24: Schematic view of the three main body axes in planarian. 33

Figure 25: Canonical and non-canonical Wnt signalling pathways. 36

Figure 26: β CATENIN-1 displays a gradient from the 37

prepharyngeal region to the tail.

Figure 27: BMP signaling in the control of the DV axis.	39
Figure 28: Wnt5 and Slit are involved in medio-lateral organization in planarian.	42
Figure 29: X1, X2 and Xin DGE expression levels of the three subunits of nuclear factor Y.	52
Figure 30: Two different NF-YB proteins in planarian.	53
FIGURE 31: <i>nf-y</i> subunits are expressed in neoblasts.	54
Figure 32: <i>Nf-y's</i> are expressed in neoblast.	55
Figure 33: <i>nf-y</i> RNAi planarian generate regeneration defects.	57
Figure 34: Phenotype observed after the injection of different combined dsRNA of <i>nf-YA</i> , <i>nf-YB2</i> and <i>nf-YC</i> during regeneration.	58
Figure 35: NF-Y inhibition affects neoblasts.	59
Figure 36: NF-Y produces a reduction of differentiated cells.	60
Figure 37: Expression pattern of the different planarian <i>klfs</i> .	68
Figure 38: Dynamic expression of <i>klfs</i> during regeneration.	69
Figure 39: <i>KLF10/11</i> inhibition accelerates regeneration.	71
Figure 40: <i>klf10/11</i> is expressed in neoblasts.	72
Figure 41: Mitotic dynamics during regeneration after <i>Smed-klf10/11</i> RNAi.	74

FIGURE GLOSSARY

Figure 42: <i>Smed-klf10/11 RNAi</i> animals are not able to remodel.	76
Figure 43: <i>Klf10/11</i> present putative AP-1 binding sites.	78
Figure 44: <i>Wnt5</i> and <i>Slit</i> have complementary expression domains and affects the CNS positioning.	82
Figure 45: rWNT5a rescues <i>wnt5</i> RNAi phenotype	84
Figure 46: ROR and ROBO-c are the <i>Wnt5</i> and <i>Slit</i> receptors.	86
Figure 47: <i>Ror</i> and <i>robo-c</i> are expressed in the CNS.	88
Figure 48: <i>ror/slit</i> and <i>robo-c/wnt5</i> co-localize in muscular cells.	90
Figure 49: <i>Wnt5</i> and <i>slit</i> are not expressed in glia cells.	91
Figure 50: Schematic representation of the results observed with respect to <i>Wnt5-Ror/Slit-Robo-c</i> .	92
Figure 51: Topology Network of the <i>Wnt5-Ror</i> and <i>Slit-Robo-c</i> system.	94
Figure 52: The boundary of expression between <i>Wnt5</i> and <i>Slit</i> is not defined at early regeneration stages.	95
Figure 53: WNT5-ROR and SLIT-ROBO-c regulation occurs by transcriptional changes.	97
Figure 54: Dependence of <i>Slit</i> expression on <i>wnt5</i> expression.	99
Figure 55: Injection of rWNT5a in the <i>slit</i> expression domain locally inhibits <i>slit</i> expression.	101

Figure 56: Planarian model for NF-Y regulation.	113
Figure 57: Possible location of Klf10/11 downstream Jnk in the planarian JNK pathway.	121
Figure 58: Wnt5 and Slit generate a mutually depend system to position the CNS.	129-130
Figure 59: Wnt5 and Slit position other tissues/structures with M-L organization.	134
Figure 60: Comparison between the acoel <i>S. Roscoffensis</i> and <i>slit</i> RNAi planarian.	136
Figure 61: Schematic representation of dsRNA injection experiments.	148

GLOSSARY OF ABBREVIATIONS

A-P	antero-posterior
APC	Adenomatosis Polyposis Coli Tumor Suppressor
ASC	Adult Stem Cell
BrdU	Bromodeoxyuridine
<i>C. elegans</i>	<i>Caenorhabditis elegans</i>
Cat1	Category 1
Cat2	Category 2
Cat3	Category 3
cm	Centimeter
c-neoblast	Clonogenic Neoblast
CNS	Central Nervous System
DBD	DNA binding domains
DGE	Digital Gene Expression
DNA	Deoxyribonucleic acid
dr	Days of regeneration
dsRNA	double strand RNA
D-V	dorso-ventral
FACS	Fluorescent Activated Cell Shorting
FISH	Fluorescent In Situ Hybridization
hr	Hours of regeneration
M-L	medio-lateral
mm	milimeter
NLS	nuclear localization signal
PCG	Positional Control Gene
PCR	Polymerase Chain Reaction

ABBREVIATION GLOSSARY

qPCRs	quantitative PCRs
RNAi	Ribonucleic Acid interference
RT-PCR	Real Time- PCR
rWNT5a	Recombinant WNT5a protein
SC	Single Cell
scRNAseq	single cell RNA sequencing
SID	Sin3 interaction domain
Smed	Schmidtea mediterranea
VNC	Ventral Nerve Cord
pVNC	preexisting Vental Nerve Cord
WISH	Whole Mount In Situ Hybridization
Xin	X insensitive
γ -neoblasts	gamma neoblast
ζ -neoblast	zeta neoblast
vNeoblasts	nu-neoblasts
σ -neoblast	sigma neoblast
wt	Wild Type
d.a.i.	Days after irradiation
CHAPS	3-[(3- Cholamidopropyl) dimethylammonio]-1-propanesulfonate
+ cells	possitive cells

GLOSSARY OF GENES

Gene	Description
ADMP	Antidorsalizing Morphogenetic Protein. It is a TGF- β homolog expressed in the Spemann organizer.
AGAT-1	Planarian gene expressed in late epidermal progeny.
AP-1	Activator Protein 1. It is a transcription factor that regulates gene expression in response to a variety of stimuli, including cytokines, growth factors, stress, and bacterial and viral infections.
Arrestin	Small family of proteins important for regulating signal transduction at G protein-coupled receptors.
BCL-2	B-Cell CLL/Lymphoma 2. Member of the Bcl-2 family of regulator proteins that regulate cell death (apoptosis), by either inducing (pro-apoptotic) or inhibiting (anti-apoptotic) apoptosis.
BMP	Bone Morphogenetic Protein. BMPs are considered to constitute a group of pivotal morphogenetic signals, orchestrating tissue architecture throughout the body.
bmp4	Bone morphogenetic protein 4. Part of the transforming growth factor-beta superfamily which includes large families of growth and differentiation factors.
Btd	Buttonhead. It is a transcriptional activator related to vertebrate Sp1.
Cabut	Drosophila's name for klf10/11. Transcription factor member of the KLF family.
cavii-1	Carbonic Anhydrase-1. Zinc metalloenzymes that catalyze the reversible hydration of carbon dioxide.
CBF	Core-Binding Factor. Pseudonym for NF-Y.
CDKs	Cyclin-dependent kinases.
Derailed	Drosophila's name for Ryk. Member of the family of growth factor receptor protein tyrosine kinases.
dMKK4	MAP kinase kinase
dpp	Decapentaplegic, homolog to the vertebrate's BMP.
E2F	Also known as Retinoblastoma-Associated Protein 1. Key

GENE GLOSSARY

	regulator of entry into cell division that acts as a tumor suppressor.
egr-1	Early growth response protein 1 is a transcription factor with zinc finger domains.
elav-2	Embryonic Lethal, Abnormal Vision 2. Stabilize several cellular mRNAs by binding to AU-rich elements in the 3' untranslated region of the mRNA.
ERK	extracellular signal–regulated kinases
FAS-L	type-II transmembrane protein that belongs to the tumor necrosis factor family
Fos	Fos Proto-Oncogene, AP-1 Transcription Factor Subunit.
Frizzled	Family of G protein-coupled receptor proteins.
gata4/5/6	GATA transcription factors are a family of transcription factors characterized by their ability to bind to the DNA sequence "GATA"
gfp	Green fluorescent protein.
gpas	G protein alpha subunit. Membrane-associated, heterotrimeric proteins composed of three subunits
h2b	Histone 2b. Involved in the structure of chromatin in eukaryotic cells.
H3P	Histone-3-phosphorylated. Histone H3 is specifically phosphorylated during both mitosis and meiosis in patterns that are specifically coordinated in both space and time.
HAP2/3/4/5	Heme-activated protein2/3/4/5. Yeast name for NF-Y.
hnf4	Hepatocyte Nuclear Factor 4 is a nuclear receptor protein.
IAP1	Inhibitor of apoptosis protein 1.
if	Intermediate filament. In planarian two intermediate filament genes has been published with the same name. One is expressed in the DV margin and the second is expressed in glial cells.
JNKK	Jun-N-terminal kinase kinase
JNKs	Jun-N-terminal kinases
Jun	Jun Proto-Oncogene, AP-1 Transcription Factor Subunit

KLF	Krüppel like factors. Family of transcription factors with three tandem zinc finger domains.
MAPKs	Mitogen-Activated Protein Kinases
msi-1	RNA-binding protein Musashi homolog. Protein containing two conserved tandem RNA recognition motifs.
MYC	V-Myc Avian Myelocytomatosis Viral Oncogene Homolog. The protein encoded by this gene is a multifunctional, nuclear phosphoprotein that plays a role in cell cycle progression, apoptosis and cellular transformation.
NB.21.11e	Planarian gene expressed in early epidermal progeny
NF-Y	Nuclear Factor-Y
nkx2.2	Homeobox protein involved in the morphogenesis of the CNS.
nlg4	Neurologin 4 is a synaptic adhesion molecule involved in synapse formation and synaptic transmission.
nlg7	Noggin-like 7. Inhibitor of bone morphogenetic proteins (BMP) signaling.
nog1	Noggin-1. Inhibitor of bone morphogenetic proteins (BMP) signaling.
Noggin	Secreted polypeptide which binds and inactivates members of the TGF-beta superfamily signaling proteins.
notum	Palmitoleoyl-Protein Carboxylesterase. Acts as a key negative regulator of the Wnt signaling pathway by specifically mediating depalmitoylation of WNT proteins.
ovo	Transcription factor involved in planarian eye maintenance and differentiation.
p53	Tumor suppressor protein.
<i>pc2</i>	Proprotein convertase 2 (PC2) also known as prohormone convertase 2 or neuroendocrine convertase 2 (NEC2) is a serine protease, an enzyme responsible for the first step in the maturation of many neuroendocrine peptides from their precursors.
Piwi-1	P-element Induced WImpy testis. Class of genes originally identified as encoding regulatory proteins responsible for maintaining incomplete differentiation in stem cells and maintaining the stability of cell division rates in germ line cells.

GENE GLOSSARY

Piwi-2	P-element Induced Wimpy testis. Class of genes originally identified as encoding regulatory proteins responsible for maintaining incomplete differentiation in stem cells and maintaining the stability of cell division rates in germ line cells.
pk1	Pantothenate kinase is the first enzyme in the Coenzyme A (CoA) biosynthetic pathway.
prog-1	Aliase for NB.21.11e.
Prog-2	Aliase for NB.32.1g.
ptprd-9	Receptor-type tyrosine-protein phosphatase delta is an enzyme which suggested role is to promote neurite growth, and regulating neurons axon guidance.
PVALS/T	Motif which is known to interact with co-repressors of the C-terminal binding protein (CtBP) family.
ROBO	Roundabout. Family of proteins which are single-pass transmembrane receptors that are highly conserved across many branches of the animal kingdom.
ROR2	Receptor Tyrosine Kinase Like Orphan Receptor 2. Belongs to the family of tyrosine kinase receptors that are important in regulating skeletal and neuronal development, cell migration and cell polarity. ROR proteins can modulate Wnt signaling by sequestering Wnt ligands.
Ryk	Receptor-Like Tyrosine Kinase. This protein is involved in stimulating Wnt signaling pathways such as the regulation of axon pathfinding.
sfrp	Secreted frizzled-related protein 1. Contains a cysteine-rich domain homologous to the putative Wnt-binding site of Frizzled proteins.
Sin3	Component of both the Rpd3S and Rpd3L histone deacetylase complexes.
Slit	Family of secreted extracellular matrix proteins which play an important signalling role in the neural development of most bilaterians.
sog	Short Gastrulation gene. Homolog to the vertebrate chordin, related to BMP signaling.
soxp1	Transcription factor that bind to the minor groove in DNA, and belong to a super-family of genes characterized by HMG-

	box.
soxp2	Transcription factor that bind to the minor groove in DNA, and belong to a super-family of genes characterized by HMG-box.
soxp3	Transcription factor that bind to the minor groove in DNA, and belong to a super-family of genes characterized by HMG-box.
SP	Specificity proteins. Famnily of transcription factors closely related to KLF family.
ston-2	Stonin-2. Membrane protein involved in regulating endocytotic complexes
Synapsin	Family of proteins that have long been implicated in the regulation of neurotransmitter release at synapses.
tbx-2	T-box gene which encode a transcription factors involved in the regulation of developmental processes.
TCF/LEF	Transcription factors which bind to DNA through a high mobility group domain.
TGF β	Transforming growth factor beta.
TNF-a	Tumor necrosis factor alpha.
tolloid	Encodes an astacin-like zinc-dependent metalloprotease and is a subfamily member of the metzincin family.
TRAIL	TNF-related apoptosis-inducing ligand.
tropomyosin	Tropomyosin is a two-stranded alpha-helical coiled coil protein found in cell cytoskeletons.
ura4	Orotidine 5'-phosphate decarboxylase. This protein is involved in pathway that synthesizes UMP, which is itself part of Pyrimidine metabolism.
Wnts	Large family of secreted glycoproteins that are cysteine-rich and highly hydrophobic.
zfp1	Zinc Finger Protein 1.
α -Tubulin	Belong to the tubulin protein superfamily. α - and β -tubulins polymerize into microtubules.
β -catenin	Subunit of the cadherin protein complex and acts as an intracellular signal transducer in the Wnt signaling pathway.

INTRODUCTION

The question of how organs and tissues have the ability to restore tissue lost after damage or during the normal ageing process is an old question that has kept researchers from many disciplines active for decades. One of the most used strategies to approach this question is to study the organisms that have the ability to regenerate either some tissues or cell types or by regenerating the whole body. The use of a wide variability of organisms to study regeneration has demonstrated that this ability is highly extended through the animal kingdom (Figure 1).

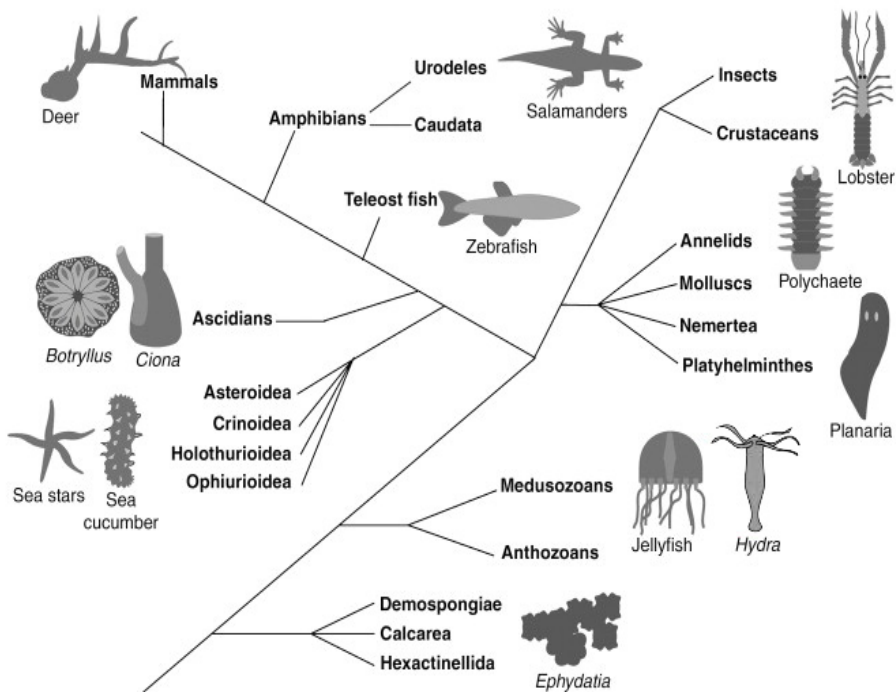


Figure 1: Phylogenetic tree showing the animal phyla that contain species with high regenerative potential, either as larvae or as adult. Modified from (Galliot & Ghila 2010).

INTRODUCTION

However, not all the organisms have the same abilities to regenerate. While some organisms show reduced regenerative ability, like mammals, others are able to fully regenerate a complete organism from a small portion of the body, like hydra or planarian, passing through organisms with specific regenerative abilities, like zebrafish, which regenerate heart, fins, retina, etc.

1. Regeneration and homeostasis

A wide range of diverse biological processes contribute to the maintenance of the anatomical form and functionality in an adult animal. For the correct maintenance of an adult structure it is necessary a continuous cell renewal to replace all the aged or damaged cells. In most metazoan, the main strategy to protect adult tissue from physiological problems is the elimination and replacement of the damaged cells. This process is called cell turn over (Galliot & Ghila 2010). The adult stem cells are the main players in this process in which they divide and differentiate in order to replace the eliminated cells. Therefore, for the correct cell turn over three main processes are required: Cell death, proliferation and differentiation (**Figure 2**).

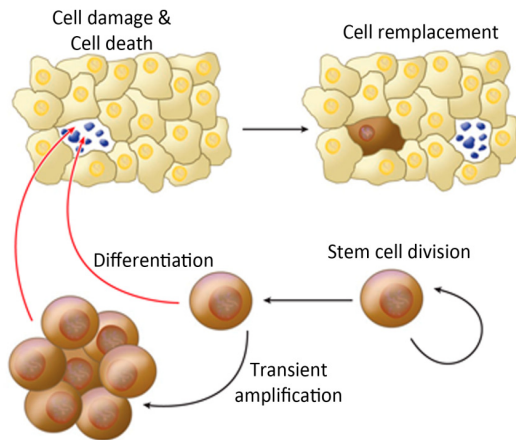


Figure 2: Schematic view of cell turnover process. Stem cells are amplified to generate the amount of cells required to replace the dead cells and differentiate into the correct cell type. Modified from (Pellettieri & Alvarado 2007).

Similar to cell turn over, the regenerative process also consist on the replacement of cells but after tissue lost. There are multiple possible means by which injured tissues could provide new cells for regeneration (**Figure 3**). First, new cell types could be produced by resident stem cells, which differentiate into one or several cell types as occurs in hydra regeneration (Galliot 2013). These stem cells can divide or not depending on the regenerative requirements. Second, new cells could be produced through dedifferentiation, which means a loss of the differentiated character of a cell type to produce a dividing cell that acts as a progenitor cell. This is the case of zebrafish heart regeneration, in which cardiomyocytes dedifferentiate and became the regenerative source cells (Jopling et al. 2010; Jopling et al. 2011). Additionally, differentiated cells could divide to produce more cells such as during liver regeneration. Finally, new cell types could arise as a result of transdifferentiation which could happen without cell division, or via a progenitor cell produced by dedifferentiation (Selman & Kafatos 1974; Jopling et al. 2011).

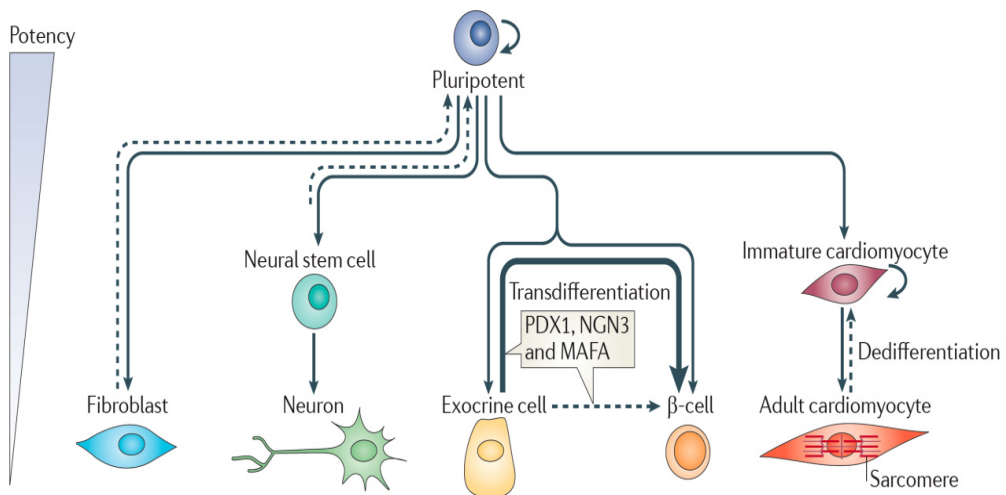


Figure 3: Overview of differentiation, transdifferentiation and dedifferentiation. Pluripotent cells are capable of differentiating (solid arrows) down any given lineage to give rise to a range of different cell types. During transdifferentiation, cells switch lineages to create another cell type. For example, pancreatic exocrine cells can be induced to transdifferentiate into β -cells by expressing the transcription factors pancreas and duodenum homeobox 1 (PDX1), neurogenin 3 (NGN3) and MAFA. It is unclear how exocrine cells transdifferentiate into β -cells. This may occur either directly (dashed arrow) or it could involve a dedifferentiation step (bold arrow). Dedifferentiation refers to a regression of a mature cell within its own lineage, which, in many cases, allows it to proliferate (curved arrow). Mature zebrafish cardiomyocytes proliferate during heart regeneration. This involves a dedifferentiation step (dashed arrow) that may facilitate this process. Modified from (Jopling et al. 2011)

In every regenerative process it is required the generation of cells that substitute the missing ones. To generate this situation, as in the case of the cell turn over, it is essential cell death to remove preexisting cells and re-pattern the tissue, proliferation to generate new cells and differentiation or cell specification to produce the correct cell types. Therefore, both regeneration and cell turnover can be seen to follow similar mechanism. In addition to these main processes, positional instruction plays an essential role, thus every single cell has to be placed in the correct position to finally form a complete and functional tissue or organ.

In this Thesis, some aspects of each described process have been studied; therefore the manuscript is divided in three main chapters corresponding to cell specification or differentiation, apoptosis/proliferation and positional information. Before going through the three processes, I will describe the animal model used in this Thesis.

2. Planarian as a model system: *Schmidtea mediterranea*

We use the planarian *Schmidtea mediterranea* as a model system to go further in the comprehension of the regeneration and the tissue turnover. *Schmidtea mediterranea* is a free living fresh water planarian which can be found living in European lakes and rivers; however there are also sea and land planarian species. These animals are relative small, with length varying between 1mm to 2cm (**Figure 4A**). Planarians are triploblastic acoelomate bilaterians that belong to the Tricladida order. This means that they possess cells types coming from the three main embryonic layers (ectoderm, mesoderm and endoderm), they present bilateral symmetry and have a blind digestive system composed by three main gut branches, one anterior and two posterior. The intake and outtake of food is through an evaginated organ called pharynx (**Figure 4B**) which is opened to the exterior by the mouth and connects to the gut through the esophagus in the three gut branches crossing.

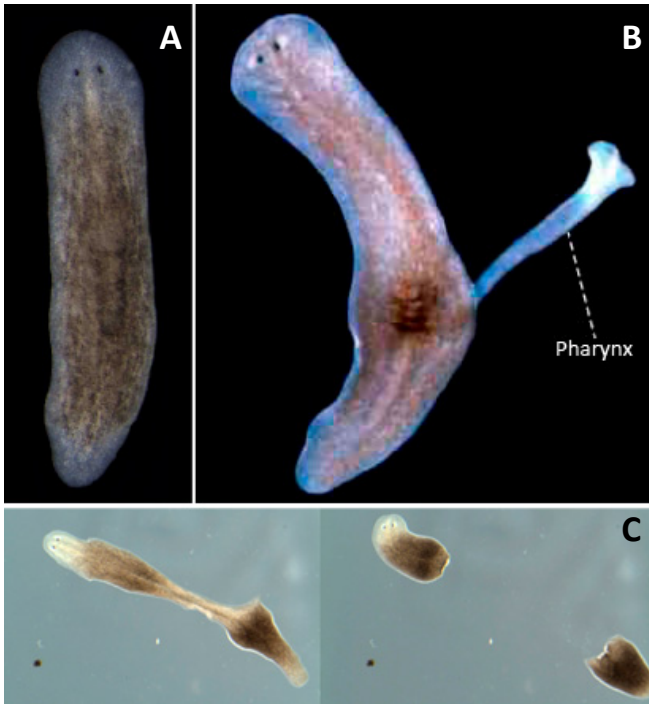


Figure 4: In vivo images of *Schmidtea mediterranea*. (A) Eyes are dorsally located in the most anterior part (head). (B) Pharynx evaginates from ventral side to food intake. Modified from (McDonald & Rossant 2014). (C) Planarian asexual reproduction. Modified from Francesc Cebria lab webpage).

Schmidtea mediterranea is composed by two different strains, sexual and asexual. The sexual strain is reproduced by laying cocoons. These individuals are hermaphrodites presenting ovaries and testis in the same organism when they arrive to their sexual maturity; they reproduce by cross fertilisation laying cocoons. On the other hand, the asexual strain reproduces by fission, where the tail of the planarian is usually attached to a surface and stretches until the tail fragment is separated from the rest of the organism (Figure 4C). After that, planarian regenerates the tail lost while the tail piece regenerates all the missing structures to form a new complete organism. The asexual strain of *Schmidtea mediterranea* studied here is a clonal line generated from one single organism coming from the Montjuic's Fountain.

2.1. Nervous system

Planarians have a centralised nervous system ventrally disposed composed by two cephalic ganglia in anterior which connects with two ventral nerve cords (**Figure 5**). The Central Nervous System (CNS) of this animal can suggest simplicity; however, molecular and morphological studies reveal the existence of unipolar, bipolar and multipolar neurones, which secrete evolutionary conserved neuroactive substances such as serotonin, dopamine, noradrenaline and a variety of neuropeptides (Cebrià 2007)(Mittal et al. 2016). Latest publications have demonstrated for the first time the presence of glia cells, which are involved in the CNS regeneration and maintenance.

The brain or cephalic ganglia is organized in two bilaterally symmetric lobules which are connected through an anterior commissure. The brain is organized as a central neuropil surrounded by the neuronal cell bodies (**Figure 5**). The brain projects neural connections towards the margins to process the signals coming from the different sensory cells distributed along the head. The planarian brain is dorsally located in respect to the ventral nerve cords (VNC) which are considered as different structures. The VNCs are projected along the anterior-posterior axis clustered in small groups of cells.

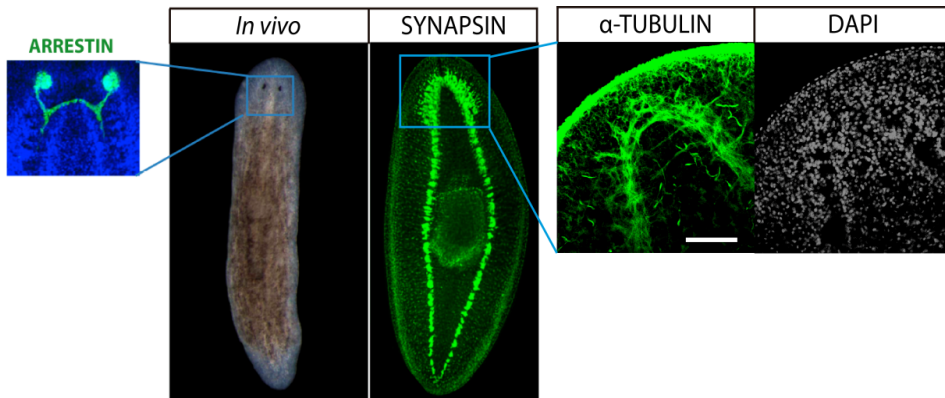


Figure 5: Planarian Central Nervous System. SYNAPSIN labelling shows the CNS: the cephalic ganglia and the ventral nerve cords. ARRESTIN antibody labels the photoreceptors (eyes) and the optic chiasm. TUBULLIN labelling shows the axons while DAPI labels the cell nuclei.

The visual system is in the anterior part, composed by two eyes, which contain photoreceptor and pigment cells. Photoreceptor cells project ipsilateral and contralateral axons towards the brain to form the optic chiasm (**Figure 5**). This visual system allows planarians to sense the light exerting their typical photophobic behavior (Okamoto et al. 2005). The new molecular tools and the presence of genes specifically expressed in the different eye cell populations have allowed a deep characterisation of this system.

In addition to the CNS and the visual system, planarians have different peripheral nervous plexus: the subepidermal, the submuscular, the gastrodermal and the pharynx plexus. Some innervations have been also observed crossing the parenchyma. This nerve net composed by these plexus is related with the control of muscular contractions, transduction of sensory organs information or gastrodermal movements (Baguña & Ballester 1978).

2.2. Digestive system

Planarians belong to Tricladida order, which means that they possess three main gut branches, one anterior and two posterior. These branches are subdivided into smaller structures (secondary, tertiary and quaternary branches) increasing the absorption surface of the gut (**Figure 6A**). The gut covers the whole body of the animals providing the nutrients to every tissue. The gastrodermis is organized into a unique columnar layer composed by two main cell types: the absorptive phagocytes which engulf the food through intracellular digestion and the goblet cells that secrete enzymes into the lumen to start the digestion of the biggest food pieces (**Figure 6B**). This intestinal epithelium or gastrodermis is surrounded by a basal lamina, enteric muscle and the gastrodermal plexus (Forsthoefel et al. 2011)(Baguña & Ballester 1978).

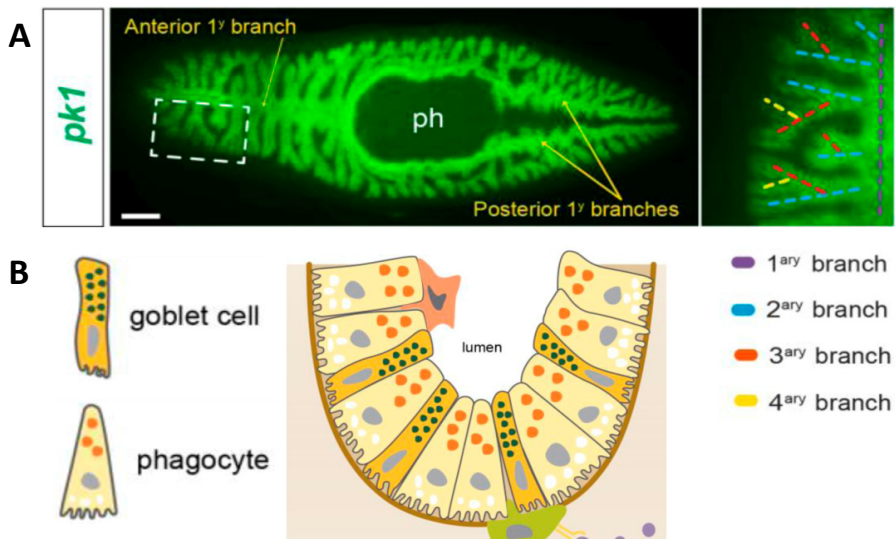


Figure 6: Planarian digestive system. (A) Planarian gut labelled by *pantotenate kinase* probe. Labelling shows the organization of the gut in a single anterior branch and two posterior and symmetrical branches. Main branches are also subdivided in secondary, tertiary and quaternary branches. (B) Schematic view of gut at cellular level. Phagocytes and goblet cells are organised in single layers. Images modified from (Barberán et al. 2016).

2.3. Excretory system

The planarian excretory system is involved in waste excretion and osmoregulation. It consists of groups of protonephridia located along the body. It is formed by epithelial blind tubules ending in a terminal cell which expulse the wastes to the exterior (Figure 7) (Rink et al. 2011).

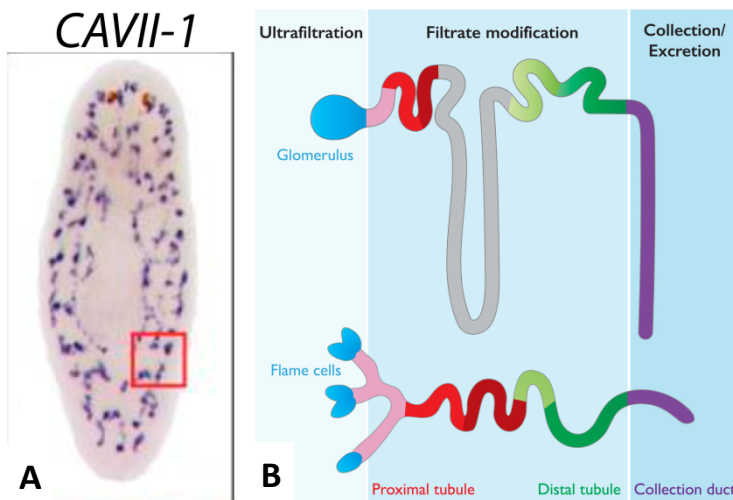


Figure 7: Planarian excretory system. (A) Protonephridial system distribution in planarian. Excretory system is labelled by *cavii-1* probe. Modified from Rink 2011. (B) Schematic view of the excretory system in planarian. Modified from (Rink et al. 2011)(Issigonis & Newmark 2015).

2.4. Reproductive system

The sexual strain of *Schmidtea mediterranea* is the only one which posses a mature and complete reproductive system. The reproductive system is formed by testis distributed in two stripes located dorsally and laterally, the ovaries which are positioned posterior to the brain and the vitelline glands placed similarly to the testis (Figure 8). Asexual planarians do not show mature reproductive organs; however, it has been shown that this strain also has germ stem cells, which in the

end are not able to differentiate to form the mature reproductive system (Wang et al. 2007).

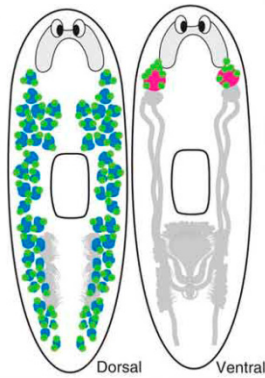


Figure 8: Generalized reproductive system in the sexual planarian. Left, testes (blue) are located dorsolaterally. Right, ovaries (pink) are located more ventrally at base of the brain. *nanos*-positive germline stem cells of the testes and ovaries (green). Accessory reproductive structures (grey). Modified from (Chong et al. 2013).

2.5. Parenchyma tissue

The parenchyma is the connective tissue which is located between the epidermis and the internal organs (RM. Rieger, S. Tyler, JPS. Smith 1991). It is mainly composed by the chromatophor cells, secretory cells and neoblast (Baguña & Romero 1981); however, the exact cell composition of this tissue is not well characterised.

2.6. Epidermal tissue

The planarian epidermis consists on a monostratified tissue with relative simple organization of multi-ciliated and non-ciliated cell types (**Figure 9**) (Baguña & Romero 1981)). As in most organisms, this tissue shows a high rate of cell renewal, since it is the most exposed tissue of the organism, which means that

INTRODUCTION

planarian stem cells have to continuously proliferate and differentiate to generate all epidermal turn over.

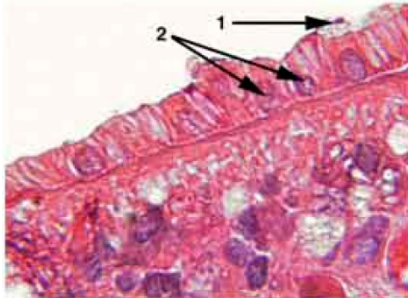


Figure 9: Photomicrograph of a longitudinal section through epidermis, showing cilia (1) and rhabdites (2). Obtained from <http://mlitvaitis.unh.edu/K-12Primer/shapesandsizes.htm>

2.7. Muscular tissue

Planarians have different layers of subepidermal muscle fibers which act as a structural skeleton. The planarian muscle is not usually used for locomotion which is due to ventral cilia, although it allows the control of movement direction. The body-wall muscle is organized in four different layers of fibers: circular, longitudinal, diagonal and again longitudinal (from exterior to interior) (**Figure 10**). In addition, another set of fibers connect dorsal and ventral body surfaces (Cebrià et al. 1997)(Francesc Cebria 2000). On the other hand, the pharynx or the gut also has a muscular plexus associated, which allows their movement to take the nutrients during evagination. Planarian muscle cells are mononucleated, like the vertebrate smooth muscle; however, phylogenetic analyses indicate that they are more similar to striated muscle. Therefore, the planarians muscle exhibits several ambiguities (Agata et al. 1998)(Francesc Cebria 2000).

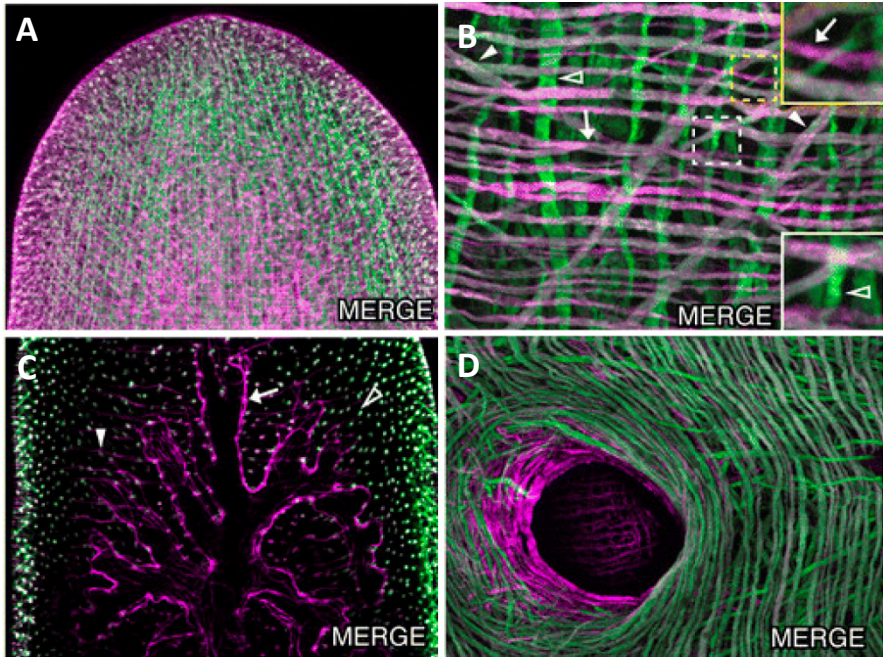


Figure 10: Immunostaining showing different types of muscular fibers in planarian. (A) Muscular labelling in the head region of the planarian. (B) Circular, longitudinal, and diagonal fibers in the body wall musculature. (C) Labelling of anterior intestinal branches where the intestinal musculature is observed in purple. (D) Labelling of circular muscle fibers of the body wall, mouth and the pharynx. Figure modified from (Ross et al. 2015).

In addition, it has been shown that the planarian muscle also takes other roles. Thus, muscle contraction is essential to close the wound during planarian regeneration (Cebrià et al. 1997)(CHANDEBOIS 1980). Recently, body-wall muscle cells have been shown to be responsible to provide the coordinates and positional information through the expression of positional control genes (PCG). The PCGs have been defined as genes that display regionalized expression along one or more body axis and either show a patterning-abnormal RNAi phenotype or encode a protein that is predicted to regulate important pathways for planarian patterning (**Figure 11**) (Reddien 2011)(Witchley et al. 2013).

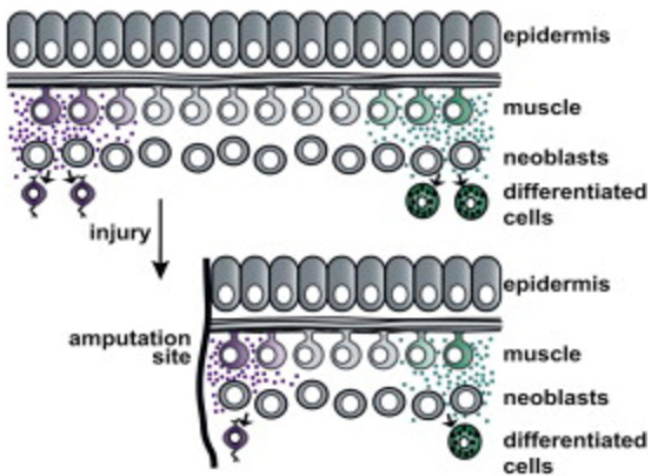


Figure 11: PCG expression in muscle specifies the identity of new cell types made in tissue turnover. Following amputation, muscle cells change their PCG expression, and these changes dictate which type of new tissue is regenerated. Modified from (Witchley et al. 2013).

2.8. Neoblast

The amazing regenerative ability of planarians is due to the presence of an abundant population of pluripotent stem cells that proliferate and divide to develop all the missing structures. These stem cells are called neoblast (Baguna et al. 1989). Planarian neoblast are the only dividing somatic cells and they show a high nuclear/cytoplasmic ratio (Figure 12). Elevated doses of γ -irradiation

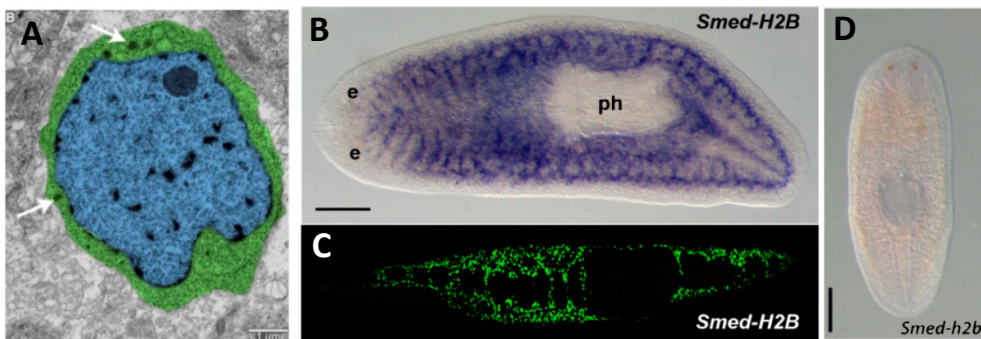


Figure 12: Planarian Neoblasts. (A) Transmission electron micrograph of a neoblast. Nucleus painted in blue and cytoplasm in green. Ribonucleoprotein complexes called chromatoid bodies pointed with arrows. Modified from (King & Newmark 2012). (B-C) Distribution of neoblast showed by *Smed-h2b* probe in intact and longitudinal section respectively. (D) Expression of *Smed-h2b* in lethally irradiated planarian. B-D Modified from (Solana et al. 2012)

specifically eliminate neoblast, as they are the only planarian cell types which go into mitosis. They are distributed along the body in the parenchyma but anterior to the photoreceptors and in the pharynx (**Figure 12**) (Forsthoefel et al. 2011)(Newmark & Sánchez Alvarado 2000).

Neoblasts have been subject of study for decades and several experiments have demonstrated that they are responsible for the regenerative potential of planarians. For example, the abolition of neoblast by γ -irradiation impairs regeneration and tissue turn over (Wolff et al. 1948)(Bardeen & Baetjer 1904). Other classical experiments have shown that injection of neoblasts could restore regenerative abilities and long-term viability to lethally irradiated planarians; Moreover, injection of neoblast derived from a sexual strain “transform” a lethally irradiated asexual planarian into sexual (Baguna et al. 1989). More recently, the new available tools allow the injection of a single neoblast into an irradiated planarian and restore the whole stem cell population. In this essay, the term clonogenic neoblast (c-neoblast) was coined, calling clonogenic to a neoblast which is able to repopulate the whole planarian (Wagner et al. 2011).

Studies using general mitotic markers like histone-3-phosphorilated (H3P) or Bromodeoxyuridine (BrdU) staining has been widely used to label and study neoblast divisions and dynamics (Newmark & Sánchez Alvarado 2000; Eisenhoffer et al. 2008; Wenemoser & Reddien 2010). In addition, the characteristic ratio nucleus/cytoplasm of neoblast allowed their extraction and purification through Fluorescent Activated Cell Shorting (FACS) (Hayashi et al. 2010). By this method, three main cell populations were identified corresponding to dividing neoblast (X1: proliferating stem cells, S/G2/M), differentiated cells

INTRODUCTION

(Xin: cells in G0/G1, cells not affected by the irradiation) and an undefined population (X2: a mix of stem cell progeny and proliferating, G0/G1) (Figure 13).

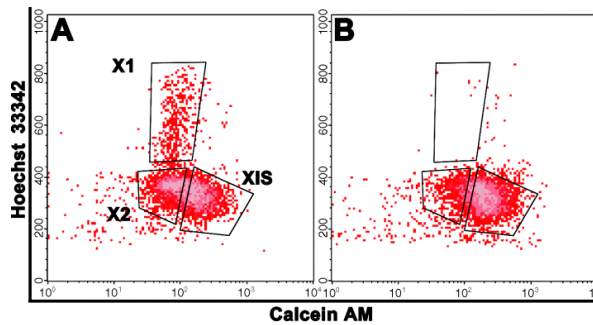


Figure 13: Fluorescence-activated cell sorting (FACS) profiles of cells derived from non-irradiated and X-ray-irradiated adult planarians. Representative FACS dot-plots obtained from dissociated control, non-irradiated (A) and 4 days past X-ray-irradiated (B) animals. Comparison of the profiles of panels (A) and (B) shows one region of high

calcein AM staining eliminated on X-ray-irradiation, which is thus absent in panel (B): this region corresponds to a population of cells designated X1. A second X-ray-sensitive region, with weak Hoechst 33342 and calcein AM staining, corresponds to a cell population designated X2. A large region separate from X1 and X2 and present on both plots (A) and (B) maps to an X-ray-insensitive fraction designated Xin. Figure from (Hayashi et al. 2006).

Both FACS and irradiation experiments allowed the design of transcriptomic studies to analyze the transcriptomic profile of neoblasts versus the other populations. These transcriptomic analysis allowed the identification of neoblast specific genes as members of the Piwi/Argonaute family (Reddien et al. 2005) or histone 2b (Solana et al. 2012) among others (Abril et al. 2010; Blythe et al. 2010; Labbé et al. 2012; Resch et al. 2012; Rouhana et al. 2012; Rodríguez-Esteban et al. 2015) providing genetic markers to further study this cell population. Interestingly, several of these neoblast-specific genes are required for their maintenance (Guo et al. 2006; Reddien et al. 2005; Salvetti et al. 2005; Solana et al. 2009).

Recent studies demonstrate that the population of neoblasts is heterogeneous, since subpopulations of neoblasts have been identified that express markers of specific cell types (eyes, gut, brain...), suggesting the existence of lineage restricted neoblasts (**Figure 14**) (Cowles et al. 2013; Currie & Pearson 2013; Lapan & Reddien 2011; Scimone et al. 2011). This lineage restricted neoblast, also called specialized neoblast, correspond to what in other organism are usually known as lineage restricted progenitors. These new findings contradict the classical neoblast view, where there is only one type of neoblast, a naive neoblast, which is able to produce all planarian cell types (**Figure 14**).

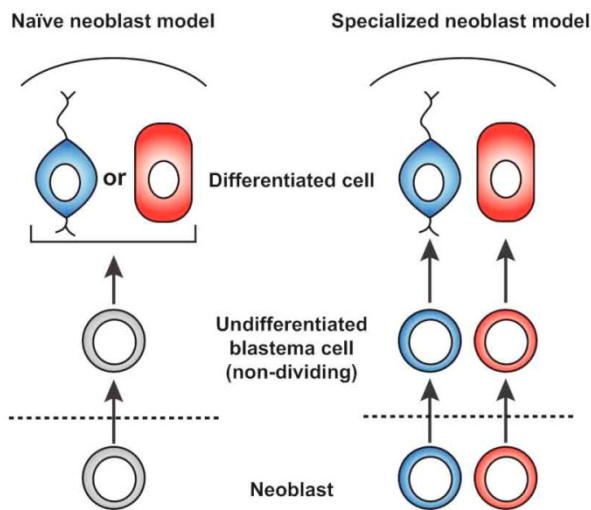


Figure 14: Schematic view of the two main theories about the generation of differentiated cells from neoblasts. On the left, the naive neoblast model and on the right side the specialized neoblast model. Figure from (Reddien 2013).

Using single cell transcriptomics, van Wolfswinkel and collaborators described subtypes of neoblast, identified by the presence of specific combinations of transcripts: the sigma neoblast (σ -neoblast) expressing mainly *Smed-soxp1* and *Smed-soxp2*, the zeta neoblast (ζ -neoblast) expressing *smed-zfp1* and the gamma neoblast (γ -neoblasts) (van Wolfswinkel et al. 2014). Later on, an additional

INTRODUCTION

subclass, the nu-neoblasts (vNeoblasts) characterized by the expression of *smed-ston-2*, *smed-msi-1* and *smed-elav-2* were described (Molinaro & Pearson 2016) σ -neoblast are responsible for the proliferative response after a wounding and, since they are able to develop to all cell types, they could respond to the already described c-neoblast. On the other hand, ζ -neoblast, γ -neoblasts and vNeoblasts are specific for epidermal, gut and neural tissues respectively (van Wolfswinkel et al. 2014)(Molinaro & Pearson 2016) .

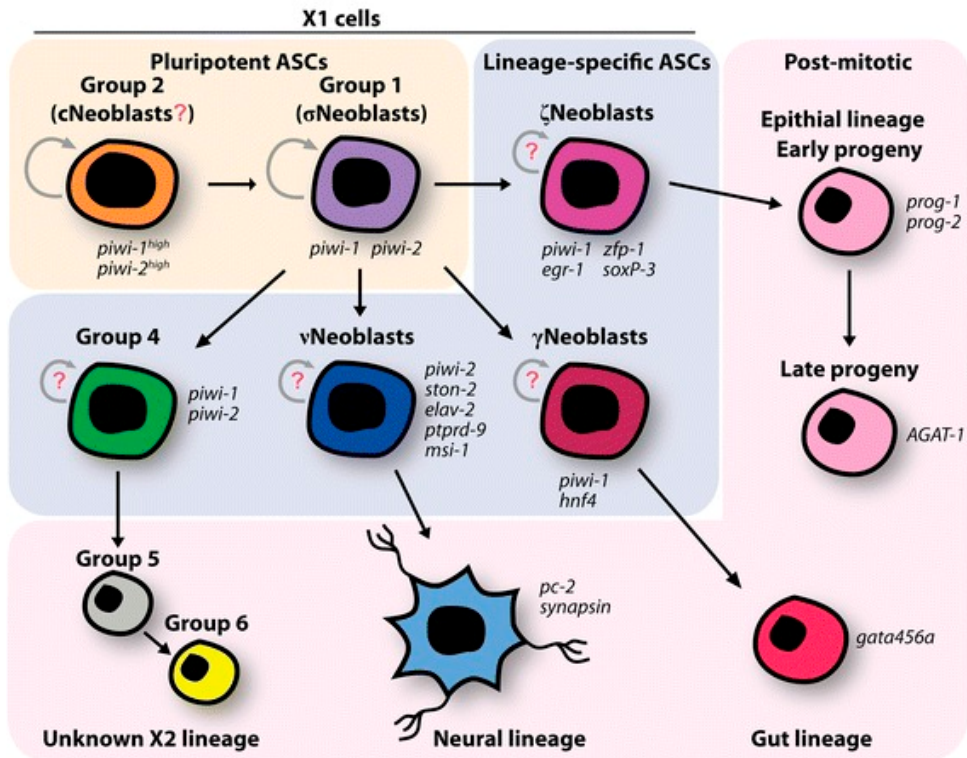


Figure 15: Model of planarian stem cell hierarchies. Summary model of the planarian cell lineages. Based on the scRNAseq and Waterfall/pseudotime analyses, it is hypothesized that cNeoblasts are represented in the Group 2 cluster, which give rise to pluripotent Group 1/ σ Neoblasts. In turn, σ Neoblasts give rise to ζ , γ , v, and Group 4 neoblasts, represented in the middle tier. The hypothesis argues that these neoblast subclasses give rise to tissue-specific lineages on the third tier, such as epithelium for ζ Neoblasts, gut for γ Neoblasts, and neurons for vNeoblasts. Red question marks denote either unknown existence or unknown ability to self-renew. Figure modified from (Currie et al. 2016).

3. Mechanisms required for proper regeneration and tissue turn over

Cell turnover and regeneration as previously described, are two different mechanisms in which adult stem cells sense the absence of tissue or specific cell types to initiate diverse mechanisms to cover this lost. In addition both require the correct specification of the stem cells into the right cell lineage or lineages to form exactly the correct differentiated cells and therefore maintain the tissue running. Both mechanisms are useless without the proper positional instructions which guide the correct positioning of the different structures. Regeneration and cell turnover are not understood without stem cell proliferation, differentiation and positioning instructions, however, these three processes are an abruption of a complex and coordinated system that involves all of them and are separated just for this comprehensive study. Due to the complexity of the whole regenerative or homeostasis process I will also divide the following sections and results into these three main events.

3.1. Control of cell number: balance between proliferation and apoptosis

Animals maintain a controlled body size to keep the whole organism the function. It is not well understood how animals control their own size. Allometry is a field of study based on the main observation that the size and shape of organs are

INTRODUCTION

always appropriated to the animal size. The process on how organs and tissues keep their proper size and proportions is an open question in biology.

The cell number in an organism or in their organs/tissues is mainly controlled by the tight balance between the cells that die by different causes (such as accumulation of mutations, DNA damage, external wound, etc) and the proliferation of stem cell to substitute the dying cells. Planarians are an ideal model to study how animals maintain their body size as they are able to grow and degrow depending on the food availability. In addition, their regenerative abilities also require the remodeling of organs and structures to keep the new proportions.

In planarians, the apoptotic and proliferative response after wounding or during cell turnover has been broadly studied. Apoptosis is one of the most important ways to naturally eliminate cells that have suffered DNA damage and stress among others. This controlled cell death has also been shown as a process with a tight regulation during planarian regeneration. After amputation, there are two main apoptotic responses (peaks), one at 4 hours after the amputation and the second one at 72 hours. The first apoptotic response is restricted to the wound area while the second one occurs all through the body (**Figure 16**)(Pellettieri et al. 2010). This apoptotic response is associated with the remodelling requirements during the regeneration process, thus after a tissue loss the pre-existent planarian tissue has to be restructured. Therefore, the amount of apoptotic response is proportional to the tissue lost(Pellettieri et al. 2010).

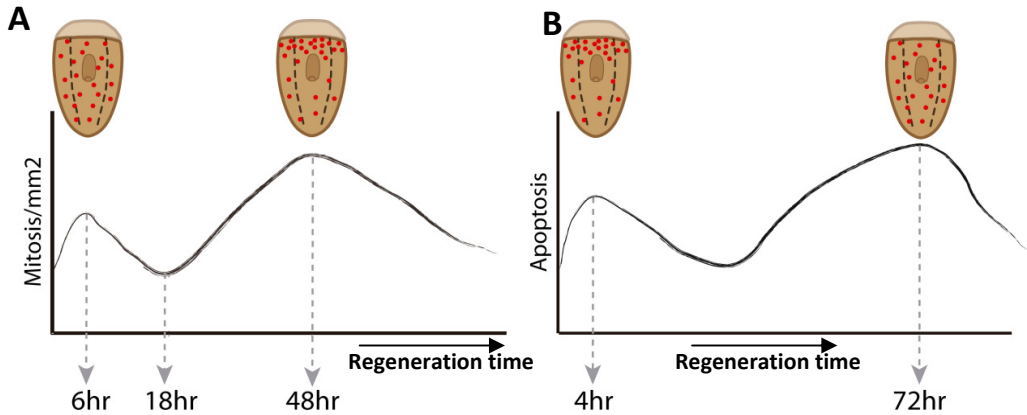


Figure 16: Mitotic and apoptotic dynamics during planarian regeneration. (A) Two proliferative peaks are present at 6 and 48 hours after amputation. First mitotic peak is associated with a general mitotic response while the second is more localized in the pre-wounding area. (B) Apoptosis is increased at 4 hours and 72 hours after amputation. First apoptotic response is localized in the wound area while the second is general.

After tissue loss, neoblasts start dividing to generate the cells required to form the new tissues. This mitotic response is highly coordinated in a spatial-temporal manner, showing two peaks (Baguña 1976; Saló & Baguña 1984; Wenemoser & Reddien 2010). The first proliferative peak takes place at 6 hours after some damage and appears through the body (Wenemoser & Reddien 2010). At 48 hours a second mitotic peak appears, localized in the post wounding region, in the area called postblastema. It has been suggested that the first mitotic activation corresponds to all the neoblast responses that are in G2 or at the end of the S phase, which need less time to go into mitosis. Between both peaks, a lesser mitosis appears at 18 hours after amputation (**Figure 16**)(Saló & Baguña 1984).

On the other hand the planarian is a very interesting model to study how body size is controlled during normal homeostasis, as they are able to grow and degrow

INTRODUCTION

depending on food availability. After feed, the mitotic response is activated, and apoptosis decreases, therefore more cells are generated allowing the planarian to grow. On the other hand, during starvation, apoptosis is increased, while mitosis is maintained at basal levels. Under no energy supply conditions, planarians take the energy to stay alive from the dying cells. Therefore, during homeostasis, the balance between proliferation and apoptosis is highly important to maintain the size and proportions of the animals depending on the energy intake conditions (Figure 17).

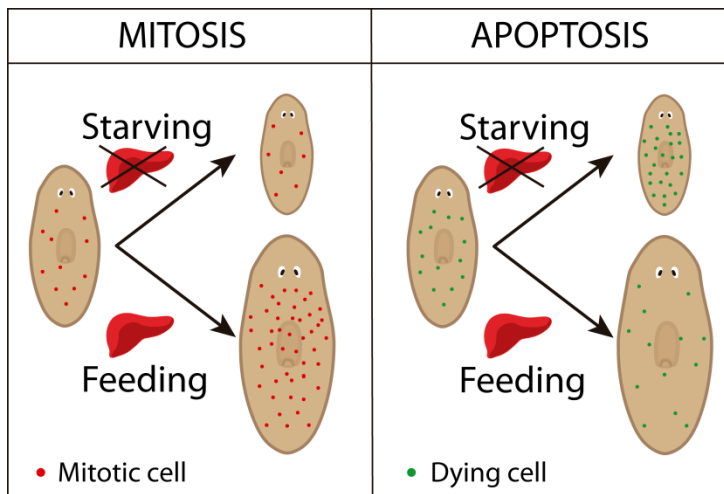


Figure 17: Proliferative and apoptotic response during growth and degrowth. (A) Proliferation is activated at 3 hours after feeding while during starvation is maintained. (B) Apoptosis is activated during degrowth.

3.1.1. Jun-N-terminal kinase: an important proliferation and apoptosis regulator

Jun-N-terminal kinases or JNKs belongs to the superfamily of MAP-kinases involved in the regulation of cell proliferation, differentiation and apoptosis. The MAP-kinases pathway transport external stress signals from the cell surface to the nucleus through the phosphorylation of a series of kinases (Kockel et al. 2001). One of the most studied roles of JNK signalling is the control of apoptosis, involved in the two broadly accepted signalling pathways which initiate it: 1) the extrinsic pathway, initiated by dead receptors such as those of TNF- α , TRAIL, and FAS-L and 2) the intrinsic pathway, initiated by mitochondrial events (Elmore 2007). On the other hand, JNK has been involved in cell cycle regulation, where it ensures the controlled onset of mitosis (Chen 2012; Gutierrez et al. 2010).

The JNK pathway has been extensively studied in *Drosophila melanogaster*, taking advantage of the broad genetic tools available for this model organism. In flies, the central JNK signalling core is formed by Basket (JNK), Hemipterous (JNKK) and dMKK4. Basket phosphorylates the transcription factors Jun and Fos allowing the formation of the heterodimer AP-1 (Activator Protein 1) which is able to regulate target genes through binding to AP-1 motives (TGACTCA) (**Figure 18**) (Lee et al. 1987; Perkins et al. 1990; Riesgo-Escovar et al. 1996). In *Drosophila*, JNK activates the apoptotic process through the activation of the inhibitor of apoptosis protein 1 (IAP1), which inhibits Caspases. JNK also promotes proliferation

INTRODUCTION

during *Drosophila* regeneration and homeostasis (Biteau et al. 2008; Jiang et al. 2010; Sun & Irvine 2011).

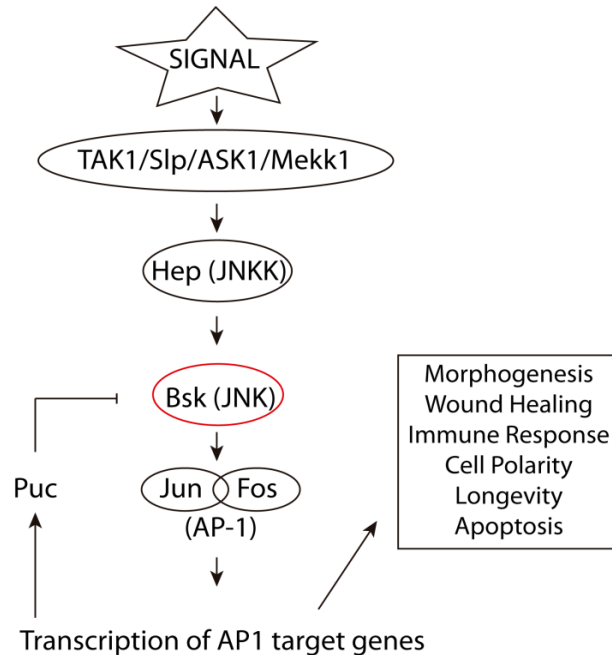


Figure 18: JNK pathway described in *drosophila*. A stress signal triggers activation of membrane proximal kinases that phosphorylate and activate different kinases. JNK translocates to the nucleus where it can regulate the activity of transcription factors like AP-1 to finally regulate a huge variety of processes.

In our model, recent studies demonstrate that planarian JNK also plays a key role in controlling the balance between proliferation and apoptosis during regeneration and homeostasis (Almuedo-Castillo et al. 2014). In this study, the inhibition of *Smed-jnk* prevents proper regeneration by attenuating the apoptotic response and accelerating the cell cycle. In homeostatic conditions, inhibition of planarian *jnk* avoids the proper remodelling of the preexisting tissue, inverting the balance

between cell death and proliferation (**Figure 19**)(Almuedo-Castillo et al. 2014). These findings pointed JNK as an essential stress response element required for the correct communication between proliferative and apoptotic response in planarians.

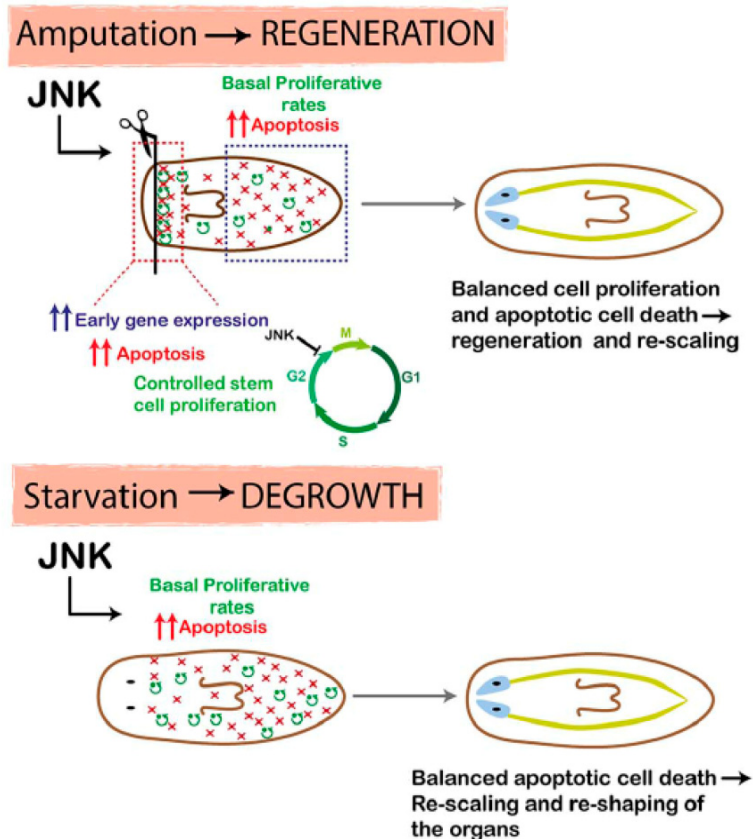


Figure 19: Schematic showing role of JNK in planarian regeneration and homeostatic degrowth. In the wound region, JNK triggers early gene expression and apoptosis, and mediates temporal control of the cell cycle progression of neoblasts, which ensures the balanced differentiation of different cell types and hence proper regeneration of missing tissues. In pre-existing regions, JNK triggers apoptosis and maintains basal levels of proliferation to ensure that body proportion is properly restored after amputation. RNA interference of JNK activity prevents all these processes in both the wound region and in pre-existing regions, as well as regeneration and rescaling. Modified from (Almuedo-Castillo et al. 2014)

3.1.2. Krüppel like factors (KLF): Their role regulating proliferation and apoptosis.

At this point, it is necessary to introduce the krüppel-like factors (KLFs), a family of transcription factors which has been shown to be especially important for the regulation of cell cycle genes and apoptosis. KLFs, together with specificity proteins (SP), are families characterized by the presence of three tandem C₂H₂ zinc finger domains located at the C-terminus and identified by their homology to the *Drosophila* Krüppel gene (Jäckle et al. 1986). These zinc finger domains are DNA binding domains (DBD) which bind to GT regions (GT boxes) and CACC elements (Kadonaga et al. 1987). These families have evolved through multiple gene-duplication events varying the number of members between species (Kaczynski et al. 2003). The N-terminal part of this proteins are much variable between members and species, containing transcriptional activation or repression domains. SPs can be differentiated from KLFs by the presence of the Buttonhead (Btd) box domain just 5' of the DBD (**Figure 20**)(Suske et al. 2005).

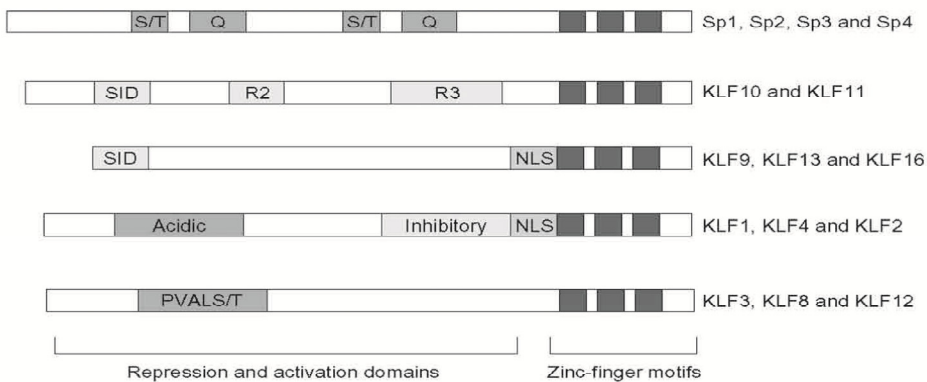
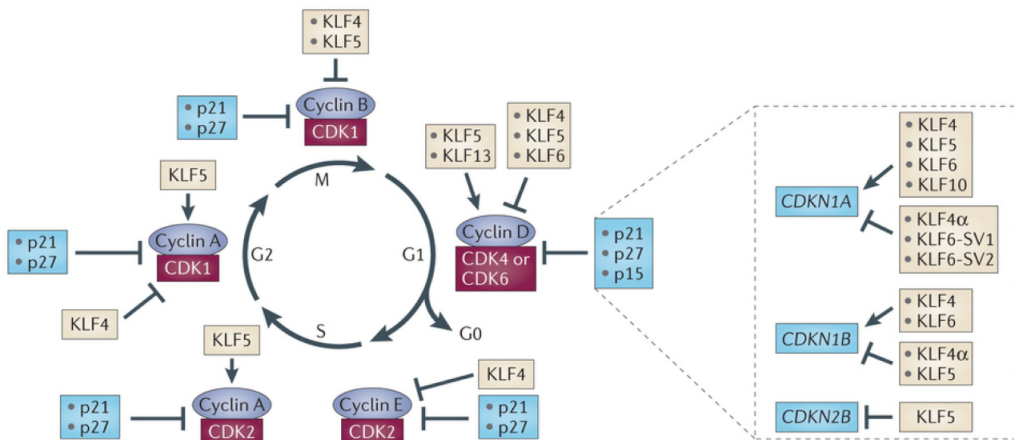


Figure 20: Structural properties of vertebrate Sp1-like/KLF proteins. Sp1-like/KLF proteins have highly homologous carboxy-terminal DNA-binding domains characterized by three Cys2His2 zinc-finger motifs and recognizing GC-rich DNA elements, and variant amino termini. SP-like contain glutamine-rich (Q) and serine/threonine-rich (S/T) amino-terminal transcription activation domains. Two members of subgroup III, KLF10 and KLF11, are TGF β -inducible repressors and have three conserved amino-terminal repression domains, including the Sin3 interaction domain (SID). KLF9, KLF13 and KLF16, are also characterized by a functional SID domain. KLF1, KLF2 and KLF4 are characterized by amino-terminal acidic activation domains, inhibitory regions adjacent to the zinc fingers and a conserved nuclear localization signal (NLS) sequence. In addition, KLF13 contains a similar nuclear localization sequence. KLF3, KLF8 and KLF12, have a conserved repression motif (PVALS/T). Figure modified from (Kaczynski et al. 2003).

By regulating gene transcription, KLFs are involved in many physiologic and pathological processes, such as cell differentiation, proliferation, cell growth, and apoptosis during normal development or in different disease conditions (Cao et al. 2010; Pearson et al. 2008). Different members of this family have been found to be highly important during several cancer types' progression. The main reason is their essential role in the control of cell cycle and apoptosis. Cyclins and CDKs are cell cycle regulators which are common targets for several KLFs (**Figure 21**) (Tetreault et al. 2013). Furthermore, as proliferation and apoptosis are interconnected, many of the proliferative factors regulated by KLF are also relevant for apoptosis, like p53, E2F, MYC or MAPKs (Senderowicz 2004). In addition, KLFs regulate specific apoptotic factors as BCL-2 family members and JNK (Tarapore et al. 2013; Muñoz-Descalzo et al. 2005). In this line, it has been described that Cabut, a drosophila KLF (homologous to vertebrate klf10/11), is controlled by JNK during wing disc regeneration by the binding of AP-1 to the Cabut promoter (Ruiz-romero et al. 2015).

INTRODUCTION

At the beginning of this Thesis, it was not known the role of any KLF member in planarians. However, during this Thesis, Scimone and collaborators described a planarian Klf required for the differentiation of *cintillo*-expressing sensory neurons and eye cells (Scimone et al. 2014; Lapan & Reddien 2012).



Nature Reviews | Cancer

Figure 21: KLF family members in the cell cycle control. KLFs control cell proliferation by targeting cell cycle regulators like cyclins, cyclin-dependent kinases (CDKs) and CDK inhibitors. Figure from (Tetreault et al. 2013).

3.2. Stem cell specification

Previously it has been introduced the importance of the generation of the proper number of cells during regeneration or cell turnover; however, cell proliferation is meaningless if all the new generated cells do not take the correct cell fate to supply the cell lost. For that reason, a correct and well regulated differentiation mechanism should be applied during regeneration and cell turnover. In regards to planarians, these last years have been specially clarifying for the identification and characterisation of this process.

As previously shown, planarian neoblasts are a heterogenic cell population in which according to the differential gene expression several cell types have been described: the σ -neoblast, the ζ -neoblast, the γ -neoblasts and the vNeoblasts. In addition, cNeoblasts have been described as the truly totipotent planarian stem cells (van Wolfswinkel et al. 2014; Molinaro & Pearson 2016). Each Neoblast subtype gives rise to specific cell types as other model systems where every tissue has their own progenitor stem cells. One of the most clarifying examples of planarian cell specification is the differentiation process of epidermal lineage. For the specification of epidermal cells in planarians different steps have been described based on the sequential and cell-type specific expression of different genes. Thus ζ -neoblast give early progeny cells labeled by *prog-1* (also known as *NB.21.11e*), then start to express the late progeny marker *agat-1*, following the expression of *zfpu-6* and finally the terminal markers corresponding to epidermal cells, like *vimentin* (**Figure 22**) (Tu et al. 2015). This process has been described in detail thanks to coexpression analysis between the different markers. In addition, irradiation experiments at lethal doses show the disappearance of first *prog-1*+ cells, then *agat-1*+ cells and finally *zfpu-6*+ cells, according to the described epidermal cell specification steps (Tu et al. 2015; Eisenhoffer et al. 2008).

In addition to the epidermal lineage specification, several genes have been shown to be required for the generation of different cell lineages as is summarised in figure 22 (Scimone et al. 2014). All these genes specifically expressed in different cell types allowed researchers to go deeper in understanding how stem cells differentiate into different cell types.

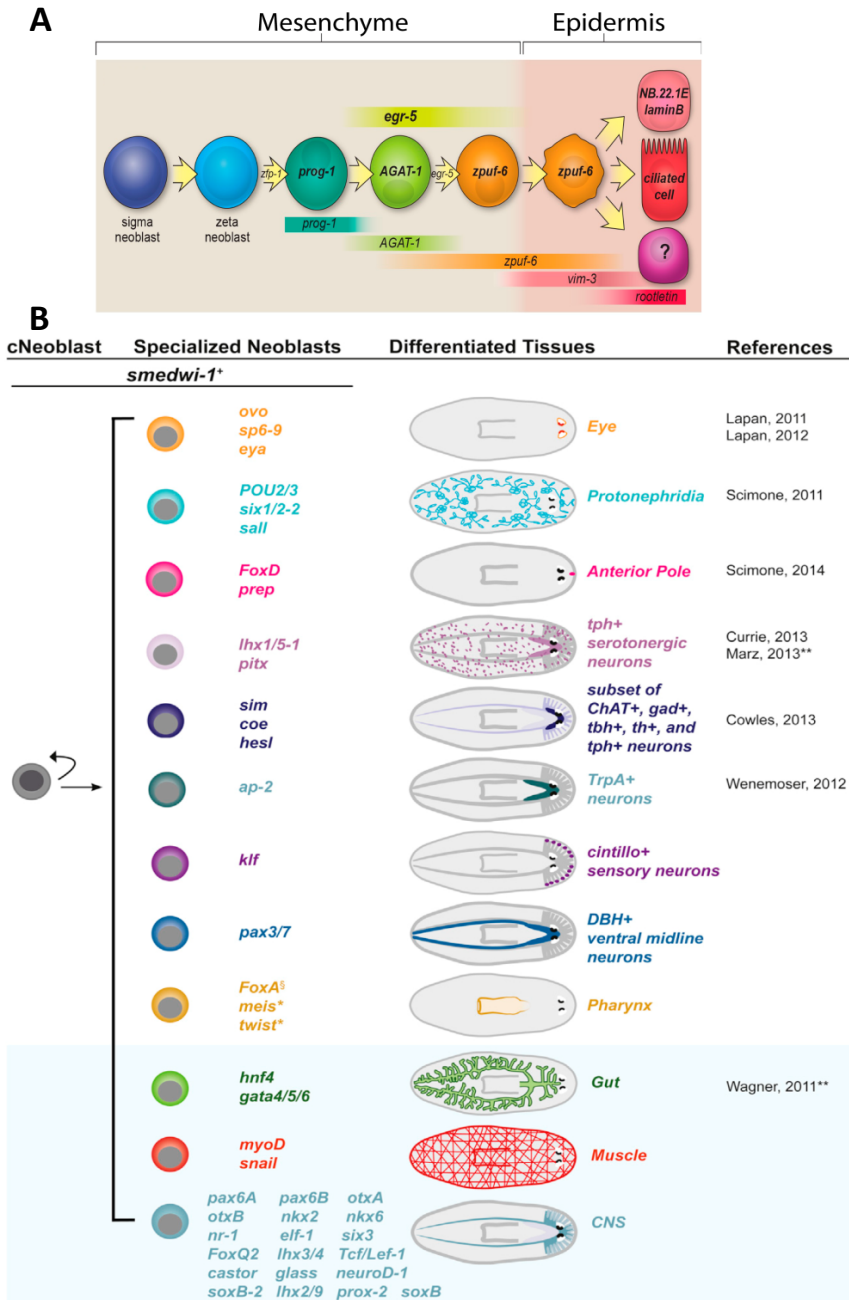


Figure 22: Overview of cell specification in planarian. (A) Genes involved in the epidermal differentiation steps. Modified from (Tu et al. 2015). (B) Scheme proposed by Scimone and collaborators: Specialization of neoblasts into different cell lineages following wounding and genes which have been found to be involved. Modified from (Scimone et al. 2014).

3.2.1. Nuclear Factor Y: a transcriptional complex required for proper cell specification.

Although several genes are involved in cell specification, here I will introduce an important transcriptional complex called Nuclear Factor-Y complex (NF-Y), which was not studied before this Thesis in planarians. I will generally describe the known roles of this complex focusing in cell specification processes.

Nuclear Factor Y, also known as CBF or HAP2/3/4/5, consists of three different subunits, NF-YA, NF-YB and NF-YC, all required for the formation of the transcriptional complex NF-Y (**Figure 23A**). It has been shown that for the correct assembly of the complex, NF-YB interacts with NF-YC forming a heterodimer that then interacts with NF-YA, to form the heterotrimeric NF-Y transcription complex (**figure 23B**)(Mantovani 1999). This complex binds to CCAAT motifs, which is common in many promoter and enhancer regions of a large number of genes in eukaryotes, related with several developmental processes like proliferation, cell death, differentiation or axon targeting (**Figure 23B**) (Hughes et al. 2011; Matuoka & Yu Chen 1999; Bhattacharya et al. 2003; Morey et al. 2008; Li et al. 1992). The fact that knock out of mouse or fly NF-YA results in early embryonic lethality corroborates these essential roles during early development (Yoshioka et al. 2007; Bhattacharya et al. 2003).

INTRODUCTION

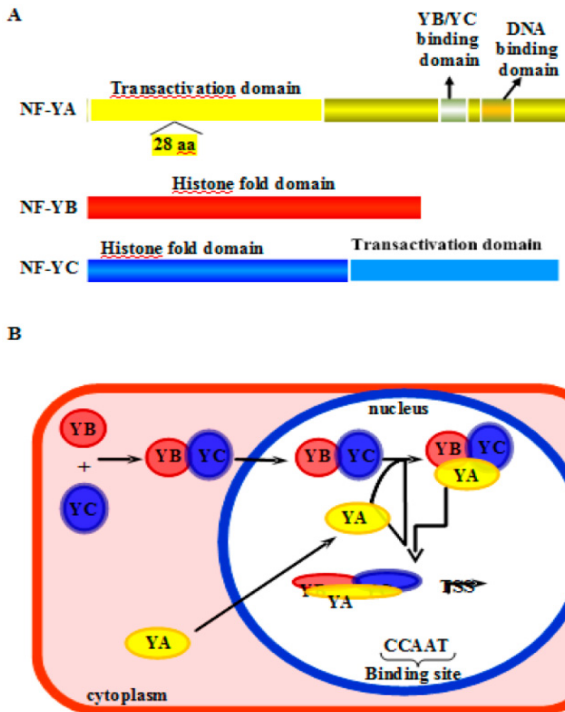


Figure 23: NF-Y complex

(A) Schematic representation of NF-Y subunits. B) A tight NF-YB/NF-YC heterodimer is assembled, translocated in the nucleus where it binds the NF-YA subunit containing the DNA binding domain. The resulting trimer is able to bind the CCAAT sequence on DNA. Modified from (Gurtner et al. 2016)

Going further into the roles of NF-Y during cell specification events, several *in vivo* studies, generally focused in one of the three subunits, are found. During *Drosophila* eye development, growth and identity specification appears to be separated (Mann 2004), allowing the identification of genes essential for one or another process. In this context, Yoshioka and collaborators showed that NF-YA can disturb eye specification, but not disc growth (Yoshioka et al. 2007). NF-YB has been also seen required during eye development, thus knock down of this subunit generates defects during R7 photoreceptor cell differentiation (Ly et al. 2013). In *C. elegans*, an RNAi screening identified NF-Y as negative regulator of the T-box gene *Tbx-2*, which is essential for the specification of neural cell fate (Milton et al. 2013).

Although the role of NF-Ys had not been studied during planarian regeneration and homeostasis, in another platyhelminth, *Schistosoma mansoni* (Human blood Fluke), NF-Y has been shown to be expressed during the whole life cycle. Furthermore, NF-YA accumulates in the nucleus of oocytes during their maturation and decreases in maturing spermatozooids (Serra et al. 1996).

3.3. Positional instructions

One common feature between all the pluricellular organisms is that they need a body plan organized in a tridimensional manner to keep the functionality of all the organs and tissues. Bilateral organisms are organized according to three main axes: The antero-posterior (AP), the dorso-ventral (DV) and the medio-lateral (ML) (**Figure 24**). The conjunction of these three axes gave to bilateral clade the characteristics which define them. For example, during evolution the bilateralization is tied to the appearance of a central nervous system, with a cephalized structure normally called brain.

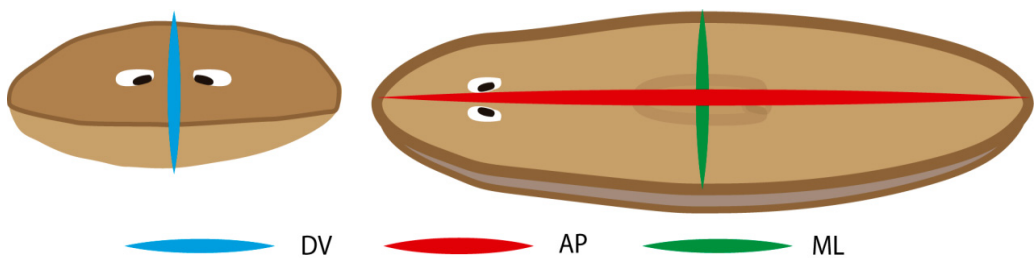


Figure 24: Schematic view of the three main body axes in planarian. DV: Dorso-Ventral; AP: Antero-Posterior; ML: Medio-Lateral.

INTRODUCTION

Pattern formation is the developmental process by which different cell types and tissues organize according to their body axes. Thus, pattern formation ensures that tissues and organs form in the correct place during embryonic development and also in adult organisms during cellular renewal or regeneration. The specification of the body axis during embryonic development and the patterning of the organs and tissues have been broadly studied; however, how this axial information is controlled post-embryonically is not well understood.

Adult organisms do not require the establishment of new axes; nevertheless during regeneration, positional information is required to properly regenerate the correct pattern of the missing tissues. Furthermore, during normal cell-turnover, cells must also receive the correct positional information to reach their final fate and position. Even more, in planarians, positional information must be especially activate at the adult stage, since they are not only able to regenerate big parts of their body but also to change the size of their body and organs during their usual cell turn-over. For that reason, planarians plasticity is a unique scenario in which to study adult pattern formation. Several studies from the last years demonstrate that the amazing plasticity of planarians is sustained by the abundant population of totipotent adult stem cells spread in their whole body (neoblasts), concomitant to the activation of the intercellular signals that direct them towards their specific fate and location. Thus, adult planarians maintain continuously active the patterning mechanisms that ensure the shape and organization of their organs and the whole body, both in regenerating and homeostatic contexts.

3.3.1 Planarian AP axis establishment:

Wnt ligands are a family of secreted glycoproteins which activate the Wnt signalling pathway by binding to a receptor (mainly Frizzled receptors). There are two main Wnt pathways described: the canonical or β -catenin dependent and the non-canonical or β -catenin independent. The β -catenin dependent signalling pathway takes the name from β -catenin, a bi-function protein which is involved in cell-cell adhesion and transcriptomic regulation. In the canonical signalling, secreted Wnt ligands bind to Frizzled receptors and LRP co-receptors to induce cytoplasmic accumulation and nuclear translocation of β -catenin (Mikels & Nusse 2006; Clevers & Nusse 2012), which is the key intracellular component that transduces the signal to the nucleus. In the nucleus, β -catenin binds to the TCF/LEF transcription factors, triggering changes in the chromatin configuration and gene transcription (Komiya & Habas 2008; Valenta et al. 2012). On the other hand, the non-canonical pathway includes the non-canonical planar cell polarity (PCP) pathway, and the non-canonical Wnt/calcium pathway. In the non canonical pathways Wnts do not bind to the LRP co-receptor, instead they mainly bind to Ryk or ROR2 co-receptors that together with Frizzled recruit Dsh and activate different signal cascades. The final effect of these non-canonical pathways has been related with actin modifications and calcium control which mainly control cell migration, cell adhesion and general cell movements like axon projections (**Figure 25**). During the following paragraphs I will focus on the canonical pathway which is mainly involved in planarian A-P control while the non-canonical will be later discussed during the M-L axis establishment.

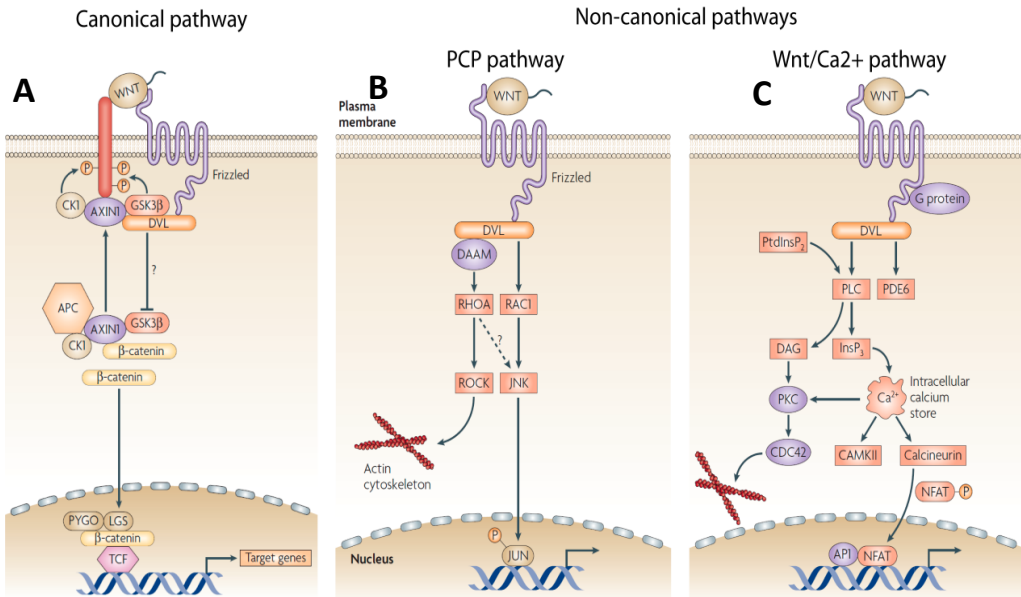


Figure 25: Canonical and non-canonical Wnt signalling pathways. (A) Upon binding of a WNT protein to the receptor, a signalling cascade is initiated. LRP is phosphorylated by CK1 and GSK3 β , and AXIN1 is recruited to the plasma membrane. The kinases in the β -catenin destruction complex are inactivated and β -catenin translocates to the nucleus to form an active transcription factor complex with TCF. (B) Planar cell polarity (PCP) signalling does not involve β -catenin, LRP or TCF molecules, but leads to the activation of the small GTPases RHOA and RAC1, which activate the stress kinase JNK (Jun N-terminal kinase) and ROCK and leads to remodelling of the cytoskeleton and changes in cell adhesion and motility. (C) WNT–Ca²⁺ signalling is mediated through G proteins and phospholipases and leads to transient increases in cytoplasmic free calcium that subsequently activate the kinases PKC (protein kinase C) and CAMKII and the phosphatase calcineurin. Modified from (Staal et al. 2008).

In planarian, inhibition of β -catenin by RNAi generates a range of A-P phenotypes, from two-headed planarians to radial-like hypercephalized planarians (Gurley et al. 2008; Iglesias et al. 2008). Inhibition of negative regulators of the canonical Wnt pathway, such as the components of the β -catenin destruction complex, APC and axin, leads to two-tailed planarians (Gurley et al. 2008; Iglesias et al. 2008). To explain these phenotypes, it is widely accepted that there is a gradient of β -catenin activity, lower in anterior and higher in posterior, which

specifies and maintains AP axial identity in planarians (**Figure 26**) (Adell et al. 2010; Sureda-Gómez et al. 2016).

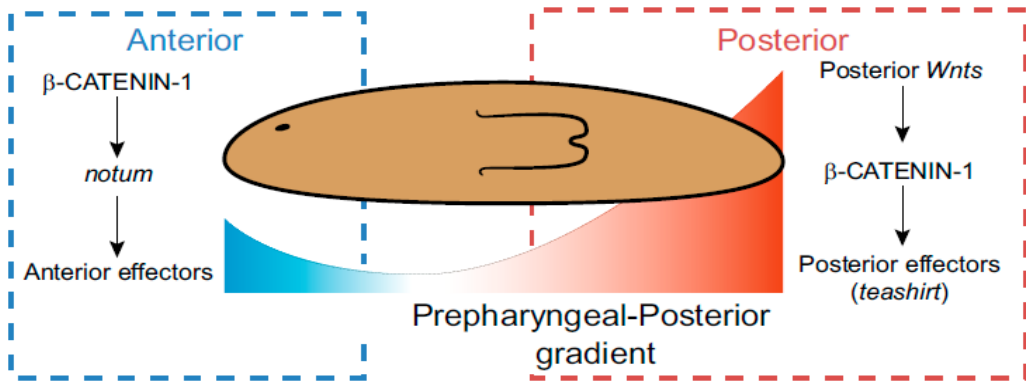


Figure 26: β CATENIN-1 displays a gradient from the prepharyngeal region to the tail. Nuclear localization of β CATENIN-1, which is responsible for activation of effectors of posterior identity, like *teashirt* (Reuter et al., 2015), would depend on the action of the posterior wnts (Wnt1, Wnt11-1, Wnt11-2, Wnt11-5). In the anterior region, β CATENIN-1 is required for expression of *notum* among other effectors of anterior morphogenesis. Figure obtained from (Sureda-Gómez et al. 2016).

3.3.2. Planarian D-V axis establishment:

The dorso-ventral axis has been shown to be mainly controlled by the Bone Morphogenetic Protein (BMP) signalling pathway in both vertebrates and invertebrates. During vertebrate development, a gradient of BMP signalling specifies cell fates along the D-V axis, with the highest levels specifying the ventral-most tissues, while increasing BMP inhibition leads to more lateral tissues and an absence of BMP signalling to dorsal tissues (Dosch et al. 1997; Knecht & Harland 1997; LaBonne & Bronner-Fraser 1998; Marchant et al. 1998; Neave et al. 1997; Wilson et al. 1997). By contrast, in invertebrates like *Drosophila*, the homolog to BMP decapentaplegic (*dpp*), is expressed dorsally and it is required in

INTRODUCTION

order to specify and maintain dorsal identity. Noggin, expressed in *Drosophila*, promotes ventral development, specifying ventral ectoderm and CNS in the absence of all endogenous ventral-specific zygotic gene expression. Dpp inhibits neural fates thus the noggin presence allows the development of the CNS ventrally located (Gerhart 2000). In both, vertebrates and invertebrates it has been proposed that spatial opposed expression of BMP and Antidorsalizing Morphogenetic Protein (ADMP) can promote the restoration of the DV axis after tissue removal.

In planarian, similar to invertebrate development, the BMP pathway is required to specify and maintain dorsal identity during planarian regeneration and homeostasis (Molina et al. 2007; Orii & Watanabe 2007; Reddien et al. 2007). It has been shown that inhibition of several elements of the BMP pathway results in ventralized planarians. On the other hand, the silencing of antagonists of the BMP signalling pathway results in the dorsalization of the animal (Molina et al. 2011). Therefore, Bmp/Admp regulatory circuit is a central feature of the Bilateria, used broadly for the establishment, maintenance, and regeneration of the D-V axis (**Figure 27**)(Gaviño & Reddien 2011).

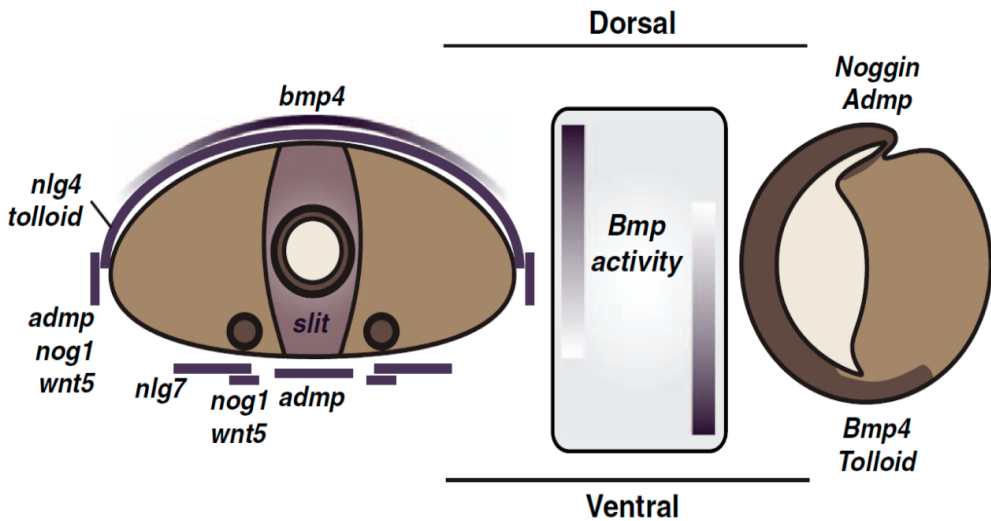


Figure 27: BMP signaling in the control of the DV axis. BMP signaling is active on the dorsal side of planarians and on the prospective ventral side of *Xenopus* gastrula-stage embryos. A transverse section of a planarian is depicted with the central hole representing a gut branch and the ventral circles representing nerve cords. The *Xenopus* embryo is depicted as a sagittal section. *Admp* and *Noggin* expression spatially oppose the site of *bmp* expression in both cases. A proposed axis inversion in the evolution of deuterostomes could explain the opposite orientation in protostomes and chordates. Modified from (Reddien 2011).

3.3.3. Planarian M-L establishment:

The evolutionary appearance of the bilateral body plan required the formation of a midline organiser (Meinhardt 2004). From the midline, different structures are organized at both sides forming a mirror image, in which each half organises the structures along the M-L axis. Although some bilaterians show left-right asymmetry, in planarians it has never been described (Inaki et al. 2016).

The midline is an elongated and narrow organising region along the M-L axis which functioning requires complex molecular interactions. Different modes of midline formation have evolved in vertebrates, insects and planarians, indicating that midline formation had a crucial role in the diversification of higher organisms (Meinhardt 2004).

3.3.3.1. Midline and CNS establishment

The formation of the midline in bilaterians is linked to the CNS formation (Christian Klämbt & Goodman 1991; C Klämbt & Goodman 1991; Meinhardt 2004). In vertebrates, the dorsal organiser promotes the elongation of the midline along the A-P axis, and consequently the CNS is formed dorsally. On the other hand, in insects the dorsal organiser represses the midline formation, promoting the formation of the midline ventrally; therefore, the CNS is ventrally formed (Arendt & Nübler-Jung 1994; De Robertis & Sasai 1996).

From the midline, axons are organized and projected ipsi- or contra-laterally to finally form the complex net of axons that covers the entire body. In all bilateral organisms, the axon paths that cross the midline allow communication between both sides of the body (Lartillot & Philippe 2008; Kaprielian et al. 2001). There are several families of molecules that guide the path and growth of neuronal axons like Netrins, Ephrins, Semaphorins, Slits and Wnts (Bashaw & Klein 2010; Dickson 2002). These molecules can exert an attractive or repulsive action towards the axons that show specific receptors in its surface.

During the formation of the CNS it is essential a proper organisation and expression domains of the axon guidance molecules (the ligands), and their receptors (Sánchez-Soriano et al. 2007). However, the mechanisms that define the proper expression boundaries of the axon cues are not well understood.

As in other bilaterians, in planarians the midline coordinates the M-L assembly of the neural circuitry through the secretion of axon guidance cues that direct the axons towards or against it. Out of the axon guidance molecules found in planarians, only a Slit homolog has been proved to control axon growth from the midline, acting as a repulsive cue, as in all studied animals (Cebrià 2007). Thus, in planarians, Slit is secreted by midline cells and acts as an axon repulsive cue to restrict the growth of the axons towards the midline. Thus, in planarians where *slit* has been silenced through RNAi, there is a collapse of the axons in the midline (Cebrià et al. 2007). However, the Slit receptor roundabout (ROBO), which is also conserved along evolution (Cardenas Castillo 2016), had not been found in planarians at the beginning of this Thesis. Although two ROBO receptors (ROBO-A and ROBO-B) had been described, their functional analysis showed that they are not the receptors of the described Slit (Cebrià & Phillip A. Newmark 2007).

Interestingly, two unrelated studies report that in planarians the non-canonical Wnt5 could be exerting the same function than Slit but from the opposite domain (**Figure 28**) (Adell et al. 2009; Almuedo-Castillo et al. 2011; Gurley et al. 2010). Wnt5 is an evolutionary conserved non-canonical Wnt which function has been related mainly with cell migration (Liang et al. 2003; Liang et al. 2007) but also with axon repulsion during the formation of the A-P commissures in *Drosophila*

INTRODUCTION

(Yoshikawa et al. 2003). Thus, in planarians, *wnt5* is expressed in the complementary domain with respect to *slit*, which is in the lateral region, and restricts the growth of the neural system towards it (Figure 28).

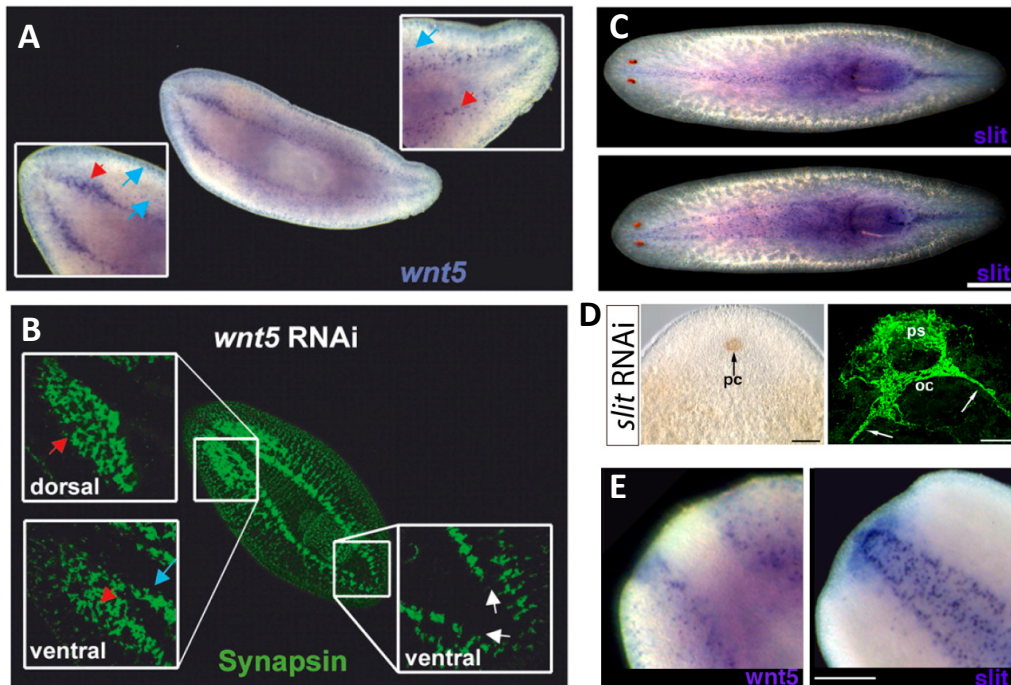


Figure 28: Wnt5 and Slit are involved in medio-lateral organization in planarian. (A) *Wnt5* is expressed from the ventral nerve cords to the margin of the animal. (B) Inhibition of *Smed-wnt5* generates a lateralization of the CNS towards the margin of the animals. (C) Dorsal and ventral view of *slit* expression. *Slit* is expressed along the planarian midline. (D) *Smed-Slit* RNAi generates cyclops planarian, viewed in vivo and with anti-ARRESTIN antibody. (E) Expression of *wnt5* and *slit* in regenerating planarian. Image shows complementary expression of both genes. (A-B) Modified from (Adell et al. 2009). (C-D) Modified from (Cebrià & Phillip A Newmark 2007). (E) Modified from (Almuedo-Castillo et al. 2011).

An important finding in the planarian field was that the three signalling pathways required for the establishment of planarian body axes (Wnt for the A-P, BMP for the D-V and Wnt5-Slit for the M-L) are also responsible for their maintenance during planarian homeostasis. Thus, the same phenotypes observed after β -*catenin*, *BMP*, *Wnt5* or *Slit* RNAi in regenerating animals are observed when intact animals are injected during several weeks (Sureda-Goez et al. 2016; Molina et al. 2011; Adell et al. 2009) Therefore, during regeneration and homeostasis the same positional instructions are used to specify and maintain the body axes in planarian.

OBJECTIVES

With the aim to improve our understanding of the process of cell renewal and regeneration in planarians, the following objectives were proposed for this Thesis:

1. Study the role of the Nuclear Factor Y complex during cell specification.

- 1.1. Identify the members of the Nuclear Factor Y transcriptional complex in planarians.
- 1.2. Study the role of the NF-Y complex during planarian regeneration and tissue turn over.

2. Study the role of Krüppel-like transcription factors in the control of proliferation and apoptosis in planarian.

- 2.1. Identify the members of the Krüppel-like transcription factor family in planarians.
- 2.2. Functionally characterise Klf10/11 during planarian regeneration and tissue turn over.
- 2.3. Study the functional relationship between Klf10/11 and c-Jun N-terminal Kinase in the control of proliferation and apoptosis.

3. Study of the molecular mechanism through which Wnt5 and Slit control the medio-lateral organization of the central nervous system in planarian.

- 3.1. Identify the receptors of Wnt5 and Slit in planarians, and describe the expression pattern and functional relationship between the ligands and receptors of the network.
- 3.2. Modelling the topology network by which Wnt5, Slit and their receptors create a self-regulatory system to establish the medio-lateral pattern in planarians.

RESULTS

CHAPTER I:

Nuclear Factor Y complex controls neoblast differentiation avoiding the proper regeneration and homeostasis.

4.1. The Nuclear Factor Y elements were found in a Digital Gene Expression Analysis

The use of high throughput techniques has been extended to many organism in the last years. In planarians, many transcriptomic studies have been done during the last 6 years analysing several conditions, tissues and even single cells (Abril et al. 2010; Blythe et al. 2010; Adamidi et al. 2011; Sandmann et al. 2011; Labbé et al. 2012; Resch et al. 2012; Kao et al. 2013; Onal et al. 2012). In our group, a Digital Gene Expression (DGE) analysis was performed analysing different cell populations extracted by Fluorescence-activated Cell Sorting (FACS) (Rodríguez-Esteban et al. 2015; Hayashi et al. 2006; Moritz et al. 2012). Using this sorting technique in planarians, it is possible to separate three different groups of cells called X1, X2 and Xin, according to the nucleus/cytoplasm ratio. As previously described the X1 fraction corresponds to neoblasts or cycling cells, which show a high amount of DNA (4n cells). This is the population that disappears after irradiation and corresponds to cycling neoblasts. The Xin fraction corresponds to differentiated cells, which show a small nucleus with respect to the cytoplasm, and the X2 population is a mix of quiescent neoblast and differentiating cells. The goal of the DGE analysis performed corresponding to these three different populations was to identify neoblast-related genes and to understand their genetic diversity (**Annex 1**).

In this analysis, we found that the three components of the Nuclear Factor Y were highly represented in the X1 population (neoblasts) (**Figure 29**). This high representation in neoblasts, together with the function described for these genes in

stem cells of other organisms (Yoshioka Y, 2012; Ly L, 2013) led us to study more in depth the function of these genes in the process of neoblast proliferation, maintenance and differentiation.

Gene	X1	X2	Xin	p-val X1-Xin	p-val X2-Xin
<i>Smed-nf-yA</i>	31.31	1.15	5.57	3.48e-007	2.50e-001
<i>Smed-nf-yB</i>	17.03	0	0	7.63e-006	1
<i>Smed-nf-yC</i>	589.38	97.74	142.93	4.54e-064	1.46e-002

Figure 29: X1, X2 and Xin DGE expression levels of the three subunits of nuclear factor Y.

Table showing the normalized expression levels of each gene with the correspondent pvalue. Modified from (Rodríguez-Esteban et al. 2015).

4.2. Protein structure of NF-Y elements.

As described before, the Nuclear Factor Y complex is composed by the subunits alpha, beta and gamma encoded by three different genes (NF-YA, NF-YB and NF-YC), all required for DNA-binding. Each subunit was represented by only one transcript in the DGE data and a single homologous to each corresponding subunit was found in close species as *Schistosoma mansoni* or *Clonorchis sinensis* (**Annex 2**). However, a different NF-YB was already described in the sexual strain of *Schmidtea mediterranea*, which is required for the maintenance and proliferation of the spermatogonial stem cells (Wang et al. 2010; Iyer et al. 2016). Research in the available transcriptomic databases (**Annex 3**) (Brandl et al. 2016) showed that two *nf-yb* were present in all planarian species, sexual and asexual

(**Figure 30**), suggesting a duplication and functional diversification of this gene in planarians. Since the one previously described in sexual planarians was called *nf-yb*, we named *Smed-nf-yb2* to the new one found in the X1 population.

Alignment NFYB protein

```

NF-YB      -----XRFLPICNVSKIMKK
NF-YB2     MDSNQENIVSDNNFDSYYENMDHQVQQGDGEYTQEFELQSPLEQDRFLPIANVSKIMKK
                                     *****
NF-YB      DLPFSAKIAKDAKQCVQECASEFISFVSSEAAEICQNDKRKTINGEDILQAFANLGFQDNY
NF-YB2     AVPTNGKISKEAKEIVQECVSEYISFITSEAAEKCCQEKRKTINGEDLLWAMANLGFQES
           :* .*:*:*:*: *****:****:***** **:*****:*.*:*****:
NF-YB      VETLQNFLQTYREANKFENDIIDLGNNNNAQGRPWSMAPVNSNSSSELNLIKLNMPHLLSM
NF-YB2     VEPLRLFLTKYREANKLDSSIMD--DSIEMGR--HMDNMGNVENTIYLRDNIIEYVQSE
           **.*. ** .*****:..*.* :. ** * .* .. : .: * : : *
NF-YB      LPLTDLTSS---NLNLENLLRDSDFQR--AVLNHLKKSSTDEDSFNMDEALLFLFKLY
NF-YB2     AGHDSTTATGTITLSTDGSSSGNIYVTYPTNLNTINGCNNNVDSNL-----
           .*: : .*. :. . : : ** : : . : * . *
NF-YB      ILWILKKKKKK
NF-YB2     -----

```

Figure 30: Two different NF-YB proteins in planarian. Alignment between *Smed-NF-YB* and *Smed-NF-YB2* proteins. Alignment done by clustalW.

4.3. Expression of *nf-y* subunits in planarian

To characterise the function of the components of the Nuclear Factors Y, we first analysed their expression pattern in wild type and irradiated animals (**Figure 31**). As mentioned in the introduction, lethal doses of irradiation eliminate the neoblast a day after irradiation, and the progeny also disappears during the following days. The three NF-Y components were expressed in the parenchyma and the CNS, and the expression in the parenchyma decayed one day after irradiation, corroborating its expression in neoblasts (**Figure 31**). The remaining

expression of the subunits one day after irradiation could be explained by its expression also found in differentiated tissues, as shown by its expression in the X2 and Xin population from the DGE data.

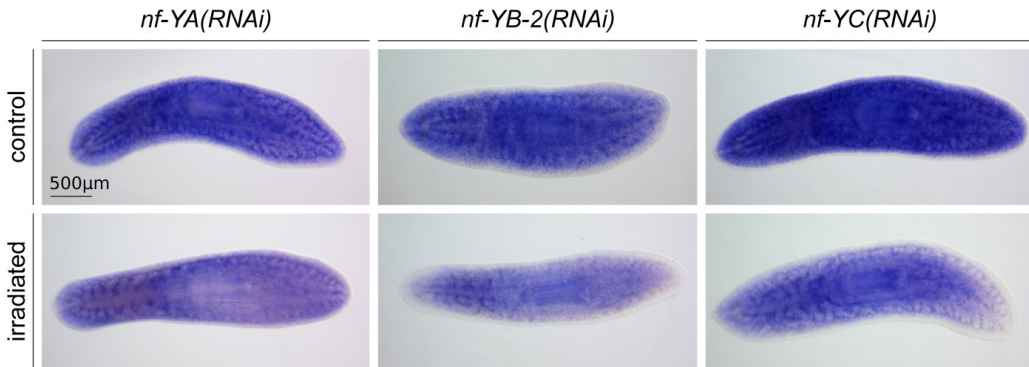
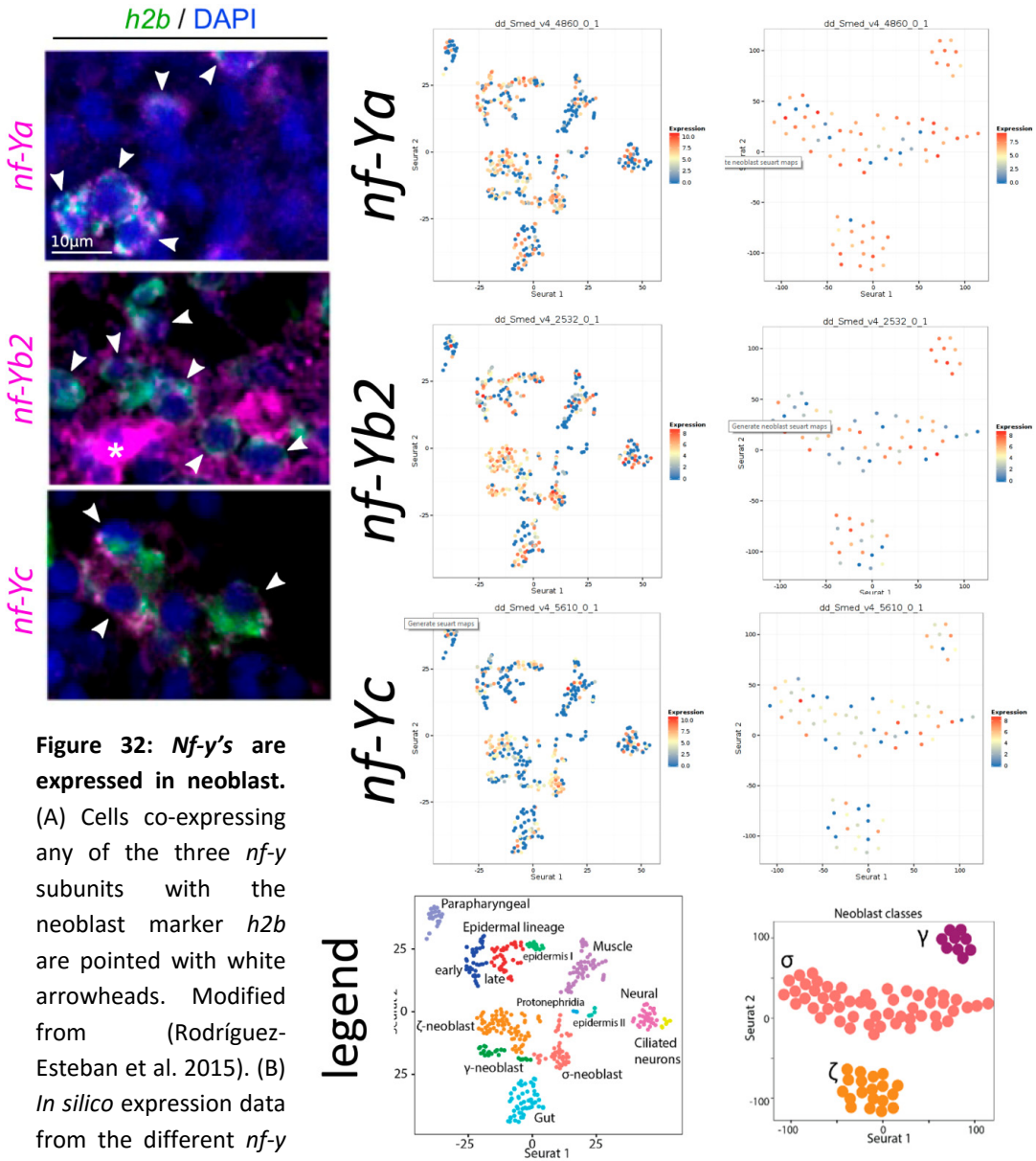


FIGURE 31: *nf-y* subunits are expressed in neoblasts. Expression of the three members of the NF-Y complex in wild type and lethally irradiated animals. Modified from (Rodríguez-Esteban et al. 2015)

To confirm the presence of the transcripts in neoblast, we performed double FISH of the three subunits with the neoblast marker *h2b*. We found co-localization of each subunit with *h2b* (white arrowheads), demonstrating that all elements of the complex are expressed in neoblast (**Figure 32**). We also were able to detect expression of the three subunits in other cell types, suggesting that the function of this complex is not restricted to neoblasts. Recent Single Cell expression data available from Reddien's lab allowed us the *in silico* search of the transcripts expression (van Wolfswinkel et al. 2014). The results confirm the ubiquitous expression of these subunits and the presence of all of them in neoblast (**Figure 32B**).



4.4. Functional analysis of *nf-y* subunits in planarian

It has been suggested that each NF-Y component could have a specific role. Therefore, to better understand the function of this complex, we performed RNAi of each subunit separately. In homeostatic conditions, inhibition of the different subunits resulted in head regression, ventral curling and the final death of the animals by lysis (**Figure 33A**). This phenotype is observed after ablation of the neoblast population (Reddien et al. 2005; Guo et al. 2006) and demonstrates the important role of the three subunits in the neoblast function.

The inhibition of the three subunits during planarian regeneration showed in all the cases a reduction on the regeneration ability, although the impairment degree was different depending on the subunit. Eleven days after the amputation, animals do not regenerate properly, showing smaller blastemas and improper regeneration of the photoreceptors (**Figure 33b**). Immunostaining with anti-synapsin and WISH with *sfrp* and *gpas* used as neural marker, showed smaller brains and fewer brain ramifications (**Figure 33c**).

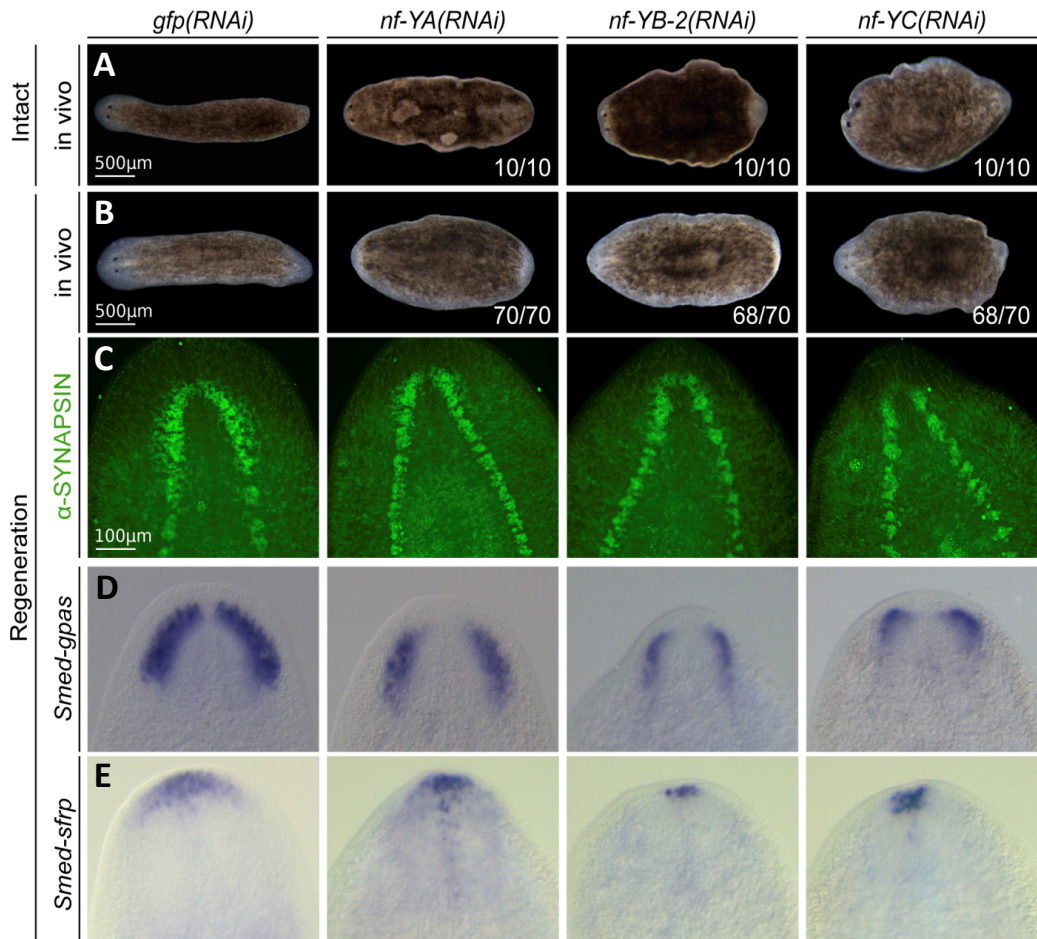


Figure 33: *nf-y* RNAi planarian generate regeneration defects. (A) *Smed-nf-Y(RNAi)* animals present wounds and curling during homeostasis. (B) *Smed-nf-Y(RNAi)* animals regenerate thinner blastemas with non well formed eyes and shape defects and fail to differentiate a proper brain, with reduced cephalic ganglia as revealed with anti-SYNAPSIN antibody and *Smed-sfrp* probe (C,E). (D) They also present reduced brain branching showed by *Smed-gpas* probe. Regeneration experiments show 11 days regenerating animals after two rounds of injection. Homeostatic animals were analyzed 26 days after the first dsRNA injection. Modified from (Rodríguez-Esteban et al. 2015)

The simultaneous inhibition of *nf-YA*, *nf-YB2* and *nf-Yc* strongly increases the phenotype, since animals cannot regenerate from the first round of inhibition (3 consecutive days of dsRNA injection following by amputation the fourth day). In addition, inhibition of the subunits in pairs also increases the single phenotype which goes in a similar direction in the inhibition of the three different subunits. These results support the role of the three subunits in the same complex (Figure 34).

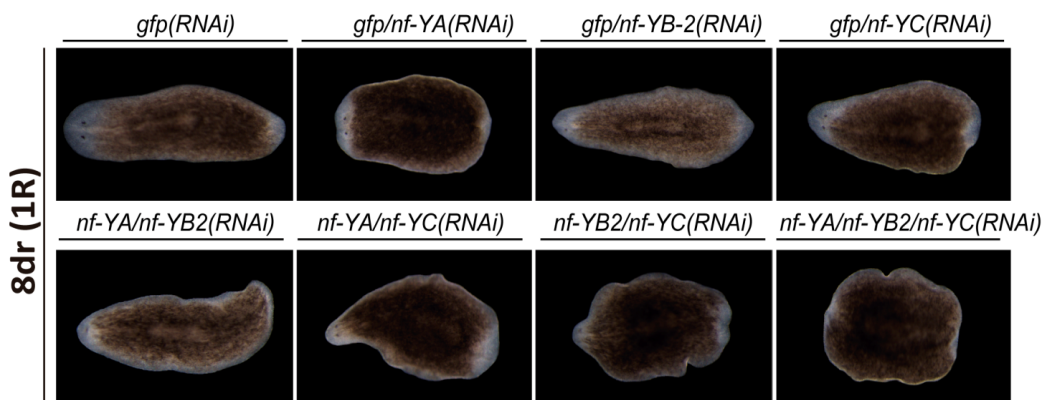


Figure 34: Phenotype observed after the injection of different combined dsRNA of *nf-YA*, *nf-YB2* and *nf-YC* during regeneration. In vivo pictures show RNAi animals 8 days after cutting.

Since the impairment of the regeneration along with the neoblasts related expression of the different subunits suggests a disturbance in the planarian stem cells, we checked the presence of this population in RNAi regenerating animals using the neoblasts marker *Smed-h2b* (Solana et al. 2012). However, the results showed that the number of *Smed-h2b*⁺ cells was not decreased but increased. Furthermore, we found *Smed-h2b*⁺ cells anterior to the photoreceptors, where they are not normally present (Oarii et al. 2005). This aberrant accumulation of

neoblasts could be caused by an excess of neoblasts divisions or, alternatively, by a possible problem in their differentiation (**Figure 35A**). Immunostaining with the antibody anti-H3P, which labels mitotic cells, shows a decrease of mitotic cells even though there were more neoblasts (**Figure 35B**). These results demonstrate that the accumulation of neoblast is not due to increased mitosis.

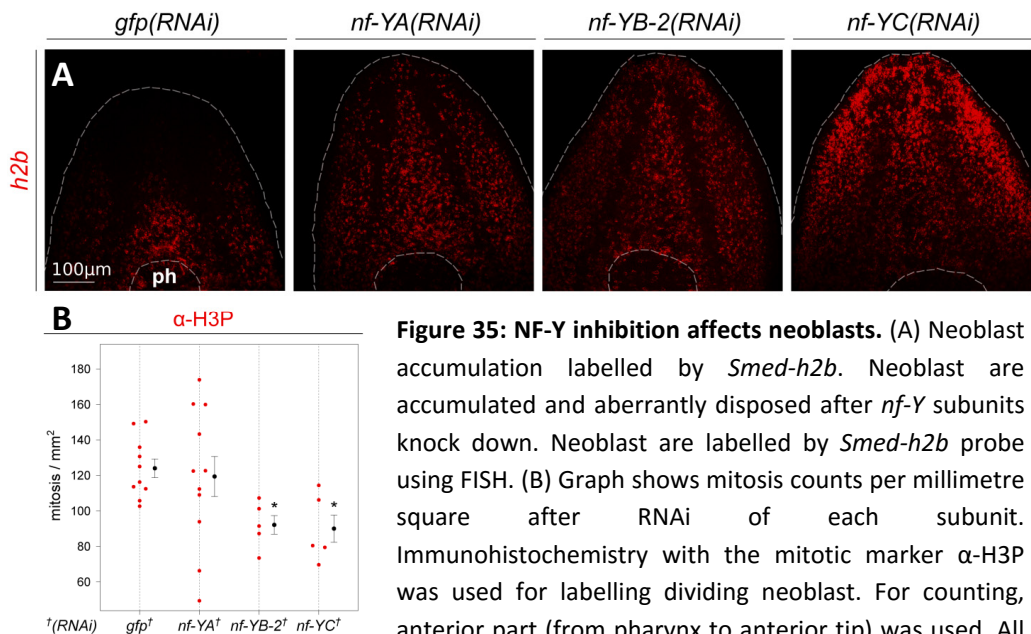


Figure 35: NF-Y inhibition affects neoblasts. (A) Neoblast accumulation labelled by *Smed-h2b*. Neoblast are accumulated and aberrantly disposed after *nf-Y* subunits knock down. Neoblast are labelled by *Smed-h2b* probe using FISH. (B) Graph shows mitosis counts per millimetre square after RNAi of each subunit. Immunohistochemistry with the mitotic marker α -H3P was used for labelling dividing neoblast. For counting, anterior part (from pharynx to anterior tip) was used. All experiments show 11 days regenerating animals. Modified from (Rodríguez-Esteban et al. 2015).

If neoblast were not accumulated by an increase of mitosis, then this could be due to a failure in the differentiation process. In planarians, the differentiation of the epidermal lineage is the most studied, since the hierarchical transition of the different cell types that give rise to epidermal cells from neoblast precursors has been characterised molecularly (Tu et al. 2015). Thus, the markers *Smed-nb.21.11e* and *Smed-agat-1* can be used to identify early and late post-mitotic

epidermal progenitors, respectively (Tu et al. 2015). WISH of these two epidermal markers after RNAi of each subunit of the NF-Y complex allowed the quantification of the early and late epidermal progenitors cells (Figure 36). The results showed a decrease in the number of early postmitotic cells (*Smed-nb.21.11e+*) in all RNAi conditions, whereas late postmitotic cells (*Smed-agat-1+*) do not show significant differences.

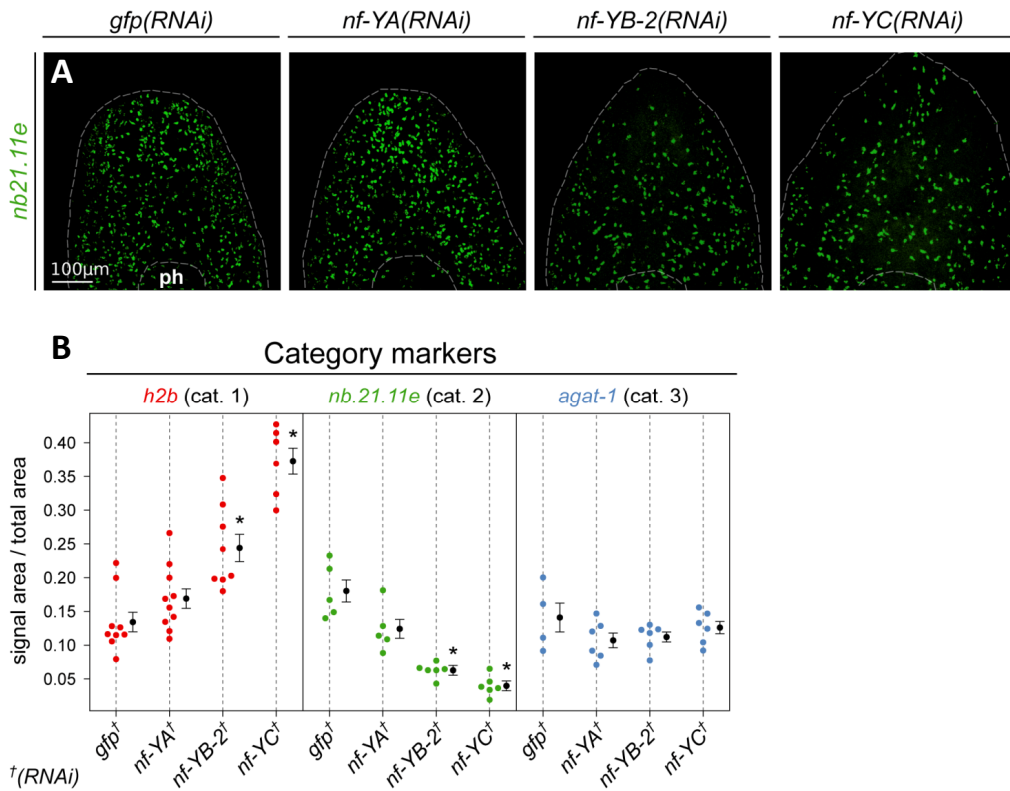


Figure 36: NF-Y produces a reduction of differentiated cells. (A) Early progeny cells marked by *Smed-nb.21.11e* probe. The early progeny is reduced in RNAi regenerating animals. (B) Graph shows quantification of *Smed-h2b* (showed in previous figure), *Smed-nb.21.11e* and *Smed-agat1* positive cells in the postblastema area. For counting, anterior part (from pharynx to anterior tip) was used. All experiments show 11 days regenerating animals after 2 rounds of dsRNA injections. Modified from (Rodríguez-Esteban et al. 2015).

The accumulation of neoblasts along with the decrease of early postmitotic cells suggests that the NF-Y complex is playing a role in the control of early epidermal differentiation events. The defects observed in the regenerating CNS suggest that the NF-Y could also be controlling the differentiation process of neural tissues. To test if NF-Y is involved in the differentiation of other cell lineages, their analysis with specific cell markers would be required.

CHAPTER II:

Krüppel-like Factor 10/11 controls the onset of mitosis in planarian stem cells and triggers apoptotic cell death required for regeneration and remodelling.

Planarian neoblasts are adult pluripotent stem cells, thus one single neoblast is able to repopulate an irradiated planarian. However, it is poorly understood how these stem cells “decide” to keep their stemness, proliferate or go ahead on the differentiation in order to maintain tissue homeostasis or to replace missing tissue. Krüppel-like transcription factors (Klf) exert multiple developmental roles and they have been described as essential master regulators of stem cells processes such as proliferation, differentiation and stemness maintenance (McConnell & Yang 2010). Since nothing was known about the role of this factors in our model, our aim was to functionally characterise the members of the KLF family during planarian regeneration and homeostasis.

5.1. Expression pattern of planarian *klf* members

We were able to identify *in silico* five putative members of the KLF family in planarian (Smed-Klf, Smed-Klfb, Smed-Klfc, Smed-Klfd and Smed-Klf10/11). One of them (Smed-Klf), was characterised during the process of this Thesis, and was shown to be required for the proper differentiation of photoreceptors cells (Lapan & Reddien 2012). Thus, we proceeded with the characterisation of the other four. The expression of *Smed-klfb*, *Smed-klfd* and *Smed-klf10/11* was ubiquitous; however *Smed-klf-c* showed a testis-related expression (**Figure 37**). Although we analysed the asexual strain of *Schmidtea mediterranea*, it has been shown that asexual planarians present germ stem cells that are not able to differentiate (Saber et al. 2016). We confirmed the expression of *Klf-c* in testis in the sexual strain (**Figure 37B**).

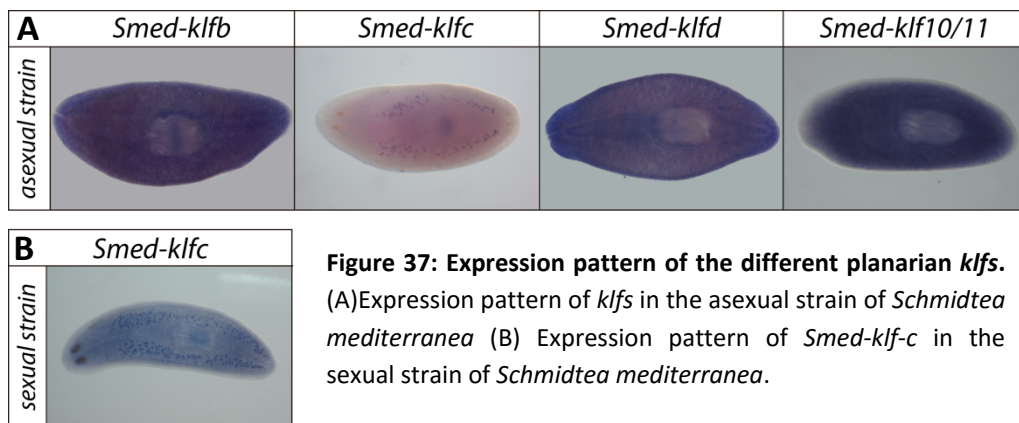


Figure 37: Expression pattern of the different planarian klfs.

(A) Expression pattern of klfs in the asexual strain of *Schmidtea mediterranea* (B) Expression pattern of *Smed-klfc* in the sexual strain of *Schmidtea mediterranea*.

To understand the possible role of Klf's during regeneration, we studied their transcriptional dynamics during regeneration through the analysis of different transcriptomic databases (Kao et al. 2013; Brandl et al. 2016). Interestingly, these transcription factors showed dynamic expression changes during regeneration suggesting a possible role during this process. *Klfb* showed two peaks of expression at 24 and 48hr, while *klfd* showed a higher expression at 6 and 24hr. On the other hand, *klfc* seemed to be down-regulated during the first hours of regeneration. *Klf10/11* showed the highest activation of the transcriptional levels during regeneration reaching expression peaks of 2.5 fold in head and tail regenerating fragments (**Figure 38A**) (Kao et al. 2013). To validate this data experimentally, we performed WISH using the *klf10/11* probe during different regenerating time points (**Figure 38B**). Although WISH is a qualitative method but not quantitative, the intensity of the probe signal shows a correlation with the previous *in silico* data. In addition, bipolar amputated trunks showed the highest expression at 12hr and 48hr (data not available in the published transcriptome) (**Figure 38B**). In any case, qPCR should be done to confirm these results. As previously described, during the first hours after amputation, there is a dynamic

proliferative response with two mitotic peaks at 6 hours and 48 hours. In the case of *klf10/11*, its expression is increased near to these time points suggesting a relationship with the mitotic response. In addition, expression of *klfb* and *klfd* at early regenerating time points suggest that they also could be involved in the control of mitotic-related genes.

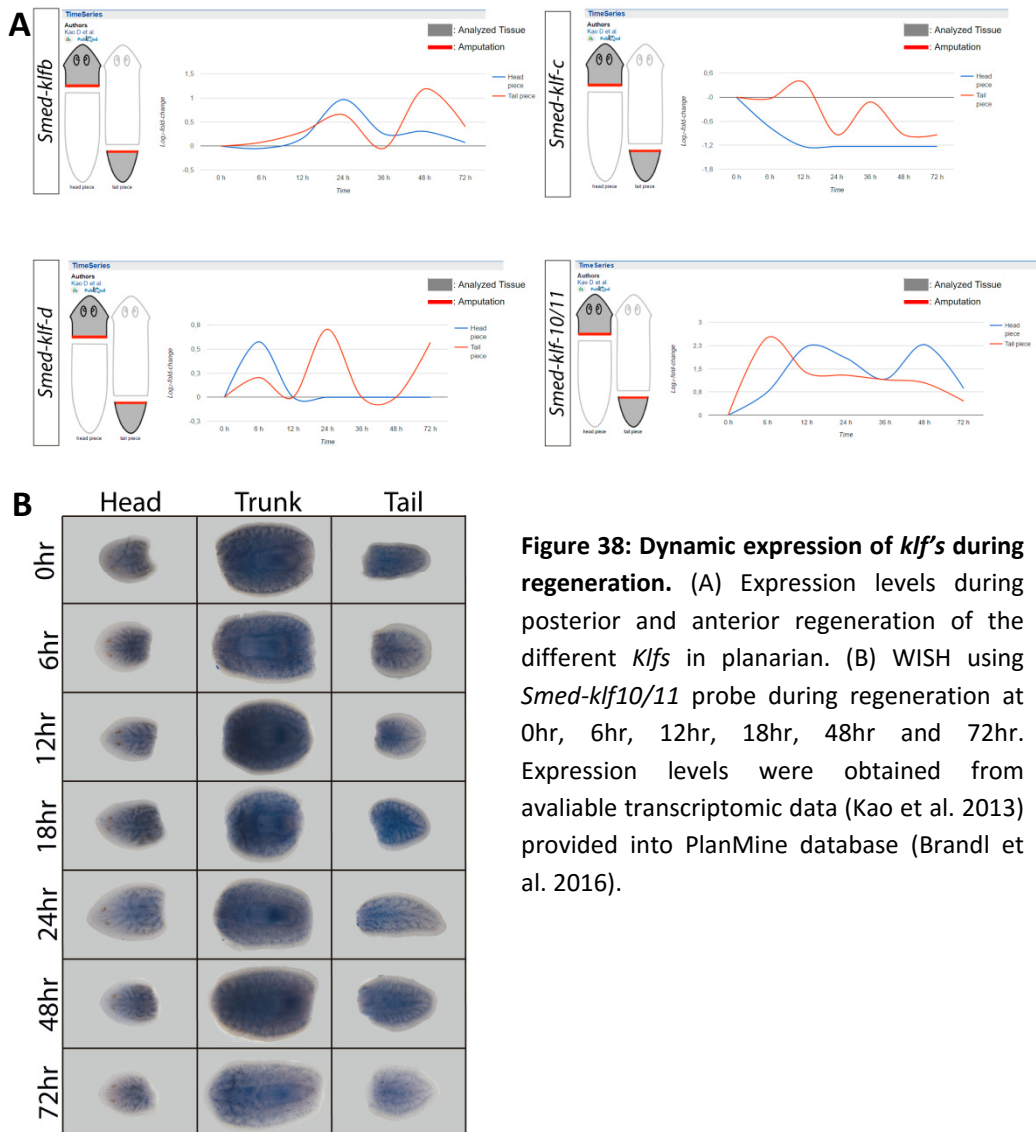


Figure 38: Dynamic expression of *klf*'s during regeneration. (A) Expression levels during posterior and anterior regeneration of the different *Klfs* in planarian. (B) WISH using *Smed-klf10/11* probe during regeneration at 0hr, 6hr, 12hr, 18hr, 48hr and 72hr. Expression levels were obtained from available transcriptomic data (Kao et al. 2013) provided into PlanMine database (Brandl et al. 2016).

5.2. Functional characterisation of the planarian Klfs

To study the possible role of these transcription factors in planarians, we performed RNAi experiments. After two rounds of dsRNA injections, only *Smed-klf10/11* inhibition gave any apparent phenotype. For that reason, along with the interesting expression pattern of *klf10/11* during regeneration lead us to focus on the study of this family member.

5.2.1. Functional analysis of *Smed-klf10/11*

The first *in vivo* phenotype found in *klf10/11* RNAi animals was an acceleration of the regeneration speed. At 3-4 days of regeneration *klf10/11* RNAi animals showed more developed photoreceptors. Thus, at 3 days of regeneration, 70% of *klf10/11* RNAi animals show eye spots, while they were not still visible in control animals. At 4 days of regeneration, RNAi animals showed bigger eyes in respect to the control, suggesting an advanced regenerative time point (**figure 39A**). To confirm our observation, we analysed the expression of *Smed-notum*, which is a Wnt inhibitor expressed in anterior blastemas and that confers anterior identity (Petersen & Reddien 2011). *Notum* shows a dynamic expression pattern in which it first appears in spread cells (12hr-1dr), it then concentrates in the anterior pole (3dr), it elongates towards the brain (4dr), and finally it reaches the definitive expression pattern, in a pool of cells in the anterior pole and two clusters associated to the cephalic ganglia (5dr) (**Figure 39B**). In *Smed-klf10/11* RNAi, *notum* brain-related expression appears earlier than *gfp* RNAi controls (**Figure**

39B) confirming the previous observation. The early appearance of photoreceptor cells in *klf10/11* RNAi planarians along with the faster progression of *notum* expression indicates that the RNAi animals regenerate faster than controls.

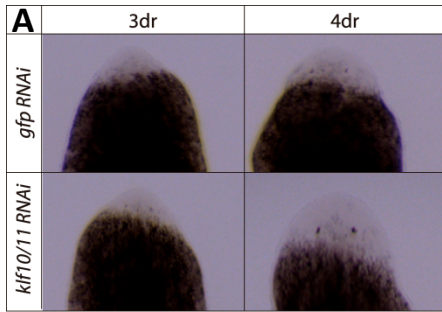
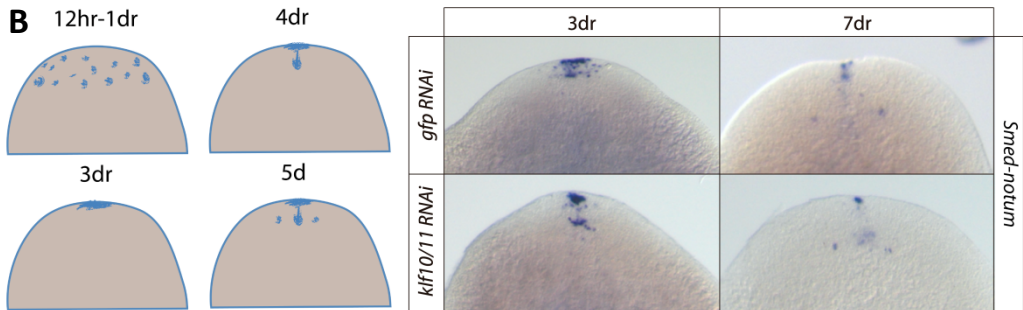


Figure 39: *KLF10/11* inhibition accelerates regeneration. (A) *Smed-klf10/11* RNAi animals showed the appearance of photoreceptors earlier than controls. (B) Schematic view of *Smed-notum* expression pattern during regeneration. *Smed-klf10/11* RNAi animals present an advanced regenerative stage according to *Smed-notum* expression pattern.



5.2.1.1. *Klf10/11* attenuates the progression of the cell cycle.

Two main ways of generating tissues and structures faster than normal during regeneration can be figured. On the one hand, the shortening of the cell cycle could generate more cells in less time. On the other hand, the increase in neoblast entering in cycle also would lead to an increase in the cells available to form the new tissue. There is a third possibility, in which the cycling population is not affected but the differentiation of cells is accelerated. In all scenarios the readout

RESULTS: CHAPTER II

could be a faster appearance of differentiated tissues, but also co-lateral effects could be expected.

If *klf10/11* is exerting its role in the cycling population, first, it should be expressed in neoblasts. To analyse it, we performed WISH using *klf10/11* probe in irradiated animals, in which neoblast are not present (Figure 40A). *Klf10/11* expression decreases after irradiation demonstrating that it is present in neoblast. To corroborate this result, we performed FISH using the *klf10/11* probe with the neoblast marker *h2b* (Figure 40B). Co-localization of both probes further demonstrates the expression of *klf10/11* in neoblast.

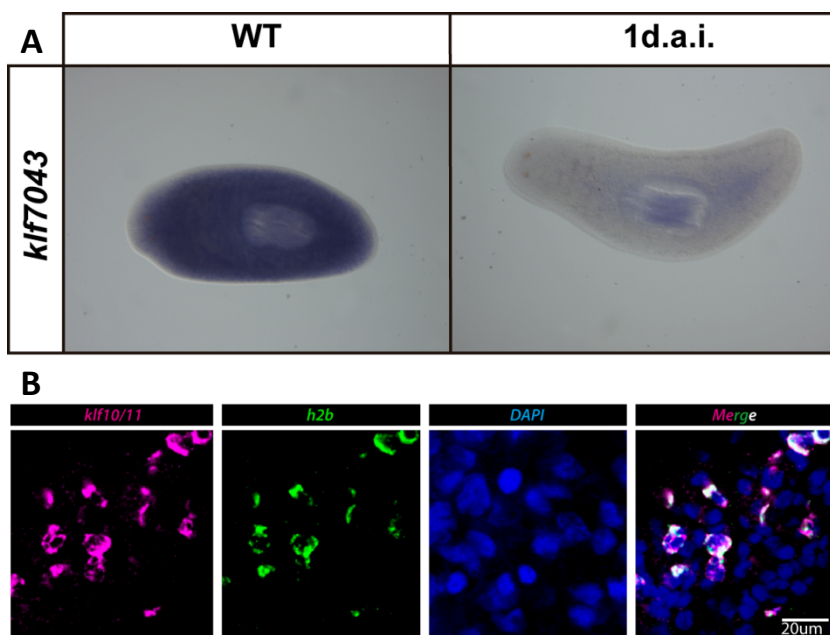


Figure 40: *klf10/11* is expressed in neoblasts. (A) WISH of *Smed-klf10/11* in wild type and lethally irradiated planarian. (B) FISH of *Smed-klf10/11* (purple) and the neoblast marker, *Smed-h2b* (green). Co-localization of both and the disappearance of *klf10/11* after irradiation demonstrate the *klf10/11* expression in neoblasts.

Once showed that *klf10/11* is expressed in neoblasts, we proceeded to the analysis of the mitotic response in *klf10/11* RNAi animals during regeneration (0hr, 6hr, 18hr, 24hr, 36hr, 48hr, and 72hr). As previously described in the introduction, during planarian regeneration two mitotic peaks have been described, at 6hr and at 48hr. As it is shown in the graphic (**Figure 41A**), in *klf10/11* RNAi animals the first mitotic peak is increased while the second mitotic peak appears earlier than in control animals. This result suggests that *klf10/11* RNAi planarians generate more neoblasts and faster than controls, which could explain the increase in the regeneration speed.

Importantly, these altered mitotic dynamics resembles the alterations observed after *jnk* RNAi in planarians (**Figure 41B**) (Almuedo-Castillo et al. 2014). However, it has been described that after *jnk* RNAi inhibition, planarians are unable to regenerate (Almuedo-Castillo et al. 2014), which does not occur in *klf10/11* RNAi planarians. An explanation could be the different expressivity of the phenotype since the percentage *jnk* RNAi animals which could not regenerate was very low (less than 10%) (Personal communication from Almuedo-Castillo).

RESULTS: CHAPTER II

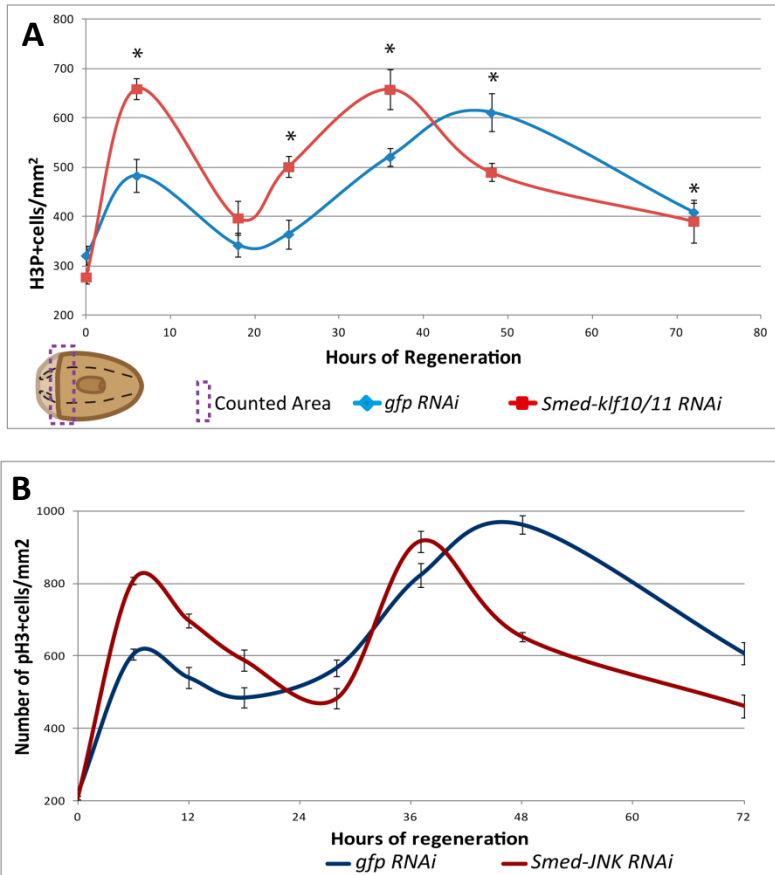


Figure 41: Mitotic dynamics during regeneration after *Smed-klf10/11* RNAi. Mitosis are detected by H3P antibody and counted in the postblastema region. (A) The first mitotic peak is higher in *klf10/11* RNAi while the second mitotic peak appears earlier than in control animals. 10 animals were used in each point. Asterisks shows significant changes, t test $p < 0,005$. (B) Graph showing the mitotic dynamics during regeneration after JNK RNAi. Modified from (Almuedo-Castillo et al. 2014).

5.2.1.2. Klf10/11 triggers the apoptosis required for proper remodelling

Previously in the introduction I already introduced that *jnk* inhibition not only affects proliferation but also inhibits apoptosis. In view of the similar phenotype observed after *klf10/11* and *jnk* RNAi regarding the mitotic response, we analyzed whether *klf10/11* RNAi was affecting apoptosis in the same manner than Jnk. To that aim, we inhibited both genes separately. After three rounds of dsRNA injections and anterior cutting both *jnk* and *klf10/11* RNAi planarian showed remodelling problems, since the relative position of the pharynx with respect to the whole body was different between RNAi and control animals (**Figure 42A, 42B**). This result already supports their role in triggering apoptosis since, as previously described in *jnk* RNAi animals, the aberrant positioning of the pharynx is caused by the lack of apoptosis and the inability to remodel the tissue and to position the pharynx according to the new proportions. In agreement, the analysis of the apoptotic response in *jnk* and *klf10/11* RNAi animals demonstrates that both apoptotic peaks, at 4 hours and at 3 days of regeneration, were highly reduced in both RNAi conditions in respect to the control.

During homeostasis, apoptosis was also reduced in both *jnk* and *klf10/11* RNAi animals. To note, apoptosis levels were equally reduced in *jnk*-RNAi and *klf10/11* RNAi. This result, along with the observation that the inhibition of both genes leads to the same disturbance of the proliferative dynamics suggests that *jnk* and *klf10/11* could be part of the same pathways, as described in *drosophila* (Muñoz-Descalzo et al. 2005).

RESULTS: CHAPTER II

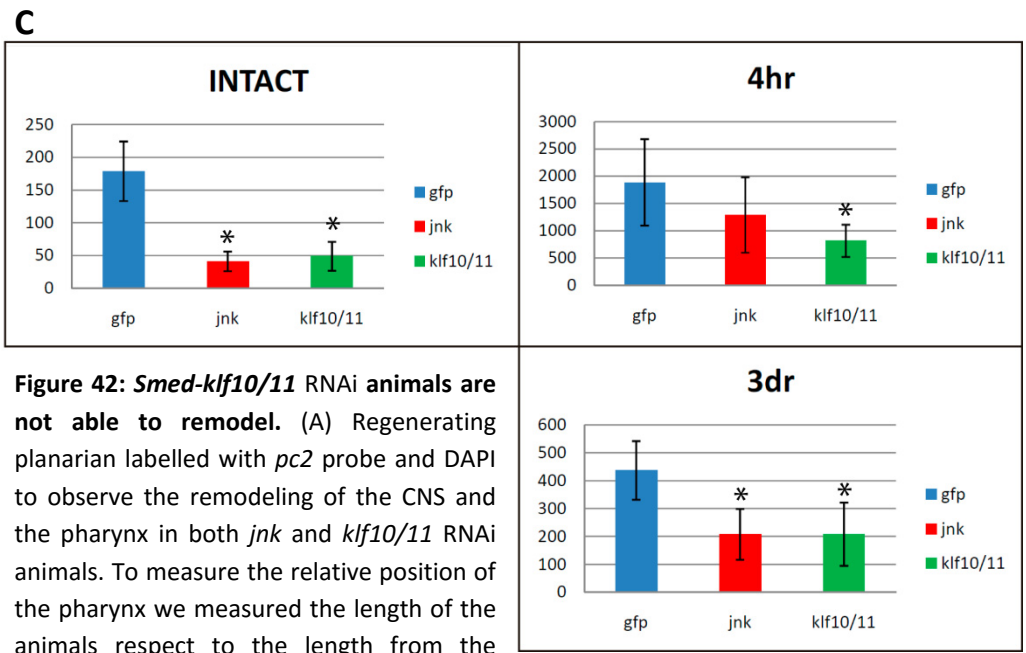
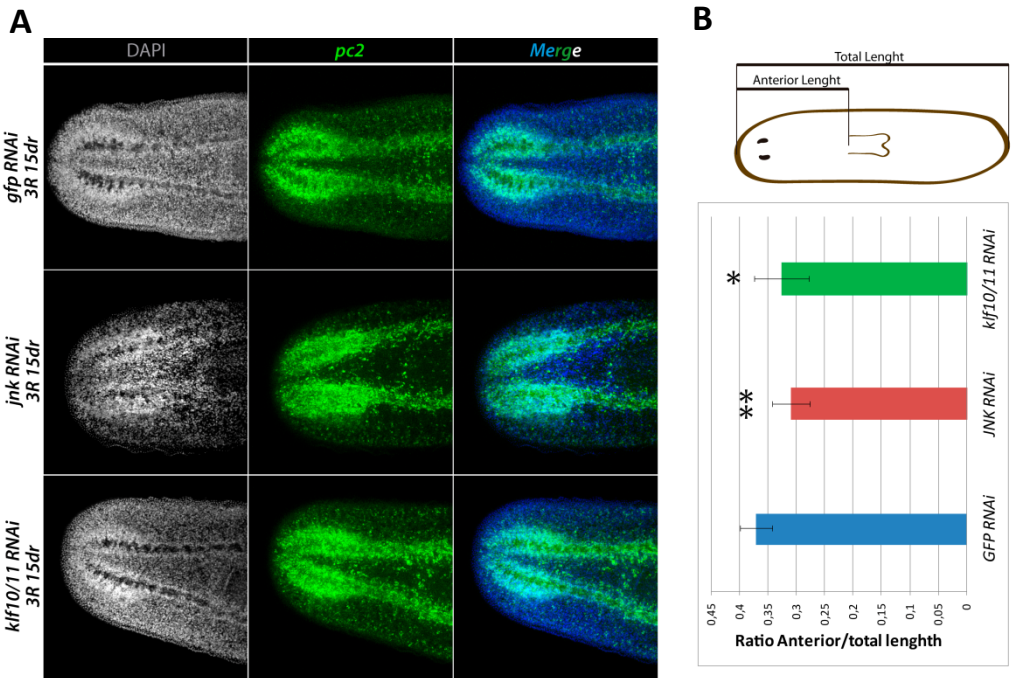


Figure 42: *Smed-klf10/11* RNAi animals are not able to remodel. (A) Regenerating planarian labelled with *pc2* probe and DAPI to observe the remodeling of the CNS and the pharynx in both *jnk* and *klf10/11* RNAi animals. To measure the relative position of the pharynx we measured the length of the animals respect to the length from the pharynx to the anterior pole.

(B) Measurements of the relative position of the pharynx. (C) Quantification of apoptotic cells labelled by tunnel assay in intact, 4 hours of regeneration and 3 days of regeneration RNAi planarian. 10 animals were used in each point in two technical replicates. Asterisks shows significant changes, ttest $p < 0,05$.

5.2.2. Klf10/11 has putative AP-1 binding sites

In the introduction section it has been explained how JNK activates the expression of its target genes through the Activator protein 1 transcription factor (AP-1) (Ruiz-romero et al. 2015; Lee et al. 1987). The *cabut* gene (the *Drosophila klf10/11* homolog) shows the consensus binding sites for AP-1, and has been shown to act downstream of the Jnk during the dorsal closure in *Drosophila* (Muñoz-Descalzo et al. 2005). We used bioinformatics prediction tools for putative binding sites (PROMO) in which we took two thousand base pairs upstream of the open reading frame of the *Klf10/11* coding region and we run the software looking for AP-1, c-Jun and c-Fos specific binding sites. We were able to identify several consensus binding sites for AP-1 upstream the *Klf10/11* coding region, suggesting that Jun and Fos are able to control *klf10/11* expression (**Figure 43A**).

To test if Jnk was controlling *Klf10/11* expression we quantified the expression levels of *klf10/11* in a *jnk* RNAi background by q-PCR. However, the result shows that inhibition of *jnk* generated a significant increase of the *klf10/11* expression levels (**Figure 43B**). This was not the expected result according to the hypothesis that *klf10/11* could be downstream of *jnk*. An explanation could be that the levels of *klf10/11* were analysed several weeks after *Jnk* inhibition. To clarify this point quantification should be done at earlier time-points.

A

PROMO prediction binding sites		
NAME	MATRIX	WIDTH
c-Jun	[T00131]	6
c-Fos	[T00124]	7
c-Jun	[T00132]	7
c-Jun	[T00133]	7
c-Fos	[T00122]	8
AP-3	[T00039]	7
AP-2alphaA	[T00035]	6
AP-1	[T00029]	8
AP-1	[T00032]	8
c-Fos	[T00123]	8
AP-2	[T00034]	10
AP-2alpha	[T00033]	9
AP-1	[T00031]	11

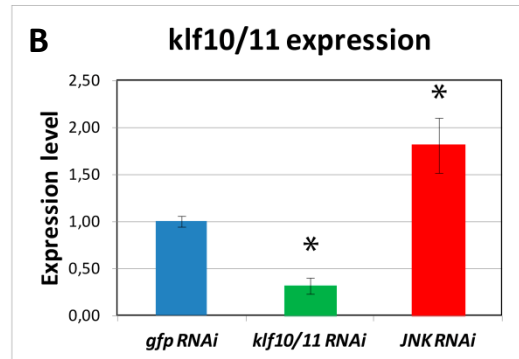


Figure 43: Klf10/11 present putative AP-1 binding sites. (A) Prediction of AP1-related binding sites upstream *Smed-klf10/11* using PROMO software. Consensus sequences for every AP-like factors and their components (jun and fos) were selected. Promo software: http://alggen.lsi.upc.es/cgi-bin/promo_v3/promo/promoinit.cgi?dirDB=TF_8.3.

B) Expression levels of *klf10/11* and *jnk* after *Smed-klf10/11* RNAi. Asterisks shows significant changes; ttest $p < 0,005$.

CHAPTER III:

WNT5-ROR2 and SLIT-ROBO-c signals
generate a mutually dependent system to
position the CNS along the medio-lateral axis
in planarians.

During evolution, Bilateralization is tied to the appearance of a CNS, composed of an anterior brain connected to the nerve cords. It is known that the symmetric organization of the CNS along the M-L axis depends on instructive signals from the midline. However, the establishment and maintenance of the M-L organization must require the integration of the midline signals with the lateral ones and the neurogenic instructions. To further understand this process, we studied the functional relationship between the Wnt-5 and the Slit signaling systems in planarians, which had been suggested to play a major role in guiding the M-L growth of the CNS.

6.1. Wnt5 acts as a repellent for neuronal growth

In planarians, *wnt5* and *slit* are expressed in complementary domains with respect to the M-L axis, being *wnt5* expressed from the CNS to the D-V border, and *slit* expressed between the CNS and the midline (**Figure 44A**) (Gurley et al. 2010; Adell et al. 2009). Furthermore, their inhibition by RNAi results in opposite phenotypes, both in intact and regenerating animals (**Figure 44B, 44C**). So, *wnt5* RNAi animals show a lateral expansion and medial disconnection of the CNS, while in *slit* RNAi animals the CNS collapses in the midline (**Figure 44B, 44C**) (Gurley et al. 2010; Adell et al. 2009). In both phenotypes, the visual axons and the photoreceptors follow the aberrant location of the CNS; *wnt5* RNAi planarians show ectopic lateral projections of their visual axons while *slit* RNAi planarians show collapsed visual axons in the midline (**Figure 44B**), and even a formation of medial ectopic eyes during homeostatic turnover (**Figure 44C**). From this data, we hypothesised that Wnt5 and Slit could be positioning the CNS

along the M-L axis through controlling neuronal growth from their domains of expression.

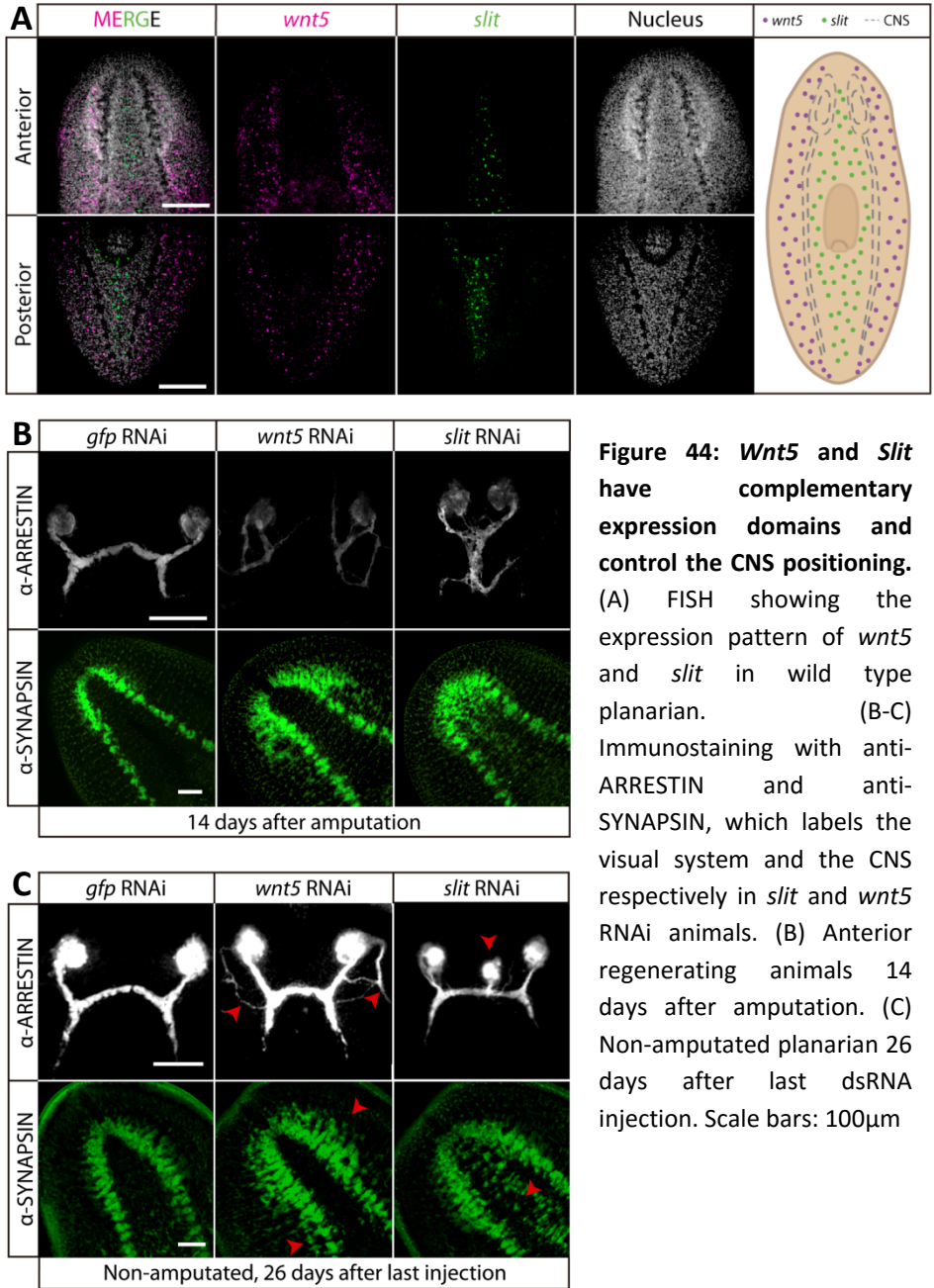


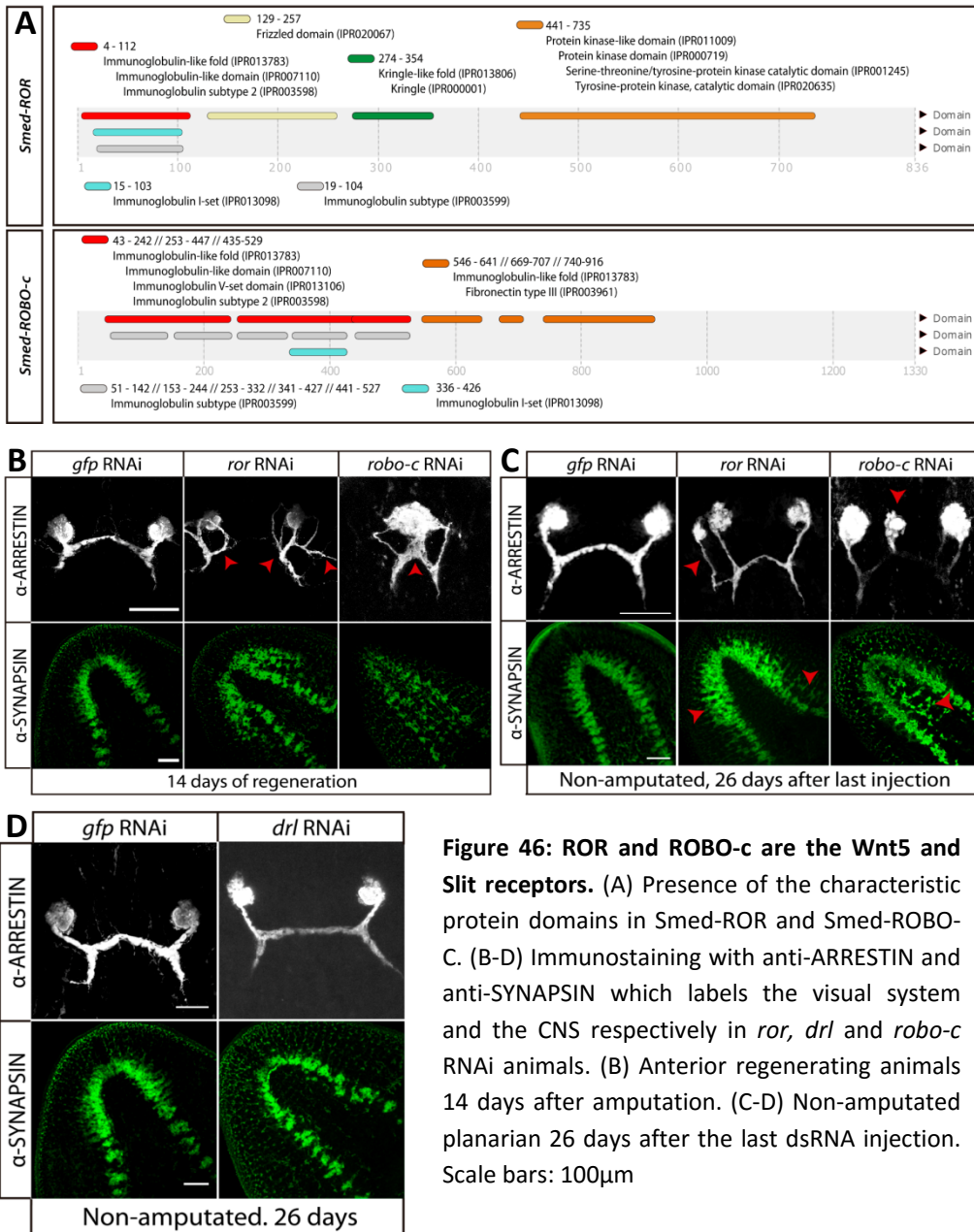
Figure 44: *Wnt5* and *Slit* have complementary expression domains and control the CNS positioning. (A) FISH showing the expression pattern of *wnt5* and *slit* in wild type planarian. (B-C) Immunostaining with anti-ARRESTIN and anti-SYNAPSIN, which labels the visual system and the CNS respectively in *slit* and *wnt5* RNAi animals. (B) Anterior regenerating animals 14 days after amputation. (C) Non-amputated planarian 26 days after last dsRNA injection. Scale bars: 100µm

The role of Slit as an axon repulsive cue is well documented in most model animals as well as in planarians (Cebrià et al. 2007). To test whether Wnt5 exerts a repulsive action for neuronal growth in planarians we tested the effect of generating an ectopic source of the WNT5 ligand through a local injection of a recombinant human/mouse WNT5 (rWNT5a), taking advantage of the high conservation of WNT5 across species (**Figure 45A**). Previously, in order to verify the activity of the rWNT5a in planarians, we tested the ability of rWNT5a to rescue the *wnt5* RNAi phenotype. We then injected rWNT5a in a regenerating blastema of *wnt5* RNAi planarians that were amputated 18-24 hours before. The injection was performed on both sides of the blastema, the region where *wnt5* is normally expressed (**Figure 45B**). The generation of these exogenous sources of rWNT5a partially rescues the *wnt5* RNAi phenotype, since 12 days after the amputation, rWNT5a injected planarians show proper connection of the brain in the midline and less lateral displacement of the brain than control planarians (**Figure 45B**). Next, we injected rWNT5a at one side of a 24 hours regenerating blastema and analysed the regeneration of the new brain 3 days later. Immunostaining with anti-synapsin shows that the exogenous source of rWNT5a produces the displacement of the newly formed nervous system towards the opposite side (**Figure 45C**). This result indicates that the function of Wnt5 in planarians is to repel the growth of the neural tissues to ensure its correct position and its integration with the pre-existent CNS.

signal via the Frizzled receptors, which are shared between canonical and non-canonical Wnts, as well as the Wnt5-specific receptors Ryk/Derailed tyrosine kinase and the Ror tyrosine kinase (Green et al. 2014). We searched for the Wnt5-specific receptors in the *S. mediterranea* transcriptomes and we found a single ortholog of a Ryk/Derailed receptor and of a Ror receptor. ROR conserve the typical domains of this type of receptors (Immunoglobulin, kringle and protein kinase domains) suggesting that it could exert similar roles than in other organisms, including the recognition of the WNT5 ligand (**Figure 46A**). Their functional analysis by RNAi demonstrates that while *Ryk/Derailed* RNAi only causes mild defects in the regeneration of the brain, which appears thinner (**Figure 46D**), *ror* RNAi phenocopies the *wnt5 RNAi* phenotype, that is lateral expansion of the CNS and disconnection of the anterior commissure and the optic chiasm, both in intact and regenerating planarian (**Figure 46B, 46C**).

Roundabouts receptors (Robos) are the evolutionary conserved SLIT receptors. Two Robo homologs (Robo-a and -b) had been described in planarians, but their RNAi phenotype was not related with the one found after *slit* inhibition (Cebrià & Newmark 2007). In the transcriptomic databases (Brandl et al. 2016) we found a third Robo receptor (*Smed-robo-c*), which also conserves the characteristic protein domains of this receptor family (Immunoglobulin and fibronectin domains)(**Figure 46A**). Importantly, its inhibition phenocopies the *slit* RNAi phenotype, producing the collapse of the CNS and the visual system in the midline (**Figure 46B, 46C**). These results indicate that ROR and ROBO-C are the receptors through which WNT5 and SLIT exert their repulsive action towards the neuronal growth in planarians.

RESULTS: CHAPTER III



6.2.1. *Ror* and *Robo-c* are co-expressed in neuronal cells.

Expression analysis shows that both *ror* and *robo-c* are expressed in the CNS, among other tissues (**Figure 47A**). Their expression in neural cells is confirmed by co-expression with *pc2*, a neural marker (Cowles et al. 2013)(**Figure 47C**). Furthermore, double FISH and quantification of *ror+/*roboC*+ cells* demonstrate that they co-localize in most cells in the cephalic ganglia and in the VNCs, as well as in the photoreceptors (>80%) (**Figure 457C, 47D, 47E**). The co-expression of *ror* and *robo-c* in neural cells is supported by *in silico* analysis of the single cell (SC) expression data from planarians recently published (**Figure 47D**) (Wurtzel et al. 2015). These results indicate that the receptors of WNT5 and SLIT are expressed in neural cells, in agreement with the hypothesis that both signals control neuronal growth, and furthermore that the same neurons are sensitive to both signals. Thus, Wnt5 and Slit, acting from opposite domains, could establish a corridor to guide the path of the growing axons (**Figure 47F**).

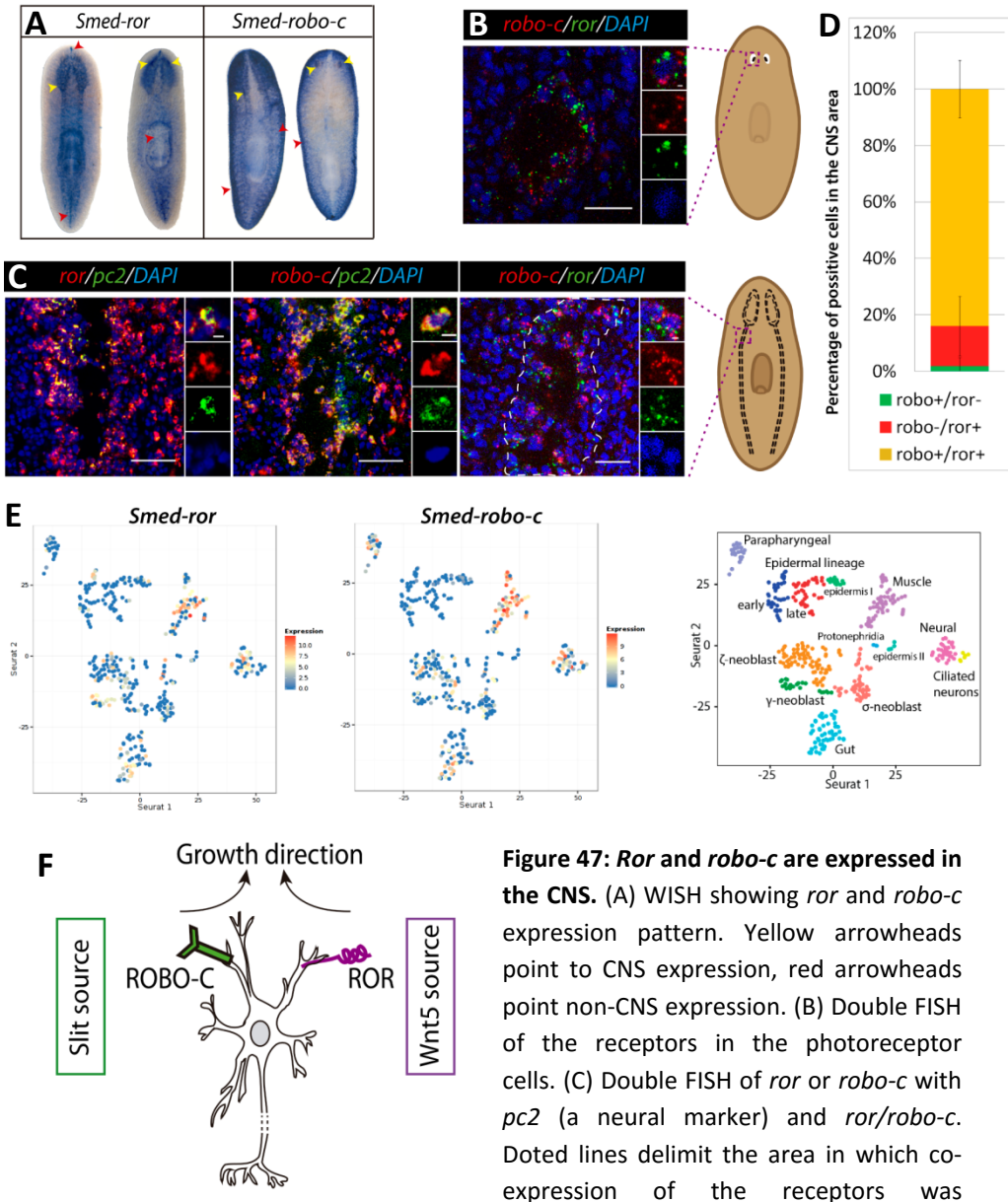


Figure 47: *Ror* and *robo-c* are expressed in the CNS. (A) WISH showing *ror* and *robo-c* expression pattern. Yellow arrowheads point to CNS expression, red arrowheads point non-CNS expression. (B) Double FISH of the receptors in the photoreceptor cells. (C) Double FISH of *ror* or *robo-c* with *pc2* (a neural marker) and *ror/robo-c*. Dotted lines delimit the area in which co-expression of the receptors was

(D) Quantification of *ror+/robo-c+* cells in the CNS. (E) Single cell expression obtained from the SC RNAseq data showing the cell types in which both receptors are expressed. (F) Scheme of the working model: neurons express Wnt5 and Slit receptors in order to respond to both signals, which arrive from opposite domains, and thus growing in the correct M-L position. Scale bars: 25µm in FISH and 5µm in magnifications.

6.3. *Ror* and *Robo-c* are expressed in muscular cells that express *slit* and *wnt5*, respectively.

Ror and *robo-c* are expressed mainly in neural cells, but both of them appear also to be localised in discrete domains outside the CNS: *ror* is expressed in the dorsal and ventral midline and *robo-c* is expressed in the margin of the animal. Interestingly, both receptors are expressed in complementary domains, but in the opposite domains with respect to their ligands. That is, *ror* is expressed in the midline as the ROBO-c ligand, *slit*, and *robo-c* is expressed in the margin, as the ROR ligand, *wnt5* (Figure 47A, red arrowheads). To test whether the ligand and the receptor of the opposite ligand were co-expressed in the same cells, we performed a double FISH (Figure 48A). The result shows that there are *slit*⁺ cells in the midline which also express *ror* while in the margin of the animal are *wnt5*⁺ cells which express *robo-c*. The quantification of these co-localization between *wnt5/robo-c* and *slit/ror* shows that all the *slit*⁺ cells in the midline are *ror*⁺, and that all *wnt5*⁺ cells in the margin of the animal are *robo-c*⁺ (Figure 48A).

Slit and *Wnt5* are described as positional control genes (PCGs), which are genes responsible to pattern the planarian body, and which are expressed in the muscular cells covering all the planarian body (Witchley et al. 2013). Co-expression of *slit* and *wnt5* with *tropomyosin*, a muscular marker, confirms that all *slit*⁺ and *wnt5*⁺ cells are muscular cells (Figure 48B) (Witchley et al. 2013), thus, the cells *slit*⁺/*ror*⁺ and *wnt5*⁺/*robo-c*⁺ are muscular cells. This result is confirmed in the *in silico* analysis of the single cell (SC) expression data (Figure 48c) (Wurtzel et al. 2015).

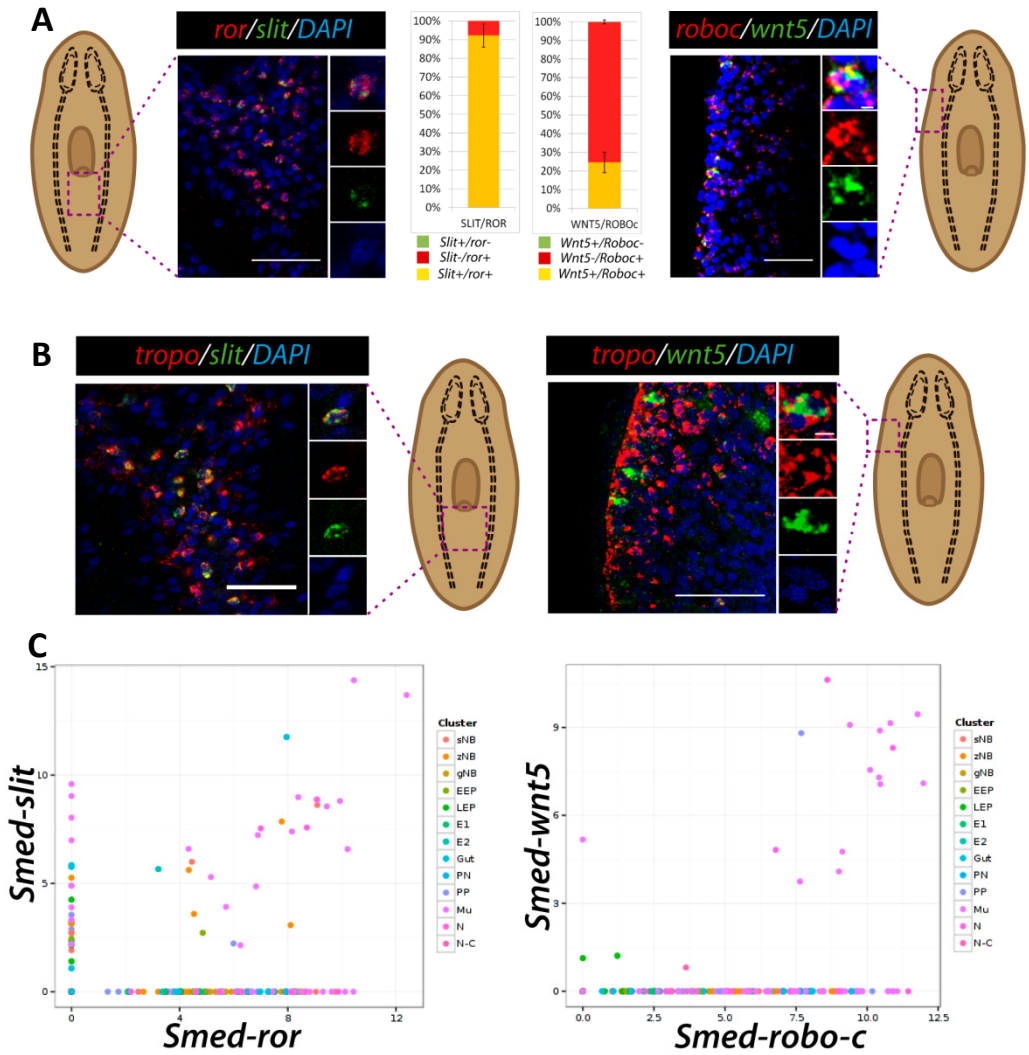


Figure 48: *ror/slit* and *robo-c/wnt5* co-localize in muscular cells. (A-B) Double FISH of *ror/slit* and *robo-c/wnt5* in wild type planarian (A) FISH shows co-localization of *ror/slit* and *robo-c/wnt5* probes. Graphs show the quantification of the co-localization. (B) *wnt5* and *slit* are expressed in muscular cells, as they co-localize with the muscular marker tropomyosin (*tropo*). (C) Single cell expression obtained from data (Wenemoser & Reddien 2010) showing cells expressing *ror/slit* and *robo-c/wnt5*. Scale bars: 25µm in FISH and 5µm in magnifications.

It was recently reported the existence of glial cells in planarians, which could also express *tropomyosin* (Roberts-Galbraith et al. 2016; Wang et al. 2016), and in other organisms they are responsible for the secretion of axon repulsive cues, such as WNT5 and SLIT (Christian Klämbt & Goodman 1991; C Klämbt & Goodman 1991; Battye et al. 2001; Cardenas Castillo 2016). Therefore, we reasoned that *slit*⁺ and/or *wnt5*⁺ cells could be glial cells. To check it we performed a double FISH using a reported glial marker in planarians (*intermediate filament-if*) (Wang et al. 2016; Roberts-Galbraith et al. 2016). The result shows that *wnt5* nor *slit* co-express with *if*, indicating that, at least those glial cells described in planarians are not secreting WNT5 or SLIT ligands (Figure 49).

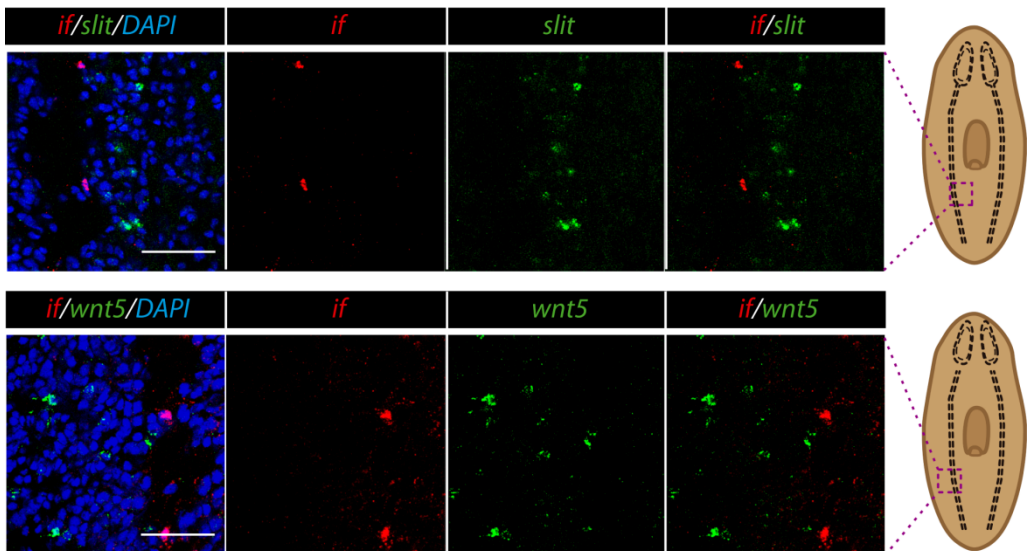


Figure 49: *Wnt5* and *slit* are not expressed in glia cells. Double FISH of the glial marker *intermediate filament (if)* with both, *wnt5* and *slit* probes. FISH shows no co-localization of this markers suggesting that *wnt5* and *slit* are not expressed in glial cells. Scale bars: 25 μ m.

Overall, our results show that besides their expression in neuronal cells, *ror* and *robo-c* are expressed in muscular cells that also express the ligand of the other receptor. Thus, the muscular *wnt5*⁺ cells in the lateral domain express the Slit receptor *robo-c*, and the muscular *slit*⁺ cells in the midline express the Wnt5 receptor *ror* (Figure 50). This result suggests that the Wnt5/Ror and Slit/Robo-c systems not only position the CNS through a repulsive action from opposite domains, but, they could also be mutually regulated, providing self-regulative properties to the M-L axis patterning.

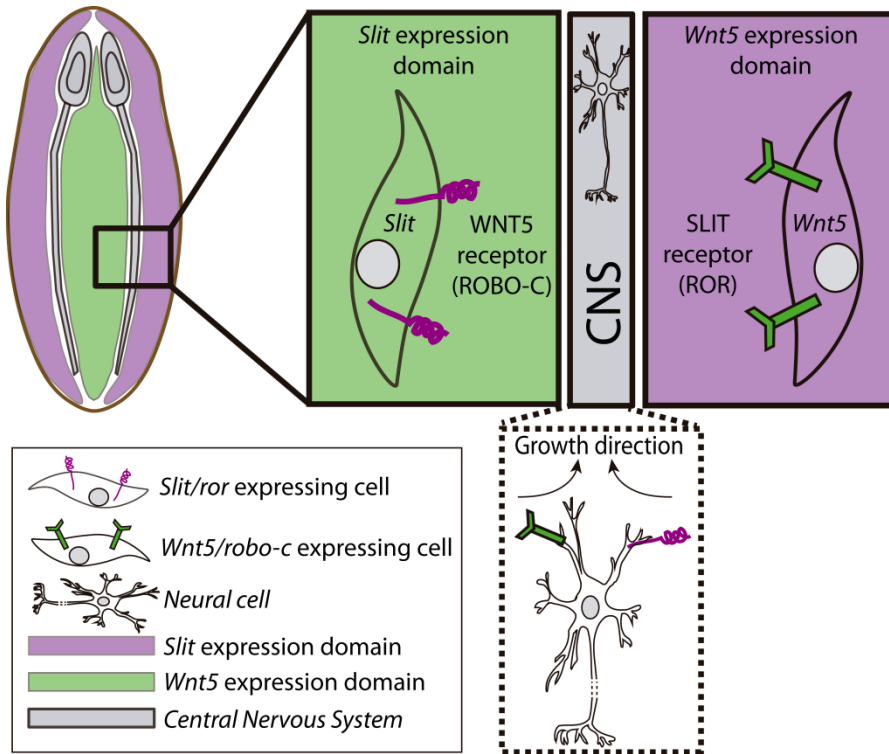


Figure 50: Schematic representation of the results observed with respect to Wnt5-Ror/Slit-Robo-c. Both receptors are expressed in neural cells, responding to the repulsive action of Wnt5 and Slit signals, which are expressed in muscular cells at both sides of the CNS. The Wnt5 receptor (ROR) is expressed in *slit* expressing cells and the Slit receptor (ROBO-C) is expressed in *wnt5* expressing cells, suggesting a regulatory link between both systems.

6.4. Wnt5-Ror/Slit-Robo-c signalling systems could act as a self-regulatory system to define their respective expression domains

According to the previous results, we hypothesized that Wnt5-Ror and Slit-Robo-c signalling systems could comprise act as a self-regulatory system to define their respective expression domains. We approach the veracity of this model we developed a mathematical model of the network and we analyzed the transcriptional relationship between the four elements of the system.

6.4.1. Modeling of the Wnt5-Ror/Slit-Robo-c signalling system

With the previous results and in collaboration with Luciano Marcon (FML Max Planck Society, Tübingen, Germany), who developed the RDNets software (Marcon et al. 2016), we generated a gene topology network to understand the interactions which could be occurring between the four elements of the Wnt5-Ror and Slit-Robo-c signalling systems.

For the generation of the topology, the requirements were the complementary expression domains of *wnt5* and *slit*, and the activation of ROR and ROBO-c receptors by the secreted molecules WNT5 and SLIT respectively. The resulting topology suggests that a Turing-like model could explain the presence of two different domains of expression that regulate on each other through the presence of the receptor of the secreted molecules in the opposite domain (**Figure 51**). In this topology, WNT5 and SLIT would activate their own receptors, ROR and ROBO-C. Moreover, ROR would inhibit ROBO-c while ROBO-c would activate ROR. In addition, SLIT would activate the Wnt5 receptor ROR.

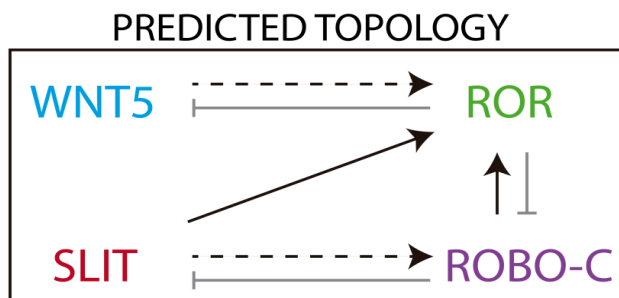


Figure 51: Topology Network of the Wnt5-Ror and Slit-Robo-c system. Doted lines designated physical activation of the receptors. Grey lines show inhibitory interaction while dark arrows show activation. Generated by RDNets software: <http://marconlab.org/RDNets/rdnets.php?name=home>

6.4.2. The boundary of expression between *Wnt5* and *Slit* is not defined at early regeneration stages

A self-regulatory system has the property to pattern an initially disorganised tissue. To test whether this is the case in planarians, we analysed whether the domains of expression of *wnt5* and *slit* were not defined during early regeneration. Our results show that between 14 hours and 2 days after amputation *wnt5* expressing cells are found at both sides of the VNCs (**Figure 52**). Thus, *wnt5* and *slit* are expressed following a salt-and-pepper expression pattern in the midline of the regenerative region. However, during the first days of regeneration, the expression of *wnt5* and *slit* is reorganized and at 3 days, *wnt5* expression is completely re-localized in the lateral domain, coinciding with the new formation of the brain primordia (**Figure 52**). The salt-and-pepper expression at early regenerating time points supports the self-regulatory properties of the topology presented.

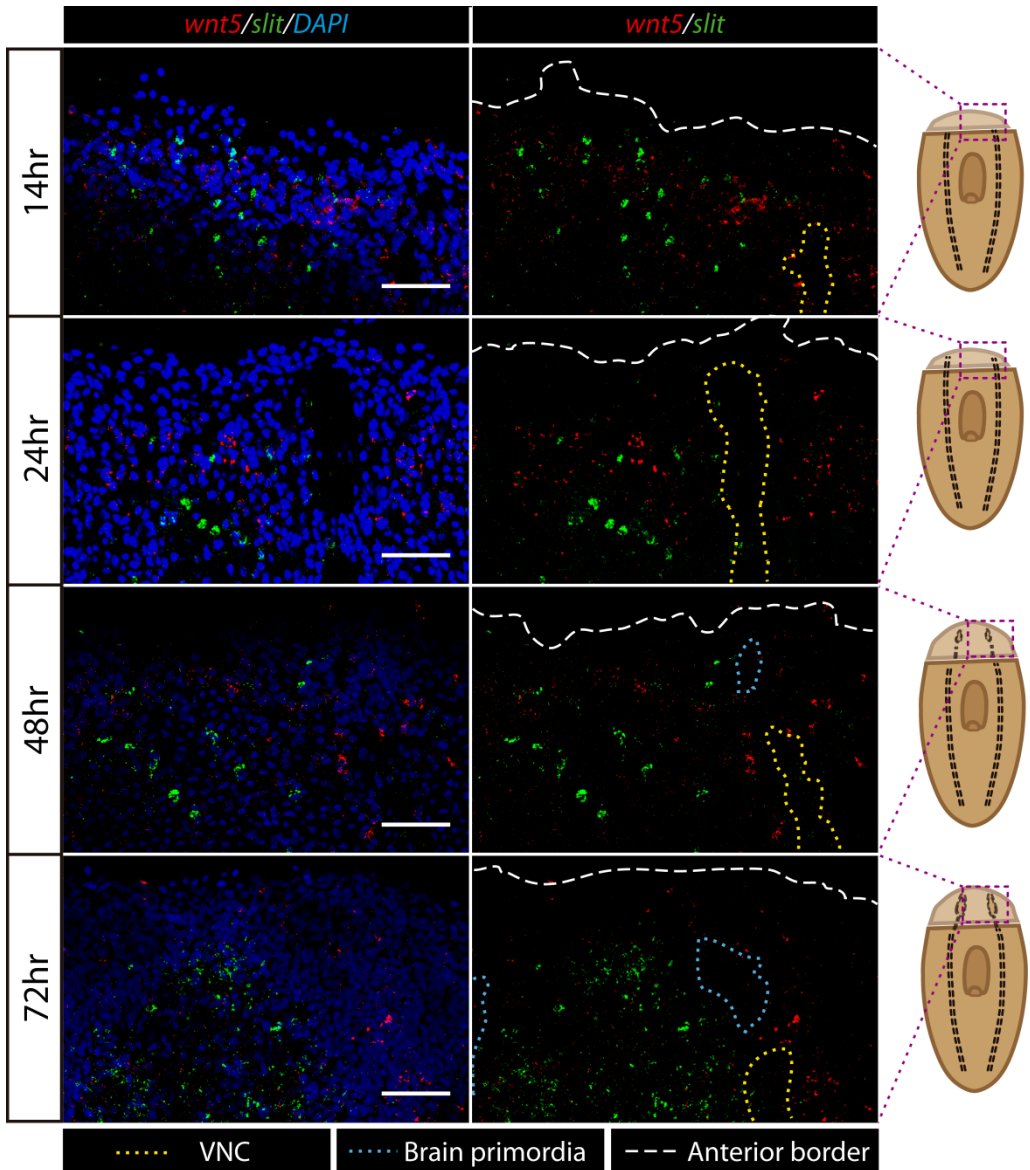


Figure 52: The boundary of expression between *Wnt5* and *Slit* is not defined at early regeneration stages. Double FISH at different early regeneration time points. Before 3 days of regeneration, *wnt5*⁺ cells are found in the *slit* expression domain, in a salt-and-pepper pattern. At two 2-3 days, when the brain primordia is forming (blue dotted line) *wnt5* expression gets confined to the lateral domain (Yellow dotted lines show VNC).

6.4.3. WNT5-ROR and SLIT-ROBO-c regulation occurs by transcriptional changes

One of the requirements for the proper execution of the previous model consists on transcriptional variations after the alteration of single elements. To experimentally understand how these changes are produced we measured through qPCR the transcriptional changes of each element after the inhibition of each one of them (**Figure 53A**). The results show that after *slit* inhibition there is a significant decrease of the Wnt5 receptor *ror*, supporting a regulative role of the Wnt5 receptor through Slit, thus both are expressed in the same muscular cells as previously described. In addition, *ror* inhibition increases *slit* expression corroborating this co-regulative effect between the Wnt5 receptor and Slit. On the other hand, *wnt5* inhibition produces an increase of *robo-c* expression, which also fits with the co-localization of both transcripts in muscular cells. Finally, the inhibition of *robo-c* also increases *slit* and *ror* expression (**Figure 53A**). Although the observation of the expression levels after the inhibition of each element of the system, we are not able to directly compare these results with the previous topology since the qPCRs are the transcriptional levels at one exactly moment and the topology predicts dynamic interactions. In addition, the transcriptional changes can be caused by direct or indirect interaction effects (**Figure 53B**). However, these results strongly suggest the veracity of the self-regulatory system between Wnt5-Ror/Slit-Robo-c.

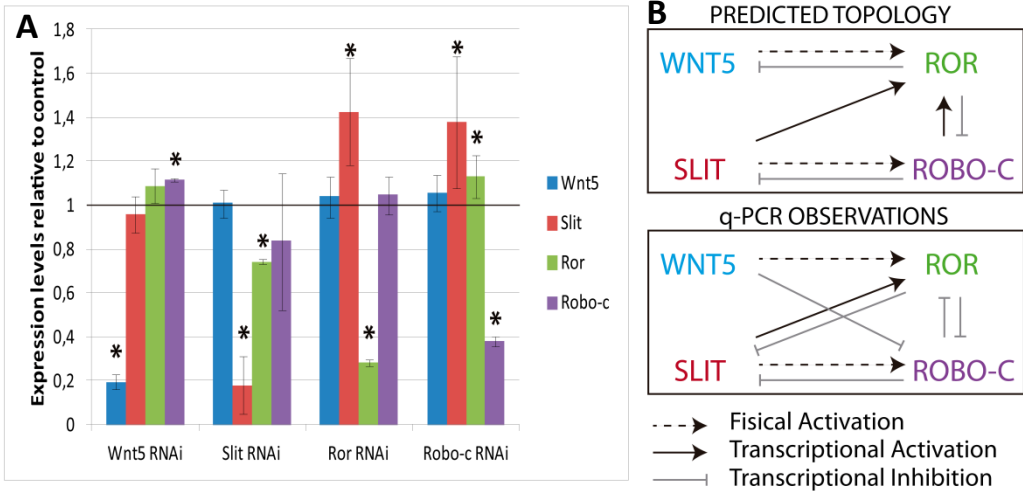


Figure 53: WNT5-ROR and SLIT-ROBO-c regulation occurs by transcriptional changes. (A) q-PCRs of *wnt5*, *slit*, *ror* and *robo-c* RNAi samples to check the expression levels of each element. Quantification respect to *gfp*RNAi animals and normalized to *ura4*. Asterisks show significant changes (ttest $p < 0.05$). (B) Comparative between the topology network predicted and the results obtained by q-PCRs.

6.4.4. Wnt5 is required to establish the *slit* expression domain

According to our initial hypothesis, the expression of *wnt5* and *slit* should be mutually regulated. To experimentally check this relationship, we analysed by in situ hybridization the expression of *wnt5* in *slit* RNAi animals and the expression of *slit* in *wnt5* RNAi planarians. The result shows that, after 3 weeks of inhibition, *wnt5*⁺ cells are found in the *slit* domain in *slit* RNAi animals, and that *slit*⁺ cells are found outside the normal *slit* expression domain (Figure 54A). After a sagittal amputation, which requires a major remodelling of the M-L axis, control animals are able to re-define the *slit* expression domain 8 days after amputation. However, at the same time point *slit* and *wnt5* RNAi planarians are not able to re-

define the expression pattern of *wnt5* or *slit*, respectively (**Figure 54B**). To further understand the mutual dependence between *wnt5* and *slit*, we performed a gain of function experiment in which rWNT5a was injected at one side of regenerating blastemas. The result shows that ectopic source of rWnt5a produces the displacement of *slit*⁺ cells towards the opposite side (**Figure 54C**). It was not possible to perform the gain of function experiment with *slit*, since we did not found a recombinant protein functional in planarians.

Overall, those experimental results indicate that the domain of expression of *slit* and *wnt5* are mutually defined. This mutual regulation takes place during homeostatic cell renewal and during the *de novo* specification of the *slit* and *wnt5* domains during regeneration.

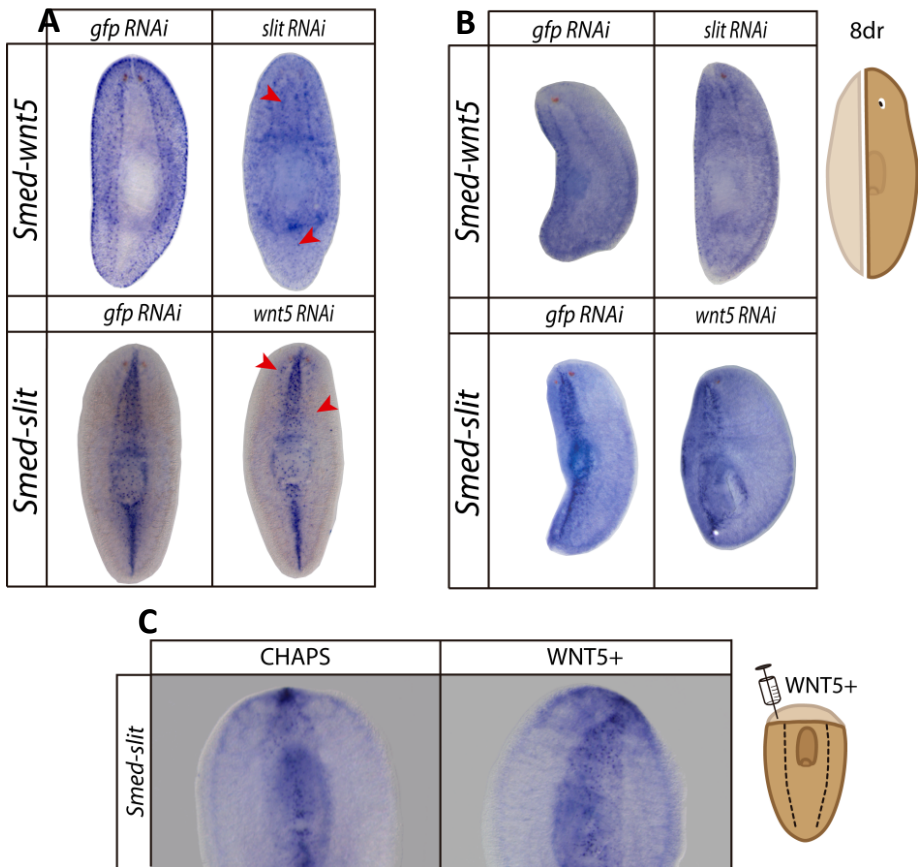


Figure 54: Dependence of *Slit* expression on *wnt5* expression. (A) *wnt5* RNAi planarians show ectopic appearance of *slit*⁺ cells outside the normal *slit* expression domain and *slit* RNAi planarian show ectopic appearance of *wnt5*⁺ cells outside their domain. (B) Sagittal amputation in *wnt5* RNAi planarian impairs the re-definition of the *slit* expression boundary. (C) rWNT5a injections at one side of a 2 days regenerating blastemas exert a repulsive role in *slit* expression, displacing it to the opposite side.

6.4.5. An ectopic source of WNT5 in the *slit* expression domain locally inhibits *slit* expression.

The previous experiment demonstrated that the *slit* expression domain is Wnt5 dependent. To test whether Wnt5 regulates *slit* transcriptional levels we injected the rWNT5a protein at the posterior midline in the *slit* expression domain. One day after the injection, *slit* expression locally disappeared in the injected area (80% of the injected animals) (**Figure 55**), suggesting that Wnt5 transcriptionally repress *slit*. An alternative explanation could be that Wnt5 could promote the migration of *slit*⁺ cells away from the rWNT5a source. However, the analysis by FISH of the *slit*⁺ cells showed that the amount of *slit*⁺ cells around the rWNT5a injected area is not different between controls and injected animals. To test whether the repression of *slit* by Wnt5 was dependent on the *ror* receptor, which is expressed in this region, the same experiment was performed in *ror RNAi* animals. The result shows that *ror RNAi* rescues the phenotype produced after rWNT5a injection, thus, in those animals *slit* expression is not affected (**Figure 55**).

These results demonstrate that the over-expression of rWNT5a locally inhibits the transcription of *slit* and that this action is through the WNT5 receptor ROR.

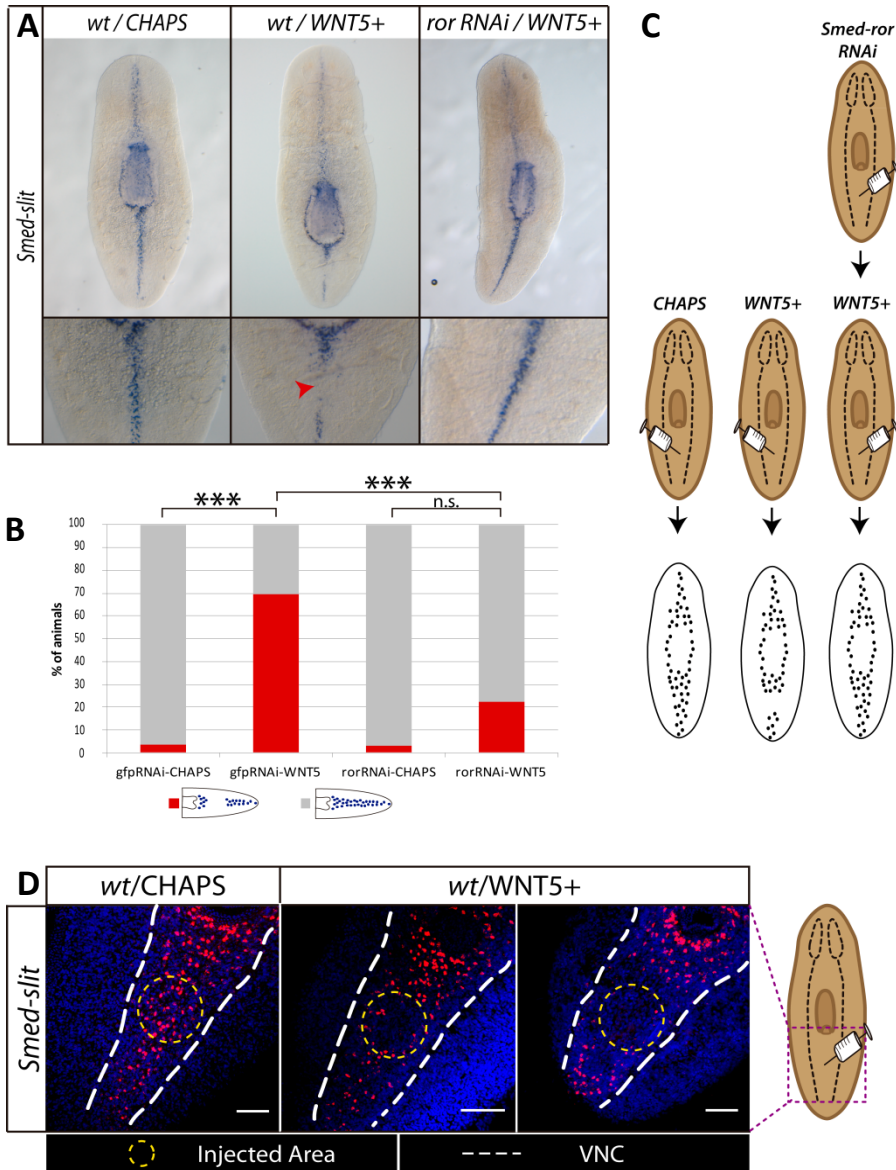


Figure 55: Injection of rWNT5a in the *slit* expression domain locally inhibits *slit* expression. (A) WISH of *slit* shows its interrupted expression in the rWNT5a injection region. Inhibition of the Wnt5 receptor *ror* rescues the *slit* interruption after rWNT5a injection. (B) Graph shows the quantification of animals with interrupted *slit* expression. Asterisk shows significant differences. (Chi Square with Bonferroni correction; critical value: 0,05). (C) Schematic view of the designed experiment. (D) FISH using *slit* probe shows that the *slit* expression disappearance is not due to migration of *slit*+ cells. Scale bars: 100µm.

RESULTS: CHAPTER III

In summary, our results support that the M-L organisation of planarian tissues is controlled by the WNT5/SLIT signalling system, which conform a self-organizing system with two main functions: 1) to position the CNS through their repulsive action from opposite domains, and 2) to define their own expression domains.

DISCUSSION

During this PhD Thesis different aspects of the regeneration and cell turnover processes in planarians have been approached. Nevertheless, the manuscript has been split into three main parts, which correspond to three main cellular processes: balance between proliferation and apoptosis, differentiation and positional instructions. It is necessary to remark that every process is interconnected. The data presented in this thesis contributes to better understand specific aspects of these three main processes showing new data and opening new questions which I will try to analyse and discuss during this section. Although in the previous sections, proliferation and apoptosis, differentiation and positional instructions have been approached separately, during this section I will discuss specific results concerning each process but also how all processes could be interconnected to regulate as a whole adult regeneration and tissue turnover.

CHAPTER I:

Nuclear Factor Y complex controls neoblast differentiation avoiding the proper regeneration and homeostasis.

NF-Y is a transcriptional complex which function relies on being the core of the transcriptional regulation. Therefore, this complex controls many genes involved in a wide variety of processes like proliferation, differentiation, axon targeting, etc (Hughes et al. 2011; Matuoka & Yu Chen 1999; Bhattacharya et al. 2003; Morey et al. 2008). Our results suggest that in planarians the NF-Y exerts a role in the functionality of neoblast during homeostasis and in their early differentiation during regeneration. Below I will discuss the specific aspects of the NF-Y function in planarians.

7.1. The NF-Y heterotrimeric complex is required to drive target gene expression in planarians

Some studies describing the NF-Y transcriptional complex propose that NF-Yb and NF-Yc could be enough to control gene expression (Romier et al. 2002). Although our results are just preliminary, they point to the requirement of the three subunits to carry gene expression in planarians. Thus, we observe a very similar phenotype after inhibition of the three subunits alone, and the combinatorial inhibition of the three subunits does not produce new phenotypes but an increase of the phenotype observed by single inhibition.

As previous described, the formation of the heterodimer NF-Yb/NF-Yc is required for the binding of the NF-Ya subunit to finally form the heterotrimeric complex. In planarian, our results show different penetrance of the phenotype, being *nf-yb2* and *nf-yc* RNAi phenotypes stronger than *nf-ya* RNAi. It could be that the

interruption of the formation of the dimer NF-Yb2/NF-Yc is enough to avoid the functionality of the entire complex. In addition, the combinatorial gene knock down of the three subunits also corroborate this hypothesis, since inhibition of both *nf-yb2* and *nf-yc* at the same time increases the phenotype with respect to the other cases. Furthermore, the inhibition of the three elements of the complex at the same time shows the stronger phenotype. To fully corroborate if all the members of the complex are required for its functionality, identification and expression analysis of different target genes should be carried out after the inhibition of each subunit.

7.2. Duplication and functional specialisation of NF-Yb

The requirement of the three subunits to make a functional transcriptional NF-Y complex opens a new question in respect to the function of this complex in planarian; thus in *Schmidtea mediterranea* two different NF-Yb subunits have been found (*Smed-NF-Yb* and *Smed-NF-Yb2*). While we have seen that NF-Yb2 seems to be controlling neoblast early differentiation events, NF-Yb has been related with self-renewal and proliferation of planarian spermatogonial stem cells (Iyer et al. 2016). Even though the NF-Yb function has been described in the planarian sexual strain, and the NF-Yb2 role is described in the asexual strain, both genes are present in both strains and in other planarian species (**Annexes II and III**). Thus, it would be necessary to study the role of both subunits in sexual and asexual strains to understand whether they exert specific roles in different cell types, since the presence of this duplication suggest a possible functional specialisation. It

would also be interesting to test whether both NF-Yb and –Yb2 require the NF-Ya and NF-Yb subunits for their function. In this case, it could be that the presence of a specific B subunit could direct the cell-specificity of the whole complex and thus its transcriptional activity and the target genes.

7.3. Function of NF-Y in *Schmidtea mediterranea*

The results of the functional characterisation of the NF-Y in planarians were published as a part of a functional validation of the Digital Gene Expression study, published by Gustavo Rodriguez-Esteban and collaborators (Rodríguez-Esteban et al. 2015)(**Annex I**). In the published manuscript we focused on the role of the NF-Y in the control of the early events of neoblast differentiation. The decrease of the early progeny after NF-Y complex RNAi, but not of the neoblasts, suggests a problem in the early differentiation event. However, despite the increase in neoblasts, a decrease in the number of mitotic cells is observed. This result could be explained by a possible function of the NF-Y complex in the cell cycle. Thus, Benatti and collaborators demonstrated that NF-YA inactivation leads to down regulation of a multitude of cell cycle genes and a delay in S-phase progression in cell culture (Benatti et al. 2008; Benatti et al. 2011). Experiments of BrdU incorporation to analyse the number of cells in S-phase would help to clarify this function. On the other hand, the findings of neoblasts aberrantly located in the anterior part of the head, is a phenotype often observed in animals which regenerate smaller blastemas and smaller brains. The underlying reason could be that the structures differentiate in the pre-existent tissue, where neoblasts

DISCUSSION: CHAPTER I

are normally located. Moreover, NF-Y could also be controlling positional information, promoting aberrant migration of neoblasts or interfering with the guiding signals that direct neoblast, or other cell types, to the right position. In this way, NF-Y has also been involved in the targeting of neural cells in *Drosophila*, showing that NF-Yc is important for R7 photoreceptor cell targeting through the control of Senseless (Morey et al. 2008).

Owing to the molecular markers available at the moment of the study, the specific role of NF-Y in cell differentiation was restricted to the study of the epidermal lineage. However, the neural defects observed, suggest that this complex could also be involved in the differentiation of different tissues. In this line, *Drosophila* NF-Y complex does not only regulate R7 targeting but also differentiation, through the control of *Sev* gene expression (Yoshioka et al. 2012). On the other hand, this complex has also been associated with the differentiation of other cell types. Using CaCo-2 cells, NF-Ya has been shown to be required for the differentiation of intestinal epithelial cells (Bevilacqua et al. 2002). Altogether, since it is very possible that NF-Y in planarians controls the differentiation of several cell types, it would be very interesting to further study the RNAi phenotypes using the current tissue-specific available markers. For instance, the process of cell specification and differentiation of photoreceptor cells has been accurately described molecularly (Lapan & Reddien 2011). The analysis of these specific markers would allow us to determine if NF-Y is affecting the determination of this lineage and for which specific stage is important. Moreover, the implementation of the current knowledge of the epidermal steps and genes specification, which is much more accurate than at the time we performed the reported experiments, would also

allow discerning the specific stage in which NF-Y is involved during epidermal differentiation.

In intact animals, inhibition of the NF-Y complex leads to a neoblast-related phenotype, which is tissue regression and curling of the animals. Although the phenotype is very similar to the one reported after ablation of the neoblast population, our results in regenerating animals suggest that the cause of the phenotype could be the inability of cells to differentiate, concomitant to problems in cell cycle progression, and not the direct ablation of the neoblast population. A deeper characterisation of the *nf-y* RNAi intact animals should be performed to further understand the role of the NF-Y complex in this context.

Altogether, our results indicate that aside to other processes in planarians, NF-Y could be mainly affecting neoblast differentiation towards different fates, as well as the cell cycle progression, as already reported in other animal models (**Figure 56**).

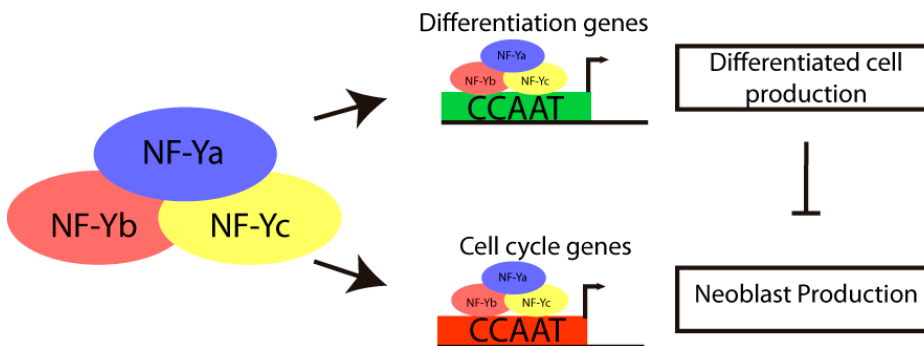


Figure 56: Planarian model for NF-Y regulation. NF-Y is controlling both, proliferation and differentiation processes. Absence of differentiated cells signals neoblast to proliferate to maintain the organism cell turnover. NF-Y is controlling both to interconnect differentiation and neoblast proliferation.

CHAPTER II:

Krüppel-like Factor 10/11 controls the onset of mitosis in planarian stem cells and triggers apoptotic cell death required for regeneration and remodelling.

KLF family genes are a set of DNA binding proteins involved in the regulation of gene expression. They control the expression of multiple genes, involved in proliferation, stem cell maintenance, differentiation and cell death (Pei & Grishin 2015; Spittau & Krieglstein 2012; Shindo et al. 2002; Aksoy et al. 2014; Suske et al. 2005; Jiang et al. 2008; Swamynathan 2010; McConnell & Yang 2010). Different members of the family have been related with one function or another. In planarians, we have found five members of the KLF family. *Smed-klf* was already published to be required for the proper differentiation of the chemo- and photoreceptor cells (Lapan & Reddien 2012), which fits with the described role of KLFs in cell fate determination. Out of the other four, we focused on the functional characterization of KLF10/11, since the other three members gave any phenotype after inhibition.

In the next section I will discuss the role of *klf10/11* in controlling cell proliferation and apoptosis during planarian regeneration and homeostasis.

8.1. *klf10/11* controls the onset of mitosis and triggers the apoptosis required for regeneration and remodelling possibly as a JNK target

Smed-klf10/11 shows a ubiquitous expression pattern; however, during regeneration the expression is dynamic, showing two peaks of expression around 24 and 48 hours. Taking into account that the entire eukaryotic cell cycle takes place in approximately 22-24 hours, the expression pattern suggest that *Smed-*

klf10/11 could have a role in the control of the cell divisions required for the regenerative process. The co-expression of *klf10/11* with the neoblast marker *h2b* supports its role in stem cells.

Furthermore, the analysis of the mitotic response after amputation in *klf10/11* RNAi animals supports its essential role in the onset of the mitotic response. Thus, the first mitotic pick observed in control planarians, at 6h, is higher in *klf10/11* RNAi animals, and the second, at 48h, appears earlier than in controls. Importantly, this pattern of the mitotic kinetics reminds us the one published in *jnk* RNAi planarians, suggesting a possible relationship between them. In addition, drosophila studies reported that Cbt, the *Drosophila* homolog to *klf10/11*, was acting downstream JNK (Muñoz-Descalzo et al. 2005), suggesting that in planarians Klf10/11 could be a target of Jnk. On the other hand, in vertebrates has been shown that Klf10 and Klf11 are downstream elements from the TGF- β signalling pathway which has also been involved in the activation of Jnk pathway (Hocevar et al. 1999; Dai et al. 1999). Moreover, in vertebrate pancreas, Klf10 and Klf11 is rapidly upregulated by TGF- β stimulation, leading to the control of pancreatic cell growth through inhibition of cell proliferation and induction of apoptosis which fits with our observation in planarian (Cook & Urrutia 2000; Kaczynski et al. 2003).

Planarian Jnk has been shown to be an important regulator not only of the mitotic response but of the balance between proliferation and apoptosis (Almuedo-Castillo et al. 2014). The unbalance caused through its inhibition impairs regeneration of the new tissues and remodelling of the old ones, and thus regeneration does not take place. Our results show that *klf10/11* could be also a

modulator of this balance in planarians, since its inhibition reduces the apoptosis and impairs remodelling in intact animals. Thus, all this data favours the hypothesis where Klf10/11 could exert the same function than Jnk acting as a target of it. However, the first observation after *klf10/11* inhibition was an acceleration of the regeneration speed, and not an impairment of the regenerative response, as described in *jnk* RNAi animals. The difference between phenotypes could be due to differences in the expressivity of the loss of function generated by *jnk* and *klf10/11* RNAi. Thus, the percentage of animals that cannot regenerate after *jnk* RNAi is very low, and they can just be observed after three rounds of inhibition. On the other hand, after three rounds of *klf10/11* dsRNA injections the phenotype described of faster regeneration cannot be observed any more but animals show a reduced blastema and do not regenerate properly. Thus, low doses of *klf10/11* inhibition favours regeneration while high doses impair regeneration. In any case, more analysis should be performed to clarify whether the acceleration in the regenerative process after *klf10/11* inhibition could be causing co-lateral defects.

To have more data about the possible regulation of Klf10/11 by Jnk, we performed an *in silico* search of the AP-1 binding sites in the up-stream region of the Klf10/11 coding sequence. Although the planarian genome is not well assembled and we lack prediction tools to study conservative promoting regions in planarians we were able to find putative AP-1 binding sites upstream the Klf10/11 open reading frame, supporting that it could be a direct target of Jnk (**Figure 57**). Unfortunately, when quantifying the levels of *klf10/11* after *jnk* inhibition, we found that they were increased and not decreased, as expected. However, this

experiment should be repeated in different conditions, since it contradicts the similar phenotypes observed after their inhibition. A possible explanation of this result could be that the quantification was performed after three weeks of *jnk* dsRNA injections. Although the phenotype of *jnk* or *klf10/11* inhibition cannot be observed earlier, the quantification of the levels of the transcripts should be performed earlier, to discard any indirect effect due to the long-term inhibition.

In any case, to finally address whether Klf10/11 is a target of Jnk in planarians, inhibition of AP-1 components followed by expression and functional analysis should be performed. Therefore, inhibition of AP-1 elements (Fos and Jun) should decrease *klf10/11* expression while knock down of Jnk inhibitors like Puc should increase the *klf10/11* expression. In addition, inhibition of more than one element of the pathway at the same time (like Jnk, Jun and Fos) could increase the phenotype observed allowing us to analyze the effect of this inhibition on *klf10/11* expression at earlier time points thus avoiding the long-term inhibition side effects.

To conclude, inhibition of *klf10/11* produces a phenotype strikingly similar to the one described after *jnk* inhibition, suggesting that it could be a Jnk target, as described in *Drosophila* (**Figure 57**). Both genes are essential for the onset of the mitotic response during regeneration of new tissues, and to trigger the apoptotic cell death that enables remodelling of the old tissues during regeneration and of the whole animal during homeostasis. The integration of the mitotic and the apoptotic response is essential for any developmental process, and especially during regeneration. In addition, the differences between inhibitory doses, which produce opposite effects (the acceleration of the regeneration speed versus the

impairment of proper regeneration), highlight the importance of the dose-dependent effect, which should be always considered in any medical application. A more in deep study of the role of the putative Jnk-Klf10/11 pathway not only in planarians but in vertebrates could help in establishing novel regenerative therapies.

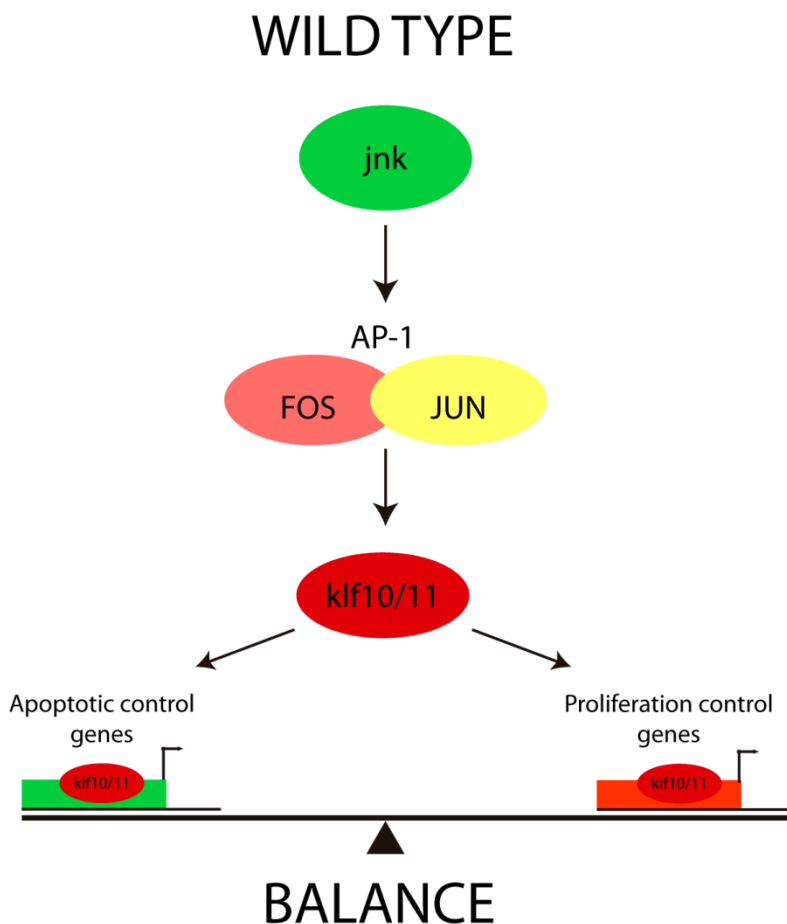


Figure 57: Possible location of Klf10/11 downstream Jnk in the planarian JNK pathway. The Jnk signalling pathway controls the balance between proliferation and apoptosis through klf10/11 in planarian.

CHAPTER III:

WNT5-ROR2 and SLIT-ROBO-c signals
generate a mutually dependent system to
position the CNS along the medio-lateral axis
in planarians.

Positional information is a key requirement to position structures and organs in every developmental process. During planarian regeneration it is essential the existence of these positional instructions thus every new tissue is organized according to the pre-existing tissue to finally form a healthy and functional organism. This process is also required during planarian homeostasis, thus the tissue turn over which naturally occurs in planarian needs these instructions to properly replace the new cells. Here, we have studied in detail the mechanism through which Wnt5-ROR and Slit-ROBO-c establish the proper M-L position of the CNS by creating a self-regulatory system to define their reciprocal domains of expression.

9.1. Wnt5/Ror and Slit/Robo-c generate a mutually dependent system

The initial definition of self-organization by Immanuel Kant as a characteristic of living systems implied the existence of a loop between organization and function (Immanuel Kant 1914). Turing already showed that a system of reactants that are initially homogeneously distributed in a solution can generate products that segregate in spatial patterns if certain conditions are met. The product of a reaction should acts as a short-range positive activator of its own production while activating the production of an inhibitor that diffuses much faster (Turing 1952).

The data presented during this thesis proposes that Wnt5 and Slit are two molecules which have the capability to self-organize, following a Turing-like

behaviour. These self-organizing systems have been typically studied in embryology, where developing organisms must organize new cells to create a functional individual. However, the high plasticity of planarians allowed us to investigate whether self-organizing systems are also responsible to create and maintain patterns during adult regeneration and cell renewal. As opposed to embryonic development, during planarian regeneration this type of spontaneous patterning mechanism could be not required, since pre-existing tissues will always provide a pre-pattern. However, the same interactions between the components of a system might be used in order to guarantee the maintenance and plasticity of expression patterns after all kind of perturbations, such as amputations or different access to food, in the case of planarians.

Here we have found that two diffusible molecules (Wnt5 and Slit) are able to regulate each other expression domain thanks to the presence of their receptor in the opposite domain. Thus *wnt5* expressing cells in the lateral domain express the SLIT receptor (*Robo-c*) while *slit* expressing cell in the midline express the WNT5 receptor (*Ror*). This self-organizing system exerts a dual function: 1) it mutually restricts the boundary of expression of its elements, and 2) it directs the growth direction of the neural cells (**Figure 58**). This dual function allows the correct position of the planarian structures along the M-L axis both during *de novo* tissue formation in regenerating blastemas and during homeostatic cell renewal.

In any case, according to our initial model and to the experimental results, WNT5 and SLIT would not only interact with the receptors found in neurons but should also activate the receptor found in muscular cells of the opposite domain with respect to the VNCs. Thus, they must travel away from their own domains of

expression. How this travel occurs and how it takes place remains unsolved. Recently, it has been proposed that Wnts, which are highly lipophilic proteins, are not able to travel long distances by simple diffusion mechanism. However, other transport systems, like lateral diffusion driven by proteoglycans, transport proteins, exovesicles or cytonemes could be occurring in our system (Stanganello & Scholpp 2016; Beckett et al. 2013; Farin et al. 2016). The proper molecular tools to localize the secreted proteins would help in solving this question. In addition, during the first hours of regeneration, when *wnt5+* and *slit+* cells are mixed and the self-organizing system is active, the ligands would not need to “travel” long distances but just use transport mechanisms to act in neighbour cells (Beckett et al. 2013; Farin et al. 2016).

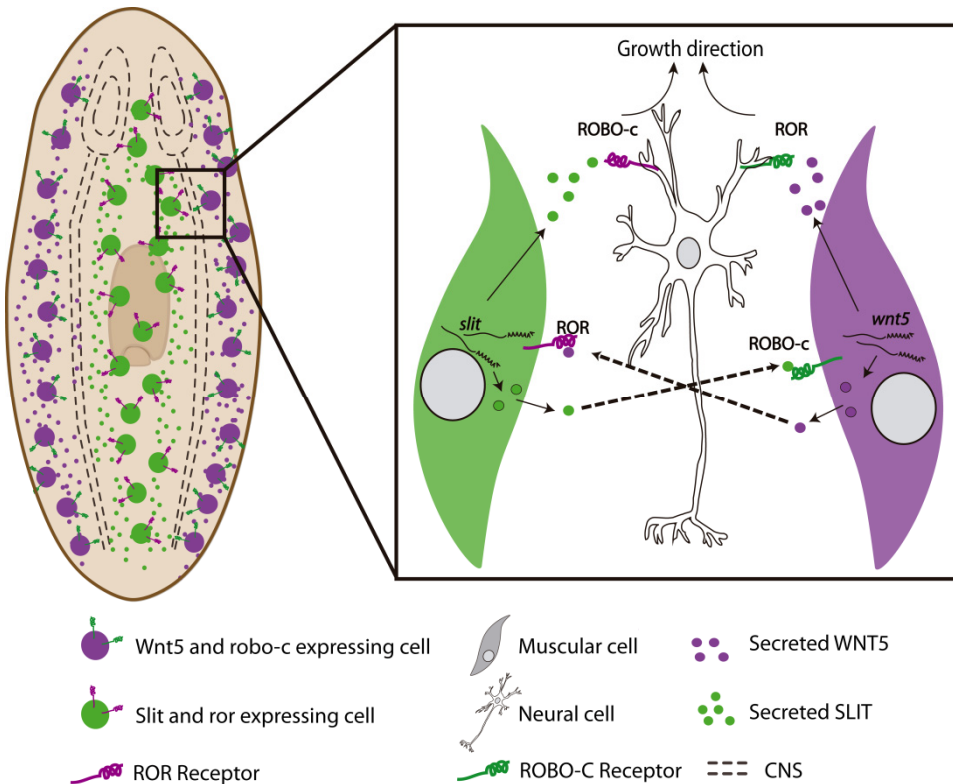


Figure 58: Wnt5 and Slit generate a mutually depend system to position the CNS.

Scheme showing the complementary expression domains of *wnt5/Robo-c* and *slit/Ror* in muscular cells in respect to the CNS. Neurons of the CNS express both receptors, being able to respond to both signals coming from opposite sides, and thus defining the path for the CNS. Muscular *wnt5+/robo-c+* cells are able to respond to SLIT while *slit+/ror+* muscular cells are able to respond to WNT5 to finally delimit their own expression domains.

9.2. Mechanism through which Wnt5 and Slit position the CNS

The preexisting tissue is one of the main differences between the formation of a new CNS during regeneration or during embryonic development. Several studies indicate that in planarian the brain primordia are formed during the first 48hr. However it is not know if the formation of brain primordia is initially dependent on the preexisting VNC (pVNC). It could be that the axonal projections from the pVNC send signals to properly position the new brain primordia. However, the first regenerating time point in which axon projection can be observed from the pVNC is at 48hr, and not earlier (Fraguas et al. 2012). On the other hand, if the site of appearance of the brain primordia is independent from direct projections of the pVNC, it could depend on the migration of neural cells close to the wound to the blastema region, or on the direct differentiation of blastema cells into neural cell types. In this situation, once the brain primordia is formed, the attractive signals to connect the old and new tissues would be established. According to our finding in this Thesis, the Wnt5/Slit system here reported could be the signal required to position the new CNS with respect to the M-L axis. However, the specific mechanism through which *slit* and *wnt5* position the CNS is still not solved. Two main mechanisms could be proposed:

WNT5/SLIT act as axon repulsive molecules: In this scenario, the pVNCs can elongate towards the region where the brain primordia should be formed. To drive this process, Wnt5 and Slit could be guiding the axonal growth to the right M-L position by exerting a repulsion action on them. Once the axons are well positioned; they could generate the required signals for the brain primordia formation. Therefore, Wnt5 and Slit, through directional axonal growth, will guide the M-L position of the new brain. A problem of this possibility is that axon projection has been never observed between the brain primordia and the pVNC at early stages.

WNT5/SLIT controls cell migration: Although Wnt5 and Slit are well established axon guidance molecules, they also have been involved in the control of cell migration. The formation of the brain primordia can be addressed by the control of neural progenitor cells to the right position where they will differentiate forming this new brain. Preliminary data supports that Wnt5 and Slit are controlling at least eye progenitor cells, thus after their inhibition *ovo+* cells are found outside their normal location (**Annex IV**). *Wnt5* inhibition leads to the lateral displacement of *ovo+* cells and *slit* RNAi produces the localization of these cells closer to the midline. In addition, both *wnt5* and *slit* RNAi animals show miss location not only of the axons but also of the neuronal bodies, supporting the role of these molecules in the control of cell migration.

According to our data, the second scenario seems more plausible, since the self-regulatory properties of the Wnt5/Slit system could be enough to position the new brain primordia with respect to the M-L axis, independently on axonal

projections from the pre-existent CNS. An interesting observation is that in early blastemas *wnt5* and *slit* are expressed in a salt-and-pepper pattern but only in the region between the pVNCs, in the slit domain, suggesting that *slit* exerts a dominant role during the *de novo* establishment of the M-L pattern. This dominant role could be explained by the essential function of *slit* in defining the midline, the organizing region essential for the general patterning of the blastema (Oderberg et al. 2017).

It must be also considered that both mechanisms, axon guidance and cell migration, could be controlled by the Wnt5/Slit system. Thus these molecules could be promoting the migration of progenitor neural cells to the right position and at the same time, guiding the pre-existing neural cells to growth in the M-L axis. Therefore, both the positioning of the new brain primordia in the blastema and the growth of the pVNC in the correct M-L position will depend on the repulsive action of WNT5 and SLIT.

In contrast to the regenerative scenario, during homeostasis there is no need of new tissue formation but of maintaining the structures according to the planarian size. Inhibition of *wnt5* and *slit* in intact planarian produces the ectopic formation of CNS. This new CNS formation must occur during the process neuronal differentiation required for normal cell renewal since in *wnt5* or *slit* RNAi animals show the same number of neural cells than controls, according to the transcriptomic data (**Annex IV**). Thus, the appearance of a miss located second CNS must be caused by the incorrect localization or migration of neural precursors. . The finding that the new CNS formed in the RNAi animals appears independent from the preexisting one also supports this notion.

These data suggest that when *wnt5* and *slit* are inhibited, the cells differentiate into neurons in an aberrant position, either by inaccurate progenitor migration or by signaling stem cells in the ectopic zone to differentiate to neurons. All these results support the hypothesis that Wnt5 and Slit are controlling the migration of neural precursor cells.

9.3. The Wnt5/Slit system controls the M-L position of all tissues

Gurley and collaborators observed that in a small proportion of *wnt5* RNAi animals' trunk developed one or two pharynges lateral to the original pharynx (Gurley et al. 2010). This result highly suggests that Wnt5 is controlling the positioning of other organs like pharynx. Therefore, *slit*, expression domain depends on Wnt5 and according to our results, will be also controlling the positioning of other structures. Preliminary data obtained during this Thesis further indicates that Wnt5/Slit are controlling the M-L positioning of structures other than the CNS (**Figure 59**). Thus, the two posterior gut branches seem to be closer to the midline in *slit* RNAi animals with respect to controls, while *wnt5* RNAi animals show a lateral displacement. In addition, rWNT5a injection produces the lateralization of the gut opposed to the injected area. Other cell types, like the posterior and anterior organizing regions, labelled with *wnt1* and *notum*, respectively, are also displaced in both *wnt5* and *slit* RNAi animals (**Figure 59**). All these results indicate that Wnt5 and Slit do not only position neural structures but also several cell types along the M-L axis. However, our studies do not allow clarifying whether the affectation of these tissues is directly related with

the Wnt5/Slit signalling or it is an indirect effect caused by the displacement of the CNS.

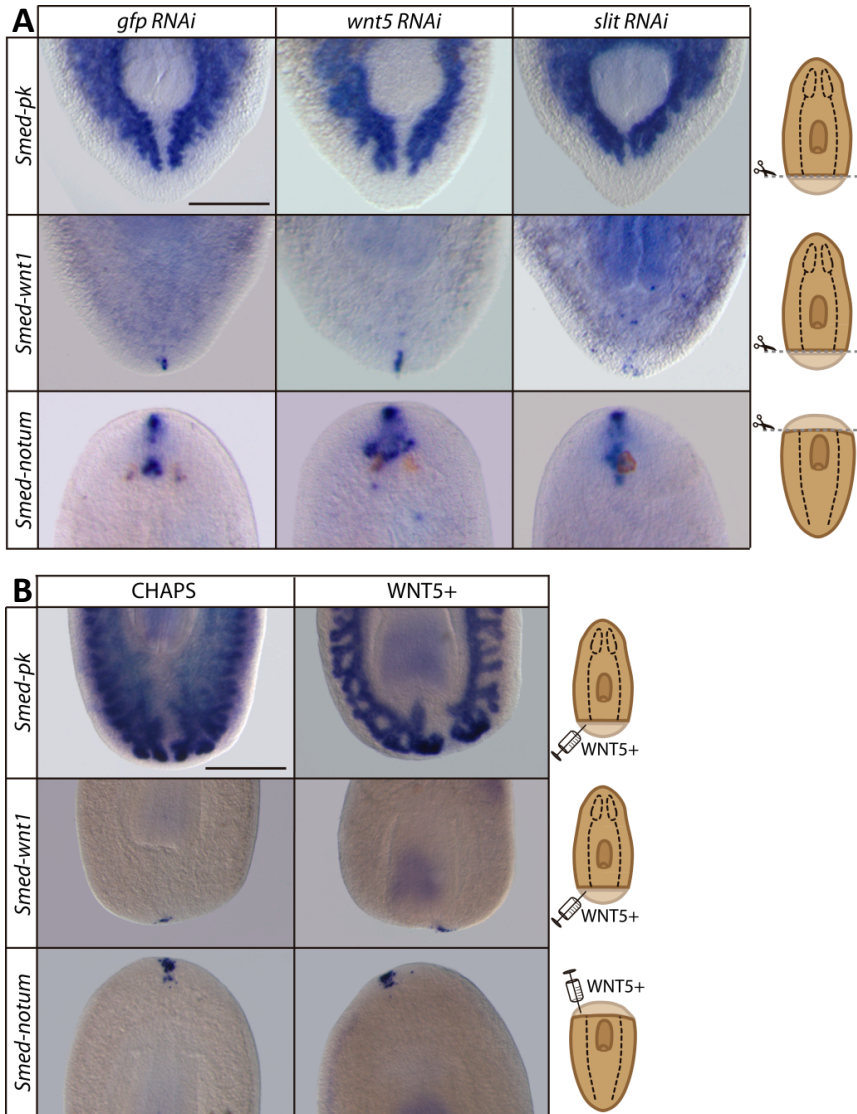


Figure 59: Wnt5 and Slit position other tissues/structures with M-L organization. (A-B) Expression of *pantotenase kinase* (a gut marker), *notum* (marker of the anterior pole) and *wnt1* (marker of the posterior pole) after (A) inhibition of *wnt5* and *slit* or after (B) rWNT5a injection.

9.4. Was the Wnt5/Slit system controlling the number of longitudinal nerve cords along evolution?

The basic orthogonal plan of the CNS of Platyhelminthes varies mainly in the number of longitudinal cords (Bullock, Theodore Holmes 1965). The presence of three to five pairs of cords is considered more primitive, with an evolutionary tendency towards reducing the number of cords to one main pair of cords (**Figure 60**). During this evolutionary process the variance of the expression pattern of *wnt5* and *slit* could explain these different morphologies. Therefore, intercalation of *wnt5* and *slit* expression domains will generate new paths for the formation of additional nerve cords.

And not only in Platyhelminthes but in all bilatelians it could be that a Wnt5/slit system, or a similar network, could be positioning the CNS along the M-L axis. The evolution of the CNS in bilateral organisms is highly studied, and it is known that Slit and Wnt5 play a role at different stages (Kapasa et al. 2010; Schubert et al. 2001; Itoh et al. 1998; Zinzen et al. 2006). However, a relationship between both molecules has never been described in a possible role of these two molecules and their receptors in the evolution of the CNS. Furthermore, it will be very interesting to study if this described system, or a similar one, is involved in the evolution of the CNS and in the acquisition of the different morphologies of bilateral organisms.

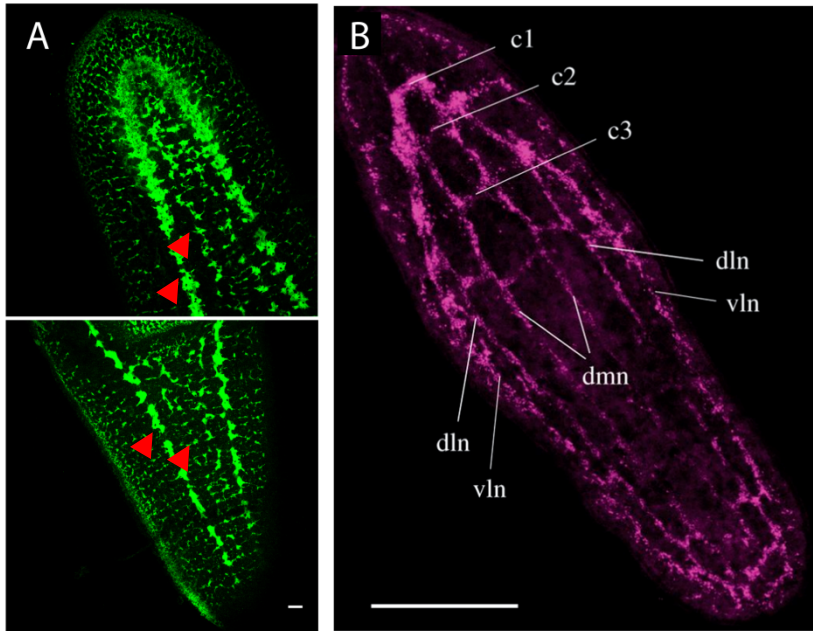


Figure 60: Comparison between the acoel *S. Roscoffensis* and *slit* RNAi planarian. (A) *slit* RNAi planarian during homeostasis shows two pairs of VNC along the body. (B) Dorsocentral projection of the *S. Roscoffensis* juvenile nervous system with the two lobes of the brain, connected by three commissures. c1, first brain commissure; c2, second brain commissure; c3, third brain commissure; dln, dorso-lateral neurite bundles; dmn, dorsomedial neurite bundles; vln, ventro-lateral neurite bundles. (A,B) Scale bar: 35 μ m. (B) Modified from (Gavilán et al. 2015)

GENERAL DISCUSSION:

During the whole development of this Thesis, different aspects of the main processes required for a proper regeneration and/or tissue renewal have been approached in the animal model *Schmidtea mediterranea*. The interconnection of these events is important for a tight regulation of this complex process where several aspects have to be controlled. Thus, balance between proliferation and apoptosis, stem cell specification events and cell positioning are interconnected through genetic and physical mechanisms. First, the characterization of the Nuclear Factor Y, a transcriptional complex involved in all these processes due to the huge variability of genes which controls is an example of the interconnectivity of these processes. On the other hand, Klf10/11 also has been shown to be required to control the balance between proliferation and apoptosis, which probably in an indirect way is also affecting stem cells specification since this unbalance will prevent the generation of correct signals for differentiation. Finally, we have presented interesting results about the control of the M-L organization exerted by Wnt5 and Slit. This M-L organization is not only required to position differentiated structures but also could provide the correct signals to neoblast to proliferate and differentiate into the correct cell types, and to differentiated cells to dye and allow remodelling.

This work clarifies important aspects essential for the field of developmental biology. The role of NF-Y in the stem cell specification can allow future research to clarify which genes controlled by this transcriptional core are controlling the stem cell specification not only in planarian but in other organisms. In addition, the finding that Klf10/11 is controlling the balance between proliferation and apoptosis possibly downstream of Jnk, as it is described in *drosophila*, suggests that

DISCUSSION

this process is conserved along evolution. Thus, its study can be helpful to understand in other organisms how proliferation and apoptosis, which are events important for almost every developmental process, are controlled.

Finally, the results supporting the M-L establishment through Wnt5 and Slit, contribute with a new mechanism through which these two molecules are regulating each other generating a plastic system that allows planarian to have the positional information in different contexts as regeneration and homeostasis. It would be interesting to clarify if this mechanism is also functional during neurogenesis in the planarian embryo. The relationship between these molecules has never been described in other species, thus it will be very interesting to test if this robust mechanism is important for the M-L specification in other organisms and is conserved along evolution.

Finally, the data presented during this Thesis can be very interesting for the growing field of regenerative medicine. All the general processes described during this Thesis; proliferation, apoptosis, stem cell specification or the axis establishment cannot be noteless in any regenerative therapy, thus all of them are essential for a successful regenerative process. Therefore, our data can be also very helpful for future research inside the regenerative medicine field making planarians a useful animal model in which study the basis of regeneration and to test in them possible regenerative therapies due to their easy handling and maintenance.

CONCLUSIONS

1. We found 3 elements of the NF-Y complex in planarians. They are ubiquitously expressed, showing clear localization in neoblasts.
2. In planarians, there is a duplication of NF-Yb, which enabled a functional specialization: NF-Yb2 is involved in stem cell differentiation and NF-Yb in germ cell specification.
3. NF-Y inhibition promotes neoblast accumulation and blocks differentiation towards the epidermal lineage.
8. We identified 5 Küppel-like factors in planarians.
9. *Klf10/11* is mainly expressed in neoblasts and its inhibition accelerates planarian regeneration and impairs remodelling of the pre-existing tissue. The underlying mechanism is an acceleration of the mitotic onset and a decrease in apoptosis. The unbalance between proliferation and apoptosis also affects remodelling ability during homeostatic cell renewal.
10. The upstream region of *Klf10/11* coding region contains putative AP-1 binding sites, which, together with reported results on the role of *Jnk* in planarians, suggests that *Klf10/11* is a *Jnk* target in planarians.
11. *Wnt5* and *Slit*, which show complementary expression domains with respect to the CNS, act as repellents for neuronal growth in planarians, guiding the path of the neural cells.
12. ROR and ROBO-c are the WNT5 and SLIT receptors, respectively, and both co-localize in the same neurons.
13. *Ror* and *robo-c* are also expressed in *slit+* and *wnt5+* muscular cells, respectively, suggesting that they create a self-regulatory network to restrict their own expression domains.

CONCLUSIONS

14. The perturbation of *wnt5* and *slit* expression further demonstrates that both ligands regulate each other expression. Wnt5 locally inhibits the transcription of *slit*.

15. The gene topology generated by mathematical modelling supports the self-regulatory properties of the WNT5-ROR/SLIT-ROBO-c signalling network.

16. The expression boundaries between *wnt5* and *slit* are not defined early in regeneration, supporting the self-regulatory properties of the system.

17. The WNT5-ROR/SLIT-ROBO-c signalling appears as a self-regulatory network responsible to pattern all tissues along the M-L axis of planarians.

**MATERIALS
AND METHODS**

1. Planarian culture

A clonal line of *Schmidtea mediterranea* (asexual strain) BCN-10 biotype was maintained in Planarian Artificial Medium (PAM) as previously described (Cebrià & Newmark 2005) and fed once or twice a week with bovine liver. Animals are maintained in aquariums with water flow moved by air pump through a filter (seraL60). Animals used for all experiments were starved for one week.

2. Cloning

All the genes used in this study either for probe synthesis or for dsRNA injections were cloned in specific vectors. Genes used for dsRNA synthesis were cloned in pCRII vector (Life Technologies) and genes used for ssRNA synthesis were cloned in pSPARK (Canvax Biotech) or pGEM-T easy (Promega). Both vectors are double-TA vectors with promoter regions for T7 and SP6 polymerases.

3. RNAi experiments

Double-stranded RNAs (dsRNAs) were synthesized by in vitro transcription as previously described (Sánchez Alvarado and Newmark, 1999). Animals were injected inside the gut three consecutive times 33nl each (1000ng/ul) using a nanojet® from Drummond Scientific. dsRNA was injected during three consecutive days, which we called a round of injection (Figure . A round of injection was followed by the amputation on the following day on the studies in

MATERIALS AND METHODS

regenerating animals. Green fluorescent protein (*gfp*) dsRNA was injected as a control. The number of rounds of injection differed depending on the experiment:

The *nf-y* complex members were injected during two rounds and planarian were let regenerate during 11 days. In homeostasis conditions, animals were injected two rounds and observed during 26 days from the first injection.

Klf10/11 and *Jnk* were inhibited during three rounds of injections. The *Klf10/11* weaker phenotype has been obtained after two rounds of injections.

Wnt5, *Slit*, *Ror* and *Robo-c* inhibition was performed differently depending on the experiment. For transcriptomic sampling, *Wnt5* and *Slit* were inhibited during three rounds and fixed for RNA extractions at day 28th from first injection. Homeostatic condition experiments were performed with two rounds of inhibition following 26 days of observation. The rest of experiments were done following two rounds of injections.

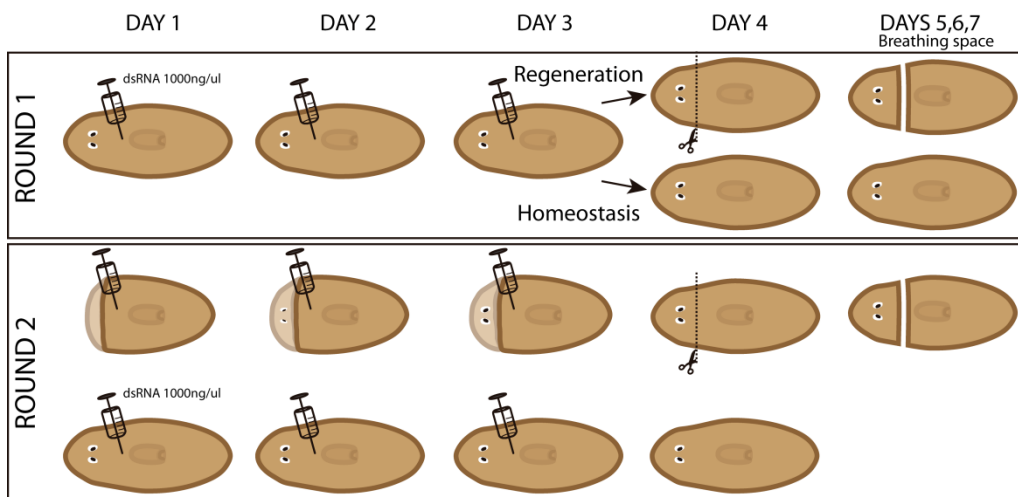


Figure 61: Schematic representation of dsRNA injection experiments.

4. In Situ Hybridization (ISH)

Probes used for ISH were synthesized by SP6 or T7 polymerase (Roche) and DIG, FITC or DNP modified nucleotides (Perkin Elmer). Whole mount ISH (WISH) or colorimetric ISH were performed as described in (Pearson BJ, 2016). Fluorescent ISHs (FISH) were performed as described in (Ryan S. King and Phillip A. Newmark, 2013). To improve the signal in the FISH a mix of several probes were used for each single gene when required. To generate this probe mix, *wnt5*, *slit*, *ror*, *roboc* and *intermediate filament* were cloned in 2-4 subfragments of 300-500bp each, thus each probe was composed by 2-4 probes. Samples were mounted in 70-80% glycerol in PBS.

5. Immunohistochemistry

Immunostaining was carried out as described previously (Ross et al. 2015). The following primary antibodies were used: anti-arrestin (VC-1, 1:15000; kindly provided by Hidefumi Orii, Himeji Institute of Technology, Hyogo, Japan), anti-synapsin (anti-SYNORF1, 1:50; Developmental Studies Hybridoma Bank), anti-alphaTubulin (AA43, 1:20; Developmental Studies Hybridoma Bank), rabbit anti-phospho-histone-H3-Ser10 (anti-H3P) (1:500; Cell Signaling Technology). Nuclei were stained with DAPI (1:5000) and/or TO-PRO (1:3000, Life Technologies). Samples were mounted in 70-80% glycerol in PBS.

MATERIALS AND METHODS

6. Generation of ectopic sources of rWNT5a

For the rescue experiment, dsRNA of *wnt5* was injected during 2 rounds following the standard protocol. Animals were cut 14 days after the first injection. 15 to 30nl of a 50ug/mL solution of recombinant Human/mouse Wnt5a Protein (R&D systems, 645-WN/CF) was ventrally injected 18-24 hours after cutting at both sides of the anterior blastema. Animals were fixed at 3 days of regeneration. Since it was important to avoid adherence of the rWnt5a ligand to the needle small volumes of the rWnt5a solution were introduced every time in the needle and the injections in the animals were carried out as fast as possible. For axon repulsion analysis, the same amount of rWNT5a was ventrally injected in wild type animals at 18-24 hours after amputation in the right blastema side. Animals were fixed at 3 days of regeneration. For the analysis of *slit* expression, the same amount of rWNT5a was ventrally injected in intact, wild type or *ror* RNAi animals in the posterior midline between the gut branches. In regenerating conditions, animals were injected as described for axon repulsion analysis. In all the cases, control animals were injected with the solution in which Wnt5a is dissolved (0.1mM EDTA, 0.5% CHAPS, 0.1% BSA in PBS 1X)

7. Whole-mount TUNEL

For TUNEL analysis, animals were fixed and treated as described (Pellettieri et al. 2010) using the ApopTag Red in Situ Apoptosis Detection Kit (Merck-Millipore

MATERIALS AND METHODS

Ref.S7165). To avoid technical variance at least two independent TUNEL experiments were performed.

8. qRT-PCR

Quantitative Real Time PCRs experiments were performed as previously described (Solana et al. 2013). Worms were killed in TRIzol® reagent following manufacturer instructions and RNA extraction was done as previous described (Rodríguez-Esteban et al. 2015). cDNAs were synthesized using SuperScriptIII Reverse Transcriptase (Invitrogen). qRT-PCR experiments were performed using the Absolute qPCR SYBR Green Master Mix (Thermo Scientific). Five animals were used per condition and each condition was done by triplicate. In each experiment, three technical replicates were performed. *Smed-Ura4* was used for normalization.

The following primers were used:

<i>Smed-klf10/11</i>	5' AGATCCGATGAGCTGTCTCG 3'	5' AATGATCGCTCCGATTGAAC 3'
<i>Smed-wnt5</i>	5' GAAGGATTGTGTTGCAATCG 3'	5' CTTGGCATTGATTTTGCAG 3'
<i>Smed-slit</i>	5' CCTGATTCTCAAGGGACCTG 3'	5' TCTTGATGACATCCGATTGC 3'
<i>Smed-ror</i>	5'AATGCCAAGATATCGGCCACA 3'	5' CCCCATGCAGTTTGGATTG 3'
<i>Smed-roboc</i>	5' CTCGCTGTGACACAAACAC 3'	5' TCTATGGGGCACTGCAGAAT 3'

Statistical significance was measured by Student's T test (* p<0.05).

MATERIALS AND METHODS

9. Gene Expression Analysis

Whole intact worms were used for *wnt5/slit* RNAi transcriptomic studies. Animals were injected with 96nl of dsRNA at 1ug/ul during 3 consecutively days per week during 3 weeks (three rounds) and fixed the day 28th after first injection. Five animals were used for condition and 3 replicates were analyzed. Worms were killed in TRIzol reagent and RNA extractions were done following manufacturer instructions.

10. Imaging

In vivo pictures were obtained under ZEISS stereomicroscope STEMI SV6, and images were captured with sCMEX Scientific 3 camera. Colorimetric ISH were observed in a Leica MZ16F stereomicroscope (Leica Microsystems, Mannheim,BW, Germany) and images were taken with a ProgRes C3 camera from Jenoptik. Fluorescent ISH and immunostaining images were obtained under a Leica TCS-SP2 confocal laser-scanning microscope (Leica Lasertchnik, Heidelberg, BW, Germany) adapted for an inverted microscope.

ANNEXES

ANNEX I:

Digital gene expression approach over multiple RNA-Seq
data sets to detect neoblast transcriptional changes in
Schmidtea mediterranea.

Rodríguez-Esteban, Gustavo; González-Sastre, Alejandro;
Rojo-Laguna, José Ignacio; Saló, Emili; Abril, Josep F.
BMC Genomics. 2015.

RESEARCH ARTICLE

Open Access

Digital gene expression approach over multiple RNA-Seq data sets to detect neoblast transcriptional changes in *Schmidtea mediterranea*

Gustavo Rodríguez-Esteban, Alejandro González-Sastre[†], José Ignacio Rojo-Laguna[†], Emili Saló^{*} and Josep F Abril^{*}

Abstract

Background: The freshwater planarian *Schmidtea mediterranea* is recognised as a valuable model for research into adult stem cells and regeneration.

With the advent of the high-throughput sequencing technologies, it has become feasible to undertake detailed transcriptional analysis of its unique stem cell population, the neoblasts. Nonetheless, a reliable reference for this type of studies is still lacking.

Results: Taking advantage of digital gene expression (DGE) sequencing technology we compare all the available transcriptomes for *S. mediterranea* and improve their annotation. These results are accessible via web for the community of researchers.

Using the quantitative nature of DGE, we describe the transcriptional profile of neoblasts and present 42 new neoblast genes, including several cancer-related genes and transcription factors. Furthermore, we describe in detail the *Smed-meis-like* gene and the three Nuclear Factor Y subunits *Smed-nf-YA*, *Smed-nf-YB-2* and *Smed-nf-YC*.

Conclusions: DGE is a valuable tool for gene discovery, quantification and annotation. The application of DGE in *S. mediterranea* confirms the planarian stem cells or neoblasts as a complex population of pluripotent and multipotent cells regulated by a mixture of transcription factors and cancer-related genes.

Keywords: Planaria, Neoblast, Stem cell, Transcriptome, Transcription factor

Background

During the last decade, there has been increasing interest in the use of *Schmidtea mediterranea* as a model organism for the study of stem cells. These freshwater planarians contain a population of adult stem cells known as neoblasts, which are essential for normal cell renewal during homeostasis and which confers them with amazing regeneration capabilities [1-4]. Although a number of studies based on massive RNA interference (RNAi) [5], gene inhibition [6], microarray [7], and proteomics [8,9]

approaches have been carried out to identify the crucial neoblast genes responsible for their stemness, our understanding of their biology is far from complete. The use of next generation sequencing (NGS) technologies provides an opportunity to study these cells in depth at a transcriptional level. For that to be accomplished, however, a reliable transcriptome and genome references are required. Up to eight versions of the transcriptome for this organism have been published to date, making use of different RNA-Seq technologies [10-16], including one meta-assembly which slightly improves each one separately [17]. Despite all these efforts, a consistent reference transcriptome is still lacking.

Some studies have provided quantitative data on transcripts and their respective assemblies, focusing

*Correspondence: esalo@ub.edu; jabril@ub.edu

[†]Equal contributors

Departament de Genètica, Facultat de Biologia, Universitat de Barcelona (UB), and Institut de Biomedicina de la Universitat de Barcelona (IBUB), Av. Diagonal 643, 08028 Barcelona, Catalonia, Spain

on regeneration [13,17,18] or directly on neoblasts [11,14,15,19]. However, RNA-Seq suffers from an intrinsic bias that affects the quantification of transcript expression in a length-dependent manner. This bias is independent of the sequencing platform and cannot be avoided nor removed by increasing the sequencing coverage or the length of the reads. Furthermore, it cannot be corrected a posteriori during the statistical analysis (by transcript length normalization, for instance). Consequently, the quantification of the transcripts and the detection of differentially expressed genes is compromised [20-22]. Digital gene expression (DGE) [23] is a sequence-based approach for gene expression analyses, that generates a digital output at an unparalleled level of sensitivity [22,24]. The output is highly correlated with qPCR [25-27] and does not suffer from sequence-length bias. The combination of DGE and RNA-Seq data has been shown to help overcome the specific limitations of RNA-Seq [28], and the usefulness of DGE has been thoroughly demonstrated in research ranging from humans [26,29] to non-model organisms [22,24]. However, to date, DGE has not been extensively applied to the study of the planarian transcriptome.

Here, we have compiled and analyzed all the transcriptomic and genomic data available for *S. mediterranea* using DGE. This has facilitated an improved annotation and provided tools to ease the comparison and browsing of all the information available for the planarian community.

We have taken advantage of the resolution of DGE to quantitatively characterize isolated populations of proliferating neoblasts, their progeny, and differentiated cells through fluorescence-activated cell sorting (FACS) [30,31]. The resulting changes in transcription levels were analyzed to obtain transcript candidates for which an extensive experimental validation was performed. This has yielded new neoblast-specific genes, including many transcription factors and cancer-related homologous genes, confirming the validity of our strategy and the utility of the tools that we have implemented. Moreover, we provide a deeper molecular description of four of those candidates, the *Smed-meis-like*, and the three subunits of the Nuclear Factor Y (NF-Y) complex *Smed-nf-YA*, *Smed-nf-YB-2*, and *Smed-nf-Y-C*. Both families of genes are attractive candidates to be studied in planaria. The Meis family of transcription factors specify anterior cell fate and axial patterning [32], whereas the NF-Y complex is a heterotrimeric transcription factor that promotes chromatin opening and is involved in the regulation of a wide number of early developmental genes [33].

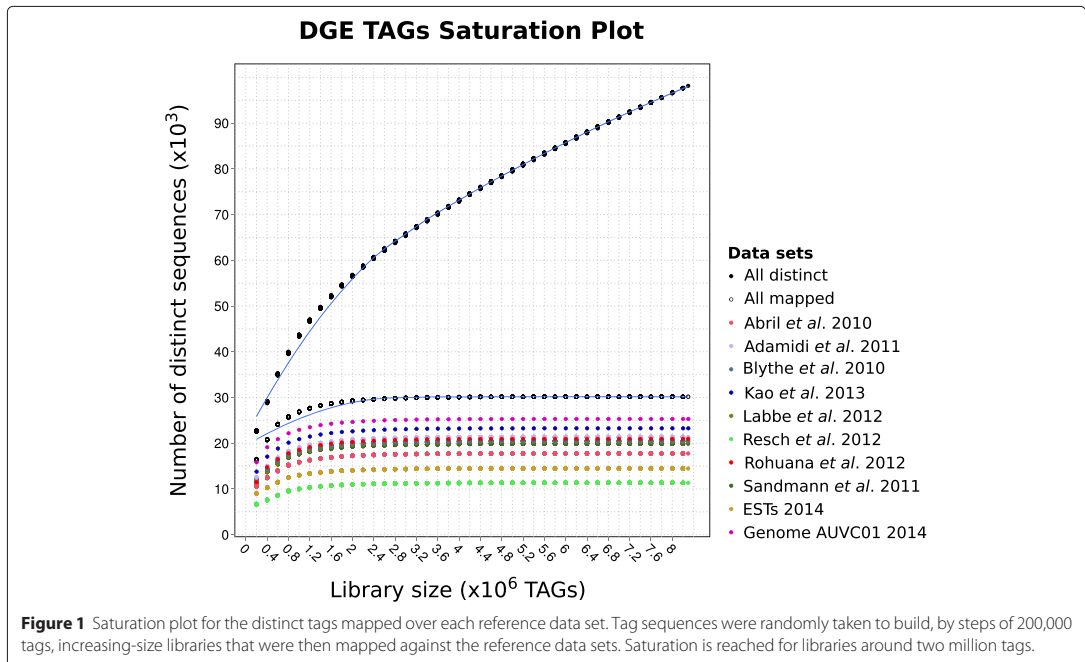
Results and discussion

Three DGE libraries were obtained from FACS-isolated cell populations X1 (proliferating stem cells, S/G2/M), X2

(a mix of stem cell progeny and proliferating, G0/G1), and Xin (differentiated cells, G0/G1) [30] (Additional file 1). 8,298,210 total reads were sequenced (X1: 3,641,099; X2: 3,488,712; Xin: 1,168,399), representing 98,156 distinct tags (X1: 70,849; X2: 24,621; Xin: 25,221), with an average of 84.5 reads per tag (X1: 51.4; X2: 141.7; Xin: 46.3). The distribution of the tags in each cell population can be observed in Additional file 2A. DGE is reported to achieve near saturation in genes detected after 6-8 million tags [22]. Furthermore, for moderately to very highly expressed genes (>2 cpm) it occurs with three or even just two million tags [22,34]. Figure 1 shows that saturation was reached at around two million tags for most of the data sets which the distinct tags were mapped to, although the slope for the total number of distinct tags decreases without saturating. It is worth noting that all the reference transcriptome sets performed similarly, achieving a maximum near 20,000 mapped tags. However, when looking at how many distinct tags map to any of those transcriptomes, about 5,000 tags appear not to be shared among all of them (see the "All mapped" and the "All distinct" data series on Figure 1, and further details on mapping below).

A critical point in this kind of experiment has to do with the number of times a tag has to be seen so that it can be considered reliable. Discarding too many tags in an attempt to increase reliability will result in a loss of information whereas keeping all of them may generate background noise. To estimate the specificity of our tags and to establish an optimal cutoff for the minimum number of counts a tag should have in order not to be considered artefactual, we performed a series of simulations mapping iteratively randomized sets of our data. The results are summarized in Additional file 3 for the different cutoffs tested (1, 5, 10, 15 and 20 minimum occurrences of tags). For cutoffs higher than five there is no substantial gain in terms of specificity (the number of hits decreases less than one order of magnitude). Thus, we defined reliable tags as those sequenced five times or more and discarded the rest. Thereafter, for the subsequent computational and experimental analyses, only those tags occurring at least five times were considered. From the initial set of 98,156 distinct tags, 40,670 passed that cutoff (Additional file 2B).

The low technical variability of DGE and its high reproducibility, together with the digital quantification of transcripts, enables direct comparison of samples across different experiments, even from different laboratories [21,22,24-26,29,35]. That property allowed us to contrast our results with those from Galloni [36], who used DGE to identify neoblast genes by comparing irradiated versus control animals over the same strain of clonal *S. mediterranea*. A Venn diagram showing the similarity of the strategies can be seen in Additional file 4. From the total distinct tags, 31.38% (30,806 out of 98,156) were sequenced 10 times or more in our study, compared with



just 11,28% (42,159 out of 373,532) in the irradiation strategy, indicating a greater representation of each tag. This suggests, as expected, that the cell-sorting approach has higher specificity. In addition, the strand-specific nature of DGE allows the discrimination of sense and antisense transcripts. Almost 30% of the transcripts successfully identified also presented antisense transcription, even though at lower levels than canonical transcription. This confirms the findings of the aforementioned study in planarians [36] and others [37], and shows that a large proportion of the genome is transcribed from both strands of the DNA. Although the purpose of these transcripts is still open to debate, evidences point to a post-transcriptional gene regulatory function [38].

Tag mapping to reference sequence data sets

An essential step in DGE is the recovery of the transcript represented by each tag. The nature of the DGE methodology, which generates reads of only 21 nucleotides, implies mapping short reads against a reference genome or a collection of ESTs to retrieve full-length sequences for the original transcripts. On the other hand, the short length facilitates the fast mapping of the tags against the reference sequence data set. To obtain the maximum number of transcripts, tags were mapped against the 94,876 *S. mediterranea* ESTs from the NCBI dbEST [39-42] and all the available transcriptomes (formally

those can also be considered as ESTs libraries). 26,822 tags (65.95%) mapped over at least one set of ESTs/transcripts, leaving a huge number (34.05%) unmapped.

In an attempt to recover tags that did not map over the transcripts, tags were also mapped over the *S. mediterranea* genome assembly draft AUVCO1 masked with the *S. mediterranea* repeats [23,43-45] (Table 1 and Figure 2). The overlap between transcriptomes was high. Although in most cases sets of reads mapping over a single transcriptome has a very low incidence, there were two cases where one could find a relatively small number of tags mapping to only one transcriptome: 327 tags (1.1%) for Labbé et al. 2012; 208 tags (0.7%) for Rohuana et al. 2012; 3,231 tags (10.7%) remarkably mapping only over the genome; and 26.1% of tags (10,617 out of 40,670) not mapping at all. For tags sequenced 10 times or more, the proportion of unmapped tags is similar: 20.5% (6,327 out of 30,806) (Additional file 2B). Even allowing up to two mismatches, 9.36% of the reads remain not mappable to the genome. This is still an important amount, considering that two mismatches is very permissive (it represents almost a 10% of nucleotide substitution in the read with respect to the reference sequence).

These results indicate that there will be a significant number of transcripts that are not represented yet neither in the current transcriptomic sets nor in the reference

Table 1 Summary of mapped tags

Reference	Mapped	One match	More than one match	Orphan	Contigs per tag
Abril et al. 2010	17,760	12,848	4,912	22,910	1.616
Adamidi et al. 2011	21,364	18,024	3,340	19,306	1.282
Blythe et al. 2010	20,518	17,649	2,869	20,152	1.204
Kao et al. 2013	23,477	15,791	7,686	17,193	1.444
Labbé et al. 2012	20,339	19,513	826	20,331	1.040
Resch et al. 2012	11,334	9,789	1,545	29,336	1.158
Rouhana et al. 2012	21,768	14,891	6,877	18,902	1.579
Sandmann et al. 2011	19,885	14,774	5,111	20,785	1.407
ESTs 2014	14,482	3,650	10,832	26,188	5.442
Genome AUVCO1 2014	25,328	19,019	6,309	15,342	1.272

Counts for the tags mapping over the reference data sets depicted in Figure 2. Total (distinct) tags: 40,670; mapped tags: 30,053; orphan tags (tags not mapped): 10,617.

genome, despite their coverage depth [46–49], and may correspond, for instance, to weakly expressed genes [50]. Mapping tags are expressed on average at 50.78 cpm, while non-mapping tags only at 19.85 cpm. Nonetheless, since transcriptomes currently available lack the complete annotation of 3'-UTR regions and the DGE libraries were made from the 3'-ends, reads that map to genomic sequences but not to current transcripts may potentially come from the 3'-UTR ends not yet sequenced. To evaluate this possibility, we have projected the transcriptome from Kao et al. 2013 [17] over the genome and looked

for the proximity of the tags mapping next to the 3'-end of the transcripts (Additional file 5). Downstream sequenced DGE tags account for 4.12% of all the possible CATG targets. This small amount of sequenced tags only mapping to the genome may correspond to potential novel unsequenced transcripts, alternative 3'-UTR exons of splicing isoforms, misannotated or alternative poly-adenylation sites, or even to non-coding RNAs not represented yet in the present transcriptome sets. Future RNA-Seq experiments may provide further sequence evidences supporting transcripts for those tags.

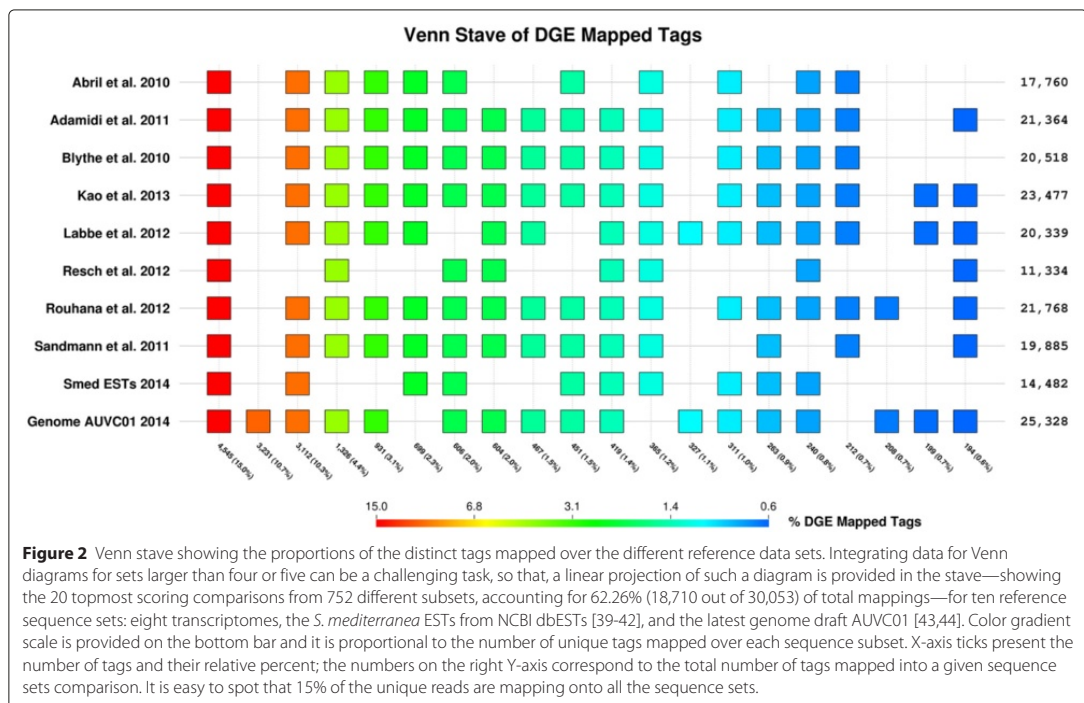


Figure 2 Venn stave showing the proportions of the distinct tags mapped over the different reference data sets. Integrating data for Venn diagrams for sets larger than four or five can be a challenging task, so that, a linear projection of such a diagram is provided in the stave—showing the 20 topmost scoring comparisons from 752 different subsets, accounting for 62.26% (18,710 out of 30,053) of total mappings—for ten reference sequence sets: eight transcriptomes, the *S. mediterranea* ESTs from NCBI dbESTs [39–42], and the latest genome draft AUVCO1 [43,44]. Color gradient scale is provided on the bottom bar and it is proportional to the number of unique tags mapped over each sequence subset. X-axis ticks present the number of tags and their relative percent; the numbers on the right Y-axis correspond to the total number of tags mapped into a given sequence sets comparison. It is easy to spot that 15% of the unique reads are mapping onto all the sequence sets.

Functional annotation

8,903 contigs from Smed454_90e—Smed454 from now on—[10] showing significant expression changes ($p < 0.001$) were selected and, from those, 7,735 contigs presented a hit to a Pfam domain model (Figure 3). For those sequences having a significant hit to a known domain/protein, gene ontology (GO) analysis was performed in order to summarize changes on the biological processes and molecular functions due to the observed expression patterns of the enriched sets of transcripts. Those transcripts were classified according to the cell type in which they were mostly expressed, then their significant GO annotations were clustered (also taking into account their parent nodes in the ontology), to calculate the terms abundance log-odds ratio. Comparison of GO categories between transcripts predominantly expressed in X1, X2 or Xin cell fractions revealed significant patterns of enrichment as indicated in Additional file 6 (see also the “Transcriptomes” tables available from the web site—planarian.bio.ub.edu/SmedDGE—for specific GO terms assigned to each transcript).

The GO comparison between the neoblast population (X1) and the differentiated cells (Xin) reflects distinct functional signatures: X1 is enriched in ubiquitin-dependent protein catabolic process, nucleic acid binding, RNA-binding, helicase activity, ATP binding, translation, and nucleosome assembly; Xin most represented categories include actin binding, actin cytoskeleton organization, small GTPase mediated signal transduction, proteolysis, and calcium ion binding; whereas in X2, markers of secretory activity such as vacuolar transport are more abundant.

Browsing data

All tag mappings over the different transcriptome versions are available in the form of dynamic tables from our web site (planarian.bio.ub.edu/SmedDGE, Figure 4A). The relationship between Smed454, along with their domains and functional annotation, with the other reference transcriptomes described in this manuscript can be browsed on a subset of those tables. In order to establish the correspondence between the transcriptomes, a megablast—NCBI BLAST+ 2.2.29 [51]—was performed, filtering the resulting hits afterwards by three levels of coverage (90%, 95% and 98%). Although the focus is set on Smed454, the user can reorder those tables by columns containing identifiers for other transcriptome versions or she can choose to jump to the transcriptome version specific summary table.

Moreover, the Smed454 contig browser [10,52] has been revamped into a more flexible interface based on GBrowse2 (planarian.bio.ub.edu/gbrowse/smed454_transcriptome). One can find there different types of annotation tracks: reads coverage, homology to known

genes/proteins, hits to Pfam domains, and also the information of the tags mapped over the sequence. One track-specific GBrowse2 Perl module was modified to display DGE tags data, such as the sequence, counts and rank position. Further customization of the GBrowse2 configuration facilitates the access to most of that information in the form of pop-up summary boxes, but also by means of additional “Details” page (see yellow panel on the right side of Figure 4B).

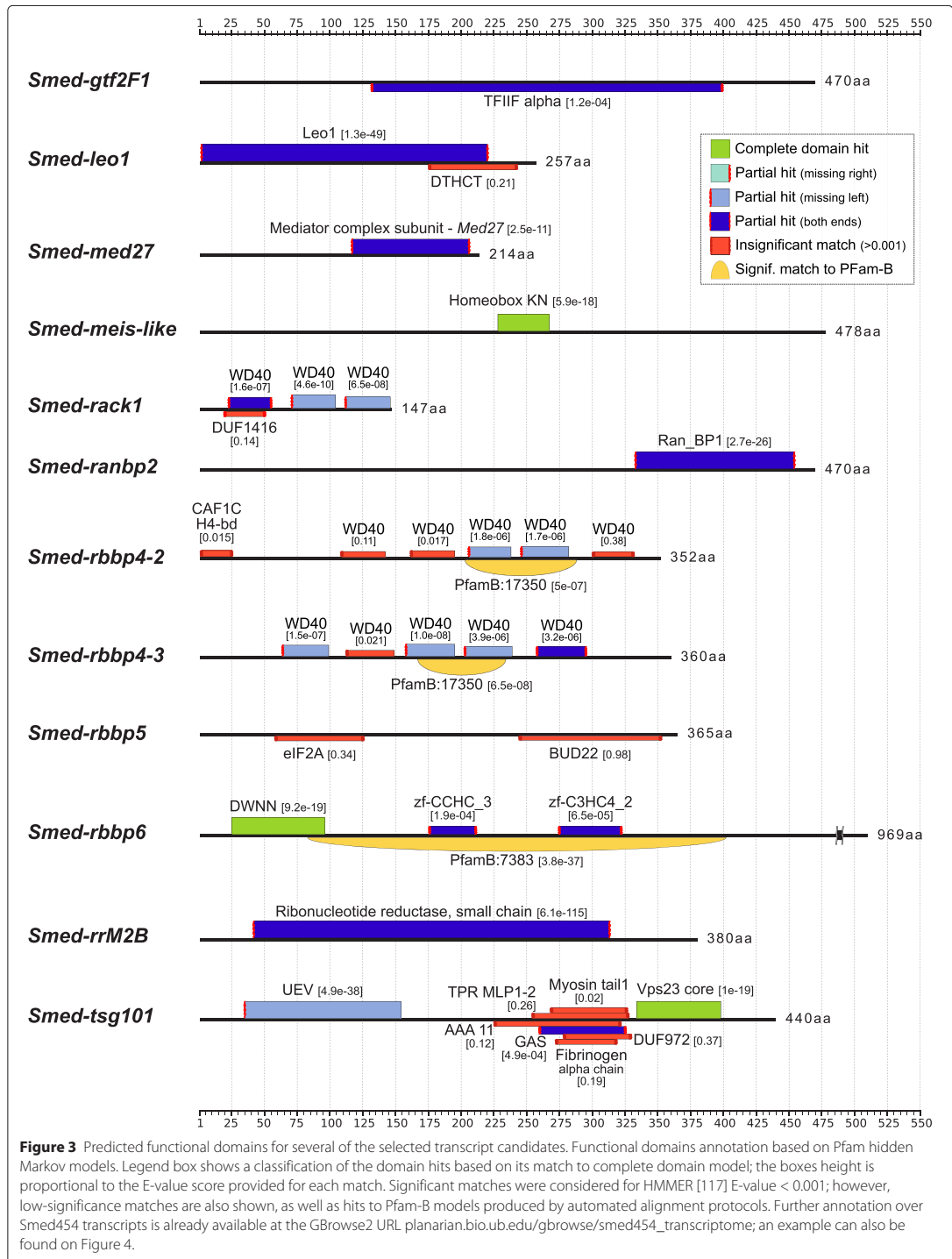
This browser has been developed under the principle of easy accessibility, in the hope that it will become a useful and informative user friendly tool for experimental researchers in their daily work.

Experimental validation

The validity of our approach is corroborated by the expression levels detected in 40 already known and well-characterized neoblast genes (Table 2), plus another 29 genes described in the literature with evidence of also being neoblast related (Table 3). As can be observed in Figure 5, both sets of genes show the expected expression pattern along the vertical right hyperbola, indicating a clear X1 specificity, with two exceptions overrepresented in X2: *Smed-nlk-1* and *Smed-prog-1*, which is described to be found in postmitotic cells [53]. *Smed-dlx* and *Smed-sp6-9* are key genes in eye formation [54]; despite their localized activation, DGE was sensitive enough to identify both of them predominantly in the X1 subfraction. Moreover, we could detect expression of genes such as *Smed-smg-1*—which is described as broadly expressed through all tissues, including neoblasts [55]—in both neoblasts and differentiated cells. Finally, 133 clones from two different studies [6,56] focussing on regeneration, stemness and tissue homeostasis are, indeed, significantly overexpressed in neoblasts (Additional file 7).

Based on their X1/Xin expression ratio, we selected a collection of potential new neoblast genes among the most represented in the X1 population. With the chosen candidates we performed expression pattern analysis by whole mount in situ hybridization (WISH) in irradiated animals. At different times after irradiation, as the neoblasts and its progeny decline, the hybridization signal disappears [57]. The expression of 42 out of 47 genes tested was diminished or completely lost in irradiated animals (Table 4 and Additional file 8).

Although neoblasts are essential also during homeostasis for normal cell renewal, the phenotype becomes more evident during regeneration. Functional analyses were therefore carried out by RNAi followed by head and tail amputation in order to visualize defects in the regenerating process. From the 42 genes whose expression was affected by irradiation, 24 showed a phenotype after RNAi (Additional file 9), most of them preventing a successful



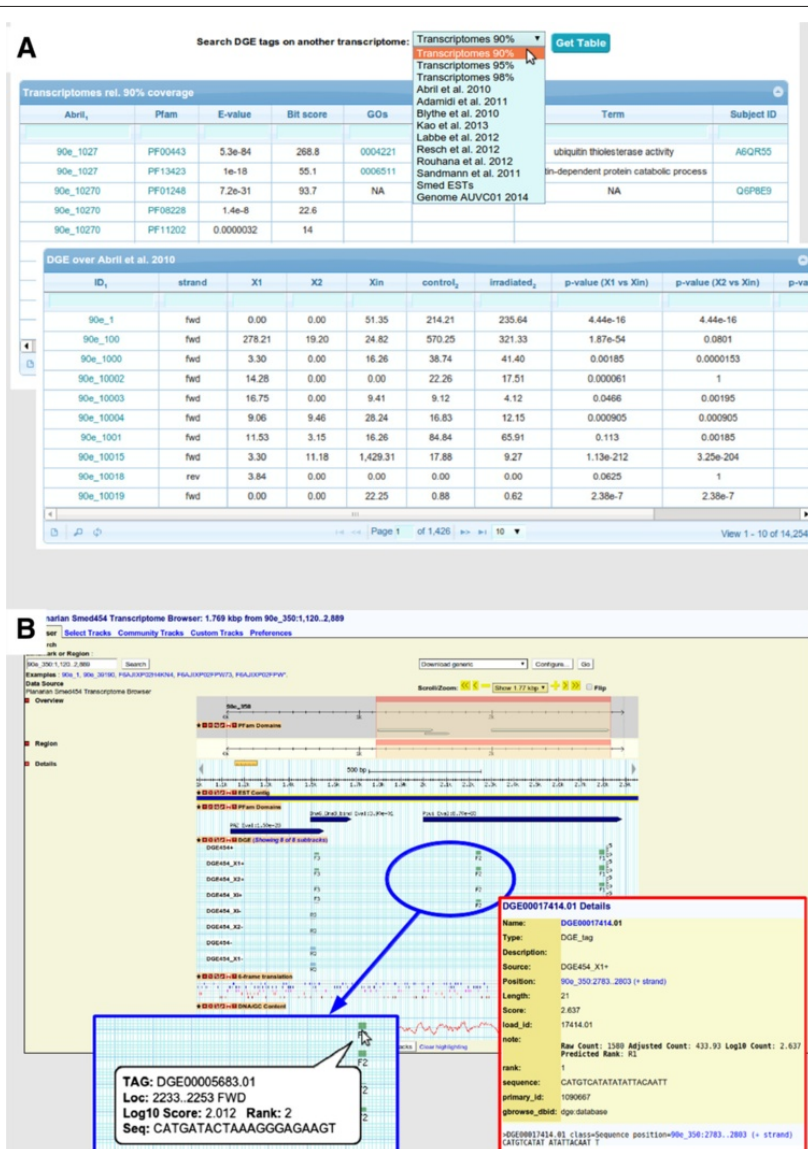


Table 2 Neoblast genes

Gene	X1	X2	Xin	p-val X1-Xin	p-val X2-Xin	Accession	PubMed
<i>Smed-bruli</i>	212.57	122.68	0	2.20e-062	1.58e-035	DQ344977	16890156
<i>Smed-chd4</i>	159.84	18.34	13.69	5.91e-032	1.10e-001	GU980571	20223763
<i>Smed-coe</i>	10.16	0	0	9.77e-004	1	KF487109	25356635
<i>Smed-cycD</i>	18.95	0	0	1.91e-006	1	JX967267	23123964
<i>Smed-dlx</i>	5.22	0	0	3.12e-002	1	JN983829	21852957
<i>Smed-e2f4-1</i>	141.72	23.50	29.96	6.24e-018	7.79e-002	JX967265	23123964
<i>Smed-egr-3</i>	19.50	0.57	0	1.91e-006	5.00e-001	HM777016	21458439
<i>Smed-egr-1</i>	510.01	37.26	153.20	9.16e-045	3.06e-017	JF914965	21846378
<i>Smed-foxA</i>	15.65	0	0	1.53e-005	1	JX010556	24737865
<i>Smed-hdac-1</i>	1086.49	0	60.77	4.19e-122	4.34e-019	JX967266	23123964
<i>Smed-hnf4</i>	30.21	8.31	8.56	3.85e-004	1.85e-001	JF802199	21566185
<i>Smed-hsp60</i>	113.43	10.32	33.38	8.64e-011	2.18e-004	GU591874	21356107
<i>Smed-hsp70</i>	326.28	0	11.13	3.98e-081	4.88e-004	GU591875	21356107
<i>Smed-jnk</i>	87.61	13.47	11.98	8.29e-016	1.55e-001	KC879720	24922054
<i>Smed-lst8</i>	43.12	1.43	0	1.14e-013	5.00e-001	JN815261	22479207
<i>Smed-msh2</i>	57.13	2.58	0	6.94e-018	1.25e-001	JF511467	21747960
<i>Smed-nanos</i>	39.27	1.15	0	1.82e-012	5.00e-001	EF153633	17390146
<i>Smed-ncoa5</i>	48.34	30.38	0	1.46e-011	5.96e-008	KF668097	24268775
<i>Smed-nf-YB</i>	11.26	2.58	0	4.88e-004	1.25e-001	HM100653	20844018
<i>Smed-p53</i>	5.22	5.73	0	3.12e-002	1.56e-002	AY068713	12421706
<i>Smed-papbc</i>	46.96	0	0	7.11e-015	1	HM100651	20844018
<i>Smed-pbx</i>	226.03	38.12	19.69	1.17e-044	6.41e-003	KC353351	23318635
<i>Smed-pcna</i>	728.63	24.08	0	3.51e-217	5.96e-008	EU856391	18786419
<i>Smed-prmt5</i>	43.67	0.57	0	5.68e-014	5.00e-001	JQ035529	22318224
<i>Smed-prog-1</i>	1.92	389.54	37.66	7.09e-010	7.42e-074	JX122762	18786419
<i>Smed-runt-1</i>	16.48	0	0	1.53e-005	1	JF720854	21846378
<i>Smed-sd-1</i>	14.28	0.57	0	6.10e-005	5.00e-001	KF990481	24523458
<i>Smed-sd-2</i>	4.67	0	0	3.12e-002	1	KF990482	24523458
<i>Smed-smB</i>	461.12	0	29.96	1.72e-099	9.31e-010	GU562964	20215344
<i>Smed-smg-1</i>	72.78	11.47	26.53	1.51e-006	4.38e-003	JF894292	22479207
<i>Smed-soxP-1</i>	15.11	3.15	0	3.05e-005	1.25e-001	JQ425151	22385657
<i>Smed-sp6-9</i>	38.72	0.57	0	1.82e-012	5.00e-001	JN983830	21852957
<i>Smed-srf</i>	40.37	0.29	16.26	5.78e-004	1.53e-005	JX010474	22549959
<i>Smed-tert</i>	19.22	0	0	1.91e-006	1	JF693290	22371573
<i>Smed-tor</i>	31.86	0	10.27	3.35e-004	9.77e-004	JF894291	22479207
<i>Smed-vasa-1</i>	1209.52	22.93	22.25	3.39e-162	1.17e-001	JQ425140	22385657
<i>Smed-wi-1</i>	644.59	13.47	0	6.01e-192	1.22e-004	DQ186985	16311336
<i>Smed-wi-2</i>	724.78	50.45	26.53	1.41e-176	2.90e-003	DQ186986	16311336
<i>Smed-wi-3</i>	433.93	76.82	21.40	9.76e-101	4.01e-009	EU586258	18456843
<i>Smed-xin-11</i>	26.64	0	0	7.45e-009	1	DQ851133	17670787

X1, X2 and Xin DGE expression levels of already known and deeply characterized neoblast genes.

Table 3 Likely neoblast genes

Gene	X1	X2	Xin	p-val X1-Xin	p-val X2-Xin	Accession	PubMed
<i>Smed-armc1</i>	20.60	2.01	0	4.77e-007	2.50e-001	JQ425158	22385657
<i>Smed-ash2</i>	17.58	0.86	0	3.81e-006	5.00e-001	KC262336	23235145
<i>Smed-cpsf3</i>	19.77	0	0	9.54e-007	1	KJ573358	24737865
<i>Smed-da</i>	13.46	0	0	1.22e-004	1	KF487093	24173799
<i>Smed-eed-1</i>	42.02	0	0	2.27e-013	1	JQ425136	22385657
<i>Smed-ezh</i>	31.03	2.01	0	4.66e-010	2.50e-001	JQ425137	22385657
<i>Smed-fer3l-1</i>	12.36	1.15	0	2.44e-004	5.00e-001	KF487094	24173799
<i>Smed-fhl-1</i>	158.19	8.31	23.11	2.79e-025	3.67e-003	JQ425148	22385657
<i>Smed-hcf1</i>	20.60	0	0	4.77e-007	1	KC262343	23235145
<i>Smed-hes-3</i>	26.09	0.57	0	1.49e-008	5.00e-001	KF487112	24173799
<i>Smed-junl-1</i>	173.30	4.59	0	1.97e-050	3.12e-002	JQ425155	22385657
<i>Smed-khd-1</i>	29.94	4.87	8.56	3.85e-004	1.22e-001	JQ425142	22385657
<i>Smed-mcm7</i>	351.82	24.08	0	5.22e-104	5.96e-008	KJ573361	24737865
<i>Smed-mls-2</i>	97.50	15.48	32.52	7.09e-008	3.88e-003	KC262344	23235145
<i>Smed-mrg-1</i>	53.28	3.44	0	1.11e-016	1.25e-001	JQ425133	22385657
<i>Smed-nlk-1</i>	0	30.10	0	1	9.31e-010	JQ425157	22385657
<i>Smed-nsd-1</i>	135.40	8.03	0	4.23e-039	3.91e-003	JQ425134	22385657
<i>Smed-pabp2</i>	191.98	2.58	8.56	2.84e-045	5.37e-002	KJ573359	24737865
<i>Smed-rbbp4-1</i>	121.67	0	0	3.13e-035	1	JQ425135	22385657
<i>Smed-sae2</i>	19.77	6.02	0	9.54e-007	1.56e-002	KJ573350	24737865
<i>Smed-setd8-1</i>	10.99	0.57	0	4.88e-004	5.00e-001	JQ425139	22385657
<i>Smed-soxP-2</i>	37.63	4.01	0	3.64e-012	6.25e-002	JQ425152	22385657
<i>Smed-soxP-3</i>	14.01	14.62	0	6.10e-005	3.05e-005	JQ425153	22385657
<i>Smed-sz12-1</i>	76.90	0	0	6.62e-024	1	JQ425138	22385657
<i>Smed-tcf15</i>	47.51	16.05	0	3.55e-015	1.53e-005	JQ425150	22385657
<i>Smed-vasa-2</i>	491.06	184.02	55.63	6.25e-087	2.39e-016	JQ425141	22385657
<i>Smed-wdr82-2</i>	195.55	16.63	0	2.66e-057	7.63e-006	KC262342	23235145
<i>Smed-zmym-1</i>	180.99	6.31	0	8.05e-053	1.56e-002	JQ425146	22385657
<i>Smed-znf207-1</i>	44.77	3.73	0	2.84e-014	6.25e-002	JQ425147	22385657

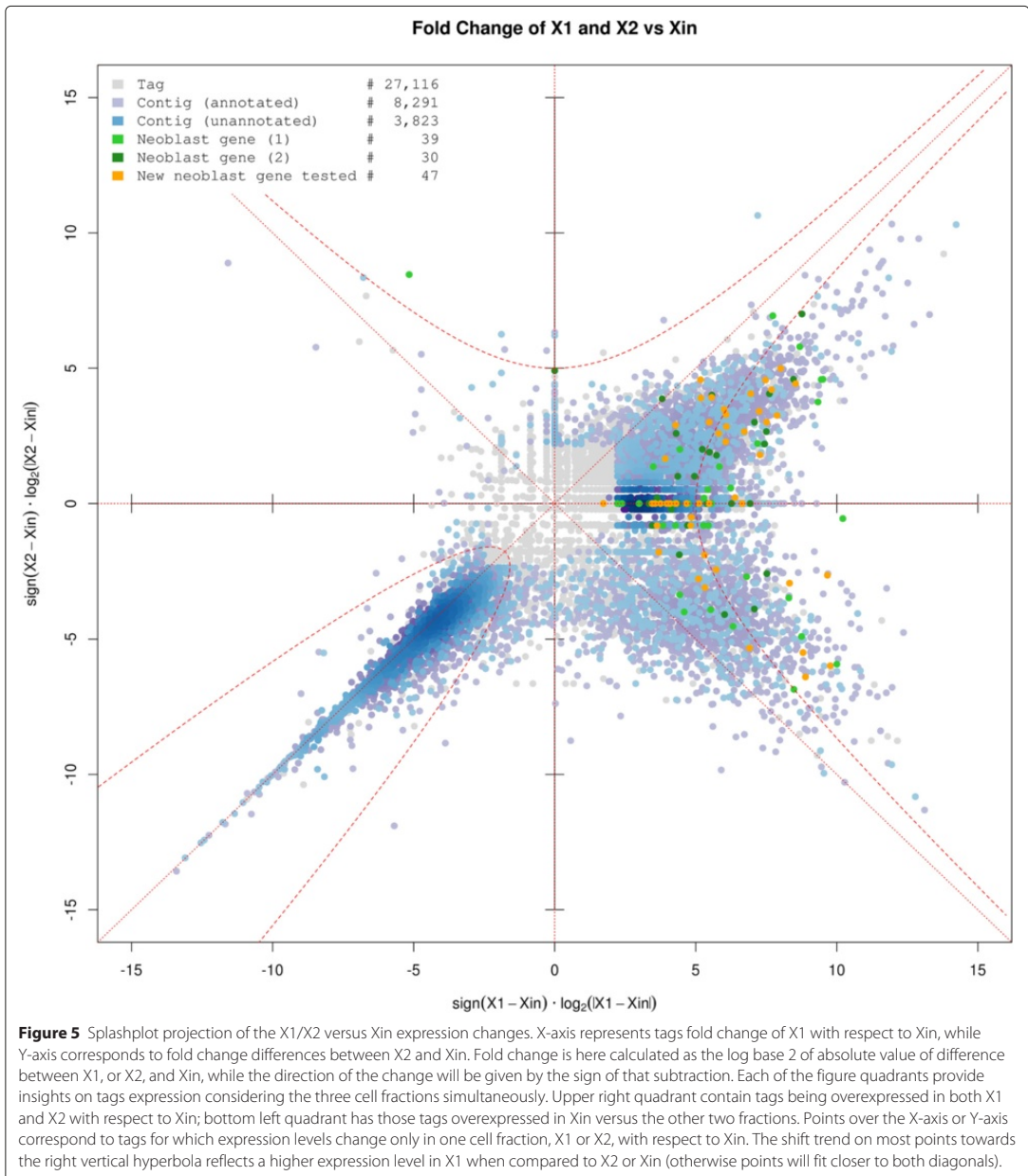
X1, X2 and Xin DGE expression levels of genes described in the literature with some evidences of being neoblast genes.

regeneration and leading to the death of the animals, the usual phenotype for neoblast genes [58,59].

New neoblast genes

Interestingly, several of the new genes identified as neoblast genes correspond to transcription factors, which are key elements implicated in cell fate decisions. Furthermore, many are also homologous to cancer related genes. We briefly describe those that produce planarian regeneration impairment after RNAi (Additional file 9). The inhibition of six of them produce a reduced blastema with defective head and eyes. *Smed-atf6A*, is a cyclic AMP-dependent transcription factor, which interacts with the Nuclear Transcription Factor Y (NF-Y) complex (further analyzed

later). *Smed-ccar1*, is a perinuclear phospho-protein that functions as a p53 coactivator modulating apoptosis and cell cycle arrest [60]. *Smed-hmrnpA1/A2B1*, a component of the ribonucleosome, is involved in the packaging of pre-mRNA into hnRNP particles in embryonic invertebrate development [61] and in stem cells [62]. *Smed-srrt*, modulates arsenic sensitivity, a carcinogenic compound that inhibits DNA repair [63]. *Smed-med7* and *Smed-med27* belong to a mediator complex essential for the assembly of general transcription factors. *Smed-ranbp2* is a member of the nuclear pore complex and is implicated in nuclear protein import. Within the same family, *Smed-nup50* shows also a stronger phenotype. The knock-down of the other 14 genes prevents the formation of the blastema completely. *Smed-gtf2E1* and *Smed-gtf2F1*, are



components of the general transcription factors IIE and IIF. *Smed-ncapD2* is necessary for the chromosome condensation during mitosis [64]. *Smed-pes1*, is required in zebrafish for embryonic stem cell proliferation [65]. *Smed-rack1*, is an intracellular adaptor of the protein kinase C in a variety of signaling processes. *Smed-lin9*, is related to the

retinoblastoma pathway interacting with Retinoblastoma 1, which is required for cell cycle progression [66]. All six different retinoblastoma binding proteins produce a non-blastema phenotype. The retinoblastoma pathway has been described to regulate stem cell proliferation in planarians [67] and some of its genes are already identified.

Table 4 New neoblast genes experimentally validated

Gene	X1	X2	Xin	p-val X1-Xin	p-val X2-Xin	TR	TF	ED	CC	OG	Accession	PubMed
<i>Smed-atf6A (Smed-atf1)</i>	12.36	0.57	0	2.44e-004	5.00e-001	•	•				JX010554	22549959
<i>Smed-ccar1</i>	184.01	79.11	0	1.02e-053	1.65e-024	•		•	•	•	KM981922	
<i>Smed-dnaIA3</i>	133.75	26.94	10.27	2.65e-028	2.53e-003	•				•	KM981923	
<i>Smed-erigc3</i>	66.74	4.87	0	6.78e-021	3.12e-002					•	KM981924	
<i>Smed-gat2 Smed-mospat</i>	106.29	7.17	0.86	1.78e-030	3.12e-002					•	KM981925	
<i>Smed-gtf2E1</i>	36.25	14.91	0	1.46e-011	3.05e-005	•	•				KM981926	
<i>Smed-gtf2F1</i>	25.54	0	0	1.49e-008	1	•	•				KM981927	
<i>Smed-hadhB</i>	153.80	12.33	1.71	4.86e-043	5.55e-003					•	KM981928	
<i>Smed-hnmpA1/A2B1</i>	341.93	13.76	21.40	3.70e-075	6.75e-002			•			KM981929	
<i>Smed-leo1 (NBE.6.06A)</i>	377.36	26.66	5.14	3.79e-104	4.69e-005	•	•			•	AY967650	15866156
<i>Smed-lin9</i>	47.51	13.76	2.57	9.25e-012	5.19e-003	•	•		•	•	KM981930	
<i>Smed-maf</i>	19.50	7.45	0	1.91e-006	7.81e-003	•	•				KM981931	
<i>Smed-med7</i>	162.86	11.18	7.70	3.59e-038	1.44e-001	•		•			KM981932	
<i>Smed-med27</i>	72.51	14.91	5.14	6.99e-017	1.48e-002	•					KM981933	
<i>Smed-meis-like</i>	10.99	0	0	4.88e-004	1	•	•			•	KM981934	
<i>Smed-mix</i>	160.12	0	40.23	1.81e-017	9.09e-013	•	•		•		KM981935	
<i>Smed-ncapD2</i>	84.86	0	0.86	1.11e-024	5.00e-001				•		KM981936	
<i>Smed-nfx1 Smed-stc</i>	28.29	0.57	0	3.73e-009	5.00e-001	•	•				KM981937	
<i>Smed-nf-YA</i>	31.31	1.15	2.57	3.48e-007	2.50e-001	•	•			•	KM981938	
<i>Smed-nf-YB-2</i>	17.03	0	0	7.63e-006	1	•	•			•	KM981939	
<i>Smed-nf-YC</i>	589.38	97.74	142.93	4.54e-064	1.46e-002	•	•			•	KM981940	
<i>Smed-nme1 Smed-nm23H1</i>	603.39	45.00	129.24	4.69e-073	6.54e-010	•	•			•	KM981941	
<i>Smed-nup50</i>	45.32	8.89	0.86	6.54e-013	9.77e-003	•	•			•	KM981942	
<i>Smed-pest1 (Smed-pescadillo-1)</i>	228.23	46.15	18.83	5.45e-046	3.34e-004	•	•			•	JX010566	22549959
<i>Smed-rack1</i>	115.90	30.10	0	1.91e-033	9.31e-010	•	•			•	KM981943	
<i>Smed-ranbp2 Smed-nup358</i>	45.32	0.86	0.86	6.54e-013	5.00e-001	•	•			•	KM981944	
<i>Smed-ribbp4-2 (Smed-ribbp-1)</i>	100.24	0	0	1.08e-028	1	•	•			•	JX010613	22549959
<i>Smed-ribbp4-3 (NBE.6.02C)</i>	254.04	27.52	17.97	7.94e-054	4.01e-002	•	•			•	AY967644	15866156
<i>Smed-ribbp4-4</i>	56.30	6.02	0	1.39e-017	1.56e-002	•	•			•	KM981945	
<i>Smed-ribbp5</i>	43.94	0.57	4.28	6.91e-010	1.56e-001	•	•			•	KM981946	
<i>Smed-ribbp6</i>	64.27	11.18	0	5.42e-020	4.88e-004			•		•	KM981947	
<i>Smed-rim2B (Smed-rim2-2)</i>	826.40	7.45	13.69	1.07e-111	5.54e-002				•	•	JX010501	22549959

Despite that, most of them are yet to be analyzed. Finally, *Smed-rrM2B*, is a subunit of the ribonucleotide reductase (RNR) complex required for DNA repair [68]. Details on these genes as well as the rest of the genes tested from the X1 population can be examined in the Additional file 10.

The four remaining genes presenting an aberrant phenotype during regeneration when inhibited by RNAi are described in detail in the following two sections: the *Smed-meis-like*, a new member of the Meis family, and the three components of the Nuclear Factor Y complex, all of them found to be overexpressed in neoblasts.

Smed-meis-like

Smed-meis-like is a member of the TALE-class homeobox family, similar to Meis genes, which was found to be overexpressed in the X1 subpopulation. This gene family is characterized by the presence of a homeobox domain with three extra amino acids between helices 1 and 2 [69]. Some of its members can act as cofactors for *Hox* genes [32]. In *S. mediterranea*, other members of the family have been described: *Smed-prep* [70], *Smed-meis* [54] and *Smed-pbx* [71,72].

WISH on intact animals shows that it is expressed in the cephalic ganglia, the pharynx, the tip of the head, and the parenchyma (Figure 6A). The downregulation observed three days after irradiation suggests that the parenchyma-associated expression is related to neoblasts and early postmitotic cells. To corroborate this, a double fluorescence in situ hybridization (FISH) together with the neoblast marker *Smed-h2b* [59] has been carried out (Figure 6B and Additional file 11A). Confocal microscopy shows colocalization of both genes in some cells, which confirms the expression of *Smed-meis-like* in neoblasts and, thus, the DGE results. Nevertheless, not all *Smed-meis-like* positive cells are expressing *Smed-h2b*, reinforcing the idea that *Smed-meis-like* is not exclusive of neoblasts.

Knockdown of *Smed-meis-like* through RNAi produced a diverse range of anterior regeneration phenotypes (Figure 6C), which can be explained by a different penetrance. The mildest phenotype produced a squared head with elongated and disorganized eyes. This phenotype was also clearly visible with fluorescence in situ hybridization (FISH) against *Smed-opsin* [5] and *Smed-tph* [73], which label the photoreceptor and the pigment cells of the eye (Figure 6D). In an intermediate phenotype, cyclopic animals are obtained, whereas in the strongest one there is no anterior blastema formation. This range of phenotypes can also be observed with the marker of brain branches *Smed-gpas* [74], which shows a gradual reduction of brain regeneration after *Smed-meis-like* inhibition. These results are also confirmed by the reduction of the brain signal of the pan-neural marker α -SYNAPSIN (Additional file 11B). Posterior regeneration was normal.

In the strongest phenotype, there is also no expression of the anterior markers *Smed-notum* [75] and *Smed-sfip-1* [76,77], and the marker of sensory-related cells *Smed-cintillo* (Figure 6E) [78]. This indicates that *Smed-meis-like* is necessary for anterior identity. In contrast, expression of the posterior marker *Smed-wnt-1* [77] remains after *Smed-meis-like* inhibition. Thus, we can conclude that *Smed-meis-like* is necessary for anterior, but not for posterior regeneration.

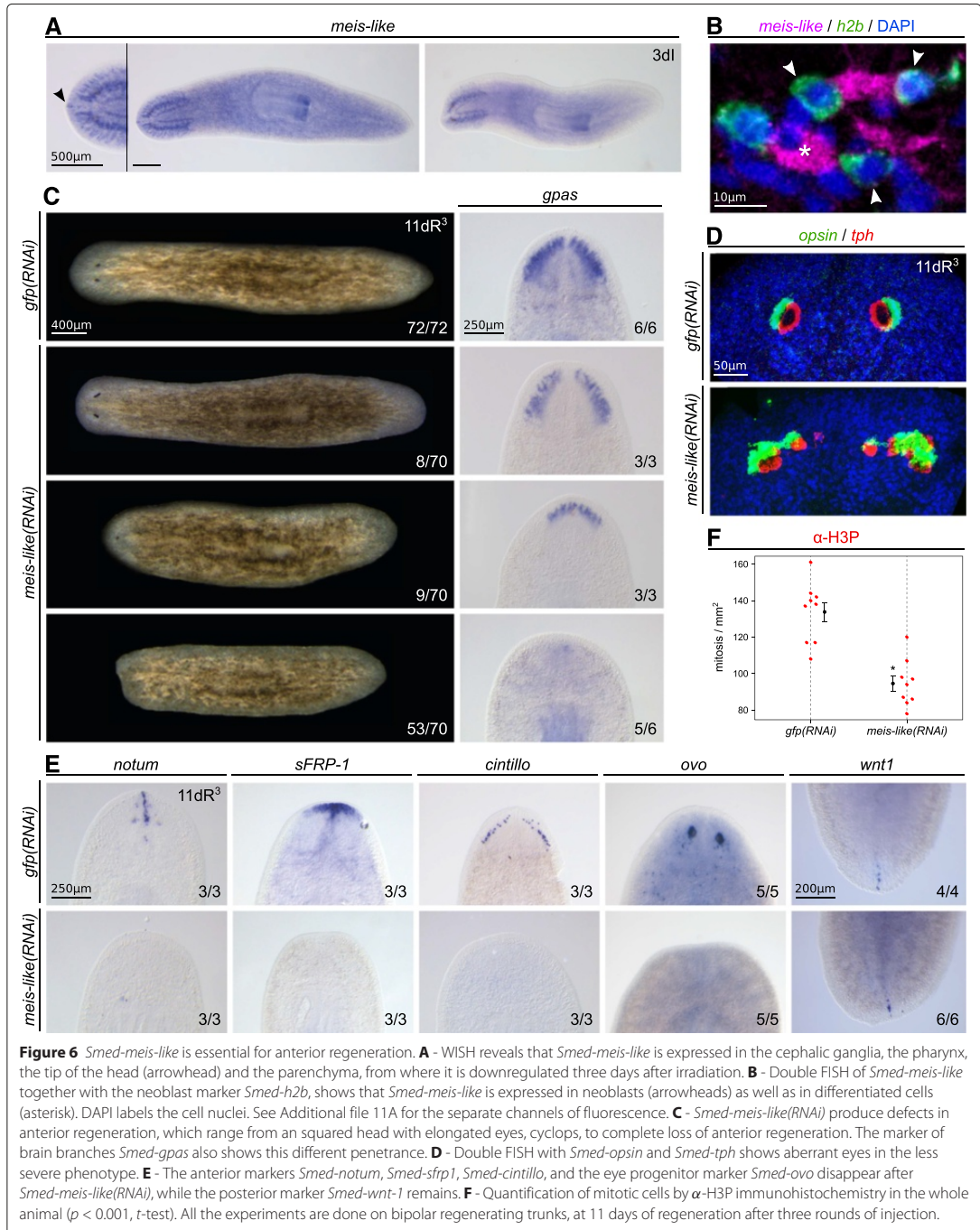
Finally, immunohistochemistry against H3P (Figure 6F) shows a slight—but significant—decrease in proliferation in the whole animal (133.8 ± 5.22 mitosis/mm² in $n=9$ controls versus 94.6 ± 4.06 cells/mm² in $n=9$ *Smed-meis-like*(RNAi), mean \pm s.e.m.). This decline in mitosis is matched by the lack of progenitors of some anterior structures, indicating also defects in differentiation. Thus, eye progenitor cells, which are labeled with *Smed-ovo* [54], are not present in *Smed-meis-like*(RNAi) animals (Figure 6E).

The requirement for *Smed-meis-like* in anterior regeneration is similar to another member of the family, *Smed-prep* [70]. This differential phenotype is also observed after the inhibition of other genes, such as *Smed-egr4* [79], *Smed-zicA* [80,81] and *Smed-FoxD* [82]. The milder phenotype, showing elongated eyes, is similar to the effect of *Smed-meis*(RNAi) [54], and also to the mild inhibition of *Smed-bmp4* [83]. Altogether, these results suggest that *Smed-meis-like* is important for eye and anterior regeneration, similarly to other members of the TALE-class homeobox family. However, given the lack of expression of *Smed-meis-like* in the eyes, the abnormal eye formation could be a consequence of the anomalous brain regeneration.

Nuclear Factor Y complex

The Nuclear Factor Y complex (NF-Y) is an important transcription factor composed by three subunits (NF-YA, NF-YB and NF-YC), each one encoded by a different gene. This heterotrimeric complex acts as both an activator and a repressor, and it regulates other transcription factors, including several growth-related genes, through the recognition of the consensus sequence CCAAT localized in the promoter region [84–88]. In addition, it has been reported that the NF-Y complex regulates the transcription of many important genes like *Hoxb4*, *y-globin*, *TGF-beta receptor II*, or the *Major Histocompatibility Complex class II* and *Sox* gene families [89]. This large number of interactions makes the NF-Y complex an important mediator in a wide range of processes, from cell-cycle regulation and apoptosis-induced proliferation to development and several kinds of cancer [90].

In the sexual strain of *S. mediterranea*, an NF-YB is necessary to maintain spermatogonial stem cells [91]. We have isolated a different NF-YB subunit (NF-YB-2), and also a member of the other two subunits (NF-YA and



NF-YC). WISH shows that the three genes are expressed ubiquitously and in the cephalic ganglia (Figure 7A). Moreover, the expression decrease one day after irradiation indicating a linkage with stem cells, as described in other organisms [92]. Double FISH of each NF-Y subunit together with *Smed-h2b* confirms the expression of this complex in neoblasts and also in some determined cells (Figure 7B and Additional file 12A).

It has been suggested that each NF-Y component could have a specific role [93]. Therefore, to better understand the function of this complex, we knocked down each subunit separately. Although the penetrance varies depending on the subunit inhibited, the phenotype observed after RNAi treatment is the same. In intact non-regenerating animals, RNAi resulted in head regression, ventral curling and, finally, death by lysis (data not shown), as described for other neoblast-related genes [58,59]. After 11 days, head and tail amputated animals failed to regenerate properly, with a smaller brain and fewer brain ramifications as revealed by *Smed-gpas* (Figure 7C) and by α -SYNAPSIN (Additional file 12B). Furthermore, we observe an increase in the number of *Smed-h2b*⁺ cells (Figure 7C,E), also in the area in front of the eyes, where there should not be undifferentiated neoblasts, even though mitosis are reduced (Figure 7D). There is also a decrease in the number of early postmitotic cells (*Smed-nb.21.11e*⁺) (Figure 7C,E), whereas late postmitotic cells (*Smed-agat-1*⁺) do not present significant differences (Figure 7E) [53]. These early progeny markers have recently been associated with epidermal renewal [94]. Hence, the accumulation of neoblasts and the decrease of the subepidermal postmitotic population suggest a defect in the early stages of the differentiation process affecting the epidermal lineage. The neural lineage may also be compromised according to the atrophied cephalic ganglia.

Conclusions

This work presents experimental validation of a collection of putative neoblast genes obtained from a DGE assay on cell fractions. As clearly depicted in the splashplot for the comparison of expression levels between X1, X2 and Xin fractions (Figure 5 and Additional file 13A), there are only a few transcripts specific to X2. The plot produced with the data provided by Labbé [14] from their RNA-Seq analysis on X1, X2 and Xin cell fractions for *S. mediterranea* shows a similar pattern (Additional file 13B). Moreover, comparison among the three sets using Pearson and Spearman correlations indicates that X1 and X2 are the most correlated populations (Additional file 14). Following these results, most of the transcripts expressed in X2 are also expressed in X1. Hence, X2 is a heterogeneous population that cannot be transcriptionally differentiated from X1 without a deeper discrimination method. In this regard, the strategy recently applied by van Wolfswinkel

and collaborators using the last sequencing technology to obtain the transcriptome of individual cells [94], represents the most promising approach to deciphering the heterogeneity of the neoblast progeny.

Randomization simulations also illustrate the specificity of the 21bp tags to detect real transcripts, corroborating previous estimations [29,46,48,49,95,96]. Furthermore, those results reinforce the assumption that most of the non-mapping tags will correspond to real transcripts [46-49], still lacking from reference data sets for this species. Antisense transcription was also detected, confirming previous reports [25,36,49]. Although further analysis will be required to determine whether this could explain a fraction of the “novel” tags, our primary focus was to characterize the canonical protein-coding transcripts. Due to the heterogeneity of this species genome, we would expect some variability—both at sequence and expression arising from individuals (the pool of animals taken for the samples), and cells (as they do not come from a cell culture). This could explain another fraction of tags not mapping onto the reference transcriptomes. Consequently, we were quite strict in the current manuscript to look for exact tag matches, taking into account that one or more mismatches represents a mappability issue even for finished transcriptomes of the quality of human [97] or *Drosophila melanogaster* [98].

DGE has proven to be reliable for transcript quantification and new gene identification in planaria. In this work, we have described a new member of the TALE-class homeobox family, *Smed-meis-like*. Similar to other members of this family, this gene seems to be involved exclusively on anterior polarity determination during regeneration. Given that the expression of this gene is not restricted to neoblasts, its role can also be important in committed cells. Our results with the NF-Y complex suggest that the knockdown of this complex blocks early differentiation of the epidermal and, probably, neural lineages, both belonging to the ectodermal line, generating a neoblast accumulation and deregulation. This effect has been shown in other organisms such as *Drosophila*, in which NF-Y knockout blocks differentiation of R7 neurons through *senseless* [89,99]. The majority of the new neoblast genes reported and validated in this study were found to participate in cell proliferation, cell cycle regulation, embryogenesis or development in other models, and many of them are involved in processes related to cancer. The pathways participating in tumorigenic processes and stem cell regulation are often the same, as has been proposed previously for planarians [100]. These genes are probably fundamental for stem cell maintenance and the control of proliferation in organisms with the capacity to regenerate [101], thus reinforcing the potential value of *S. mediterranea* as an in vivo model for stem cell research [102].

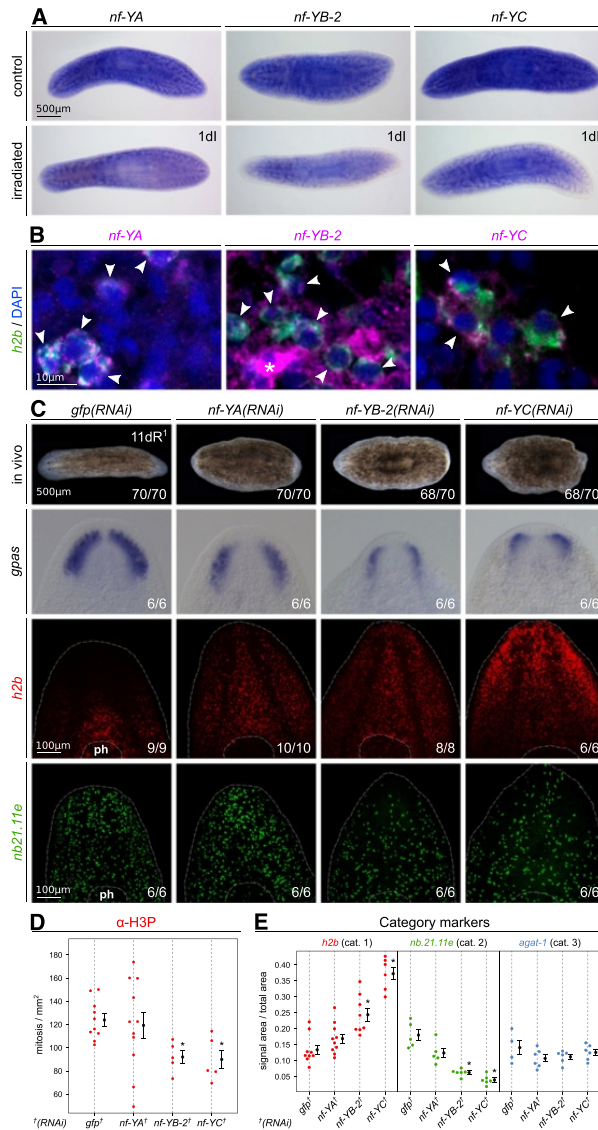


Figure 7 *Smed-nf-Y* gene complex is required for the proper neoblast differentiation and localization. **A** - WISH shows that the three *Smed-nf-Y* genes are expressed ubiquitously and in the cephalic ganglia, and one day after irradiation their expressions decrease. **B** - Double FISH of *Smed-nf-YA*, *Smed-nf-YB-2*, and *Smed-nf-YC* together with the neoblast marker *Smed-h2b* shows colocalization with the NF-Y subunits (arrowheads), demonstrating the expression of this complex in neoblasts as well as in differentiated cells (asterisk). DAPI labels the cell nuclei. See Additional file 12A to check each channel of fluorescence separately. **C** - *Smed-nf-Y(RNAi)* animals regenerate thinner blastemas with non well formed eyes and shape defects, and fail to differentiate a proper brain, with reduced cephalic ganglia as revealed with *Smed-gpas*. FISH with the neoblast marker *Smed-h2b* shows an accumulation of neoblasts in the region in front of the eyes while the early progeny marker *Smed-nb.21.11e* reveals a decrease of early postmitotic cells in *Smed-nf-Y(RNAi)* animals. **D** - Immunohistochemistry with the mitotic marker α -H3P shows a reduction in the number of mitosis. **E** - Quantification with category markers indicate a significant increase of *Smed-h2b*⁺ cells in *Smed-nf-YB-2(RNAi)* and *Smed-nf-YC(RNAi)* animals and a significant decrease of *nb.21.11e*⁺ cells in all of the RNAi animals, whereas *Smed-agat-1*⁺ cells do not show significant changes ($p < 0.001$, *t*-test). Counts are referred to the whole body. ph: pharynx. All the experiments are done on bipolar regenerating trunks, at 11 days of regeneration after one round of injection.

Our DGE analysis pointed out a high resemblance among all the transcriptomes available for *S. mediterranea*. We have also shown the redundancy of the transcriptomes currently available for *S. mediterranea* in agreement with Kao [17], together with their incompleteness under the light of the DGE data. Although our results provide a comprehensive comparison among them, it would be desirable to agree on a unique transcriptome to be used by the whole community. To this end, the PlanMine initiative [103] is attempting to obtain consensus among the researchers on an appropriate reference. Nonetheless, the need for a completely sequenced and well-annotated genome remains. The DGE strategy can help in this endeavour, since short sequences can be rapidly projected over the reference genome or the transcriptome, even from different laboratories, in order to improve their annotation [46]. Similarly, DGE allows the data generated to be reassessed as many times as required, as a more complete genome and transcriptome references for this species become available. Hence, the quantitative data provided here by DGE will prove useful in order to recover and annotate more undescribed genes in the future.

Methods

Animal samples

Planarians used in this study were from the asexual clonal line of *S. mediterranea* BCN10. Animals were maintained in artificial water and were starved at least seven days prior to experimentation.

Cell dissociation, cell sorting and RNA extraction

To trigger neoblast proliferation and differentiation, two days head and tail regenerating animals were used for the preparation of the libraries. Three animals per library were used in order to obtain the required amount of RNA. Cell dissociation and FACS were carried out as described by Möritz [31] and Hayashi [30]. Briefly, after cell staining with Calcein AM and Hoechst 33342 (Molecular Probes, Life Technologies), one million cells were separated for each population in a FACS Aria sorter (Becton Dickinson) at the Scientific and Technological Centers of the University of Barcelona (CCiTUB) cytometry facilities. A representative plot of the cell populations after the sorting can be seen in Additional file 1A. Cells were directly collected in TRIzol LS (Life Technologies) at 4°C and maintained in ice to preserve RNA integrity. RNA extraction followed to obtain 1 µg of total RNA for each library. Quantification of RNA was assessed with a Nanodrop ND-1000 spectrophotometer (Thermo Scientific) and quality check was performed by capillary electrophoresis in an Agilent 2100 Bioanalyzer (Agilent Technologies) prior to library preparation.

DGE sequencing

Unlike RNA-Seq, this method only sequences a short read of a fixed length, named tag, derived from a single site proximal to the 3'-end of polyadenylated transcripts. This short read is later used to identify the full transcript. The number of times that the very same tag has been sequenced—its number of occurrences—is proportional to the abundance of the transcript which it belongs to. Since it only counts one sequence per transcript, its ability to quantify is not affected by the transcript length. For that reason, DGE is better suited for the detection of short transcripts and low expressed genes when compared with RNA-Seq [20-22].

Sequence tag preparation was done with Illumina's DGE Tag Profiling Kit according to the manufacturer's protocol as described [104]. In short, the most relevant steps included the incubation of 1 µg of total RNA with oligo-dT beads to capture the polyadenylated RNA fraction followed by cDNA synthesis. Then, samples were digested with NlaIII to retain a cDNA fragment from the most 3' CATG proximal site to the poly(A)-tail. Subsequently, a second digestion with MmeI was performed, which cuts 17 bp downstream of the CATG site, generating, thus, the 21 bp tags.

Cluster generation was performed after applying 4pM of each sample to the individual lanes of the Illumina 1G flowcell. After hybridization of the sequencing primer to the single-stranded products, 18 cycles of base incorporation were carried out on the 1G analyzer according to the manufacturer's instructions. Image analysis and base calling were performed using the Illumina pipeline, where tag sequences were obtained after purity filtering. Generation of expression matrices, data annotation, filtering and processing were performed by using the Biotag software (SkuldTech, France) [104].

Raw sequencing data in FASTQ format as well as processed tag sequences and their associated expressions have been deposited at NCBI Gene Expression Omnibus (GEO) [105] and are accessible through GEO Series accession number GSE51681 [106].

Comparison of expression data

Tag raw expression was normalized to counts per million (cpm). The statistical value of DGE data comparisons, as a function of tag counts, was calculated by assuming that each tag has an equal chance to be detected, in fair agreement with a binomial law. An internal algorithm allows the comparison between different libraries and measures the significance threshold for the observed variations and p-value calculation (see Mathematical Appendix of Piqueval et al. 2002 [104]).

Different Perl [107] scripts were designed for the subsequent analyses. All of them are available from the web site planarian.bio.ub.edu/SmedDGE.

Tag mapping

A database with all the possible CATG + 17bp theoretical tag sequences was constructed for each one of the reference data sets. Tags were compared to these databases to identify all perfect matches and, when more than one tag mapped over the same transcript, only the tag closer to the 3'-end was considered. For the genome reference, 2 mismatches were also considered for unmappable tags with the SeqMap mapper [108,109].

In addition, tags were also mapped against a database of 8,662,308 CDS and 5,189 genomic sequences from bacteria directly downloaded from GenBank [110] repositories to check sample contaminations. Only two tags mapped on bacterial transcripts, confirming the purity of our libraries.

For the 3'-UTR prediction, all 23,020 contigs of the transcriptome from Kao et al. 2013 [17], were mapped over the genome using Exonerate 2.2.0 [111] to characterize the putative 3'-UTR ends (poly-A sites were not predicted though). Apart from aligning the transcripts to the genomic contigs, the strand for the longest ORF contained was also considered to ensure proper transcript orientation. For each transcript, 1,000bp upstream and downstream regions around the genomic coordinate for the putative 3'-UTR ends found were considered to retrieve DGE tags (noted as transcripts 3'-end relative position in Additional file 5).

Libraries and reference sequence data sets randomization

Libraries and reference data sets were randomized using Perl [107] scripts and the Inline::C library to generate analogous sets of random sequences. This method resembles the original data sets in terms of size and nucleotide abundance in comparison with other approximations which generate virtual sequences based on mathematical distributions [49]. 500 and 100 randomizations for each library and data sets respectively were generated. Mapping was performed using cutoffs of 1, 5, 10, 15 and 20 occurrences (Additional file 3).

Browsing data sets

Mapped tags are also available from the web site through a set of dynamic tables (Figure 4A). They were implemented using the jQuery jqGrid-4.5.2 [112] library, an Ajax-enabled JavaScript control to represent and manipulate tabular data on the web. Those tables summarize the tags along with their mappings on the different transcriptomes publicly available (which were downloaded from the locations cited at the respective papers [10-17]), their correspondence with the Smed454 transcriptome, and their annotation.

The transcriptome browser shown in Figure 4B was initialized with the Smed454 [10] contigs using the GBrowse2 engine [113]. The browser also includes

high-scoring segment pairs (HSPs) from whole-transcriptome BLAST searches performed over the UniProt database [114] (NCBI BLAST+ 2.2.29 [51] with default parameters), as well as the Pfam [115,116] domains mapped by HMMER—with E-val=1 and domain E-val=1—[117] on the six-frame translations for the contigs sequences. DGE tag sequences—together with the corresponding counts, normalized scores, their ranks, etc.—were uploaded to the GBrowse2 MySQL database, and they are shown in the browser using a customized version of the Bio::Graphics::Glyph::xyplot module.

Functional annotation was projected from the UniProt GO annotations over the homologous Smed454 contig sequences. Two-tailed hypergeometric test, which accounts for significant overrepresented (positive-tail) or under-represented (negative-tail), was performed by comparing the set of GO assigned to transcriptome contigs over-represented on each of the cell fractions against the set of GO annotations for the whole set of contigs. Significance threshold was set to $p < 10^{-5}$ and the results are summarized in Additional file 6 for the different cell fraction sets.

Gene nomenclature

New genes were named following the nomenclature proposed for *S. mediterranea* [118] based on their BLASTx homology—NCBI BLAST+ 2.2.29 [51] with default parameters against the UniProt database [114]—to its human homologous gene according to the official gene name approved by the HUGO Gene Nomenclature Committee (HGNC) [119] whenever possible, and trying to honor the names of other members of the family if they were already stated for *S. mediterranea*. When no significant homology for the corresponding gene was available, its characteristic domain found at the Pfam site [115,116] was used to identify it.

Gene sequences and primers used for cloning are deposited at the GenBank [110] site—see Table 4 for the accession numbers of the sequences.

Irradiation

For experimental protocols requiring irradiated animals, irradiation was carried out at 75 Gy (1,66 Gy/minute) in a X-ray cabinet MaxiShot 200 (Yxlon Int.) at the facilities of the Scientific and Technological Centers of the University of Barcelona (CCIUB).

In situ hybridization

WISH was conducted for gene expression analysis, as previously described [120,121]. Images from representative organisms of each experiment were captured with a ProgRes C3 camera (Jenoptik) through a Leica MZ16F stereomicroscope. Animals were fixed and hybridized at the indicated time points.

Fluorescence in situ hybridization

For double FISH animals were treated as described elsewhere [122]. Confocal laser scanning microscopy was performed with a Leica SP2.

Immunohistochemistry

Immunostaining was carried out as described previously [123]. The following antibodies were used: α -SYNORF-1, a monoclonal antibody specific for SYNAPSIN, which was used as a pan-neural marker [124] (1:50; Developmental Studies Hybridoma Bank); and α -phospho-histone H3 (H3P), which was used to detect mitotic cells (1:500; Cell Signaling Technology). Alexa 488-conjugated goat α -mouse (1:400) and Alexa 568-conjugated goat α -rabbit (1:1000; Molecular Probes) were used as secondary antibodies.

RNAi experiments

Double-stranded RNAs (dsRNA) were produced by in vitro transcription (Roche) and injected into the gut of the planarians as previously described [5]. Three aliquots of 32 nl (400-800ng/ μ l) were injected on three consecutive days with a Drummond Scientific Nanoject II injector. Head and tail ablation pre- and post-pharyngeally followed the fourth day. If no phenotype was observed after two weeks, a second round of injection and amputation was carried out in the same manner, unless otherwise stated. Control organisms were injected with *gfp* dsRNA.

Availability of supporting data

All data sets are fully available without restriction. Yet relevant data sets were already included within this article and its additional files, further supporting material, as well as updates, will be publicly available through the project web site [<https://planarian.bio.ub.edu/SmedDGE>].

Raw sequencing data in FASTQ format, along with processed tag sequences and their associated expressions, have been deposited at NCBI Gene Expression Omnibus (GEO) [105]; they are accessible through GEO Series accession number GSE51681 [106]. Gene sequences and primers used for cloning are deposited at the GenBank [110] repository, the corresponding accession numbers for the gene sequences are listed on Table 4.

Additional files

Additional file 1: Fluorescence-activated cell sorting plot.

A - Representative FACS plot of the cell sorting experiment carried out in this study showing the selection criteria applied for the isolation of the X1, X2, and Xin cell populations as described by Möritz [31] and Hayashi [30]. The cytoplasm of the cells is stained with Calcein AM while their nuclei are labeled with Hoechst 33342. Then, cells are separated by their nucleus/cytoplasm ratio. **B** - Same FACS plot from a cell dissociation experiment with lethally irradiated planarians four days after irradiation. A complete ablation of X1 and an important reduction of cells in X2 can be

observed. The sensitivity of the cells in these populations to irradiation responds to their composition of neoblasts in different stages of the cell cycle and distinct levels of determination: X1, proliferating stem cells in S/G2/M, and X2, stem cell progeny and proliferating neoblasts in G0/G1. Neoblasts are the only proliferating cells in this organism.

Additional file 2: Distribution of mapped and orphan tags by number of occurrences. **A** - Venn diagrams showing the tags overlap between the three cell populations, by occurrence (top), and by significant p-value, ($p < 0.05$, bottom). The number of mapping tags is detailed in italics.

B - Frequency distribution of tags grouped by its number of occurrences, i.e., sequencing events, in all libraries. Tags detected in a low copy number are prone to be produced by sequencing errors—likely from more abundant tags. As can be appreciated, most of the tags with less than five occurrences do not map over any of the reference data sets, suggesting that those tags are less reliable [49], which is in agreement with the results of the randomization simulations (see the text and Additional file 3). Due to that, tags detected less than five times were discarded in further analysis.

Additional file 3: Randomization simulations. Number of tags mapped over the randomized reference data sets, and vice versa, at different occurrences cutoffs. When compared with the theoretical number of matches expected by chance, this facilitates the assessment of the minimum number of counts for a tag to be considered reliable.

Additional file 4: X1 and X2 in irradiated animals. Venn diagram showing the overlap between the results presented here and the DGE study conducted over irradiated planarians of the same clonal line by Galloni [36]. The number of mapping tags out of the total is detailed in italics. It can easily be appreciated that most of the tags present in X1 and X2 are not detected by the irradiation approach.

Additional file 5: Tags potentially mapping in the 3'-UTR regions. Y-axis represents the number of tags (tag counts) per nucleotide genomic position. The sequenced DGE tags were then classified in two groups: those mapping within the genomic region delimited by the transcript exons (green area), and those mapping outside (blue area). As position 0 depicts the last nucleotide for all the transcripts, we can only observe green marks upstream; blue marks can distribute across all the downstream region too. Background is defined by all those genomic CATG target sequences that do not match to any of the sequenced DGE tags (red areas). Dashed line depicts the average value for the downstream background tag counts.

Additional file 6: Bar plots of the GO significant terms for different comparisons among X1, X2 and Xin annotation sets. Each panel presents a list of the significant functional annotations ($p < 10^{-5}$, hypergeometric test), along with the corresponding GO code, that are over- or under-represented (computed as log-odds of the term abundance by sequence set) on each of the three ontology domains (Biological Processes, BP; Molecular Functions, MF; and Cellular Components, CC). Bar plots compare results obtained when considering the following four non-overlapping sets: X1-only (red bars), X2-only (green bars), the intersection between X1 and X2 not in Xin (orange), and Xin-only (blue bars). Bars color-filling is proportional to the p-value for the given GO code, thus darker colors corresponds to smaller p-values (all below the significant threshold anyway). A Venn diagram on top of each page represents the comparison made among the fraction sets.

Additional file 7: Genes involved in stemness, regeneration or tissue homeostasis overexpressed in neoblasts and their progeny. DGE expression of clones reported in two experimental high-throughput screenings by Reddien [6] and Wenemoser [56] related to regeneration, stemness or tissue homeostasis identified as being overexpressed in neoblasts ($p < 0.001$).

Additional file 8: Whole mount in situ hybridization of new neoblast genes. Expression by WISH of new neoblast genes in control (left panel) and irradiated planarians (right panel). 38 out of the 42 genes tested are presented here. The remaining four are characterized in Figures 6A and 7A. Time after irradiation in days is shown in the top right corner for each gene. As expected for neoblast genes, expression is reduced or disappears after irradiation.

Additional file 9: RNA interference of new neoblast genes showing defects in regeneration. The stronger and most representative phenotype obtained after RNAi for those new neoblast genes producing

aberrant regeneration after head and tail ablation. Days of regeneration and round of injection in superscript, and number of individuals affected with respect to the total are shown in the top right and bottom right corners of each panel. All pictures are dorsal except *Smed-bbp4-4*, which illustrates the typical ventral curling of dying animals. The inhibition of most of the genes completely prevented the formation of the blastema. For those cases in which a small blastema was allowed to develop, a detail of the anterior part is shown to appreciate the defective head and eyes. For a regenerating control animal see Figures 6C and 7C.

Additional file 10: Literature review of the new neoblast genes presented in this study. A description is provided for each one of the new neoblast genes proposed in this study (summarized in Table 4) based on the literature about their homologs in other species.

Additional file 11: Double fluorescence in situ hybridization of *Smed-h2b* with *Smed-meis-like*. A - Double FISH of *Smed-meis-like* together with the neoblast marker *Smed-h2b* shows colocalization of both genes, demonstrating the expression of *Smed-meis-like* in neoblasts. Expression is also detected in differentiated cells. B - The pan-neural marker α -SYNAPSIN shows the different penetrance of phenotypes of *Smed-meis-like*(RNAi).

Additional file 12: Double fluorescence in situ hybridization of *Smed-h2b* with *Smed-nf-YA*, *Smed-nf-YB-2*, and *Smed-nf-YC*. A - Double FISH of *Smed-nf-YA*, *Smed-nf-YB-2*, and *Smed-nf-YC* shows colocalization of the NF-Y subunits with the neoblast marker *Smed-h2b*, corroborating the expression of this complex in neoblasts. Expression is also detected in differentiated cells. B - The pan-neural marker α -SYNAPSIN shows reduced cephalic ganglia of RNAi animals compared with *gfp* controls.

Additional file 13: Splashplot projection of the X1/X2 versus Xin expression changes of upregulated contigs by cell population.

A - Splashplot for overrepresented contigs in the three cell fractions X1, X2 and Xin according to our DGE data over the *Smed454* transcriptome [10]. B - Same representation using the data published by Labbé [14]. Both plots show a similar composition, revealing a low number of transcripts overexpressed specifically in X2/progeny cells.

Additional file 14: Pearson and Spearman correlations of the normalized expression levels among X1, X2 and Xin. Diagonal panels show violin plots with the distribution of the normalized expression levels for each of the three cell populations data sets. Panels on the upper diagonal summarize both Pearson (parametric) and Spearman (non-parametric) correlations, along with the p-values and the linear regression model estimates for the pairwise comparison between data sets. On the bottom diagonal panels, for each pair of cell fractions the scatterplots show differences in expression for each DGE tag. Blue dotted line is defined by the intercept and slope values for the linear regression model presented on the corresponding upper panel, confidence interval is drawn as a grey shadow along that regression line. Those tags having a normalized expression value of zero in one or both of the cell types, when considering each pair-wise comparisons, were removed before computing correlations and for the plots. One can notice that X1 and X2 are the more correlated pair of cell fractions, then X2 and Xin, and finally X1 and Xin. Those results match to what would be expected.

Abbreviations

3'-UTR: Three prime untranslated region; cpm: Counts per million; DGE: Digital gene expression; EST: Expressed sequence tag; FACS: Fluorescence-activated cell sorting; FISH: Fluorescence in situ hybridization; GO: Gene ontology; ORF: Open reading frame; RNAi: RNA interference; TALE: Three amino acid loop extension; WISH: Whole mount in situ hybridization.

Competing interests

The authors declare that they have no competing interests.

Authors' contributions

ES, GRE and JFA conceived the project. GRE prepared the cell fractions for the DGE sequencing, and did the screening of the selected genes. AGS and JIR carried out the experimental characterization of the *Smed-meis-like* and *Smed-nf-Y* genes respectively. GRE and JFA performed the computational analyses and set up the web material. GRE drafted the manuscript with contributions from all authors. All authors read and approved the final manuscript.

Acknowledgements

DGE libraries were produced by Skuldtech under supervision of David Piquemal. We thank Mireille Galloni (University of Montpellier 2 and CNRS) for sharing the DGE libraries of irradiated organisms before they were publicly available. Further thanks to Jaume Comas and Ricard Álvarez (Scientific and Technological Centers of the University of Barcelona) for their excellent technical assistance at the cytometry facilities. We are especially grateful to Luca Gentile and Sören Moritz (Max-Planck-Institut für molekulare Biomedizin) for the cell dissociation protocol and their inestimable advice. We also thank all the members of the Emili Saló and Francesc Cebrià labs for encouragement and discussion, and Enrique Blanco and Iain K. Patten for critical comments on the manuscript. We want to acknowledge the helpful comments made by the referees in order to improve the final manuscript version. This work was funded by grants BFU2008-01544 and BFU2011-22786 (MICINN), and 2009SGR-1018 and SGR2014-687 (AGAUR) to ES and BFU2009-09102 (MICINN) to JFA. GRE and JRL were supported by FPI (MICINN and MECC respectively), and AGS by FPU (MECC) fellowships. The funders had no role in study design, data collection and analysis, decision to publish, or preparation of this manuscript.

Received: 14 November 2014 Accepted: 13 April 2015

Published online: 08 May 2015

References

- Reddien PW. Specialized progenitors and regeneration. *Development*. 2013;140(5):951–7.
- Rink J. Stem cell systems and regeneration in planaria. *Dev Genes Evol*. 2013;223(1-2):67–84.
- Elliott S, Sánchez Alvarado A. The history and enduring contributions of planarians to the study of animal regeneration. *Rev Dev Biol*. 2013;2(3):301–26.
- Baguña J. The planarian neoblast: the rambling history of its origin and some current black boxes. *Int J Dev Biol*. 2012;56(1-3):19–37.
- Sánchez Alvarado A, Newmark PA. Double-stranded RNA specifically disrupts gene expression during planarian regeneration. *Proc Natl Acad Sci USA*. 1999;96(9):5049–54.
- Reddien PW, Bermange AL, Murfitt KJ, Jennings JR, Sánchez Alvarado A. Identification of genes needed for regeneration, stem cell function, and tissue homeostasis by systematic gene perturbation in planaria. *Dev Cell*. 2005;8(5):635–49.
- Rossi L, Salvetti A, Marincola FM, Lena A, Deri P, Mannini L, et al. Deciphering the molecular machinery of stem cells: a look at the neoblast gene expression profile. *Genome Biol*. 2007;8(4):62.
- Fernández-Taboada E, Rodríguez-Esteban G, Saló E, Abril JF. A proteomics approach to decipher the molecular nature of planarian stem cells. *BMC Genomics*. 2011;12:133.
- Böser A, Drexler HC, Reuter H, Schmitz H, Wu G, Schöler HR, et al. SILAC proteomics of planarians identifies ncoa5 as a conserved component of pluripotent stem cells. *Cell Reports*. 2013;5(4):1142–55.
- Abril JF, Cebrià F, Rodríguez-Esteban G, Horn T, Fraguas S, Calvo B, et al. *Smed454* dataset: unravelling the transcriptome of *Schmidtea mediterranea*. *BMC Genomics*. 2010;11(1):731.
- Blythe MJ, Kao D, Malla S, Rowsell J, Wilson R, Evans D, et al. A dual platform approach to transcript discovery for the planarian *Schmidtea mediterranea* to establish RNAseq for stem cell and regeneration biology. *PLoS One*. 2010;5(12):15617.
- Adamidi C, Wang Y, Gruen D, Mastrobucchi G, You X, Tolle D, et al. De novo assembly and validation of planaria transcriptome by massive parallel sequencing and shotgun proteomics. *Genome Res*. 2011;21(7):1193–200.
- Sandmann T, Vogg MC, Owlarn S, Boutros M, Bartscherer K. The head-regeneration transcriptome of the planarian *Schmidtea mediterranea*. *Genome Biol*. 2011;12(8):76.
- Labbé RM, Irimia M, Currie KW, Lin A, Zhu SJ, Brown DD, et al. A comparative transcriptomic analysis reveals conserved features of stem cell pluripotency in planarians and mammals. *Stem Cells*. 2012;30(8):1734–45.
- Resch AM, Palakodeti D, Lu YC, Horowitz M, Graveley BR. Transcriptome analysis reveals strain-specific and conserved stemness genes in *Schmidtea mediterranea*. *PLoS One*. 2012;7(4):34447.
- Rouhana L, Vieira AP, Roberts-Galbraith RH, Newmark PA. PRMT5 and the role of symmetrical dimethylarginine in chromatid bodies of planarian stem cells. *Development*. 2012;139(6):1083–94.

17. Kao D, Felix D, Aboobaker A. The planarian regeneration transcriptome reveals a shared but temporally shifted regulatory program between opposing head and tail scenarios. *BMC Genomics*. 2013;16(14):797.
18. Solana J, Kao D, Mihaylova Y, Jaber-Hijazi F, Malla S, Wilson R, et al. Defining the molecular profile of planarian pluripotent stem cells using a combinatorial RNAseq, RNA interference and irradiation approach. *Genome Biol*. 2012;13(3):19.
19. Scimone M, Kravarik K, Lapan S, Reddian P. Neoblast specialization in regeneration of the planarian *Schmidtea mediterranea*. *Stem Cell R*. 2014;3(2):339–52.
20. Oshlack A, Wakefield MJ. Transcript length bias in RNA-seq data confounds systems biology. *Biol Direct*. 2009;4:14.
21. Raz T, Kapranov P, Lipson D, Letovsky S, Milos PM, Thompson JF. Protocol dependence of sequencing-based gene expression measurements. *PLoS One*. 2011;6(5):19287.
22. Hong LZ, Li J, Schmidt-Kuntzel A, Warren WC, Barsh GS. Digital gene expression for non-model organisms. *Genome Res*. 2012;21(11):1905–15.
23. Hanriot L, Keime C, Gay N, Faure C, Dossat C, Wincker P, et al. A combination of LongSAGE with Solexa sequencing is well suited to explore the depth and the complexity of transcriptome. *BMC Genomics*. 2008;16(9):418.
24. Veitch NJ, Johnson PC, Trivedi U, Terry S, Wildridge D, MacLeod A. Digital gene expression analysis of two life cycle stages of the human-infective parasite, *Trypanosoma brucei* gambiense reveals differentially expressed clusters of co-regulated genes. *BMC Genomics*. 2010;11(1):124.
25. 't Hoen PAC, Ariyurek Y, Thygesen HH, Vreugdenhil E, Vossen RHAM, de Menezes RX, et al. Deep sequencing-based expression analysis shows major advances in robustness, resolution and inter-lab portability over five microarray platforms. *Nucleic Acids Res*. 2008;36(21):141.
26. Asmann YW, Klee EW, Thompson EA, Perez EA, Middha S, Oberg AL, et al. 3' tag digital gene expression profiling of human brain and universal reference RNA using Illumina Genome Analyzer. *BMC Genomics*. 2009;10(1):531.
27. de Lorgeril J, Zenagui R, Rosa RD, Piquemal D, Bachère E. Whole transcriptome profiling of successful immune response to vibrio infections in the oyster *Crassostrea gigas* by digital gene expression analysis. *PLoS ONE*. 2011;6(8):23142.
28. Philippe N, Bou Samra E, Boreux A, Mancheron A, Ruffe F, Bai Q, et al. Combining DGE and RNA-sequencing data to identify new polyA+ non-coding transcripts in the human genome. *Nucleic Acids Res*. 2014;42(5):2820–32.
29. Dong H, Ge X, Shen Y, Chen L, Kong Y, Zhang H, et al. Gene expression profile analysis of human hepatocellular carcinoma using SAGE and LongSAGE. *BMC Med Genomics*. 2009;2(1):5.
30. Hayashi T, Asami M, Higuchi S, Shibata N, Agata K. Isolation of planarian X-ray-sensitive stem cells by fluorescence-activated cell sorting. *Dev Growth Differ*. 2006;48(6):371–80.
31. Moritz S, Stöckle F, Ortmeier C, Schmitz H, Rodríguez-Esteban G, Key G, et al. Heterogeneity of planarian stem cells in the S/G2/M phase. *Int J Dev Biol*. 2012;56(1-3):117–25.
32. Mukherjee K, Bürglin TR. Comprehensive analysis of animal TALE homeobox genes: new conserved motifs and cases of accelerated evolution. *J Mol Evol*. 2007;65(2):137–53.
33. Bhattacharya A, Deng J, Zhang Z, Behringer R, de Crombrugge B, Maity S. The B subunit of the CCAAT box binding transcription factor complex (CBF/NF-Y) is essential for early mouse development and cell proliferation. *Cancer Res*. 2003;63(23):8167–72.
34. Zhang X, Hao L, Meng L, Liu M, Zhao L, Hu F, et al. Digital Gene Expression tag profiling analysis of the gene expression patterns regulating the early stage of mouse spermatogenesis. *PLoS ONE*. 2013;8(3):58680.
35. Gowda M, Jantasuriyarat C, Dean RA, Wang GL. Robust-LongSAGE (RL-SAGE): a substantially improved LongSAGE method for gene discovery and transcriptome analysis. *Plant Physiol*. 2004;134(3):890–7.
36. Galloni M. Global irradiation effects, stem cell genes and rare transcripts in the planarian transcriptome. *Int J Dev Biol*. 2012;56(1-3):103–16.
37. Taft A, Vermeire J, Bernier J, Birkeland S, Cipriano M, Papa A, et al. Transcriptome analysis of *Schistosoma mansoni* larval development using serial analysis of gene expression (SAGE). *Parasitology*. 2009;136(05):469.
38. Pelechano V, Steinmetz L. Gene regulation by antisense transcription. *Nat Rev Genet*. 2013;14(12):880–93.
39. Boguski MS, Lowe TMJ, Tolstoshev CM. dbEST - database for "expressed sequence tags". *Nat Genet*. 1993;4(4):332–3.
40. Sánchez Alvarado A, Newmark PA, Robb SM, Juste R. The *Schmidtea mediterranea* database as a molecular resource for studying platyhelminthes, stem cells and regeneration. *Development*. 2002;129(24):5659–65.
41. Zayas RM, Bold TD, Newmark PA. Spliced-leader trans-splicing in freshwater planarians. *Mol Biol Evol*. 2005;22(10):2048–54.
42. Zayas RM, Hernández A, Habermann B, Wang Y, Stary JM, Newmark PA. The planarian *Schmidtea mediterranea* as a model for epigenetic germ cell specification: analysis of ESTs from the hermaphroditic strain. *Proc Natl Acad Sci U S A*. 2005;102(51):18491–6.
43. The *Schmidtea mediterranea* Genome Sequencing Project. <http://genome.wustl.edu/genomes/detail/schmidtea-mediterranea>.
44. NCBI Genome Database: *Schmidtea mediterranea*. <http://www.ncbi.nlm.nih.gov/genome/232>.
45. Reverter A, McWilliam S, Barris W, Dalrymple B. A rapid method for computationally inferring transcriptome coverage and microarray sensitivity. *Bioinformatics*. 2004;21(1):80–9.
46. Saha S, Sparks A, Rago C, Akmaev V, Wang C, Vogelstein B, et al. Using the transcriptome to annotate the genome. *Nat Biotechnol*. 2002;20(5):508–12.
47. Chen J, Sun M, Lee S, Zhou G, Rowley J, Wang S. Identifying novel transcripts and novel genes in the human genome by using novel SAGE tags. *Proc Natl Acad Sci U S A*. 2002;99(19):12257–62.
48. Pleasance E, Marra M, Jones S. Assessment of SAGE in transcript identification. *Genome Res*. 2003;13(6):1203–15.
49. Keime C, Sémon M, Mouchiroud D, Duret L, Gandrillon O. Unexpected observations after mapping LongSAGE tags to the human genome. *BMC Bioinf*. 2007;8(1):154.
50. Hene L, Sreenu V, Vuong M, Abidi S, Sutton J, Rowland-Jones S, et al. Deep analysis of cellular transcriptomes-LongSAGE versus classic MPSS. *BMC Genomics*. 2007;8(1):333.
51. Camacho C, Coulouris G, Avagyan V, Ma N, Papadopoulos J, Bealer K, et al. BLAST+: architecture and applications. *BMC Bioinf*. 2009;10(1):421.
52. Smed454 Contig Browser. https://planarian.bio.ub.edu/datasets/454/planarian_menu.php.
53. Eisenhoffer G, Kang H, Sánchez Alvarado A. Molecular analysis of stem cells and their descendants during cell turnover and regeneration in the planarian *Schmidtea mediterranea*. *Cell Stem Cell*. 2008;3(3):327–39.
54. Lapan S, Reddian P. Transcriptome analysis of the planarian eye identifies ovo as a specific regulator of eye regeneration. *Cell Rep*. 2012;2(2):294–307.
55. González-Estévez C, Felix DA, Smith MD, Paps J, Morley SJ, James V, et al. SMG-1 and mTORC1 act antagonistically to regulate response to injury and growth in planarians. *PLoS Genet*. 2012;8(3):1002619.
56. Wenemoser D, Lapan SW, Wilkinson AW, Bell GW, Reddian PW. A molecular wound response program associated with regeneration initiation in planarians. *Genes Dev*. 2012;26(9):988–1002.
57. Wolff E, Dubois F. Sur la migration des cellules de regeneration chez les planaires. *Rev Suisse Zool*. 1948;55:218–27.
58. Reddian P, Oviedo N, Jennings J, Jenkin J, Sánchez Alvarado A. SMEDWI-2 is a PIWI-Like protein that regulates planarian stem cells. *Science*. 2005;310(5752):1327–30.
59. Guo T, Peters A, Newmark P. A Bruno-like gene is required for stem cell maintenance in planarians. *Dev Cell*. 2006;11(2):159–69.
60. Kim JH, Yang CK, Heo K, Roeder RG, An W, Stallcup MR. CCAR1, a key regulator of mediator complex recruitment to nuclear receptor transcription complexes. *Mol Cell*. 2008;31(4):510–9.
61. Ball EE, Rehm EJ, Goodman CS. Cloning of a grasshopper cDNA coding for a protein homologous to the A1, A2/B1 proteins of mammalian hnRNP. *Nucleic Acids Res*. 1991;19(2):397.
62. Rigbolt KTG, Prokhorova TA, Akimov V, Henningsen J, Johansen PT, Kratchmarova I, et al. System-wide temporal characterization of the proteome and phosphoproteome of human embryonic stem cell differentiation. *Sci Signal*. 2011;4(164):3.
63. Rossman T, Wang Z. Expression cloning for arsenite-resistance resulted in isolation of tumor-suppressor *fauc* cDNA: possible involvement of the ubiquitin system in arsenic carcinogenesis. *Carcinogenesis*. 1999;20(2):311–6.

64. Kimura K, Cuvier O, Hirano T. Chromosome condensation by a human condensin complex in *Xenopus* egg extracts. *J Biol Chem*. 2001;276(8):5417–20.
65. Allende ML, Amsterdam A, Becker T, Kawakami K, Gaiano N, Hopkins N. Insertional mutagenesis in zebrafish identifies two novel genes, pescadillo and dead eye, essential for embryonic development. *Genes Dev*. 1996;10(24):3141–55.
66. Knight AS, Notaridou M, Watson RJ. A Lin-9 complex is recruited by B-Myb to activate transcription of G2/M genes in undifferentiated embryonal carcinoma cells. *Oncogene*. 2009;28(15):1737–47.
67. Zhu SJ, Pearson BJ. The Retinoblastoma pathway regulates stem cell proliferation in freshwater planarians. *Dev Biol*. 2013;373(2):442–52.
68. Nakamura Y, Tanaka H, Arakawa H, Yamaguchi T, Shiraishi K, Fukuda S, et al. A ribonucleotide reductase gene involved in a p53-dependent cell-cycle checkpoint for DNA damage. *Nature*. 2000;404(6773):42–9.
69. Bertolino E, Reimund B, Wildt-Perinic D, Clerc RG. A novel homeobox protein which recognizes a TGT core and functionally interferes with a retinoid-responsive motif. *J Biol Chem*. 1995;270(52):31178–88.
70. Felix DA, Aboobaker AA. The TALE class homeobox gene *Smed-prep* defines the anterior compartment for head regeneration. *PLoS Genet*. 2010;6(4):1000915.
71. Chen CC, Wang IE, Reddien PW. *pbx* is required for pole and eye regeneration in planarians. *Development*. 2013;140(4):719–29.
72. Blassberg RA, Felix DA, Tejada-Romero B, Aboobaker AA. PBX/extradenticle is required to re-establish axial structures and polarity during planarian regeneration. *Development*. 2013;140(4):730–9.
73. Fraguas S, Barberán S, Cebrià F. EGFR signaling regulates cell proliferation, differentiation and morphogenesis during planarian regeneration and homeostasis. *Dev Biol*. 2011;354(1):87–101.
74. Iglesias M, Almuedo-Castillo M, Aboobaker AA, Saló E. Early planarian brain regeneration is independent of blastema polarity mediated by the Wnt/ β -catenin pathway. *Dev Biol*. 2011;358(1):68–78.
75. Petersen CP, Reddien PW. Polarized *notum* activation at wounds inhibits wnt function to promote planarian head regeneration. *Science*. 2011;332(6031):852–5.
76. Gurley KA, Rink JC, Sánchez Alvarado A. Beta-catenin defines head versus tail identity during planarian regeneration and homeostasis. *Science*. 2008;319(5861):323–7.
77. Petersen C, Reddien P. Smed-beta-catenin-1 is required for anteroposterior blastema polarity in planarian regeneration. *Science*. 2008;319(5861):327–30.
78. Oviedo NJ, Newmark PA, Sánchez Alvarado A. Allometric scaling and proportion regulation in the freshwater planarian *Schmidtea mediterranea*. *Dev Dyn*. 2003;226(2):326–33.
79. Fraguas S, Barberán S, Iglesias M, Rodríguez-Esteban G, Cebrià F. *egr-4*, a target of EGFR signaling, is required for the formation of the brain primordia and head regeneration in planarians. *Development*. 2014;141(9):1835–47.
80. Vogg MC, Owlarn S, Pérez Rico YA, Xie J, Suzuki Y, Gentile L, et al. Stem cell-dependent formation of a functional anterior regeneration pole in planarians requires Zic and Forkhead transcription factors. *Dev Biol*. 2014;390(2):136–48.
81. Vázquez-Doorman C, Petersen CP. *zic-1* expression in planarian neoblasts after injury controls anterior pole regeneration. *PLoS Genet*. 2014;10(7):1004452.
82. Scimone ML, Lapan SW, Reddien PW. A forkhead transcription factor is wound-induced at the planarian midline and required for anterior pole regeneration. *PLoS Genet*. 2014;10(1):1003999.
83. González-Sastre A, Molina MD, Saló E. Inhibitory Smads and bone morphogenetic protein (BMP) modulate anterior photoreceptor cell number during planarian eye regeneration. *Int J Dev Biol*. 2012;56(1–2–3):155–63.
84. Dolfini D, Mantovani R. Targeting the Y/CCAAT box in cancer: YB-1 (YBX1) or NF-Y? *Cell Death Differ*. 2013;20(5):676–85.
85. Maity S, Golumbek P, Karsenty G, de Crombrugge B. Selective activation of transcription by a novel CCAAT binding factor. *Science*. 1988;241(4865):582–5.
86. Hatamochi A, Golumbek P, Van Schaftingen E, de Crombrugge B. A CCAAT DNA binding factor consisting of two different components that are both required for DNA binding. *J Biol Chem*. 1988;263(12):5940–7.
87. Hoof van Huijsdijnen R, Bollekens J, Dom A, Benoist C, Mathis D. Properties of a CCAAT box-binding protein. *Nucleic Acids Res*. 1987;15(18):7265–82.
88. Kim C, Sheffery M. Physical characterization of the purified CCAAT transcription factor, alpha-CP1. *J Biol Chem*. 1990;265(22):13362–9.
89. Yoshioka Y, Ly L, Yamaguchi M. Transcription factor NF-Y is involved in differentiation of R7 photoreceptor cell in *Drosophila*. *Biol Open*. 2012;1(1):19–29.
90. Ly L, Yoshida H, Yamaguchi M. Nuclear transcription factor γ and its roles in cellular processes related to human disease. *Am J Cancer Res*. 2013;3(4):339–46.
91. Wang Y, Stary J, Wilhelm J, Newmark P. A functional genomic screen in planarians identifies novel regulators of germ cell development. *Genes Dev*. 2010;24(18):2081–92.
92. Zhu J, Zhang Y, Joe G, Pompetti R, Emerson S. NF- γ activates multiple hematopoietic stem cell (HSC) regulatory genes and promotes HSC self-renewal. *Proc Natl Acad Sci*. 2005;102(33):11728–33.
93. Benatti P, Dolfini D, Viganò A, Ravo M, Weisz A, Imbriano C. Specific inhibition of NF-Y subunits triggers different cell proliferation defects. *Nucleic Acids Res*. 2011;39(13):5356–68.
94. van Wolfswinkel J, Wagner D, Reddien P. Single-cell analysis reveals functionally distinct classes within the planarian stem cell compartment. *Cell Stem Cell*. 2014;15(3):326–39.
95. Unneberg P, Wennborg A, Larsson M. Transcript identification by analysis of short sequence tags—influence of tag length, restriction site and transcript database. *Nucleic Acids Res*. 2003;31(8):2217–26.
96. Li B, Ruotti V, Stewart R, Thomson J, Dewey C. RNA-Seq gene expression estimation with read mapping uncertainty. *Bioinformatics*. 2009;26(4):493–500.
97. Koehler R, Issac H, Cloonan N, Grimmond SM. The uniqueome: a mappability resource for short-tag sequencing. *Bioinformatics*. 2010;27(2):272–4.
98. Sims D, Sudbery I, Illott NE, Heger A, Ponting CP. Sequencing depth and coverage: key considerations in genomic analyses. *Nat Rev Genet*. 2014;15(2):121–32.
99. Morey M, Yee S, Herman T, Nern A, Blanco E, Zipursky SL. Coordinate control of synaptic-layer specificity and rhodopsins in photoreceptor neurons. *Nature*. 2008;456(7223):795–9.
100. Pearson BJ, Sánchez Alvarado A. A planarian p53 homolog regulates proliferation and self-renewal in adult stem cell lineages. *Development*. 2009;137(2):213–21.
101. Oviedo N, Beane W. Regeneration: the origin of cancer or a possible cure? *Semin Cell Dev Biol*. 2009;20(5):557–64.
102. Pearson B, Sánchez Alvarado A. Regeneration, stem cells, and the evolution of tumor suppression. *Cold Spring Harb Symp Quant Biol*. 2008;73(0):565–72.
103. PlanMine. <http://planmine.mpi-cbg.de>.
104. Piquemal D, Commes T, Manchon L, Lejeune M, Ferraz C, Pugnère D, et al. Transcriptome analysis of monocytic leukemia cell differentiation. *Genomics*. 2002;80(3):361–71.
105. Barrett T, Wilhite SE, Ledoux P, Evangelista C, Kim IF, Tomashevsky M, et al. NCBI GEO: archive for functional genomics data sets—update. *Nucleic Acids Res*. 2013;41(D1):991–5.
106. NCBI Gene Expression Omnibus. <http://www.ncbi.nlm.nih.gov/geo/query/acc.cgi?acc=GSE51681>.
107. The Perl Programming Language. <https://www.perl.org/>.
108. Jiang H, Wong W. SeqMap: mapping massive amount of oligonucleotides to the genome. *Bioinformatics*. 2008;24(20):2395–6.
109. SeqMap - A Tool for Mapping Millions of Short Sequences to the Genome. <http://www-personal.umich.edu/~jianghui/seqmap>.
110. Benson D, Clark K, Karsch-Mizrachi I, Lipman D, Ostell J, Sayers E. Genbank. *Nucleic Acids Res*. 2013;42(D1):32–7.
111. Slater G, Birney E. Automated generation of heuristics for biological sequence comparison. *BMC Bioinf*. 2005;6(1):31.
112. jQuery jqGrid JavaScript Library. <http://plugins.jquery.com/jqGrid>.
113. GBrowse2. <http://gmod.org/wiki/GBrowse>.
114. Dimmer E, Huntley R, Alam-Faruque Y, Sawford T, O'Donovan C, Martin M, et al. The UniProt-GO Annotation database in 2011. *Nucleic Acids Res*. 2011;40(D1):565–70.
115. Finn RD, Bateman A, Clements J, Coggill P, Eberhardt RY, Eddy SR, et al. Pfam: the protein families database. *Nucleic Acids Res*. 2014;42(D1):222–30.

116. Pfam Database of Protein Families. <http://pfam.xfam.org>.
117. HMMER: Biosequence Analysis Using Profile Hidden Markov Models. <http://hmmer.org>.
118. Reddien PW, Newmark PA, Sánchez Alvarado A. Gene nomenclature guidelines for the planarian *Schmidtea mediterranea*. *Dev Dyn*. 2008;237(11):3099–101.
119. Gray KA, Daugherty LC, Gordon SM, Seal RL, Wright MW, Bruford EA. Genenames.org: the HGNC resources in 2013. *Nucleic Acids Res*. 2013;41(D1):545–52.
120. Molina M, Saló E, Cebrià F. The BMP pathway is essential for re-specification and maintenance of the dorsoventral axis in regenerating and intact planarians. *Dev Biol*. 2007;311(1):79–94.
121. Cebrià F, Guo T, Jopek J, Newmark P. Regeneration and maintenance of the planarian midline is regulated by a slit orthologue. *Devel Biol*. 2007;307(2):394–406.
122. King R, Newmark P. In situ hybridization protocol for enhanced detection of gene expression in the planarian *Schmidtea mediterranea*. *BMC Dev Biol*. 2013;13(1):8.
123. Cebrià F, Newmark P. Planarian homologs of *netrin* and *netrin receptor* are required for proper regeneration of the central nervous system and the maintenance of nervous system architecture. *Development*. 2005;132(16):3691–703.
124. Cebrià F. Organization of the nervous system in the model planarian *Schmidtea mediterranea*: an immunocytochemical study. *Neurosci Res*. 2008;61(4):375–84.

**Submit your next manuscript to BioMed Central
and take full advantage of:**

- Convenient online submission
- Thorough peer review
- No space constraints or color figure charges
- Immediate publication on acceptance
- Inclusion in PubMed, CAS, Scopus and Google Scholar
- Research which is freely available for redistribution

Submit your manuscript at
www.biomedcentral.com/submit



ANNEX II:

Alignment of planarian NF-Y with different species

ANNEX II

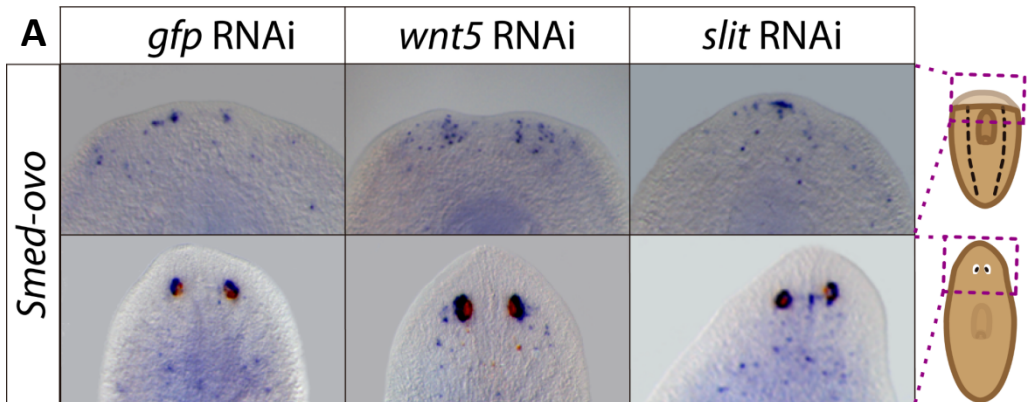
Annex1: Orthology analysis of *Schmidtea mediterranea* NF-Ys. Protein alignment of the three planarian members of the nuclear factor Y shows the conservation of the main protein domain of each element (black boxes). Alignment done by ClustalW and bioedit.

ANNEX III:

Alignment of planarian NF-Y with different planarian species

ANNEX IV:

Expression levels of neural genes after *wnt5* and *slit* RNAi.
Ovo+ cells positioning is affected after *wnt5* and *slit* RNAi

**B**

Gene	Contig	SLIT RNAi		WNT5 RNAi		Gene Reference
		log2FoldChange	padj	log2FoldChange	padj	
synaptotagmin	Smed_v4_21069_0_1	-0,22	1,00	-0,19	1,00	Tazaki A., 1999
synapsin	dd_Smed_v4_3135_0_1	0,09	1,00	0,27	0,21	Klagges BR, 1996
NeuroD	dd_Smed_v4_21717_0_1	-0,10	1,00	-0,07	1,00	Cowles M.W., 2013
ovo	dd_Smed_v4_48430_0_1	0,02	1,00	-0,05	1,00	Lapan SW, 2012
sp6-9	dd_Smed_v4_17385_0_1	0,01	1,00	0,13	1,00	Lapan SW, 2011
arrestin	dd_Smed_v4_17854_0_1	0,14	1,00	0,00	1,00	Agata et al., 1998
opsin	dd_Smed_v4_15036_0_1	0,27	0,43	-0,11	1,00	Pineda D., 2002

Annex 4: (A) WISH of *ovo* probe showing eye precursors after *wnt5* and *slit* RNAi in 2 days regenerating planarians and intact planarians. (B) Table shows the expression levels of different neural genes after *wnt5* or *slit* RNAi. The data has been extracted from a transcriptome of *wnt5* RNAi and *slit* RNAi done in collaboration with Kerstin Bartscherer lab.

BIBLIOGRAPHY

- Abril, J.F. et al., 2010. Smed454 dataset: unravelling the transcriptome of *Schmidtea mediterranea*. *BMC genomics*, 11(1), p.731. Available at: <http://www.biomedcentral.com/1471-2164/11/731> [Accessed September 25, 2014].
- Adamidi, C. et al., 2011. De novo assembly and validation of planaria transcriptome by massive parallel sequencing and shotgun proteomics. *Genome Research*, 21(7), pp.1193–1200. Available at: <http://www.ncbi.nlm.nih.gov/pubmed/21536722> [Accessed April 10, 2017].
- Adell, T. et al., 2009. Smed-Evi/Wntless is required for beta-catenin-dependent and -independent processes during planarian regeneration. *Development (Cambridge, England)*, 136(6), pp.905–910. Available at: <http://www.ncbi.nlm.nih.gov/pubmed/19211673> [Accessed September 24, 2014].
- Adell, T., Cebrià, F. & Saló, E., 2010. Gradients in planarian regeneration and homeostasis. *Cold Spring Harbor perspectives in biology*, 2(1), p.a000505. Available at: <http://www.pubmedcentral.nih.gov/articlerender.fcgi?artid=2827897&tool=pmcentrez&rendertype=abstract> [Accessed September 25, 2014].
- Agata, K. et al., 1998. Structure of the Planarian Central Nervous System (CNS) Revealed by Neuronal Cell Markers. *Zoological Science*, 15(3), pp.433–440. Available at: <http://www.bioone.org/doi/abs/10.2108/zsj.15.433> [Accessed January 26, 2017].
- Aksoy, I. et al., 2014. Klf4 and Klf5 differentially inhibit mesoderm and endoderm differentiation in embryonic stem cells. *Nature communications*, 5, p.3719. Available at: <http://www.ncbi.nlm.nih.gov/pubmed/24770696> [Accessed August 7, 2014].
- Almuedo-Castillo, M. et al., 2014. JNK controls the onset of mitosis in planarian stem cells and triggers apoptotic cell death required for regeneration and remodeling. *PLoS genetics*, 10(6), p.e1004400. Available at: <http://www.pubmedcentral.nih.gov/articlerender.fcgi?artid=4055413&tool=pmcentrez&rendertype=abstract> [Accessed December 10, 2014].
- Almuedo-Castillo, M., Saló, E. & Adell, T., 2011. Dishevelled is essential for neural connectivity and planar cell polarity in planarians. *Proceedings of the National Academy of Sciences of the United States of America*, 108(7), pp.2813–8. Available at: <http://www.pubmedcentral.nih.gov/articlerender.fcgi?artid=3041082&tool=pmcentrez&rendertype=abstract> [Accessed February 25, 2014].
- Arendt, D. & Nübler-Jung, K., 1994. Inversion of dorsoventral axis? *Nature*, 371(6492), pp.26–26. Available at: <http://www.ncbi.nlm.nih.gov/pubmed/8072524> [Accessed April 7, 2017].
- Baguna, J., Saló, E. & Auladell, C., 1989. Regeneration and pattern formation in planarians III. Evidence that neoblasts are totipotent stem cells and the source of blastema cells. *Development*, 107, pp.77–86. Available at: <http://dev.biologists.org/content/develop/107/1/77.full.pdf> [Accessed March 28, 2017].

BIBLIOGRAPHY

- Baguña, J., 1976. Mitosis in the intact and regenerating planarian *Dugesia mediterranea* n.sp. II. Mitotic studies during regeneration, and a possible mechanism of blastema formation. *Journal of Experimental Zoology*, 195(1), pp.65–79. Available at: <http://doi.wiley.com/10.1002/jez.1401950107> [Accessed April 7, 2017].
- Baguña, J. & Ballester, R., 1978. The nervous system in planarians: Peripheral and gastrodermal plexuses, pharynx innervation, and the relationship between central nervous system structure and the acoelomate organization. *Journal of Morphology*, 155(2), pp.237–252. Available at: <http://dx.doi.org/10.1002/jmor.1051550208>.
- Baguña, J. & Romero, R., 1981. Quantitative analysis of cell types during growth, degrowth and regeneration in the planarians *Dugesia mediterranea* and *Dugesia tigrina*. *Hydrobiologia*, 84(1), pp.181–194. Available at: <http://link.springer.com/10.1007/BF00026179> [Accessed March 28, 2017].
- Barberán, S., Fraguas, S. & Cebrià, F., 2016. The EGFR signaling pathway controls gut progenitor differentiation during planarian regeneration and homeostasis. *Development*, 143(April), p.dev.131995. Available at: <http://dev.biologists.org/lookup/doi/10.1242/dev.131995>.
- Bardeen, C.R. & Baetjer, F.H., 1904. The inhibitive action of the Roentgen rays on regeneration in planarians. *Journal of Experimental Zoology*, 1(1), pp.191–195. Available at: <http://dx.doi.org/10.1002/jez.1400010107>.
- Bashaw, G.J. & Klein, R., 2010. Signaling from axon guidance receptors. *Cold Spring Harbor perspectives in biology*, 2, pp.1–17.
- Battye, R. et al., 2001. Repellent signaling by Slit requires the leucine-rich repeats. *The Journal of neuroscience : the official journal of the Society for Neuroscience*, 21(12), pp.4290–8. Available at: <http://www.ncbi.nlm.nih.gov/pubmed/11404414> [Accessed April 7, 2017].
- Beckett, K. et al., 2013. *Drosophila* S2 Cells Secrete Wingless on Exosome-Like Vesicles but the Wingless Gradient Forms Independently of Exosomes. *Traffic*, 14(1), pp.82–96. Available at: <http://doi.wiley.com/10.1111/tra.12016> [Accessed March 21, 2017].
- Benatti, P. et al., 2008. A balance between NF-Y and p53 governs the pro- and anti-apoptotic transcriptional response. *Nucleic Acids Research*, 36(5), pp.1415–1428.
- Benatti, P. et al., 2011. Specific inhibition of NF-Y subunits triggers different cell proliferation defects. *Nucleic acids research*, 39(13), pp.5356–68. Available at: <http://www.pubmedcentral.nih.gov/articlerender.fcgi?artid=3141247&tool=pmcentrez&rendertype=abstract> [Accessed January 6, 2014].
- Bevilacqua, M.A. et al., 2002. Transcription factor NF-Y regulates differentiation of CaCo-2 cells. *Archives of biochemistry and biophysics*, 407(1), pp.39–44. Available at: <http://www.ncbi.nlm.nih.gov/pubmed/12392713> [Accessed April 10, 2017].

- Bhattacharya, A. et al., 2003. The B subunit of the CCAAT box binding transcription factor complex (CBF/NF-Y) is essential for early mouse development and cell proliferation. *Cancer research*, 63(23), pp.8167–72. Available at: <http://www.ncbi.nlm.nih.gov/pubmed/14678971> [Accessed April 7, 2017].
- Biteau, B., Hochmuth, C.E. & Jasper, H., 2008. JNK activity in somatic stem cells causes loss of tissue homeostasis in the aging *Drosophila* gut. *Cell stem cell*, 3(4), pp.442–55. Available at: <http://linkinghub.elsevier.com/retrieve/pii/S1934590908003925> [Accessed April 7, 2017].
- Blythe, M.J. et al., 2010a. A dual platform approach to transcript discovery for the planarian *Schmidtea mediterranea* to establish RNAseq for stem cell and regeneration biology. J. Jaeger, ed. *PloS one*, 5(12), p.e15617. Available at: <http://dx.plos.org/10.1371/journal.pone.0015617> [Accessed April 10, 2017].
- Blythe, M.J. et al., 2010b. A dual platform approach to transcript discovery for the planarian *Schmidtea mediterranea* to establish RNAseq for stem cell and regeneration biology. J. Jaeger, ed. *PloS one*, 5(12), p.e15617. Available at: <http://dx.plos.org/10.1371/journal.pone.0015617> [Accessed March 28, 2017].
- Brandl, H. et al., 2016. PlanMine – a mineable resource of planarian biology and biodiversity. *Nucleic Acids Research*, 44(D1), pp.D764–D773. Available at: <http://www.ncbi.nlm.nih.gov/pubmed/26578570> [Accessed April 10, 2017].
- Bullock, Theodore Holmes, and G.A.H., 1965. *Structure and Function in the Nervous System of Invertebrates.*, Akademie Verlag, Berlin. Available at: <http://doi.wiley.com/10.1002/iroh.19660510312> [Accessed April 20, 2017].
- Cao, Z. et al., 2010. Role of Kruppel-like factors in leukocyte development, function, and disease. *Blood*, 116(22), pp.4404–14. Available at: <http://www.bloodjournal.org/cgi/doi/10.1182/blood-2010-05-285353> [Accessed April 7, 2017].
- Cardenas Castillo, A., 2016. Robo receptors regulate neurogenesis along vertebrate brain evolution. , p.1. Available at: <https://dialnet.unirioja.es/servlet/tesis?codigo=60982> [Accessed April 7, 2017].
- Cebrià, F. et al., 1997. Myocyte differentiation and body wall muscle regeneration in the planarian *Girardia tigrina*. *Development genes and evolution*, 207(5), pp.306–316. Available at: <http://link.springer.com/10.1007/s004270050118> [Accessed March 28, 2017].
- Cebrià, F., 2007. Regenerating the central nervous system: how easy for planarians! *Development Genes and Evolution*, 217(11–12), pp.733–748. Available at: <http://www.ncbi.nlm.nih.gov/pubmed/17999079> [Accessed January 26, 2017].
- Cebrià, F. et al., 2007. Regeneration and maintenance of the planarian midline is regulated by a slit orthologue. *Developmental Biology*, 307(2), pp.394–406. Available at:

BIBLIOGRAPHY

- <http://www.ncbi.nlm.nih.gov/pubmed/17553481> [Accessed April 7, 2017].
- Cebrià, F. & Newmark, P.A., 2007. Morphogenesis defects are associated with abnormal nervous system regeneration following roboA RNAi in planarians. *Development (Cambridge, England)*, 134(5), pp.833–837.
- Cebrià, F. & Newmark, P.A., 2007. Morphogenesis defects are associated with abnormal nervous system regeneration following roboA RNAi in planarians. *Development (Cambridge, England)*, 134(5), pp.833–7. Available at: <http://dev.biologists.org/cgi/doi/10.1242/dev.02794> [Accessed April 7, 2017].
- Cebrià, F. & Newmark, P.A., 2005. Planarian homologs of netrin and netrin receptor are required for proper regeneration of the central nervous system and the maintenance of nervous system architecture. *Development*, 132(16).
- CHANDEBOIS, R., 1980. THE DYNAMICS OF WOUND CLOSURE AND ITS ROLE IN THE PROGRAMMING OF PLANARIAN REGENERATION. II — DISTALIZATION. *Development, Growth & Differentiation*, 22(4), pp.693–704. Available at: <http://dx.doi.org/10.1111/j.1440-169X.1980.00693.x>.
- Chen, F., 2012. JNK-Induced Apoptosis, Compensatory Growth, and Cancer Stem Cells. *Cancer Research*, 72(2), pp.379–386. Available at: <http://www.ncbi.nlm.nih.gov/pubmed/22253282> [Accessed April 7, 2017].
- Chong, T. et al., 2013. A sex-specific transcription factor controls male identity in a simultaneous hermaphrodite. *Nature communications*, 4, p.1814. Available at: <http://www.nature.com/doi/10.1038/ncomms2811> [Accessed March 28, 2017].
- Clevers, H. & Nusse, R., 2012. Wnt/ β -catenin signaling and disease. *Cell*, 149(6), pp.1192–205. Available at: <http://linkinghub.elsevier.com/retrieve/pii/S0092867412005867> [Accessed April 7, 2017].
- Cook, T. & Urrutia, R., 2000. TIEG proteins join the Smads as TGF-beta-regulated transcription factors that control pancreatic cell growth. *American journal of physiology. Gastrointestinal and liver physiology*, 278(4), pp.G513-21. Available at: <http://www.ncbi.nlm.nih.gov/pubmed/10762604> [Accessed April 17, 2017].
- Cowles, M.W. et al., 2013. Genome-wide analysis of the bHLH gene family in planarians identifies factors required for adult neurogenesis and neuronal regeneration. *Development (Cambridge, England)*, 140(23), pp.4691–702. Available at: <http://www.ncbi.nlm.nih.gov/pubmed/24173799> [Accessed January 10, 2014].
- Currie, K.W., Molinaro, A.M. & Pearson, B.J., 2016. Neuronal sources of hedgehog modulate neurogenesis in the adult planarian brain. *eLife*, 5. Available at: <http://www.ncbi.nlm.nih.gov/pubmed/27864883> [Accessed November 28, 2016].

- Currie, K.W. & Pearson, B.J., 2013. Transcription factors *lhx1/5-1* and *pitx* are required for the maintenance and regeneration of serotonergic neurons in planarians. *Development*, 140(17), pp.3577–3588. Available at: <http://www.ncbi.nlm.nih.gov/pubmed/23903188> [Accessed March 28, 2017].
- Dai, J.L. et al., 1999. Transforming growth factor-beta responsiveness in DPC4/SMAD4-null cancer cells. *Molecular carcinogenesis*, 26(1), pp.37–43. Available at: <http://www.ncbi.nlm.nih.gov/pubmed/10487520> [Accessed April 14, 2017].
- Dickson, B.J., 2002. Molecular Mechanisms of Axon Guidance. *Science*, 298(5600), pp.1959–1964. Available at: <http://www.ncbi.nlm.nih.gov/pubmed/12471249> [Accessed April 7, 2017].
- Dosch, R. et al., 1997. Bmp-4 acts as a morphogen in dorsoventral mesoderm patterning in *Xenopus*. *Development (Cambridge, England)*, 124(12), pp.2325–34. Available at: <http://www.ncbi.nlm.nih.gov/pubmed/9199359> [Accessed April 7, 2017].
- Eisenhoffer, G.T., Kang, H. & Sánchez Alvarado, A., 2008. Molecular analysis of stem cells and their descendants during cell turnover and regeneration in the planarian *Schmidtea mediterranea*. *Cell stem cell*, 3(3), pp.327–39. Available at: <http://www.ncbi.nlm.nih.gov/pubmed/18786419> [Accessed November 8, 2016].
- Elmore, S., 2007. Apoptosis: A Review of Programmed Cell Death. *Toxicologic Pathology*, 35(4), pp.495–516. Available at: <http://www.ncbi.nlm.nih.gov/pubmed/17562483> [Accessed April 7, 2017].
- Farin, H.F. et al., 2016. Visualization of a short-range Wnt gradient in the intestinal stem-cell niche. *Nature*, 530(7590), pp.340–343. Available at: <http://www.ncbi.nlm.nih.gov/pubmed/26863187> [Accessed March 21, 2017].
- Forsthoefel, D.J., Park, A.E. & Newmark, P.A., 2011. Stem cell-based growth, regeneration, and remodeling of the planarian intestine. *Developmental Biology*, 356(2), pp.445–459. Available at: <http://www.ncbi.nlm.nih.gov/pubmed/21664348> [Accessed January 26, 2017].
- Fraguas, S. et al., 2012. Regeneration of neuronal cell types in *Schmidtea mediterranea*: an immunohistochemical and expression study. *The International journal of developmental biology*, 56(1–3), pp.143–53. Available at: <http://www.intjdevbiol.com/paper.php?doi=113428sf> [Accessed April 17, 2017].
- Francesc Cebria, 2000. *Determination, Differentiation and Restitution of the Muscle Pattern During Regeneration and Cell Renewal in Freshwater Planarians*. Ph.D Thesi. U. de Barcelona, ed.,
- Galliot, B., 2013. Regeneration in Hydra.
- Galliot, B. & Ghila, L., 2010. Cell plasticity in homeostasis and regeneration. *Molecular Reproduction and Development*, 77(10), pp.837–855.

BIBLIOGRAPHY

- Gavilán, B., Perea-Atienza, E. & Martínez, P., 2015. Xenacoelomorpha: a case of independent nervous system centralization? *Philosophical Transactions of the Royal Society of London B: Biological Sciences*, 371(1685). Available at: <http://rstb.royalsocietypublishing.org/content/371/1685/20150039> [Accessed April 25, 2017].
- Gaviño, M.A. & Reddien, P.W., 2011. A Bmp/Admp regulatory circuit controls maintenance and regeneration of dorsal-ventral polarity in planarians. *Current biology: CB*, 21(4), pp.294–9. Available at: <http://linkinghub.elsevier.com/retrieve/pii/S0960982211000406> [Accessed April 7, 2017].
- Gerhart, J., 2000. Inversion of the chordate body axis: are there alternatives? *Proceedings of the National Academy of Sciences of the United States of America*, 97(9), pp.4445–8. Available at: <http://www.ncbi.nlm.nih.gov/pubmed/10781041> [Accessed April 7, 2017].
- Green, J., Nusse, R. & van Amerongen, R., 2014. The role of Ryk and Ror receptor tyrosine kinases in Wnt signal transduction. *Cold Spring Harbor perspectives in biology*, 6(2). Available at: <http://www.ncbi.nlm.nih.gov/pubmed/24370848> [Accessed April 3, 2017].
- Guo, T., Peters, A.H.F.M. & Newmark, P.A., 2006. A bruno-like Gene Is Required for Stem Cell Maintenance in Planarians. *Developmental Cell*, 11(2), pp.159–169. Available at: <http://www.ncbi.nlm.nih.gov/pubmed/16890156> [Accessed March 28, 2017].
- Gurley, K.A. et al., 2010. Expression of secreted Wnt pathway components reveals unexpected complexity of the planarian amputation response. *Dev Biol*, 347(1), pp.24–39.
- Gurley, K.A., Rink, J.C. & Alvarado, A.S., 2008. -Catenin Defines Head Versus Tail Identity During Planarian Regeneration and Homeostasis. *Science*, 319(5861), pp.323–327. Available at: <http://www.ncbi.nlm.nih.gov/pubmed/18063757> [Accessed April 7, 2017].
- Gurtner, A., Manni, I. & Piaggio, G., 2016. NF-Y in cancer: Impact on cell transformation of a gene essential for proliferation. *Biochimica et Biophysica Acta (BBA) - Gene Regulatory Mechanisms*. Available at: <http://www.sciencedirect.com/science/article/pii/S1874939916302838> [Accessed April 7, 2017].
- Gutierrez, G.J. et al., 2010. JNK-mediated Phosphorylation of Cdc25C Regulates Cell Cycle Entry and G2/M DNA Damage Checkpoint. *Journal of Biological Chemistry*, 285(19), pp.14217–14228. Available at: <http://www.ncbi.nlm.nih.gov/pubmed/20220133> [Accessed April 7, 2017].
- Hayashi, T. et al., 2006. Isolation of planarian X-ray-sensitive stem cells by fluorescence-activated cell sorting. *Development, growth & differentiation*, 48(6), pp.371–80. Available at: <http://doi.wiley.com/10.1111/j.1440-169X.2006.00876.x> [Accessed March 28, 2017].
- Hayashi, T. et al., 2010. Single-cell gene profiling of planarian stem cells using fluorescent

- activated cell sorting and its “index sorting” function for stem cell research. *Development, Growth & Differentiation*, 52(1), pp.131–144. Available at: <http://www.ncbi.nlm.nih.gov/pubmed/20078655> [Accessed March 28, 2017].
- Hocevar, B.A., Brown, T.L. & Howe, P.H., 1999. TGF-beta induces fibronectin synthesis through a c-Jun N-terminal kinase-dependent, Smad4-independent pathway. *The EMBO Journal*, 18(5), pp.1345–1356. Available at: <http://www.ncbi.nlm.nih.gov/pubmed/10064600> [Accessed April 14, 2017].
- Hughes, R. et al., 2011. NF-Y is essential for expression of the proapoptotic bim gene in sympathetic neurons. *Cell Death and Differentiation*, 18(6), pp.937–947. Available at: <http://www.ncbi.nlm.nih.gov/pubmed/21164521> [Accessed April 7, 2017].
- Iglesias, M. et al., 2008. Silencing of Smed-betacatenin1 generates radial-like hypercephalized planarians. *Development (Cambridge, England)*, 135(7), pp.1215–21. Available at: <http://www.ncbi.nlm.nih.gov/pubmed/18287199> [Accessed September 24, 2014].
- Immanuel Kant, K., 1914. *Critique of Judgement* 2nd ed., London.
- Inaki, M., Liu, J. & Matsuno, K., 2016. Cell chirality: its origin and roles in left–right asymmetric development. *Philosophical Transactions of the Royal Society of London B: Biological Sciences*, 371(1710).
- Issigonis, M. & Newmark, P.A., 2015. Heal Thy Cell(f): A Single-Cell View of Regeneration. *Developmental Cell*, 35(5), pp.527–528. Available at: <http://www.ncbi.nlm.nih.gov/pubmed/26651286> [Accessed March 28, 2017].
- Itoh, A. et al., 1998. Cloning and expressions of three mammalian homologues of Drosophila slit suggest possible roles for Slit in the formation and maintenance of the nervous system. *Brain research. Molecular brain research*, 62(2), pp.175–86. Available at: <http://www.ncbi.nlm.nih.gov/pubmed/9813312> [Accessed April 25, 2017].
- Iyer, H. et al., 2016. NF-YB Regulates Spermatogonial Stem Cell Self-Renewal and Proliferation in the Planarian *Schmidtea mediterranea*. *PLoS genetics*, 12(6), p.e1006109. Available at: <http://www.ncbi.nlm.nih.gov/pubmed/27304889> [Accessed April 7, 2017].
- Jäckle, H. et al., 1986. Probing gene activity in Drosophila embryos. *Journal of embryology and experimental morphology*, 97 Suppl, pp.157–68. Available at: <http://www.ncbi.nlm.nih.gov/pubmed/2442279> [Accessed April 7, 2017].
- Jiang, H. et al., 2010. Palmitic acid promotes endothelial progenitor cells apoptosis via p38 and JNK mitogen-activated protein kinase pathways. *Atherosclerosis*, 210(1), pp.71–77. Available at: <http://www.ncbi.nlm.nih.gov/pubmed/20226460> [Accessed April 7, 2017].
- Jiang, J. et al., 2008. A core Klf circuitry regulates self-renewal of embryonic stem cells. *Nature cell biology*, 10(3), pp.353–60. Available at: <http://www.ncbi.nlm.nih.gov/pubmed/18264089>

BIBLIOGRAPHY

[Accessed July 16, 2014].

- Jopling, C. et al., 2010. Zebrafish heart regeneration occurs by cardiomyocyte dedifferentiation and proliferation. *Nature*, 464(7288), pp.606–9. Available at: <http://www.nature.com/doi/10.1038/nature08899> [Accessed March 29, 2017].
- Jopling, C., Boue, S. & Izpisua Belmonte, J.C., 2011. Dedifferentiation, transdifferentiation and reprogramming: three routes to regeneration. *Nature reviews. Molecular cell biology*, 12(2), pp.79–89. Available at: <http://www.nature.com/doi/10.1038/nrm3043> [Accessed March 29, 2017].
- Kaczynski, J., Cook, T. & Urrutia, R., 2003. Sp1- and Krüppel-like transcription factors. *Genome biology*, 4(2), p.206. Available at: <http://www.ncbi.nlm.nih.gov/pubmed/12620113> [Accessed April 7, 2017].
- Kadonaga, J.T. et al., 1987. Isolation of cDNA encoding transcription factor Sp1 and functional analysis of the DNA binding domain. *Cell*, 51(6), pp.1079–90. Available at: <http://www.ncbi.nlm.nih.gov/pubmed/3319186> [Accessed April 7, 2017].
- Kao, D., Felix, D. & Aboobaker, A., 2013. The planarian regeneration transcriptome reveals a shared but temporally shifted regulatory program between opposing head and tail scenarios. *BMC Genomics*, 14(1), p.797. Available at: <http://www.ncbi.nlm.nih.gov/pubmed/24238224> [Accessed April 10, 2017].
- Kapasa, M., Arhondakis, S. & Kossida, S., 2010. Phylogenetic and regulatory region analysis of Wnt5 genes reveals conservation of a regulatory module with putative implication in pancreas development. *Biology direct*, 5(1), p.49. Available at: <http://biologydirect.biomedcentral.com/articles/10.1186/1745-6150-5-49> [Accessed April 25, 2017].
- Kaprielian, Z., Runko, E. & Imondi, R., 2001. Axon guidance at the midline choice point. *Developmental Dynamics*, 221(2), pp.154–181. Available at: <http://doi.wiley.com/10.1002/dvdy.1143> [Accessed December 13, 2016].
- King, R.S. & Newmark, P.A., 2012. The cell biology of regeneration. *Journal of Cell Biology*, 196(5), pp.553–562.
- Klämbt, C. & Goodman, C.S., 1991. Role of the midline glia and neurons in the formation of the axon commissures in the central nervous system of the Drosophila embryo. *Annals of the New York Academy of Sciences*, 633, pp.142–59. Available at: <http://www.ncbi.nlm.nih.gov/pubmed/1789544> [Accessed April 7, 2017].
- Klämbt, C. & Goodman, C.S., 1991. The diversity and pattern of glia during axon pathway formation in the drosophila embryo. *Glia*, 4(2), pp.205–213. Available at: <http://www.ncbi.nlm.nih.gov/pubmed/1827779> [Accessed April 7, 2017].

- Knecht, A.K. & Harland, R.M., 1997. Mechanisms of dorsal-ventral patterning in noggin-induced neural tissue. *Development (Cambridge, England)*, 124(12), pp.2477–88. Available at: <http://www.ncbi.nlm.nih.gov/pubmed/9199373> [Accessed April 7, 2017].
- Kockel, L., Homsy, J.G. & Bohmann, D., 2001. Drosophila AP-1: lessons from an invertebrate. *Oncogene*, 20(19), pp.2347–2364. Available at: <http://www.ncbi.nlm.nih.gov/pubmed/11402332> [Accessed April 7, 2017].
- Komiya, Y. & Habas, R., 2008. Wnt signal transduction pathways. *Organogenesis*, 4(2), pp.68–75. Available at: <http://www.ncbi.nlm.nih.gov/pubmed/19279717> [Accessed April 7, 2017].
- Labbé, R.M. et al., 2012. A comparative transcriptomic analysis reveals conserved features of stem cell pluripotency in planarians and mammals. *Stem cells (Dayton, Ohio)*, 30(8), pp.1734–45. Available at: <http://doi.wiley.com/10.1002/stem.1144> [Accessed March 28, 2017].
- LaBonne, C. & Bronner-Fraser, M., 1998. Neural crest induction in *Xenopus*: evidence for a two-signal model. *Development (Cambridge, England)*, 125(13), pp.2403–14. Available at: <http://www.ncbi.nlm.nih.gov/pubmed/9609823> [Accessed April 7, 2017].
- Lapan, S.W. & Reddien, P.W., 2011. *dlx* and *sp6-9* Control optic cup regeneration in a prototypic eye. C. Desplan, ed. *PLoS genetics*, 7(8), p.e1002226. Available at: <http://dx.plos.org/10.1371/journal.pgen.1002226> [Accessed March 28, 2017].
- Lapan, S.W. & Reddien, P.W., 2012. Transcriptome analysis of the planarian eye identifies *ovo* as a specific regulator of eye regeneration. *Cell reports*, 2(2), pp.294–307. Available at: <http://www.sciencedirect.com/science/article/pii/S2211124712001921> [Accessed August 21, 2014].
- Lartillot, N. & Philippe, H., 2008. Improvement of molecular phylogenetic inference and the phylogeny of Bilateria. *Philosophical Transactions of the Royal Society of London B: Biological Sciences*, 363(1496).
- Lee, W., Mitchell, P. & Tjian, R., 1987. Purified transcription factor AP-1 interacts with TPA-inducible enhancer elements. *Cell*, 49(6), pp.741–52. Available at: <http://www.ncbi.nlm.nih.gov/pubmed/3034433> [Accessed April 7, 2017].
- Li, X.Y. et al., 1992. Evolutionary variation of the CCAAT-binding transcription factor NF-Y. *Nucleic acids research*, 20(5), pp.1087–91. Available at: <http://www.ncbi.nlm.nih.gov/pubmed/1549471> [Accessed April 7, 2017].
- Liang, H. et al., 2007. Noncanonical Wnt signaling promotes apoptosis in thymocyte development. *The Journal of Experimental Medicine*, 204(13), pp.3077–3084. Available at: <http://www.ncbi.nlm.nih.gov/pubmed/18070933> [Accessed April 7, 2017].
- Liang, H. et al., 2003. Wnt5a inhibits B cell proliferation and functions as a tumor suppressor in hematopoietic tissue. *Cancer cell*, 4(5), pp.349–60. Available at:

BIBLIOGRAPHY

- <http://www.ncbi.nlm.nih.gov/pubmed/14667502> [Accessed April 5, 2017].
- Ly, L.L. et al., 2013. dNF-YB plays dual roles in cell death and cell differentiation during *Drosophila* eye development. *Gene*, 520(2), pp.106–118. Available at: <http://www.ncbi.nlm.nih.gov/pubmed/23470843> [Accessed April 7, 2017].
- Mann, R.S., 2004. Two Pax are better than one. *Nature genetics*, 36(1), pp.10–1. Available at: <http://www.nature.com/doifinder/10.1038/ng0104-10> [Accessed April 7, 2017].
- Mantovani, R., 1999. The molecular biology of the CCAAT-binding factor NF-Y. *Gene*, 239(1), pp.15–27. Available at: <http://www.ncbi.nlm.nih.gov/pubmed/10571030> [Accessed April 7, 2017].
- Marchant, L. et al., 1998. The inductive properties of mesoderm suggest that the neural crest cells are specified by a BMP gradient. *Developmental biology*, 198(2), pp.319–29. Available at: <http://www.ncbi.nlm.nih.gov/pubmed/9659936> [Accessed April 7, 2017].
- Marcon, L. et al., 2016. High-throughput mathematical analysis identifies Turing networks for patterning with equally diffusing signals. *eLife*, 5, pp.839–841. Available at: <http://www.ncbi.nlm.nih.gov/pubmed/27058171> [Accessed April 12, 2017].
- Matuoka, K. & Yu Chen, K., 1999. Nuclear factor Y (NF-Y) and cellular senescence. *Experimental cell research*, 253(2), pp.365–71. Available at: <http://linkinghub.elsevier.com/retrieve/pii/S0014482799946050> [Accessed April 7, 2017].
- McConnell, B.B. & Yang, V.W., 2010. Mammalian Kruppel-Like Factors in Health and Diseases. *Physiological Reviews*, 90(4), pp.1337–1381. Available at: <http://www.ncbi.nlm.nih.gov/pubmed/20959618> [Accessed April 12, 2017].
- McDonald, A.C.H. & Rossant, J., 2014. Gut endoderm takes flight from the wings of mesoderm. *Nature Cell Biology*, 16(12), pp.1128–1129. Available at: <http://www.ncbi.nlm.nih.gov/pubmed/25434463> [Accessed March 28, 2017].
- Meinhardt, H., 2004. Different strategies for midline formation in bilaterians. *Nature reviews. Neuroscience*, 5(6), pp.502–510.
- Mikels, A.J. & Nusse, R., 2006. Wnts as ligands: processing, secretion and reception. *Oncogene*, 25(57), pp.7461–7468. Available at: <http://www.ncbi.nlm.nih.gov/pubmed/17143290> [Accessed April 7, 2017].
- Milton, A.C. et al., 2013. The NF-Y complex negatively regulates *Caenorhabditis elegans* *tbx-2* expression. *Developmental biology*, 382(1), pp.38–47. Available at: <http://linkinghub.elsevier.com/retrieve/pii/S0012160613004132> [Accessed April 7, 2017].
- Mittal, R. et al., 2016. Neurotransmitters: The Critical Modulators Regulating Gut-Brain Axis. *Journal of Cellular Physiology*. Available at: <http://www.ncbi.nlm.nih.gov/pubmed/27512962> [Accessed March 29, 2017].

- Molina, M.D., Saló, E. & Cebrià, F., 2011. Organizing the DV axis during planarian regeneration. *Communicative & integrative biology*, 4(4), pp.498–500. Available at: <http://www.pubmedcentral.nih.gov/articlerender.fcgi?artid=3181533&tool=pmcentrez&rendertype=abstract> [Accessed January 7, 2014].
- Molina, M.D., Saló, E. & Cebrià, F., 2007. The BMP pathway is essential for re-specification and maintenance of the dorsoventral axis in regenerating and intact planarians. *Developmental biology*, 311(1), pp.79–94. Available at: <http://linkinghub.elsevier.com/retrieve/pii/S0012160607012651> [Accessed April 7, 2017].
- Molinaro, A.M. & Pearson, B.J., 2016. In silico lineage tracing through single cell transcriptomics identifies a neural stem cell population in planarians. *Genome biology*, 17, p.87. Available at: <http://www.ncbi.nlm.nih.gov/pubmed/27150006> [Accessed March 28, 2017].
- Morey, M. et al., 2008. Coordinate control of synaptic-layer specificity and rhodopsins in photoreceptor neurons. *Nature*, 456(7223), pp.795–9. Available at: <http://www.nature.com/doi/10.1038/nature07419> [Accessed April 7, 2017].
- Moritz, S. et al., 2012. Heterogeneity of planarian stem cells in the S/G2/M phase. *The International Journal of Developmental Biology*, 56(1-2-3), pp.117–125. Available at: <http://www.ncbi.nlm.nih.gov/pubmed/22450999> [Accessed April 10, 2017].
- Muñoz-Descalzo, S., Terol, J. & Paricio, N., 2005. Cabut, a C2H2 zinc finger transcription factor, is required during *Drosophila* dorsal closure downstream of JNK signaling. *Developmental biology*, 287(1), pp.168–79. Available at: <http://www.ncbi.nlm.nih.gov/pubmed/16198331> [Accessed December 1, 2014].
- Neave, B., Holder, N. & Patient, R., 1997. A graded response to BMP-4 spatially coordinates patterning of the mesoderm and ectoderm in the zebrafish. *Mechanisms of development*, 62(2), pp.183–95. Available at: <http://www.ncbi.nlm.nih.gov/pubmed/9152010> [Accessed April 7, 2017].
- Newmark, P.A. & Sánchez Alvarado, A., 2000. Bromodeoxyuridine Specifically Labels the Regenerative Stem Cells of Planarians. *Developmental Biology*, 220(2), pp.142–153. Available at: <http://www.ncbi.nlm.nih.gov/pubmed/10753506> [Accessed March 28, 2017].
- Oderberg, I.M. et al., 2017. Landmarks in existing tissue at wounds are utilized to generate pattern in regenerating tissue. , pp.1–10.
- Okamoto, K., Takeuchi, K. & Agata, K., 2005. Neural Projections in Planarian Brain Revealed by Fluorescent Dye Tracing. *Zoological Science*, 22(5), pp.535–546. Available at: <http://www.bioone.org/doi/abs/10.2108/zsj.22.535> [Accessed January 26, 2017].
- Onal, P. et al., 2012. Gene expression of pluripotency determinants is conserved between mammalian and planarian stem cells. *The EMBO journal*, 31(12), pp.2755–69. Available at: <http://www.pubmedcentral.nih.gov/articlerender.fcgi?artid=3380209&tool=pmcentrez&rendertype=abstract>

BIBLIOGRAPHY

- dertype=abstract [Accessed December 16, 2013].
- Orii, H., Sakurai, T. & Watanabe, K., 2005. Distribution of the stem cells (neoblasts) in the planarian *Dugesia japonica*. *Development Genes and Evolution*, 215(3), pp.143–157. Available at: <http://www.ncbi.nlm.nih.gov/pubmed/15657737> [Accessed April 10, 2017].
- Orii, H. & Watanabe, K., 2007. Bone morphogenetic protein is required for dorso-ventral patterning in the planarian *Dugesia japonica*. *Development, growth & differentiation*, 49(4), pp.345–9. Available at: <http://doi.wiley.com/10.1111/j.1440-169X.2007.00931.x> [Accessed April 7, 2017].
- Pearson, R. et al., 2008. Krüppel-like transcription factors: a functional family. *The international journal of biochemistry & cell biology*, 40(10), pp.1996–2001. Available at: <http://www.sciencedirect.com/science/article/pii/S1357272507002567> [Accessed February 7, 2014].
- Pei, J. & Grishin, N. V., 2015. C2H2 zinc finger proteins of the SP/KLF, Wilms tumor, EGR, Hucklebein, and Klumpfuss families in metazoans and beyond. *Gene*, 573(1), pp.91–99. Available at: <http://linkinghub.elsevier.com/retrieve/pii/S0378111915008562>.
- Pellettieri, J. et al., 2010. Cell death and tissue remodeling in planarian regeneration. *Developmental Biology*, 338(1), pp.76–85. Available at: <http://www.ncbi.nlm.nih.gov/pubmed/19766622> [Accessed April 7, 2017].
- Pellettieri, J. & Alvarado, A.S., 2007. Cell Turnover and Adult Tissue Homeostasis: From Humans to Planarians. *Annual Review of Genetics*, 41(1), pp.83–105. Available at: <http://www.ncbi.nlm.nih.gov/pubmed/18076325> [Accessed March 28, 2017].
- Perkins, K.K. et al., 1990. The *Drosophila* Fos-related AP-1 protein is a developmentally regulated transcription factor. *Genes & development*, 4(5), pp.822–34. Available at: <http://www.ncbi.nlm.nih.gov/pubmed/2116361> [Accessed April 7, 2017].
- Petersen, C.P. & Reddien, P.W., 2011. Polarized notum Activation at Wounds Inhibits Wnt Function to Promote Planarian Head Regeneration. *Science*, 332(6031), pp.852–855. Available at: <http://www.ncbi.nlm.nih.gov/pubmed/21566195> [Accessed April 12, 2017].
- Reddien, P.W. et al., 2007. BMP signaling regulates the dorsal planarian midline and is needed for asymmetric regeneration. *Development*, 134(22), pp.4043–4051. Available at: <http://www.ncbi.nlm.nih.gov/pubmed/17942485> [Accessed April 7, 2017].
- Reddien, P.W., 2011. Constitutive gene expression and the specification of tissue identity in adult planarian biology. *Trends in genetics: TIG*, 27(7), pp.277–85. Available at: <http://www.pubmedcentral.nih.gov/articlerender.fcgi?artid=3125669&tool=pmcentrez&rendertype=abstract> [Accessed September 25, 2014].
- Reddien, P.W. et al., 2005. SMEDWI-2 is a PIWI-like protein that regulates planarian stem cells.

- Science (New York, N.Y.)*, 310, pp.1327–1330.
- Reddien, P.W., 2013. Specialized progenitors and regeneration. *Development (Cambridge, England)*, 140(5), pp.951–7. Available at: <http://www.pubmedcentral.nih.gov/articlerender.fcgi?artid=3583037&tool=pmcentrez&rendertype=abstract> [Accessed December 28, 2013].
- Resch, A.M. et al., 2012. Transcriptome analysis reveals strain-specific and conserved stemness genes in *Schmidtea mediterranea*. *PloS one*, 7(4), p.e34447. Available at: <http://www.pubmedcentral.nih.gov/articlerender.fcgi?artid=3319590&tool=pmcentrez&rendertype=abstract> [Accessed January 6, 2014].
- Riesgo-Escovar, J.R. et al., 1996. The *Drosophila* Jun-N-terminal kinase is required for cell morphogenesis but not for DJun-dependent cell fate specification in the eye. *Genes & development*, 10(21), pp.2759–68. Available at: <http://www.ncbi.nlm.nih.gov/pubmed/8946916> [Accessed April 7, 2017].
- Rink, J.C., Vu, H.T.-K. & Alvarado, A.S., 2011. The maintenance and regeneration of the planarian excretory system are regulated by EGFR signaling. *Development*, 138(17).
- RM. Rieger, S. Tyler, JPS. Smith, G.R., 1991. *Microscopic Anatomy of Invertebrates. Volume 3. Platyhelminthes and Nemertinea.*, Inc, New York: Wiley-Liss.
- De Robertis, E.M. & Sasai, Y., 1996. A common plan for dorsoventral patterning in Bilateria. *Nature*, 380(6569), pp.37–40. Available at: <http://www.ncbi.nlm.nih.gov/pubmed/8598900> [Accessed April 7, 2017].
- Roberts-Galbraith, R.H. et al., 2016. A functional genomics screen in planarians reveals regulators of whole-brain regeneration. *eLife*, 5, pp.433–440. Available at: <http://www.ncbi.nlm.nih.gov/pubmed/27612384> [Accessed November 30, 2016].
- Rodríguez-Esteban, G. et al., 2015. Digital gene expression approach over multiple RNA-Seq data sets to detect neoblast transcriptional changes in *Schmidtea mediterranea*. *BMC Genomics*, 16.
- Romier, C. et al., 2002. The NF-YB/NF-YC Structure Gives Insight into DNA Binding and Transcription Regulation by CCAAT Factor NF-Y*. Available at: <http://www.jbc.org/content/278/2/1336.full.pdf> [Accessed April 10, 2017].
- Ross, K.G. et al., 2015. Novel monoclonal antibodies to study tissue regeneration in planarians. *BMC developmental biology*, 15, p.2. Available at: <http://www.ncbi.nlm.nih.gov/pubmed/25604901> [Accessed November 30, 2016].
- Rouhana, L. et al., 2012. PRMT5 and the role of symmetrical dimethylarginine in chromatoid bodies of planarian stem cells. *Development (Cambridge, England)*, 139(6), pp.1083–94. Available at: <http://dev.biologists.org/cgi/doi/10.1242/dev.076182> [Accessed March 28,

BIBLIOGRAPHY

2017].

- Ruiz-romero, M. et al., 2015. Cabut / dTIEG associates with the transcription factor Yorkie for growth control. , pp.1–8.
- Saberi, A. et al., 2016. GPCRs Direct Germline Development and Somatic Gonad Function in Planarians. M. F. Wolfner, ed. *PLoS biology*, 14(5), p.e1002457. Available at: <http://dx.plos.org/10.1371/journal.pbio.1002457> [Accessed April 12, 2017].
- Saló, E. & Baguñà, J., 1984. Regeneration and pattern formation in planarians. *J. Embryol exp. Morph.*, 83, pp.63–80.
- Salvetti, A. et al., 2005. DjPum, a homologue of Drosophila Pumilio, is essential to planarian stem cell maintenance. *Development (Cambridge, England)*, 132(8), pp.1863–74. Available at: <http://dev.biologists.org/cgi/doi/10.1242/dev.01785> [Accessed March 28, 2017].
- Sánchez-Soriano, N. et al., 2007. Drosophila as a genetic and cellular model for studies on axonal growth. *Neural Development*, 2(1), p.9. Available at: <http://neuraldevelopment.biomedcentral.com/articles/10.1186/1749-8104-2-9> [Accessed December 29, 2016].
- Sandmann, T. et al., 2011. The head-regeneration transcriptome of the planarian Schmidtea mediterranea. *Genome biology*, 12(8), p.R76. Available at: <http://genomebiology.biomedcentral.com/articles/10.1186/gb-2011-12-8-r76> [Accessed April 10, 2017].
- Schubert, M. et al., 2001. Three Amphioxus Wnt Genes (AmphiWnt3, AmphiWnt5, and AmphiWnt6) Associated with the Tail Bud: the Evolution of Somitogenesis in Chordates. *Developmental Biology*, 240(1), pp.262–273. Available at: <http://www.ncbi.nlm.nih.gov/pubmed/11784062> [Accessed April 25, 2017].
- Scimone, M.L. et al., 2011. A regulatory program for excretory system regeneration in planarians. *Development*, 138(20), pp.4387–4398.
- Scimone, M.L. et al., 2014. Neoblast Specialization in Regeneration of the Planarian Schmidtea mediterranea. *Stem Cell Reports*, 3(2), pp.339–352. Available at: <http://www.cell.com/article/S2213671114001866/fulltext> [Accessed August 27, 2014].
- Selman, K. & Kafatos, F.C., 1974. Transdifferentiation in the labial gland of silk moths: is DNA required for cellular metamorphosis? *Cell differentiation*, 3(2), pp.81–94. Available at: <http://www.ncbi.nlm.nih.gov/pubmed/4277742> [Accessed March 29, 2017].
- Senderowicz, A.M., 2004. Targeting cell cycle and apoptosis for the treatment of human malignancies. *Current Opinion in Cell Biology*, 16(6), pp.670–678. Available at: <http://www.ncbi.nlm.nih.gov/pubmed/15530779> [Accessed April 7, 2017].
- Serra, E. et al., 1996. Expression of NF-Y nuclear factor in Schistosoma mansoni. *Parasitology*,

- pp.457–64. Available at: <http://www.ncbi.nlm.nih.gov/pubmed/8893531> [Accessed April 7, 2017].
- Shindo, T. et al., 2002. Krüppel-like zinc-finger transcription factor KLF5/BTEB2 is a target for angiotensin II signaling and an essential regulator of cardiovascular remodeling. *Nature medicine*, 8(8), pp.856–63. Available at: <http://www.ncbi.nlm.nih.gov/pubmed/12101409> [Accessed August 17, 2014].
- Solana, J. et al., 2012. Defining the molecular profile of planarian pluripotent stem cells using a combinatorial RNA-seq, RNA interference and irradiation approach. *Genome Biology*, 13(3), p.R19. Available at: <http://www.ncbi.nlm.nih.gov/pubmed/22439894> [Accessed March 28, 2017].
- Solana, J., Lasko, P. & Romero, R., 2009. Spoltud-1 is a chromatoid body component required for planarian long-term stem cell self-renewal. *Developmental Biology*, 328(2), pp.410–421. Available at: <http://www.ncbi.nlm.nih.gov/pubmed/19389344> [Accessed March 28, 2017].
- Spittau, B. & Krieglstein, K., 2012. Klf10 and Klf11 as mediators of TGF-beta superfamily signaling. *Cell and tissue research*, 347(1), pp.65–72. Available at: <http://www.ncbi.nlm.nih.gov/pubmed/21574058> [Accessed February 7, 2014].
- Staal, F.J.T., Luis, T.C. & Tiemessen, M.M., 2008. WNT signalling in the immune system: WNT is spreading its wings. *Nature reviews. Immunology*, 8(8), pp.581–93. Available at: <http://www.ncbi.nlm.nih.gov/pubmed/18617885>.
- Stanganello, E. & Scholpp, S., 2016. Role of cytonemes in Wnt transport. *Journal of Cell Science*, 129(4). Available at: <http://jcs.biologists.org/content/129/4/665.long> [Accessed April 19, 2017].
- Sun, G. & Irvine, K.D., 2011. Regulation of Hippo signaling by Jun kinase signaling during compensatory cell proliferation and regeneration, and in neoplastic tumors. *Developmental biology*, 350(1), pp.139–51. Available at: <http://linkinghub.elsevier.com/retrieve/pii/S0012160610012418> [Accessed April 7, 2017].
- Sureda-Gómez, M., Martín-Durán, J.M. & Adell, T., 2016. Localization of planarian β CATENIN-1 reveals multiple roles during anterior-posterior regeneration and organogenesis. *Development (Cambridge, England)*, (October), p.dev.135152. Available at: <http://dev.biologists.org/lookup/doi/10.1242/dev.135152%5Cnhttp://www.ncbi.nlm.nih.gov/pubmed/27737903>.
- Suske, G., Bruford, E. & Philipsen, S., 2005. Mammalian SP/KLF transcription factors: Bring in the family. *Genomics*, 85(5), pp.551–556. Available at: <http://www.ncbi.nlm.nih.gov/pubmed/15820306> [Accessed April 7, 2017].
- Swamynathan, S.K., 2010. Krüppel-like factors: three fingers in control. *Human genomics*, 4(4), pp.263–270.

BIBLIOGRAPHY

- Tarapore, R.S., Yang, Y. & Katz, J.P., 2013. Restoring KLF5 in esophageal squamous cell cancer cells activates the JNK pathway leading to apoptosis and reduced cell survival. *Neoplasia (New York, N.Y.)*, 15(5), pp.472–80. Available at: <http://www.ncbi.nlm.nih.gov/pubmed/23633919> [Accessed April 7, 2017].
- Tetreault, M.-P., Yang, Y. & Katz, J.P., 2013. Krüppel-like factors in cancer. *Nature reviews. Cancer*, 13(10), pp.701–13. Available at: <http://www.ncbi.nlm.nih.gov/pubmed/24060862> [Accessed March 2, 2014].
- Tu, K.C. et al., 2015. Egr-5 is a post-mitotic regulator of planarian epidermal differentiation Kimberly. , (October).
- Turing, A.M., 1952. The Chemical Basis of Morphogenesis. *Philosophical Transactions of the Royal Society of London*, 237(641), pp.37–72. Available at: <http://cba.mit.edu/events/03.11.ASE/docs/Turing.pdf> [Accessed April 17, 2017].
- Valenta, T., Hausmann, G. & Basler, K., 2012. The many faces and functions of β -catenin. *The EMBO Journal*, 31(12), pp.2714–2736. Available at: <http://www.ncbi.nlm.nih.gov/pubmed/22617422> [Accessed April 7, 2017].
- van Wolfswinkel, J.C., Wagner, D.E. & Reddien, P.W., 2014. Single-Cell Analysis Reveals Functionally Distinct Classes within the Planarian Stem Cell Compartment. *Cell Stem Cell*, 15(3), pp.326–339. Available at: <http://www.ncbi.nlm.nih.gov/pubmed/25017721> [Accessed March 28, 2017].
- Wagner, D.E., Wang, I.E. & Reddien, P.W., 2011. Clonogenic neoblasts are pluripotent adult stem cells that underlie planarian regeneration. *Science (New York, N.Y.)*, 332(6031), pp.811–6. Available at: <http://www.pubmedcentral.nih.gov/articlerender.fcgi?artid=3338249&tool=pmcentrez&rendertype=abstract> [Accessed July 19, 2014].
- Wang, I.E. et al., 2016. Hedgehog signaling regulates gene expression in planarian glia. *eLife*, 5, pp.905–910. Available at: <http://www.ncbi.nlm.nih.gov/pubmed/27612382> [Accessed December 5, 2016].
- Wang, Y. et al., 2007. nanos function is essential for development and regeneration of planarian germ cells. *Proceedings of the National Academy of Sciences of the United States of America*, 104(14), pp.5901–6. Available at: <http://www.ncbi.nlm.nih.gov/pubmed/17376870> [Accessed March 28, 2017].
- Wang, Y. et al., 2010. regulators of germ cell development A functional genomic screen in planarians identifies novel regulators of germ cell development. *Genes & Development*, pp.2081–2092.
- Wenemoser, D. & Reddien, P.W., 2010. Planarian regeneration involves distinct stem cell responses to wounds and tissue absence. *Developmental biology*, 344(2), pp.979–91.

- Available at: <http://linkinghub.elsevier.com/retrieve/pii/S0012160610008377> [Accessed March 28, 2017].
- Wilson, P.A. et al., 1997. Concentration-dependent patterning of the *Xenopus* ectoderm by BMP4 and its signal transducer Smad1. *Development (Cambridge, England)*, 124(16), pp.3177–84. Available at: <http://www.ncbi.nlm.nih.gov/pubmed/9272958> [Accessed April 7, 2017].
- Witchley, J.N. et al., 2013. Muscle cells provide instructions for planarian regeneration. *Cell Reports*, 4(4), pp.633–641. Available at: <http://dx.doi.org/10.1016/j.celrep.2013.07.022>.
- Witchley, J.N. et al., 2013. Muscle cells provide instructions for planarian regeneration. *Cell reports*, 4(4), pp.633–41. Available at: <http://www.ncbi.nlm.nih.gov/pubmed/23954785> [Accessed March 28, 2017].
- Wolff, E., Dubois, F. & Dubois, F., 1948. Sur la migration des cellules de régénération chez les Planaires. *Revue suisse de zoologie.*, 55, pp.218–227. Available at: <http://www.biodiversitylibrary.org/part/117877> [Accessed March 28, 2017].
- Wurtzel, O. et al., 2015. A Generic and Cell-Type-Specific Wound Response Precedes Regeneration in Planarians. *Developmental Cell*, 35(5), pp.632–645. Available at: <http://linkinghub.elsevier.com/retrieve/pii/S1534580715007182>.
- Yoshikawa, S. et al., 2003. Wnt-mediated axon guidance via the *Drosophila* Derailed receptor. *Nature*, 422(6932), pp.583–588. Available at: <http://www.nature.com/doi/10.1038/nature01522> [Accessed April 5, 2017].
- Yoshioka, Y. et al., 2007. Complex interference in the eye developmental pathway by *Drosophila* NF-YA. *Genesis (New York, N.Y.: 2000)*, 45(1), pp.21–31. Available at: <http://doi.wiley.com/10.1002/dvg.20260> [Accessed April 7, 2017].
- Yoshioka, Y., Ly, L.L. & Yamaguchi, M., 2012. Transcription factor NF-Y is involved in differentiation of R7 photoreceptor cell in *Drosophila*. *Biology open*, 1(1), pp.19–29. Available at: <http://www.pubmedcentral.nih.gov/articlerender.fcgi?artid=3507159&tool=pmcentrez&rendertype=abstract> [Accessed January 6, 2014].
- Zinzen, R.P. et al., 2006. Evolution of the Ventral Midline in Insect Embryos. *Developmental Cell*, 11(6), pp.895–902. Available at: <http://www.ncbi.nlm.nih.gov/pubmed/17141163> [Accessed April 25, 2017].

